2016

Identifying Genetic Interactions and Target Genes of Schizosaccharomyces pombe Transcription Factors by Functional Genomics

Chatfield-Reed, Katherine

UNIVERSITY OF CALGARY

Identifying Genetic Interactions and Target Genes of *Schizosaccharomyces pombe* Transcription Factors by Functional Genomics

by

Katherine Chatfield-Reed

A THESIS

SUBMITTED TO THE FACULTY OF GRADUATE STUDIES

IN PARTIAL FULFILMENT OF THE REQUIREMENTS FOR THE

DEGREE OF DOCTOR OF PHILOSOPHY

GRADUATE PROGRAM IN BIOLOGICAL SCIENCES

CALGARY, ALBERTA

JULY, 2016

Abstract

Transcriptional regulation of target genes is a critical component of cellular regulation. Changes in expression profiles characterize different cell types, stages of the cell cycle, reactions to the environment, and many diseases including cancer. Knowledge of transcriptional regulation is critical to understanding environmental adaption, cell fate, and targeted treatment of genetic diseases. Transcription factors do not act in isolation, and often have overlapping target genes or coordinated activity. As such, understanding transcription factors requires a global approach that can be achieved with high-throughput genomics. This study used *Schizosaccharomyces pombe* as a model organism to look at transcriptional regulation. Expression and chIP microarrays were used to look for the target genes of the calcineurin-responsive transcription factor Prz1. This work uncovered hundreds of putative target genes that were both positively and negatively regulated by Prz1. These genes illuminated an evolutionarily conserved function in the cell wall, and novel roles in flocculation and reproduction. The interplay between transcription factors was examined with a synthetic genetic array screen between the transcription factors. The double deletion mutants that were sicker suggest transcription factors that share target genes or regulate related processes. A full genome screen of Prz1 was used to look for possible genetic activators of Prz1. The *pmr1*$^{+}$ calcium transporter gene was shown to negatively interact with *prz1*$^{+}$, and increase Prz1 activity in the cell. While the *alp31*$^{+}$ cofactor A gene also shared a negative genetic interaction with *prz1*$^{+}$, it did not increase Prz1 activity. Finally, a synthetic dosage lethality screen was adapted for *S. pombe* and used to look for regulators of fourteen transcription factors. This screen found 195 sick interactions between the transcription factors and a miniarray of putative

regulators. These interactions included two known upstream regulators of Yox1 and Scr1. It also showed interactions between Scr1 and two genes involved in protein degradation, the E3 ligase Ubr1 and the MYND domain protein SPBC31F10.10c, which are likely responsible for the ubiquitination of Scr1. These results introduce new insight into the *S. pombe* transcriptional-regulatory network, as well as providing a new methodology for examining genetic relationships in *S. pombe* in the future.

Acknowledgements

I would like to thank Dr. Gordon Chua for inviting me into the lab and teaching me molecular biology. Thank you very much for the support I got from the department, especially from my committee members Dr. Dave Hansen and Dr. Mark Bieda. Thank you to the members of the lab who were available to teach me new techniques or discuss difficult ideas. Finally, I would like to thank my friends and family for their continued support.

Table of Contents

List of Tables

List of Figures and Illustrations

List of Symbols, Abbreviations and Nomenclature

Symbol	Definition
A L U	Adenine, leucine, and uracil
ANOVA	Analysis of variance
CDRE	Calcineurin-dependent response element
chIP	Chromatin immunoprecipitation
CORVET	Class C core vacuole/endosome tethering
DNA	Deoxyribonucleic acid
DTT	Dithiothreitol
EMM	Edinburgh minimal medium
EV	Empty vector
GFP	Green fluorescent protein
GO	Gene ontology
H2BK123	Histone H2B, lysine 123
H3K4	Histone H3, lysine 4
HA	Human influenza hemagglutinin
HAT	Histone acetyltransferase
HCS	High-content screening
Kan	Geneticin
Lowess	Locally weighted scatterplot smoothing
MEME	Multiple Em for motif enrichment
mRNA	Messenger ribonucleic acid
MYND	Myeloid, Nervy, and DEAF-1
Nat	Nourseothricin
Nmt	No message in thiamine
OD_{600}	Optical density at 600 nm
OE	Overexpression
ORF	Open reading frame
PCR	Polymerase chain reaction
PMG	Pombe glutamate medium
PML	Promyelocytic leukemia
RFG	Red fluorescent protein
RNA	Ribonucleic acid
RNAi	Ribonucleic acid interference
RPM	Revolutions per minute
RSA	Random spore analysis
SAGA	Spt-Ada-Gcn5 acetyltransferase
SDL	Synthetic dosage lethality
SGA	Synthetic genetic array
SPAS	Sporulation agar
SUMO	Small ubiquitin-like modifier
TE	Tris-EDTA

Tuni	Tunicamycin
WT	Wild type
YES	Yeast extract with supplements
Zym	Zymolyase

Chapter One: **Introduction**

1.1 Transcriptional regulation

The information for encoding living things is stored in DNA. The information is not static, but is dynamically expressed by the molecular machinery of each cell. The specific expression of genes can create different cell lines, advance the cell cycle, and react to changing environments (Chan *et al*. 2009; Lemercier *et al.* 1998; Aligianni *et al.* 2009; Tanaka *et al.* 1998). A specific subset of genes is transcribed to mRNA and translated to proteins in reaction to the different needs of each cell. The RNA polymerase II complex transcribes genes by binding to conserved motifs in the promoters of genes, such as the TATA box or the initiator elements, and creating mRNA copies to be translated into proteins. The complex consists of multiple subunits that are responsible for the recruitment of RNA polymerase II to the promoter followed by transcriptional elongation (Chen *et al.* 1994; Corey *et al.* 2003). The genes activated by the RNA polymerase II complex are regulated by the chromatin state and sequence-specific transcription factors (Stringer *et al.* 1990; Chen *et al.* 1994; Corey *et al.* 2003). Chromatin is modified through small molecules added to histones, which change their interaction with DNA. The most well-known modifications are acetylation of histones, which is associated with open chromatin, and methylation, which can open or condense the chromatin structure depending on the amino acid residue (Lee *et al*. 1993; Brownell *et al.* 1996; Suka *et al.* 2002; Noma *et al.* 2001; Huang *et al.* 2005). Other modifications such as phosphorylation, sumoylation, and ubiquitination are also added to histones and affect the chromatin structure (Chwang *et al.* 2006; Lo *et al.* 2001; Robzyk *et al.* 2000; Joo *et al.* 2007).

Transcription factors have a DNA-binding domain that can recognize specific DNA motifs in the promoters of their target genes. On binding to these promoters they are able to activate or repress expression of the associated gene. Transcriptional activators have an activation domain that recruits general transcription machinery, improves the effectiveness of transcription, or alters chromatin structure (Stringer *et al.* 1990; Atanesyan *et al.* 2012, Chen *et al*. 1994; Yudkovsky *et al.* 2000; Ogryzko *et al.* 1996). These effects can be through direct interaction between the activation domain and the transcriptional machinery or through the recruitment of cofactors (Stringer *et al.* 1990; Kim *et al*. 1994). The activation domain can interact with components of the RNA polymerase II initiation complex or additional mediators and increase the DNA binding, stability, or processivity of the complex (Stringer *et al*. 1990; Kim *et al*. 1994; Kim *et al.* 2002). The transcriptional activators can also recruit factors that affect the chromatin state to increase access to the target genes (Ogryzko *et al.* 1996; Kadam and Emerson 2003; Corey *et al.* 2003).

Transcription factors can also act as repressors that reduce the expression of their target genes. There are multiple methods used to inhibit gene expression such as neutralizing a positive activator by blocking a DNA recognition motif, obscuring an activation domain, or competing for a coactivator (Hagen *et al.* 1994; Lemercier *et al.* 1998; Kakkis *et al.* 1989). Some repressors have repression domains that can reduce expression when fused with other activators, while others work by binding specific promoters or transcription factor activators (Hagen *et al.* 1994; Lemercier *et al.* 1998; Lillycrop *et al.* 1994; Yet *et al*. 1998). Specific recruitment of chromatin remodeling elements such as histone deacetylases can also result in gene repression (Lu *et al.* 2000).

Some transcription factors can act as either activators or repressors depending on posttranslational modifications or associated cofactors (Lillycrop *et al.* 1994; Lu *et al.* 2000).

1.2 Transcriptional-regulatory networks

The transcriptional-regulatory network describes the direct interactions between transcription factors and the promoters of their target genes (Lee *et al*. 2002). These networks govern the expression patterns of each cell and are a critical component of the regulation for the cell cycle, response to different environmental conditions, development, and cell type (Aligianni *et al*. 2009; Chen *et al.* 2008; Chan *et al*. 2009). These networks are incredibly complex and involve thousands of interactions working together to create the specific gene expression profile needed for each cell. Transcription factors can work together to regulate target genes by forming protein complexes that fine-tune their activity (Aligianni *et al*. 2009; Lemercier *et al.* 1998). It is also possible for different transcription factors to independently regulate identical, or overlapping target genes (Kwon *et al*. 2012). The overlap creates some redundancy between transcription factors, as well as allowing the same gene to be activated in response to different conditions or phases of the cell cycle.

Specific patterns of regulation have been identified in small network motifs that consistently arise in biological networks. These motifs include feed forward loops, single input motifs, multiple input motifs, and auto-regulatory motifs, which are small reoccurring regulatory motifs that are described in Figure 1.1 (Luscombe *et al*. 2004; Lee *et al*. 2002). The small motifs combine into a larger regulatory network with specific

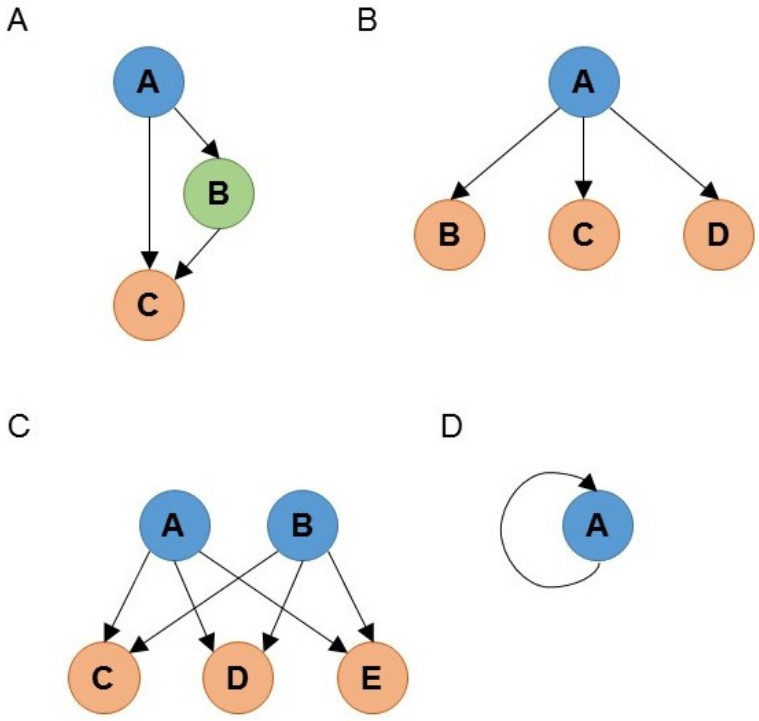

Figure 1.1: Small network motifs that reoccur in transcriptional regulation. The figure was adapted from Lee *et al*. (2002). A) The feed forward loop in which an activator A activates a second activator B and both activate a third downstream target C. B) The single input motif where one regulator is the only input for many targets. C) The multiple input motif in which the targets have multiple independent regulators. D) The auto-regulatory motif where a transcription factor regulates its own transcription.

properties associated with specific tasks. Several of these motifs are present in the transcriptional regulation of flocculation in fission yeast, including a negative feed forward loop, multiple input motifs, and auto-regulation (Figure 1.2) (Kwon *et al.* 2012). The transcription factors that are responsive to environmental stress tend to have simple networks with fewer layers of regulation, whereas transcription factors that are involved in normal cell cycle progression are more likely to interact with other factors in concert or cascades of regulatory activity (Luscombe *et al.* 2004). The cell cycle uses chains of transcriptional activation where transcription factors regulate each other in sequence to time the progression of gene expression (Lee *et al*. 2002; Luscombe *et al*. 2004). Some transcription factors act as hubs that have a large number of targets and link multiple processes together (Lee *et al*. 2002; Luscombe *et al*. 2004).

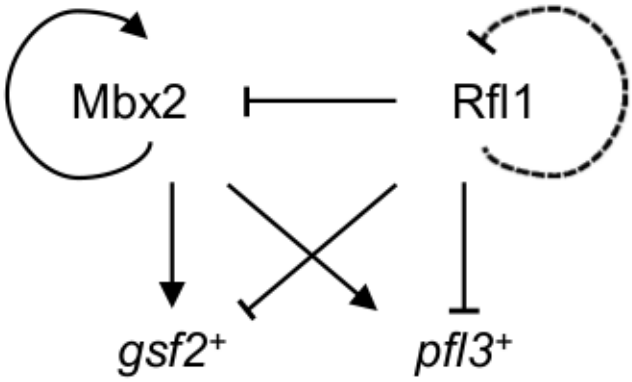

Figure 1.2: A portion of the transcriptional-regulatory network of flocculation in *S. pombe*. This figure was adapted from Kwon *et al.* (2012). This partial network shows a negative feed forward loop in which one of the transcription factors is an inhibitor. Rfl1 inhibits *mbx2*$^{+}$ expression, as well as multiple downstream target genes that are activated by Mbx2. The partial network also shows a multiple input motif and auto-regulation.

Transcriptional-regulatory networks can be inferred from gene expression data or from physical interaction data, which describe the mRNA levels and gene promoters bound by the transcription factor, respectively (Hu *et al.* 2007; Harbison *et al.* 2004). Both have drawbacks: the gene expression based functional regulatory network can connect indirect links, while the physical regulatory network can create edges that could be non-functional in a biological context (Marbach *et al.* 2012). The physical regulatory network can be examined in vivo or in vitro, and in metazoans, in vitro experiments are predominant due to the low levels and specific expression of transcription factors in multicellular organisms (Deplancke *et al.* 2006). Integrative approaches in deciphering regulatory networks attempt to combine data from multiple sources to get a more complete picture of gene regulation (Marbach *et al.* 2012). The networks generated should ideally be predictive of gene function or coexpression, in addition to providing insight into the network topology (Marbach *et al.* 2012). As these networks have been created for multiple organisms, the patterns in topology such as scale-free distribution, short path lengths, high clustering coefficients, and enrichment for feedforward and feedback loops, have been consistently observed (Lee *et al.* 2002; Deplancke *et al.* 2006; Boyer *et al.* 2005; Hu *et al.* 2007; Marbach *et al.* 2012). These network features arise consistently because they are important for robustness and adaptiveness of the organism (Marbach *et al.* 2012). The evolution of transcription-regulatory networks can occur through changes in the DNA motif of the target gene, or changes to the binding specificity and regulation of the transcription factor (Jarvela and Hinman. 2015). The evolution of transcriptional-regulatory networks is a crucial component of evolutionary adaption (Jarvela and Hinman 2015). Large-scale experiments looking at transcriptional

regulation help in building these networks, which in turn offer biological insight into cellular function and evolution.

1.3 Modes of transcription factor regulation

The activity of transcription factors is tightly regulated (Chuikov *et al*. 2004; Salghetti *et al*. 2001). An error in regulation of a transcription factor can cause severe defects and disease because it can affect the transcription of many target genes (Lu *et al.* 2000; Barlev *et al*. 2001). The regulation of transcription factors is accomplished by strict control of their levels, location, and activity in the cell. The upstream regulation is accomplished by enzymes that modify the transcription factor through the addition of small chemical groups. One of the most prevalent forms of posttranslational modification is phosphorylation and dephosphorylation. The addition or removal of a phosphoryl group can change the localization signal for the protein, change the transcription factor's ability to bind with cofactors, or target it for degradation (Hirayama *et al.* 2003; Lu *et al.* 2000; Gómez-Escoda *et al*. 2011; Andreson *et al.* 2010). These changes often affect the addition of other small molecules, such as ubiquitin, which can have further consequences on transcription factor abundance or activity (Aberle *et al*. 1997; Chi *et al*. 2001).

Ubiquitination is often used as a signal for proteolysis and regulates protein stability (Bai *et al.* 1996; Aberle *et al.* 1997; Kuras *et al*. 2002). This degradation can be an important component of the transcriptional response. Ubiquitination can be a part of rapid transcriptional activation. Some transcription factors like β-catenin are constitutively degraded, until another signaling molecule alters the ubiquitination of the

transcription factor resulting in a rapid increase in its protein level (Aberle *et al*. 1997). Protein degradation can also be closely related to target activation, where transcription factors are actively targeted for degradation as part of the transcriptional activation of their target genes (Chi *et al*. 2001; Salghetti *et al*. 2001). Ubiquitination also regulates transcription directly through histone modification and changes to the chromatin structure, which can affect the expression of transcription factors (Robzyk *et al*. 2000; Sun and Allis 2002). Ubiquitin has the ability to affect the affinity of transcription factors for specific promoters and influence their localization through cleavage from a membrane component (Hoppe *et al*. 2000; Stewart *et al*. 2011; Kuras *et al.* 2002). Small ubiquitin-like modifiers (SUMOs) are a related small molecule that use the same classes of enzymes to interact with their targets. Sumoylation of transcription factors is common and can result in activation or repression of their target genes (Gómez-del Arco *et al.* 2005; Yang and Sharrocks 2004). The activity of a transcription factor can be altered by sumoylation through nuclear export, localization to PML nuclear bodies, or interactions with cofactors such as components of the histone modification machinery (Santiago *et al.* 2013; Sachdev *et al*. 2001; Gómez-del Arco *et al*. 2005; Yang and Sharrocks 2004).

Acetylation is used extensively on histones, and is usually associated with open chromatin (Lee *et al*. 1993; Brownell *et al*. 1996; Suka *et al.* 2002). More recently, acetylation has been observed regulating the activity of other proteins directly, including transcription factors (Yao *et al.* 2001). Acetyltransferases and deacetyltransferases can activate or repress the activity of transcription factors (Yao *et al.* 2001; Soutoglou *et al.* 2000). The acetyl group can change the affinity for DNA binding, alter protein stability, or change the interaction with other regulators (Yao *et al.* 2001; Soutoglou *et al.* 2000;

Barlev *et al.* 2001; Matsuzaki *et al.* 2005). Methylation also controls transcription through histone modifications. Histone methylation is associated with both heterochromatin and euchromatin depending on the specific amino acid residue targeted (Noma *et al.* 2001; Huang *et al.* 2005). Methylation can also occur on non-histone proteins such as transcription factors and affect their activity by influencing posttranslational modification, protein-protein interaction, protein stability, protein localization, and the affinity for DNA (Kontaki and Talianidis 2010; Huang *et al.* 2007; Chuikov *et al.* 2004; Yamagata *et al*. 2008; Ea and Baltimore 2009).

There is a lot of crosstalk between posttranslational modifications of transcription factors to allow for complex regulation of transcriptional activity. For example, the tumor suppressor transcription factor p53 is regulated by phosphorylation, ubiquitination, sumoylation, methylation, and acetylation (Sakaguchi *et al.* 1998; Lukashchuk and Vousden 2007; Gostissa *et al.* 1999; Chuikov *et al*. 2004; Barlev *et al*. 2001).

Protein expression can also be regulated at the mRNA level. RNA-binding proteins can alter the levels and localization of mRNA under different conditions (Gerber *et al.* 2006). Sequence-specific RNA-binding proteins can bind in the 3' or 5' UTR to change the splicing, translation, localization, stability, and decay of the mRNA (Lillycrop *et al*.1994; Peng *et al*. 1998; Satoh *et al.* 2012; Gerber *et al.* 2004; Gerber *et al*. 2006). There are multiple RNA binding domains such the K-homology domain, RNA recognition motif, and Pumilio domain (Lorković and Barta 2002; Gerber *et al*. 2006). These RNA-binding factors alter gene expression at a posttranscriptional level and can affect the activity transcription factors, their regulators, or their target genes (Peng *et al*. 1998; Gerber *et al.* 2006).

1.4 *Schizosaccharomyces pombe* as a model organism

The fission yeast *S. pombe* is an excellent model organism for eukaryotic cells. *S. pombe* cells are normally haploid with 4914 genes, of which 26.1% are essential (Kim *et al*. 2010). It is a single celled organism that divides by binary fission making it an excellent model system for looking at components involved in cell cycle progression, as cell division follows the same progression observed in multicellular organisms (Nurse 1975; Nurse *et al*. 1976; Russell and Nurse 1987). This property made the discovery of the G2/M checkpoint of the cell cycle possible (Nurse 1975; Nurse *et al*. 1976). It also has more extensive intron splicing than the other popular model yeast, *S. cerevisiae* (Wood *et al*. 2002). *S. pombe* has 4730 introns spread through 43% of the genome, compared to 272 predicted introns in only 5% of the *S. cerevisiae* genome (Wood *et al*. 2002). The intron length is much shorter than those of metazoans, but the processing machinery is orthologous, and *S. pombe* possesses the machinery to excise mammalian introns (Wood *et al.* 2002; Käufer *et al.* 1985; Käufer and Potashkin 2000). It has a longer and more complex centromere than *S. cerevisiae*, which is more similar to metazoan centromeres (Wood *et al*. 2002). In contrast to *S. cerevisiae*, *S. pombe* is also capable of RNAi mediated chromatin silencing, another important regulatory mechanism it shares with higher eukaryotes (Cam *et al.* 2005). The RNAi chromatin silencing is important for silencing the centromeres, telomeres, and mating loci (Cam *et al.* 2005). Unlike *S. cerevisiae*, *S. pombe* did not undergo a whole genome duplication event (Wood *et al*. 2002). The lower percentage of duplicated gene classes may reduce the amount of redundancy and simplify the process of functionally characterizing genes (Wood *et al.*

2002). Together these features make it a good model organism to investigate a wide variety of conserved eukaryotic cellular processes.

S. pombe has a rapid doubling time of approximately two hours in rich media at 30°C. It can be easily transformed using plasmids, or linear DNA to create deletion or epitope-tagged strains by homologous recombination (Moreno *et al.* 1991; Maundrel 1993; Janke *et al*. 2004). There is a large deletion library available with 4836 and 3400 diploids and haploids respectively (Kim *et al*. 2010). The deletion library uses the kanamycin resistant cassette (KanMX4) for the gene replacements and is in a triple auxotrophic background, lacking the ability to synthesize adenine, leucine, and uracil (Kim *et al.* 2010). This background makes it a flexible tool for high-throughput screens and assays (Ryan *et al.* 2012; Dixon *et al.* 2008; Kennedy *et al.* 2008).

1.5 *Schizosaccharomyces pombe* transcription factors

S. pombe has 129 transcription factors, determined from the double-stranded DNA-binding domains predicted by multiple algorithms (Beskow and Wright 2006). In metazoans, transcription factor genes make up 5-10% of the genome compared to only ~1.9% in *S. pombe*, which makes it an attractive system to look for a global view of transcriptional regulation (Chua *et al.* 2013; Deplancke *et al.* 2006). Of these 129 transcription factors, Vachon *et al.* (2013) identified 99 sequence-specific transcription factors looking for genes that were not a part of the general transcription factor machinery. For the work in this study, the 99 transcription factors identified by Vachon *et al.* (2013) will be used, despite a few cases where alternate evidence suggests that some may not have sequence-specific activity (Wood *et al.* 2012). These transcription factors

have 19 different DNA-binding domains, some like the fungal Zn(2)-Cys(6) that are specific to yeast, and others that are conserved in higher eukaryotes (Table 1.1) (Kummerfeld and Teichmann 2006; Wood *et al*. 2012).

Of the 99 transcription factors, 91 have viable gene deletions, and only eight of those 91 show a significant growth defect in rich medium (Kim *et al.* 2010; Vachon *et al.* 2013). Considerably more of these transcription factors have defects when ectopically overexpressed with the *nmt1* promoter, with 64 showing growth defects and 43 displaying abnormal cell length phenotypes (Vachon *et al*. 2013). Sixty-eight of the 99 genes have been assigned a function based on experimentation or sequence homology, the functions include cell cycle, meiosis, ion homeostasis, stress response, and metabolism (Chua *et al*. 2013).

Table 1.1: The DNA-binding domains of the 99 sequence-specific transcription factors in *S. pombe.*

DNA-Binding Domain	Transcription Factors with the Domain
APSES	4
C2H2 Zn Finger	18
CAAT	1
CBF/LAG-1	2
Copperfist	2
Forkhead	5
Fungal Zn(2)-Cys(6)	30
GATA Zn Finger	3
Helix-loop-helix	4
Histone-like	3
HMG box	6
HMG-1/HMG-Y	4
Homeobox	2
HSF-type	2
IPT-TIG	1
Leucine zipper/bZIP	6
Myb-like	2
RFX	1
SRF-type	3

1.6 High-throughput approaches in identifying transcription factor targets

The function of *S. pombe* transcription factors has only been partially mapped (Chua *et al.* 2013). One important method to classify the function of transcription factors is to identify their target genes and decipher the transcriptional-regulatory network. The targets of transcription factors reveal how the cell regulates expression in response to important environmental signals and over time. Expression microarray technology allows for a view of global mRNA levels, which gives a picture of transcriptome changes within the cell (Chua *et al.* 2006; Převorovský *et al.* 2015). Two channel microarrays compare global mRNA isolated from two separate cell cultures and detect differential gene expression in response to perturbations. The design of a microarray experiment to uncover transcription factor targets must have an experimental sample in which the transcription factor of interest is active, and a control sample in which it is not (Chua *et al.* 2006; Kwon *et al.* 2012). The simplest experimental design looks at the transcription factor deletion strain relative to wild-type cells. This has been used to successfully discover target genes of several *S. pombe* transcription factors such as Gsf1, Sep1, Ace2, Yox1, and Cdc10 (Kwon *et al.* 2012; Rustici *et al*. 2004, Aligianni *et al.* 2009). A major obstacle to this simple design is that many transcription factor deletion strains do not have an obvious phenotype under standard laboratory conditions, which make it unlikely that the transcription factor is required or active, indicating that the targets may not be expressed (Vachon *et al*. 2013; Kim *et al.* 2010). Alternate designs use chemical or environmental sensitivities of the transcription factor deletion strain to identify conditions in which the transcription factor is necessary and presumably active. These treatments can be used to induce the expression of the transcription factor and its targets. *S. pombe*

transcription factors such Zip1, Atf1, Pap1, Prr1, Toe1, Sre1, Cuf1, and Fep1 have had target genes identified with chemical treatments or environmental perturbations (Harison *et al.* 2005; Chen *et al.* 2008; Vachon *et al.* 2013; Todd *et al.* 2006; Rustici *et al.* 2007). Cell cycle targets can also be identified by using synchronized cultures (Rustici *et al.* 2004; Aligianni *et al*. 2009). In addition, gene deletions that increase the activity of the transcription factor can be used to uncover the target genes by doing microarray experiments using this genetic background (Zheng *et al.* 2010). Finally, ectopic overexpression can be used to identify the targets of many transcription factors (Vachon *et al.* 2013; Převorovský *et al.* 2015). Although transcriptional activity is tightly regulated, in many cases overexpression will overcome this regulation and result in the transcription factor binding to the promoters of its target genes due to mass action (Vachon *et al.* 2013; Chua *et al.* 2006). Several transcription factors in *S. pombe* have been characterized in this manner, such as Mbx2, Toe1, Toe2, Toe3, Cbf12, and Cbf11 (Kwon *et al.* 2012; Vachon *et al.* 2013; Převorovský *et al.* 2015).

The main drawback of using DNA microarrays to uncover transcription factor target genes is that they do not show direct interaction with the promoter. The conditions used could result in some off target effects that differentially regulate genes through some mechanism other than the transcription factor, although good microarray design should limit this effect. The other issue is that the transcription factor may indirectly affect the expression levels of some genes through an intermediary, for example by affecting the expression of other transcription factors. Therefore, binding data of the transcription factor to the promoter is important to establish direct regulation of the target genes. Chromatin immunoprecipitation (chIP) microarrays can be used to uncover the DNA that

is directly bound by the transcription factor of interest (Aligianni *et al*. 2009; Kwon *et al*. 2012; Převorovský *et al.* 2015).

ChIP microarray experiments also require a design in which the transcription factor is active. The same types of conditions used to activate transcription factors for expression microarrays can be used for chIP microarrays. The transcription factors can be ectopically overexpressed or investigated in a sensitizing genetic background (Kwon *et al.* 2012; Vachon *et al.* 2013). The transcription factor can also be activated by exposing the cells to chemical or other environmental perturbations, or synchronizing the cells to the same stage of the cell cycle before performing the chIP experiment (Převorovský *et al*. 2015; Vachon *et al.* 2013). These methods have been used to uncover transcription factor target genes for Yox1, Cdc10, Gsf1, Mbx2, Toe1, Toe2, and Toe3 (Aligianni *et al.* 2009; Kwon *et al.* 2012; Vachon *et al.* 2013). A similar technique called chIP sequencing can also be used to uncover transcription factor targets by sequencing the fragments of DNA bound by the transcription factors, which has been used on the *S. pombe* transcription factors Cbf11 and Cbf12 (Převorovský *et al*. 2015).

Few *S. pombe* transcription factors (~20%) have been tested by microarray based approaches to uncover their direct target genes. This is in contrast to *S. cerevisiae* where most of the transcription factors have identified target genes either from targeted studies, or large-scale microarray screens (Hirayama *et al.* 2003; Marion *et al.* 2004; Hu *et al.* 2007; Chua *et al.* 2006). In two studies alone, 263 transcription factor deletion mutants and 55 transcription factor overexpression mutants were analyzed by expression microarrays (Hu *et al.* 2007; Chua *et al.* 2006). The deletion microarray experiments identified putative transcriptional regulators for 45% of the yeast genome (Hu *et al.*

2007). This provides significant coverage, while also supporting the need for activation of many transcription factors for microarray experiments. The 55 overexpression mutants exhibiting reduced fitness phenotypes provide an alternative method to identify target genes of a substantial number of transcription factors, although it is clearly not the only solution as an additional 23 transcription factors did not show an overexpression phenotype or activate their targets (Chua *et al.* 2006). The DNA binding of 203 transcription factors has also been examined with chIP microarrays in a study that looked at 1-12 different environmental conditions for 84 of the aforementioned transcription factors (Harbison *et al.* 2004). The binding specificity has also been examined for 89 transcription factors in vitro using 8 base pair DNA fragments (Zhu *et al.* 2009). Another 112 *S. cerevisiae* transcription factor binding specificities were tested using a protein-binding microarray, which had every unique 10 base pair double DNA sequence represented (Badis *et al.* 2008). In vitro screens have the advantage of providing the binding specificity of the transcription factor domain without needing to know the activating conditions (Badis *et al.* 2008). The drawback is that the binding specificity of the transcription factor does not necessarily reveal the in vivo DNA binding to the promoter of the target genes or address the impact of other regulatory factors (Badis *et al*. 2008). This type of large-scale screening for transcription factor target genes is crucial for the construction of transcriptional-regulatory network models of the cell, and has yet to be performed in *S. pombe*.

1.7 Synthetic genetic array screens

The budding and fission yeast genomes contain ~20% (Giaever *et al.* 2002) and 26.1% (Kim *et al.* 2010) essential genes respectively, under standard laboratory conditions. Genes are often nonessential because they are only needed under specific environmental conditions or because they are functionally redundant with one or more other genes. It is common for genes to be regulated by multiple transcription factors, making a single transcription factor redundant in most conditions (Lee *et al.* 2002). Synthetic genetic array (SGA) technology looks for redundancy or other relationships between genes by creating pairwise deletions in a high-throughput manner. Negative interactions are when the double deletion is lethal or much sicker than expected based on the single deletion, where each gene directly or indirectly compensates for the loss of the other (Tong *et al*. 2001). Conversely, positive interactions are healthier than expected based on the fitness of the two single mutants. This could result from a sick single mutant phenotype being masked by a second mutation, but more often it is the result of the double mutant fitness being less severe than expected based on a multiplicative model of the combined fitness of the two single mutants. Positive interactions are enriched among genes in signalling cascades and genes whose protein products are physically associated (Costanzo *et al.* 2010).

The high-throughput SGA screens are performed by mating genes together using high density yeast arrays and robotic pinning tools (Figure 1.3A) (Tong *et al*. 2001). The two collections of genes, the query and array genes, are distinguished by their different selection markers and opposing mating types (Tong *et al*. 2001). To perform the screen, each query is mated against the entire set of array genes and the double mutant progeny

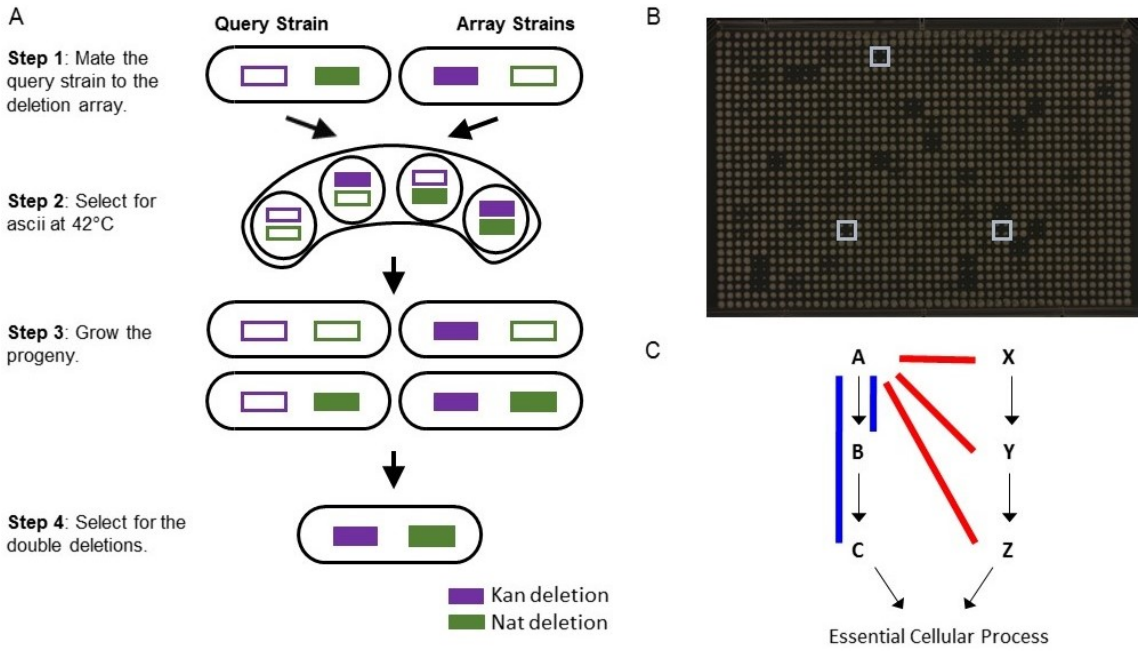

Figure 1.3: The SGA methodology in yeast. A) The protocol for the creation of double mutants in *S. pombe* based on the one described by Dixon *et al.* (2008). The Kan-resistant deletion array strains are pinned on a high density yeast array. The Nat-resistant deletion query strain is crossed with the deletion array in step 1. The cells mate for three days on SPAS plates at 25°C and spend 3 days at 42°C for selection of the spores. This was followed by recovery for three days on rich medium with no drugs. The double deletion mutants were selected by three days of growth on rich media with Kan and Nat. The final colony size was imaged and scored using SGAtools. B) The final image of the screen. The light blue boxes indicate negative interactions. C) The basic model for positive and negative interactions. The negative interactions are shown in red, and usually occur between two redundant pathways. The positive interactions are shown in blue, and often occur between genes in the same pathway or complex.

are selected using the two antibiotic resistant markers. The arrays are photographed and the colony sizes of the double mutants are then scored and normalized to assess the relative health of each double mutant combination (Figure 1.3B) (Tong *et al*. 2001). The score uses a multiplicative model of genetic interactions in which the double mutant combination is expected to be as sick as the multiplied sickness of each single mutant (Dixon *et al*. 2008; Baryshnikova *et al.* 2010). Double mutants that are sicker than the expected combination are called synthetic sick or negative interactions, and combinations that are healthier than the predicted combination are called positive interactions (Figure 1.3C) (Dixon *et al*. 2008; Baryshnikova *et al.* 2010).

The SGA technique was originally developed for *S. cerevisiae*, and to date, this organism has the most complete interaction network. There are twice as many negative as positive interactions among the *S. cerevisiae* genes profiled, which includes full or partial coverage of 75% of the genome (Costanzo *et al*. 2010). The overall network shows a power law distribution, with a few genes having many genetic interactions and many genes having very few genetic interactions (Tong *et al.* 2004; Costanzo *et al*. 2010). The sicker the single deletion mutant, the more likely it is to be a hub gene with a higher number of negative and positive interactions (Costanzo *et al.* 2010). The similarity between the interaction networks of genes can be used to uncover the functions and relationships of unknown genes (Tong *et al*. 2004; Costanzo *et al*. 2010). If a gene of unknown function genetically interacts with the same genes as a collection of genes with known function, then the unknown gene likely shares that function (Tong *et al.* 2004; Costanzo *et al.* 2010). A high degree of similarity can also indicate that the genes are in the same complex (Costanzo *et al.* 2010). Gene complexes often have a lot of shared

interactions between their component proteins and these interactions tend to be all positive or all negative within a complex (Baryshnikova *et al.* 2010). Genes in the same biological process are highly connected by genetic interactions (Costanzo *et al.* 2010; Baryshnikova *et al.* 2010). There are also higher level patterns between biological processes that have a lot of interactions between their genes, but represent completely distinct processes (Costanzo *et al.* 2010). One example is the large number of connections between protein folding, glycosylation and the cell wall with genes involved in cell polarity and morphogenesis (Costanzo *et al.* 2010). Different components of the cell have different properties in their genetic interaction network (Zheng *et al.* 2010). The kinase and phosphatase network is highly connected and enriched for positive interactions (Fiedler *et al*. 2009), while the sequence-specific transcription factor network is sparse and enriched for negative interactions (Zheng *et al.* 2010). The volume and types of interactions give an indication about the topology of the regulatory networks.

The SGA approach has been applied to several other organisms including *S. pombe* (Roguev *et al.* 2007; Dixon *et al.* 2008; Ryan *et al.* 2012), *Escherichia coli* (Babu *et al*. 2011), *Caenorhabditis elegans* (Lehner *et al*. 2006; Byrne *et al*. 2007), *Drosophila melanogaster* (Horn *et al.* 2011), mouse cell lines (Roguev *et al.* 2013), and human cell lines (Deshpande *et al.* 2013; Vizeacoumar *et al.* 2013). The interactions between the two popular model yeasts, *S. pombe* and *S. cerevisiae,* showed some conserved interactions, with the majority of interactions being species specific (Dixon *et al.* 2008). The overlap of genes between these two yeasts is considerable, with 75% of the genes sharing one or more orthologs between the two fungi (Dixon *et al.* 2008). In a SGA study that focused on conserved processes in *S. pombe,* 222 array and query genes were screened and

compared to the *S. cerevisiae* genetic interaction data (Dixon *et al.* 2008). The conservation of genetic interactions between the two organisms was estimated to be 29% among the highly-conserved processes queried. This number was supported for both positive and negative interactions in a larger comparative study (Ryan *et al*. 2012). The highest conservation was observed among genes in the same complex with 70% of the positive interactions and 68% of the negative interactions conserved (Ryan *et al.* 2012). The conservation also remained high in genes that were in the same biological process, with 58% and 38% of the positive and negative interactions conserved respectively (Ryan et al. 2012). The conservation was much lower, 19% and 15% of the positive and negative interactions conserved, respectively, when the genes were in distinct biological processes (Ryan *et al.* 2012). Even when specific genetic interactions were not conserved, the overall trend of crosstalk between biological processes often was conserved (Ryan *et al.* 2012). Genes that are essential in one yeast generally have a larger number of genetic interactions in the other yeast (Ryan *et al.* 2012). In contrast, genes with no orthologs identified in another species have very few interactions indicating little functional dependency with other systems (Ryan *et al*. 2012). By looking at networks across a variety of species, a core genetic interactome should emerge (Dixon *et al*. 2008). The ability to identify conserved genetic interactions becomes more difficult when comparing between unicellular and multicellular organisms (Dixon *et al.* 2008). The use of knockdowns, instead of complete knockouts, and the difference in fitness scoring systems in the higher eukaryotes make direct comparison more challenging (Byrne *et al.* 2007). The overlap probed to date is very low because metazoan screens preferentially choose genes that usually cannot be studied in yeast, like those involved in development

(Lehner *et al.* 2006; Byrne *et al.* 2007). The overlap between genetic interactions in *C. elegans* and *S. cerevisiae* was 4.7%, which was not significantly more than would be expected by chance (Bryne *et al.* 2007). There have been some conserved genetic interactions with medical relevance to the treatment of cancer (Deshpande *et al*. 2013; Vizeacoumar *et al.* 2013). Genes that interact with genes misregulated in cancer can provide targets for future drug therapies, which could minimize the impact on healthy cells (Deshpande *et al*. 2013; Vizeacoumar *et al*. 2013).

1.8 Synthetic dosage lethality screens

The basic SGA technique of mating and scoring the progeny has been expanded in *S. cerevisiae* to different genetic relationships such as triple gene deletions (Tong *et al.* 2004; Haber *et al.* 2013), dosage suppression interactions (Magtanong *et al.* 2011), and synthetic dosage lethality interactions (Measday *et al.* 2005; Sopko *et al*. 2006; Liu *et al.* 2009; Sharifpoor *et al.* 2012; Duffy *et al.* 2012). A synthetic dosage lethality (SDL) interaction is a growth defect observed due to gene overexpression in a target deletion background that is not present in a wild-type background (Measday and Hieter 2002). Many genes do not have a strong phenotype when overexpressed, which can be exploited in a SDL screen (Sopko *et al*. 2006). The lack of a strong phenotype could be due to upstream regulation by multiple mechanisms, such as a kinase or phosphatase that regulates the activity of its substrates (Sopko et al. 2006). Another possibility is that the deletion and overexpression genes have opposing regulatory roles for a common process (Duffy *et al.* 2012). A third explanation for a SDL interaction could be that the two mutations disrupt the stoichiometry of a protein complex (Duffy *et al*. 2012).

Several screens have been performed in *S. cerevisiae* to look for SDL interactions (Measday *et al.* 2005; Sopko *et al.* 2006; Liu *et al.* 2009; Sharifpoor *et al.* 2012; Duffy *et al*. 2012). The first steps of the SDL protocol are similar to SGA in that the query deletion is mated with an array of overexpression strains and the double mutants are selected. The SDL screen requires a final step to induce the plasmid from the query strain before the colonies are imaged and the double mutant fitness is assessed (Sopko *et al.* 2006). The first high-throughput SDL screen was used to study chromosome segregation in *S. cerevisiae* by looking for mutants sensitive to increased dosage of kinetochore proteins (Measday *et al*. 2005). SDL interactions have also been used to look for substrates of ubiquitin-binding proteins, kinases, and lysine deacetylases (Sopko *et al.* 2006; Liu *et al.* 2009; Sharifpoor *et al.* 2012; Duffy *et al*. 2012). A high-throughput SDL screen looking at the ubiquitin-binding proteins Rad23 and Dsk2 was able to identify multiple pathways affected by these gene deletions, as well as direct regulation of two proteolytic substrates (Liu *et al.* 2009). Sopko *et al.* (2006) identified the calcineurin-responsive transcription factor Crz1 as a substrate of the kinase Pho85. These results indicate that SDL interactions can be used to identify substrates in multiple regulatory pathways (Sopko *et al.* 2006; Liu *et al.* 2009). Interactions between kinase deletion strains and a whole genome overexpression array showed enrichment between kinases and known substrates, physically associated kinases, and phosphoproteins (Sharifpoor *et al.* 2012). There were also a large number of interactions that could not be accounted for through direct kinase substrate interactions and therefore likely reflect information about related pathways (Sharifpoor *et al.* 2012). One example is when the deletion of a kinase gene and its SDL partner have opposing regulatory roles in the same pathway. Increasing

the activation or inhibition of the process through overexpression, while simultaneously removing the opposing force through gene deletion, resulting in increased sickness in the double mutant (Sharifpoor *et al.* 2012). Sharifpoor *et al*. (2012) also observed that under standard laboratory conditions, not all of the existing interactions were detected because the interaction may only occur under specific environmental conditions. The kinases that interacted with more genes under standard growth conditions were mostly cell cycle genes (Sharifpoor *et al*. 2012). A similar set of interaction types was observed with the lysine deacetylase gene deletion mutants (Duffy *et al.* 2012). The interactions from SDL screens can also be compared with interactions from SGA screens to determine more complex regulatory interactions (Sharifpoor *et al*. 2012).

1.9 Specific aims

The aim of this study was to characterize multiple levels of regulation of *S. pombe* transcription factors using high-throughput functional genomics techniques. These levels include the identification of downstream target genes, functional redundancy among the transcription factors, as well as the upstream regulators. All of these levels contribute to the global view of transcriptional regulation in the cell. Applying multiple techniques in the highly tractable model of fission yeast allows large portions of this network to be explored. The interactions and regulatory patterns discovered in *S. pombe* are an important step in understanding transcriptional regulatory networks in higher eukaryotes. Specific Aim 1: The first aim was to use expression and chIP microarrays to uncover the downstream targets of the calcium-responsive transcription factor Prz1. The identity of

the target genes can then be used to explore the function of Prz1 transcription in the cell and the conservation of function between Prz1 and its orthologs in other yeast species.

Specific Aim 2: The second aim was to look at functional redundancy among the 99 sequence-specific transcription factors using the SGA method. This was achieved by crossing 38 query with 92 array transcription factor deletion strains to examine the genetic interactions among the sequence-specific transcription factors. In addition to looking at genetic interactions among the transcription factors, a full genome screen was performed on Prz1 and used to explore negative interactions as a source to identify activating conditions of the transcription factor.

Specific Aim 3: The final aim was to develop an SDL protocol for *S. pombe*, and apply the technique to look for upstream regulators of several transcription factors. Fourteen transcription factor overexpression query strains were crossed to a regulator miniarray containing gene deletions of kinases, phosphatases, ubiquitin ligases, methyltransferases, acetyltransferases, and RNA-binding proteins.

Chapter Two: **Conserved and diverged functions of the calcineurin-activated Prz1 transcription factor in fission yeast**

Kate Chatfield-Reed, Lianne Vachon, Eun-Joo Gina Kwon, and Gordon Chua

Published in Genetics, April 2016. 202: 1365-1375.

This chapter describes the characterization of the downstream target genes of the transcription factor Prz1. The work was done using *prz1*$^{+}$ mutant strains that were created by Gina Kwon and Lianne Vachon. The sensitivity of the Δ*prz1* strain to tunicamycin was discovered in a larger drug screen performed by Lianne Vachon, and she also performed that microarray experiment. I conducted the rest of the experiments and the analysis with the guidance of my supervisor Gordon Chua.

2.1 Abstract

Gene regulation in response to intracellular calcium is mediated by the calcineurin-activated transcription factor Prz1 in the fission yeast *Schizosaccharomyces pombe*. Genome-wide studies of the Crz1 and CrzA fungal orthologs have uncovered numerous target genes involved in conserved and species-specific cellular processes. In contrast, very few target genes of Prz1 have been published. This paper identified an extensive list of genes using transcriptome and ChIP-chip analyses under inducing conditions of Prz1, including $CaCl_2$, and tunicamycin treatment, as well as a Δ*pmr1* genetic background. We identified 165 upregulated putative target genes of Prz1 in which the majority contained a

calcium-dependent response element in their promoters, similar to that of the *Saccharomyces cerevisiae* ortholog Crz1. These genes were functionally enriched for Crz1-conserved processes such as cell wall biosynthesis. Overexpression of *prz1*$^+$ increased resistance to the cell wall degradation enzyme zymolyase, likely from upregulation of the O-mannosyltransferase encoding gene *omh1*$^+$. Loss of *omh1*$^+$ abrogates this phenotype. We uncovered a novel inhibitory role in flocculation for Prz1. Loss of *prz1*$^+$ resulted in constitutive flocculation and upregulation of genes encoding the flocculins Gsf2 and Pfl3, as well as the transcription factor Cbf12. The constitutive flocculation of the Δ*prz1* strain was abrogated by the loss of *gsf2*$^+$ or *cbf12*$^+$. This study reveals that Prz1 functions as a positive and negative transcriptional regulator of genes involved in cell wall biosynthesis and flocculation, respectively. Moreover, comparison of target genes between Crz1/CrzA and Prz1 indicate some conservation in DNA-binding specificity, but also substantial rewiring of the calcineurin-mediated transcriptional-regulatory network.

2.2 Introduction

Calcineurin is a highly-conserved phosphatase central to Ca^{2+} signaling. In metazoans, calcineurin regulates a wide array of Ca^{2+}-dependent processes including T-cell activation (Clipstone and Crabtree 1992), cardiac hypertrophy (Molkentin *et al.* 1998), neutrophil motility (Hendey *et al.* 1992), apoptosis (Wang *et al.* 1999), angiogenesis (Graef *et al.* 2001), and memory development (Mansuy *et al.* 1998). One of the primary effectors of calcineurin is the NFAT family of transcription factors that translocates into the nucleus to regulate target genes when dephosphorylated (reviewed in Macian 2005). In fungi, the

activity of the Crz1 C_2H_2 zinc finger transcription factor is modulated by calcineurin in a similar way (reviewed in Thewes 2014). Crz1 orthologs have been identified in various fungal species and their function appears conserved in cell wall-related processes and resistance to external stressors (Thewes 2014).

The *S. cerevisiae* Crz1 is localized in the cytosol under optimal growth conditions, but is activated and rapidly translocated into the nucleus through dephosphorylation by calcineurin in response to exogenous Ca^{2+} (Stathopoulos-Gerontides *et al.* 1999). In addition to exogenous Ca^{2+}, Crz1 is activated by numerous external stresses including high salt, prolonged exposure to α-factor, alkaline pH, antifungal compounds, blue light, nutrient deprivation, heavy metals, and ethanol (Matheos *et al.* 1997; Stathopoulos and Cyert 1997; Edlind *et al.* 2002; Serrano *et al.* 2002; Zhang and Rao 2007; Araki *et al.* 2009; Zakrzewska *et al.* 2005; Ruiz *et al.* 2008; Ferreira *et al.* 2012; Bodvard *et al.* 2013). Transcriptome profiling of *CRZ1* was initially performed with Ca^{2+} or Na^{+} treatment, which identified 163 target genes (Yoshimoto et al. 2002), and this list has been expanded subsequently with similar profiling under alkaline stress, nutrient deprivation, and transcription factor overexpression (Viladevall *et al.* 2004; Ruiz *et al.* 2008; Chua *et al.* 2006). The Crz1 target genes are known to function in ion homeostasis, small molecule transport, cell wall maintenance, lipid and sterol metabolism, and vesicle transport. Many of these target genes contain the calcineurin-dependent response element (CDRE) motif (5'-GNGGC(G/T)CA-3') in their promoter (Yoshimoto *et al.* 2002). Crz1 binds this motif, which was originally discovered in the promoter of *FKS2,* and is sufficient to drive the transcriptional activation of a reporter gene (Stathopoulos and Cyert 1997; Yoshimoto *et al.* 2002).

In *S. pombe*, the Ppb1 calcineurin catalytic subunit dephosphorylates the transcription factor Prz1 in response to elevated Ca^{2+} levels (Hirayama *et al.* 2003). Similar to other Crz1 orthologs, dephosphorylation of Prz1 causes nuclear translocation and transcriptional regulation of its target genes through binding of a CDRE-like motif (5'-AGCCTC-3') (Deng *et al*. 2006) or a Ca^{2+}-dependent response element (5'-CAACT-3') (Hamasaki-Katagiri and Ames 2010). Loss of *prz1*$^+$ produces a normal phenotype under optimal growth conditions, but results in hypersensitivity to Ca^{2+} and reduced mating efficiency (Hirayama *et al.* 2003; Sun *et al.* 2013). In contrast, the calcineurin Δ*ppb1* strain exhibits a more severe phenotype with additional defects in cytokinesis, cell polarity, and chloride hypersensitivity (Yoshida et al. 1994; Hirayama *et al.* 2003). These defects are not suppressed by *prz1*$^+$overexpression indicating that Prz1 is not the sole target of calcineurin (Hirayama *et al.* 2003). Besides Ca^{2+}, activation of Prz1 occurs upon exposure to NaCl, DTT and tunicamycin (ER stressors), micafungin (a β glucanase inhibitor), and heat shock, when assayed by either a CDRE-regulated reporter, nuclear translocation, or *prz1*$^+$ mRNA levels (Deng *et al.* 2006; Hirayama *et al.* 2003). In addition, *prz1*$^+$overexpression activates the CDRE-regulated reporter, thus indicating positive autoregulation (Koike *et al.* 2012). The response to diverse external stimuli indicates that Prz1 must regulate genes involved in multiple cellular processes as observed in other fungal orthologs. However, the current target gene list of Prz1 is far from complete. Only five target genes have been identified: *pmc1*$^+$ (Hirayama *et al*. 2003), *pmr1*$^+$ (Maeda *et al.* 2004), *ncs1*$^+$ (Hamasaki-Katagiri and Ames 2010), *cmk1*$^+$ (Cisneros-Barroso *et al*. 2014), and *prz1*$^+$ (Deng *et al.* 2006). This is in contrast to other fungal Crz1 orthologs that have more extensive target gene lists, ranging from dozens up

to several hundred genes, functioning in cellular processes such as cell wall biosynthesis, ion transport, lipid metabolism, and vesicle transport (Yoshimoto *et al*. 2002; Karababa *et al*. 2006; Chen *et al*. 2012; Hagiwara *et al*. 2008; Soriani *et al*. 2008).

Here, we substantially expand the number of putative target genes for Prz1 by transcriptome and ChIP-chip profiling and uncover novel biological roles in reproduction, cell wall structure, and flocculation. We discovered that the DNA-binding specificity of the calcineurin-responsive transcription factors is conserved between budding and fission yeasts, but considerable differences exist among orthologous target genes. The role in cell wall biosynthesis is conserved between Prz1 and its orthologs, and several putative target genes for this role were identified. Finally, we show that Prz1 directly represses target genes implicated in flocculation.

2.3 Materials and methods

2.3.1 Yeast strains, media and general methods

Table A1 contains a list of yeast strains used in this study. Strains were grown in yeast extract with supplements (YES) or EMM and supplemented with adenine (225 mg/L), leucine (225 mg/L), uracil (225 mg/L), thiamine (15 μM), geneticin (150 mg/L) and nourseothricin (100 mg/L) when required. Calcium chloride, and tunicamycin (T7765: Sigma Aldrich, St. Louis, MO) were added to YES medium at 0.15 M and 2.5 μg/mL, respectively. Cell wall sensitivity was assayed with 0.5 μg/mL micafungin (A13270-1: AdooQ Bioscience, Irvine, CA) and 25 U/mL Zymolyase 100T (E1005: Zymo Research, Irvine, CA). Deletion and epitope-tagged strains were constructed by a PCR-based stitching method as described in Kwon *et al*. (2012). All constructed strains

were verified by colony PCR and sequencing of the amplicons. For deletion strains, the entire open reading frame (ORF) was replaced with the KanMX6 or NatMX4 cassettes, while for endogenously-tagged *prz1* strains, GFP and HA epitopes were PCR-amplified from pYM27 and pYM14 plasmids, respectively (Janke *et al.* 2004), and inserted in-frame at the C-terminal end of the *prz1*$^+$ ORF. Functionality of the *prz1-HA* and *prz1-GFP* strains was determined by comparing their growth to wild type on 0.15 M $CaCl_2$-containing medium. Overexpression of *prz1*$^+$ with the *nmt1* or *nmt41* promoter was accomplished by cloning the ORF into the *pREP1/pREP2* and *pREP41* vectors, respectively. Standard genetic and molecular methods were performed as described in Moreno *et al.* (1991).

2.3.2 Microarray expression profiling

Wild type and Δ*prz1* cultures were concurrently grown in 100 ml liquid YES at 30°C for 16-20 hours to a matching cell density of ~8 × 10^6 cells/mL before harvesting. Calcium chloride and tunicamycin treatment were 0.15 M for 0.5 hour and 2.5 µg/mL for 1.5 hours, respectively, prior to harvesting. The Δ*pmr1* and Δ*prz1* cultures were also grown concurrently in 100 mL liquid YES at 30°C for 16-20 hours to a matching cell density of ~8 × 10^6 cells/mL. For *prz1*$^+$ overexpression, cultures of the *prz1OE* strain and empty vector control were concurrently grown in 100 mL of EMM (supplemented with adenine and uracil) without thiamine at 30°C for 18-22 hours to ~8 × 10^6 cells/mL and then harvested. The same procedure was used in the heterologous overexpression of *S. cerevisiae CRZ1* with the *nmt1* or *nmt41* promoter in the Δ*prz1* strain. Sample preparation for hybridization to 8 × 15,000 Agilent *S. pombe* expression microarrays and

scanning were carried out as described in detail in Kwon *et al.* (2012). All microarray experiments were performed with a single dye-swap and normalized using the R Limma package with Lowess scaling (Smyth and Speed 2003) and the eBayes method was used to combine the replicates by fitting to a linear model (Smyth 2004). Hierarchical clustering was performed using the uncentered Pearson correlation with Cluster 3.0 (Eisen *et al.* 1999) and the tree image was generated using Java Treeview (Saldanha 2004). The microarray expression data has been submitted to the NCBI Gene Expression Omnibus Database (GSE77761).

2.3.3 ChIP-chip profiling

The endogenous C-terminal-tagged *prz1-HA* strain was grown in 200 mL liquid YES medium at 30°C for 16-20 hours and treated with calcium chloride or tunicamycin as described above. A detailed description in sample preparation for hybridization to 4 × 44,000 Agilent *S. pombe* Genome ChIP-on-chip microarrays is found in Kwon *et al.* (2012). All ChIP-chip experiments were performed with dye swaps for two biological replicates. The data was normalized using the median correction method and replicates were combined with eBayes from the R limma package (Smyth and Speed 2003; Smyth 2004). Significant peaks were identified using chIPOTle (Buck *et al.* 2005). To detect potential promoter occupancy, the peak was considered only when within 1000 base pairs (the average length of the sonicated DNA fragments) of the promoter region, defined as 0-1500 base pairs upstream of the start codon. The chIP-chip data has been submitted to the NCBI Gene Expression Omnibus Database (GSE77761).

2.3.4 Motif and functional enrichment analyses

Motif searching for the DNA-binding specificity of Prz1 was carried out in MEME using promoter sequences consisting of 1000 base pairs upstream of the start codon (Bailey and Elkan 1994). The maximum size of the motif was set at 10 base pairs and at zero or one motif per promoter sequence. Functional enrichment was performed with the Princeton GO term finder (Boyle *et al.* 2004).

2.3.5 Crz1 target genes:

A list of Crz1 target genes in *S. cerevisiae* was assembled from a literature review of genome wide, as well as smaller scale, studies (Ruiz *et al.* 2008; Yoshimoto *et al.* 2002; Matheos *et al.* 1997; Cai *et al.* 2008; Chua *et al.* 2006; Fardeau *et al.* 2007; Hu *et al.* 2007). In most cases, the Crz1 target genes identified as significant were used. For the Chua *et al.* (2006) study, no specific cut-off was defined and a $\log_{10}$-fold change of 3 was selected. The Crz1/CrzA target genes used for *C. albicans*, *C. glabrata*, *A. nidulans*, and *A. fumigatus* were from individual studies in each organism which performed transcriptome analysis using microarray experiments (Karababa *et al.* 2006; Chen *et al*. 2012; Hagiwara *et al*. 2008; Soriani *et al.* 2008).

The list of *S. pombe* genes with orthologs in *S. cerevisiae* was obtained from the V2.18 orthologue list (Wood *et al.* 2012). The orthologs in the other species were determined using Inparanoid datasets (Sonnhammer and Östlund 2015) and from the Fungal Orthogroups Repository (Wapinski *et al.* 2007), except for *A. fumigatus* which relied solely on Inparanoid data.

2.3.6 Cell wall degradation assays

Strains were grown with their respective controls as described for the expression microarray experiments. Wild type and Δ*prz1* strains were grown in liquid YES medium, while genetic backgrounds containing *nmt1*-driven *prz1*$^{+}$ or empty vector were grown in liquid EMM minus thiamine for 18-24 hours. The cells were washed twice with 0.9% saline solution and resuspended in TE buffer at ~1.2 x 10^7 cells/mL. Three milliliters of cell suspension was transferred to test tubes in the presence and absence of 25 U/mL Zymolyase 100T (Zymo Research, Irvine, CA) and shaken at 37°C. OD_{600} readings were taken every 15 minutes to assess the degree of cell wall degradation. The significance of the different treatments was assessed at the two hour time point with an ANOVA followed by a two tailed t-test.

2.3.7 Flocculation assays

Constitutive flocculation was assessed by inoculating cells in liquid YES at an initial cell density of ~10^7 cells/mL and growing at 30°C in a shaking incubator. After 24 hours, 10 mL of culture was transferred to a 90 mm plastic petri dish and rotated slowly on an orbital low-speed shaker (Labnet International, Woodridge, NJ) for 10 minutes at room temperature. Images of flocs were acquired with a SPImager (S&P Robotics Inc., Toronto, ON).

2.3.8 Fluorescence microscopy

The intracellular localization of natively-regulated Prz1-GFP was determined in the *prz1-GFP* strain treated with $CaCl_2$ or tunicamycin and in the Δ*pmr1 prz1-GFP*

strain. Cells were grown and treated as described for the expression microarray experiments. Images of live *prz1-GFP* cells were captured with a Zeiss Imager Z1 microscope and AxioCam MRM digital camera (Zeiss, Thornwood, NY). The proportion of cells containing Prz1-GFP predominantly in the cytoplasm, nucleus, or both compartments was determined manually in ~300 cells from three biological replicates.

2.4 Results

2.4.1 Chemical and genetic activation of Prz1

Identification of target genes using genome-wide approaches requires that the transcription factor be in an active state. Dephosphorylation of Prz1 by calcineurin results in nuclear translocation and regulation of its target genes. Therefore, we first determined whether several types of chemical treatment and a change in genetic background resulted in activation of Prz1 by promoting its translocation into the nucleus. Several studies have examined the intracellular localization of GFP-tagged Prz1, but expression of the fusion protein was controlled by the *nmt1* promoter. The elevated expression in this strain could potentially increase the nuclear localization of Prz1 through mass action. As a result, we constructed a strain expressing a Prz1-GFP fusion protein under control of the native promoter to examine its nuclear localization in response to $CaCl_2$ and tunicamycin treatment, as well as deletion of *pmr1*$^+$, which encodes a Golgi Ca^{2+}/Mn^{2+} ATPase. The *prz1-GFP* strain exhibited sensitivity to $CaCl_2$ comparable to wild type, indicating the fusion protein was functional. When cells were grown in rich medium, Prz1-GFP was primarily localized in the cytoplasm and not in the nucleus in the majority (>85%) of cells (Figure 2.1A and B). Only ~2% of these cells exhibited predominantly nuclear

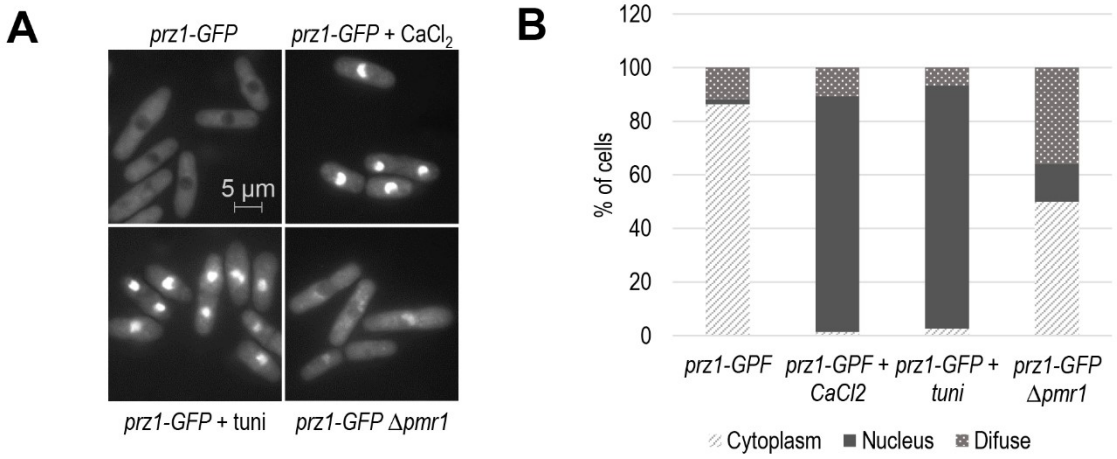

Figure 2.1: Intracellular localization of endogenously-controlled Prz1-GFP. A) Wild-type cells expressing endogenously-controlled Prz1-GFP were exponentially grown in YES medium (upper left), and treated with 0.15 M $CaCl_2$ (upper right) or 2.5 µg/mL tunicamycin (lower left) for 0.5 and 1.5 hours, respectively. The lower right panel shows the intracellular localization of endogenously-controlled Prz1-GFP in Δ*pmr1* cells grown in rich medium. B) Bar graph showing the percentage of cells in each category of Prz1-GFP localization from Figure 2.1A. The data is from three replicates of approximately 100 cells each.

localization. In contrast, Prz1- GFP exhibited mostly nuclear localization (~90%) when exposed to 0.15 M $CaCl_2$ and 2.5 µg/mL tunicamycin for 0.5 and 1.5 hours, respectively (Figure 2.1A and B). These results indicate that Prz1 is activated when treated with $CaCl_2$ and tunicamycin, which is in agreement with previous studies (Hirayama *et al.* 2003; Deng *et al.* 2006). We also investigated the intracellular localization of Prz1-GFP when *pmr1*$^+$ was deleted. Loss of *pmr1*$^+$ was synthetic lethal with the Δ*prz1* strain (Ryan *et al.* 2012), suggesting that Prz1 function is required in the Δ*pmr1* background. Moreover, calcium homeostasis may be disrupted in the Δ*pmr1* strain (Maeda *et al.* 2004) which could result in activation of Prz1. The frequency of nuclear localization of Prz1-GFP in Δ*pmr1* cells (~14%) was greater than unperturbed wild-type cells (Figure 2.1A and B). Interestingly, a substantial proportion of Δ*pmr1* cells (~38%) displayed Prz1-GFP present in both the nucleus and cytoplasm. These results suggest a robust activation of Prz1 in response to $CaCl_2$ or tunicamycin treatments and intermediate activation in Δ*pmr1* cells compared to untreated wild type.

2.4.2 Identification of Prz1 target genes by genome-wide analyses

There are currently only a handful of known direct target genes of Prz1. To expand the list of Prz1 target genes, we performed transcriptome profiling and ChIP-chip analysis under the inducing conditions determined by our Prz1-GFP intracellular localization studies. Transcriptomes were compared between the Δ*prz1* mutant with wild type exposed to 0.15 M $CaCl_2$ or 2.5 µg/mL tunicamycin, as well as between the untreated Δ*prz1* and the Δ*pmr1* strains. As a control, transcriptome profiling was performed on the Δ*prz1* and wild-type strains grown in rich medium. We identified 339

genes that were differentially regulated by more than two-fold with a $p < 0.001$ in at least one of the four expression microarray experiments (Figure 2.2A). Lower expression levels in the Δ*prz1* strain, relative to the wild type or Δ*pmr1* strain, represented positively-regulated target genes of Prz1, while higher expression indicated negatively-regulated targets. $CaCl_2$ treatment resulted in the most differentially-expressed genes (150 lower and 67 higher in Δ*prz1*), followed by the Δ*pmr1* strain (109 lower and 67 higher in Δ*prz1*) and the tunicamycin treatment (94 lower and 51 higher in Δ*prz1*) (Figure 2.2A). In contrast, only 17 and 51 genes had lower and higher expression, respectively, in the Δ*prz1* strain relative to wild type. This is consistent with previous observations that transcriptome profiling of most transcription factor deletion strains does not uncover many direct target genes in *S. pombe* under optimal growth conditions (Chua 2013; Vachon *et al.* 2013). Hierarchical clustering revealed that the tunicamycin treatment and the Δ*pmr1* strain expression profiles were the most similar (Figure 2.2A), which is in agreement with the observations that both tunicamycin and $pmr1^+$ are involved in endoplasmic reticulum stress (Deng *et al*. 2006; Dürr *et al.* 1998) and therefore may activate Prz1 in a similar way.

ChIP-chip profiling of a natively-regulated Prz1-HA strain was performed to further confirm that the differentially-expressed genes retrieved from the transcriptome studies are putative target genes of Prz1. These ChIP-chip experiments were carried out under inducing conditions of Prz1 in the presence of $CaCl_2$ or tunicamycin with the same dosages as the transcriptome studies. We found that Prz1 bound to the promoters of 254 and 257 genes during $CaCl_2$ and tunicamycin treatments, respectively, and the overlap of genes (197 genes or ~77%) between both treatments was substantial (Figures 2.2B and

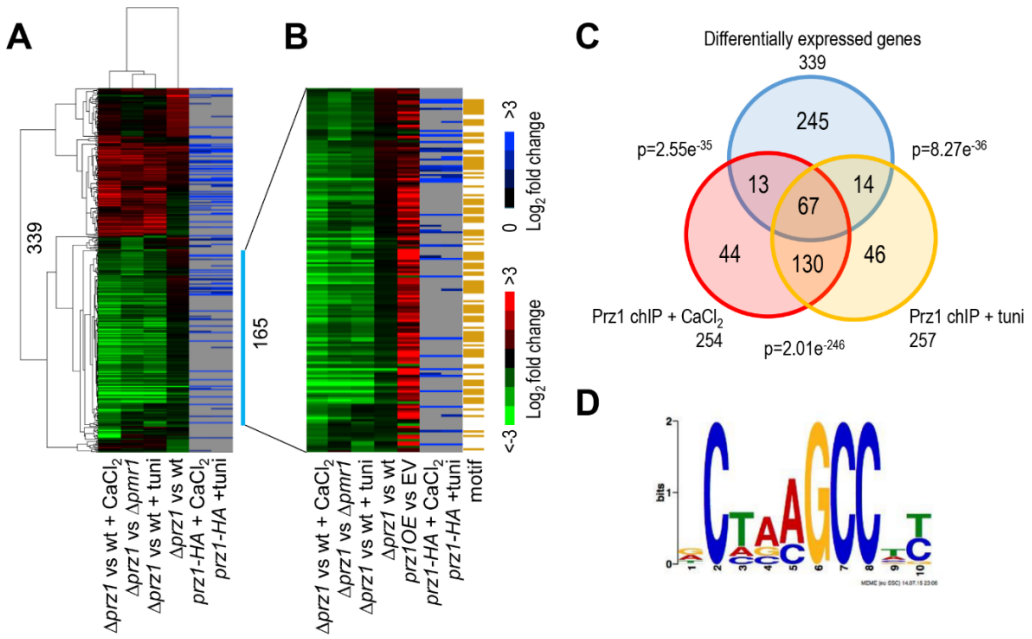

Figure 2.2: Identification of Prz1 target genes by transcriptome and chIP-chip profiling. A) The heat map shows two dimensional hierarchical clustering of 339 genes that were differentially expressed by at least 2-fold in at least one of the microarray experiments. The first four columns of the heat map compare transcriptomes of the following conditions: the Δ*prz1* strain and wild type, the Δ*prz1* strain and wild type supplemented with 0.15 M $CaCl_2$ for 0.5 hours, the Δ*prz1* strain and wild type supplemented with 2.5 µg/mL tunicamycin for 1.5 hours, and the Δ*prz1* strain compared to the Δ*pmr1* strain. All of the above experiments were performed in rich medium. In the heat map, genes upregulated and downregulated in the Δ*prz1* strain relative to the control are indicated in red and green, respectively. The two rightmost columns in the heatmap show ChIP-chip analysis of a *prz1-HA* strain treated with 0.15 M $CaCl_2$ or 2.5 µg/mL tunicamycin for 0.5 and 1.5 hours, respectively. B) The heat map shows the expression profiles of 165 putative target genes that are positively-regulated by Prz1. The first four columns of the heat map match the expression data from Figure 2.2A while the fifth column shows the expression profiles of the same target genes upregulated in a *prz1*$^+$ overexpression strain compared to the empty vector (EV) control. The next two columns in the heat map show ChIP-chip analysis of a *prz1-HA* strain treated with 0.15 M $CaCl_2$ or 2.5 µg/mL tunicamycin for 0.5 and 1.5 hours, respectively. The rightmost column of the heat map shows the 91 genes containing the CDRE motif within their promoter in orange. The colour bars indicate relative expression and chIP enrichment ratios between experimental and control strains. All microarray expression and chIP-chip experiments were performed in replicate with dye reversal. C) The Venn diagram shows the overlap between the 339 differentially-expressed genes in the transcriptome experiments and the genes identified from the chIP-chip analysis with Prz1 promoter occupancy in the presence of $CaCl_2$ or tunicamycin. The significance of the overlap is indicated as p-values that were determined using a hypergeometric distribution. D) A DNA motif generated by MEME from promoter analysis of the 165 putative target genes of Prz1. This motif is similar to the CDRE motif (5'-AGCCTC-3') previously discovered in Deng *et al.* (2006).

C). Moreover, we detected Prz1 occupancy in its own promoter in response to both $CaCl_2$ and tunicamycin treatments (Tables A2 and A3), which is in agreement with other studies (Deng *et al.* 2006). For the $CaCl_2$ treatment, 80 of the 254 promoter-bound genes (31.4%) were differentially expressed in the Δ*prz1* strain ($p=2.55e^{-35}$ using a hypergeometric distribution) (Figures 2.2B and C). In response to tunicamycin treatment 81 of the 257 promoter bound genes (31.5%) were differentially expressed in the Δ*prz1* strain ($p=8.27e^{-36}$) (Figures 2.2B and C). Overall, 94 of the 339 genes (27.7%) differentially-expressed in the transcriptome experiments were bound in one of the chIP-chip experiments (Figures 2.2B and C). This amount of overlap between transcriptome and chIP-chip analyses of Prz1 is comparable to a similar study on the fission yeast CSL transcription factors Cbf11 and Cbf12 (Převorovský *et al.* 2015).

Among the 339 differentially-regulated genes, 165 genes were consistently lower in the Δ*prz1* strain relative to wild type when treated with $CaCl_2$ or tunicamycin, indicating that Prz1 may positively regulate these target genes (Figure 2.2B). We next subjected these 165 putative target genes of Prz1 to gene ontology analysis using the Princeton GO Term Finder. The gene products were enriched for biological process categories such as reproduction ($p=5.1e^{-4}$), cell wall organization or biogenesis ($p=4.9e^{-3}$), as well as components of membranes ($p=2.2e^{-6}$) and the Golgi apparatus ($p=1.1e^{-5}$) (Table 2.1). Moreover, the vast majority of these target genes were also upregulated in the *prz1*$^{+}$ overexpression strain, and Prz1 was found to be associated with the promoters of 37 of these genes ($p=2.3e^{-12}$) (Figure 2.2B). All the known target genes of Prz1 (*prz1*$^{+}$, *pmc1*$^{+}$, *pmr1*$^{+}$, *ncs1*$^{+}$, and *cmk1*$^{+}$) were also found within these 165 genes (Table 2.1).

Table 2.1: The gene ontology terms that are significantly enriched among the 165 putative target genes positively regulated by Prz1 using Princeton GO Term Finder. The target genes that have the CDRE motif in their promoter (Figure 2.2D) are indicated in bold and those with an ortholog that is regulated by Crz1 in *S. cerevisiae* are underlined. Only the genes with enriched gene ontology terms are shown.

Gene Ontology Term	P-value	Gene List
Reproduction (GO:0000003)	$5.1e^{-4}$	*cdc1*$^+$, *dic1*$^+$, ***gpa1***$^+$, *gwt1*$^+$, *isp3*$^+$, *krp1*$^+$, *mam2*$^+$, *map1*$^+$, ***matPc***$^+$, *mcp2*$^+$, ***mcp5***$^+$, *mde6*$^+$, *mei2*$^+$, ***meu13***$^+$, *meu17*$^+$, ***meu22***$^+$, ***meu27***$^+$, *mfm2*$^+$, *mst2*$^+$, ***mug108***$^+$, ***mug133***$^+$, *mug136*$^+$, *mug63*$^+$, *mug8*$^+$, ***ncs1***$^+$, *pmp31*$^+$, ***ppk35***$^+$, *rec10*$^+$, ***scd2***$^+$, *set3*$^+$, **SPAPB1A10.08**, *ste11*$^+$, ***ste4***$^+$, *bgs1*$^+$, *cfr1*$^+$, ***pvg5***$^+$
Cell wall organization or biogenesis (GO:0071554)	$4.9e^{-3}$	*bgs1*$^+$, *cfr1*$^+$, ***pvg5***$^+$, ***cfh2***$^+$, *gas2*$^+$, ***gmh2***$^+$, ***omh1***$^+$, *pun1*$^+$, ***pvg1***$^+$, ***rga5***$^+$, **SPAC13C5.05c**, **SPAC9G1.10c**, SPBC1198.07c, **SPBC19C7.05**, SPBC21B10.07
Membrane (GO:0016020)	$2.18e^{-6}$	***gda1***$^+$, *sen54*$^+$, SPAC977.02, ***mug133***$^+$, *ima1*$^+$, *pet2*$^+$, SPBC21B10.07, ***git3***$^+$, SPBC1271.03c, ***ppk35***$^+$, ***ncs1***$^+$, *pun1*$^+$, **SPAC23C11.06c**, **SPCPB1C11.02**, *gas2*$^+$, *krp1*$^+$, **SPAC14C4.07**, ***dnf1***$^+$, SPBC15C4.06c, *pmp31*$^+$, *imt2*$^+$, *mfm2*$^+$, *cki2*$^+$, ***frp1***$^+$, **SPAC18B11.03c**, SPCC1529.01, ***ost2***$^+$, *mam2*$^+$, ***omh1***$^+$, *fur4*$^+$, **SPAC212.01c**, *bgs1*$^+$, ***isp5***$^+$, *ggc1*$^+$, ***cfh2***$^+$, *rsn1*$^+$, *psd2*$^+$, **SPAC630.04c**, ***erg1***$^+$, **SPBC1348.03**, ***meu22***$^+$, *tco1*$^+$, ***bst1***$^+$, SPAC869.03c, *meu17*$^+$, **SPAC5D6.04**, **SPAC750.04c**, ***ppr3***$^+$, **SPAC1687.08**, **SPBC19C7.05**, ***mac1***$^+$, *gwt1*$^+$, ***yip5***$^+$, SPBC1198.07c, ***itr2***$^+$, ***gga21***$^+$, *pet1*$^+$, SPCC553.12c, *lcb4*$^+$, ***pvg1***$^+$, **SPAC869.05c**, SPCC794.03, **SPAC4C5.03**, *str1*$^+$, ***tvp15***$^+$, ***gmh2***$^+$, ***pmr1***$^+$, **SPCC4B3.02c**, *mfs1*$^+$, SPAC23D3.12, ***gpa1***$^+$, ***imt1***$^+$, ***pvg5***$^+$
Golgi apparatus (GO:005794)	$1.08e^{-5}$	*fmd2*$^+$, ***gda1***$^+$, *tco1*$^+$, ***bst1***$^+$, *cfr1*$^+$, ***mug133***$^+$, **SPAC869.05c**, *pet2*$^+$, SPAC869.03c, *meu17*$^+$, **SPAC3A11.10c**, ***omh1***$^+$, ***tvp15***$^+$, *fur4*$^+$, **SPBC19C7.05**, ***gmh2***$^+$, *pun1*$^+$, ***yip5***$^+$, **SPCC4B3.02c**, ***gga21***$^+$, SPAC23D3.12, *krp1*$^+$, *pet1*$^+$, **SPAC14C4.07**, ***dnf1***$^+$, *lcb4*$^+$, ***imt1***$^+$, *mug136*$^+$, ***pvg5***$^+$, ***pvg1***$^+$, *imt2*$^+$

Strikingly, promoter analysis by MEME revealed a common motif in 91 of the 165 putative Prz1 target genes that closely resembled the CDRE sequence 5'-AGCCTC-3' (Deng *et al.* 2006) (Figures 2.2D and Table A4). Altogether, these results indicate that the majority of these 165 genes are likely direct targets that are positively regulated by Prz1.

Interestingly, 92 genes were upregulated at least two-fold in the Δ*prz1* strain during $CaCl_2$ or tunicamycin treatment (Figure 2.3), indicating that Prz1 may also negatively regulate a different set of target genes. In addition, 46 of these genes were downregulated in the *prz1*$^+$ overexpression strain, and Prz1 was associated with the promoters of 40 of the 92 putative target genes ($p=5.2e^{-25}$) (Figure 2.3). However, unlike the positively-regulated genes, no common binding motif was detected by MEME. Gene ontology analysis of these 92 genes detected functional enrichment in ion transmembrane transport ($p=4.7e^{-4}$) and small molecule catabolic processes ($p=3.0e^{-4}$) (Tables 2.2 and A5). Direct transcriptional repression of target genes has not been detected for Prz1 or confirmed in fungal Crz1 orthologs (Thewes 2014).

Table 2.2: The gene ontology terms that are significantly enriched among the 92 putative target genes negatively regulated by Prz1 using Princeton GO Term Finder. The genes that have an ortholog regulated by Crz1 in *S. cerevisiae* are underlined. Only the genes with enriched gene ontology terms are shown.

Gene Ontology Term	P-value	Gene List
Small molecule catabolic process (GO:0044282)	$3.0e^{-4}$	SPAC2F3.05c, *car1*$^+$, SPAC139.05, SPAC4H3.08, *gut2*$^+$, *gpd3*$^+$, *atd1*$^+$, *tms1*$^+$, SPCC1223.09, *eno102*$^+$
Ion transmembrane transport (GO:0034220)	$4.7e^{-4}$	*gti1*$^+$, *tgp1*$^+$, *pho1*$^+$, *mfs3*$^+$, *mug86*$^+$, SPCPB1C11.03, SPBPB2B2.01, SPBC36.02c, SPBC1683.01, *pho84*$^+$, *mae1*$^+$, SPBPB10D8.01, SPBC3H7.02, *pgt1*$^+$, SPCC794.04c

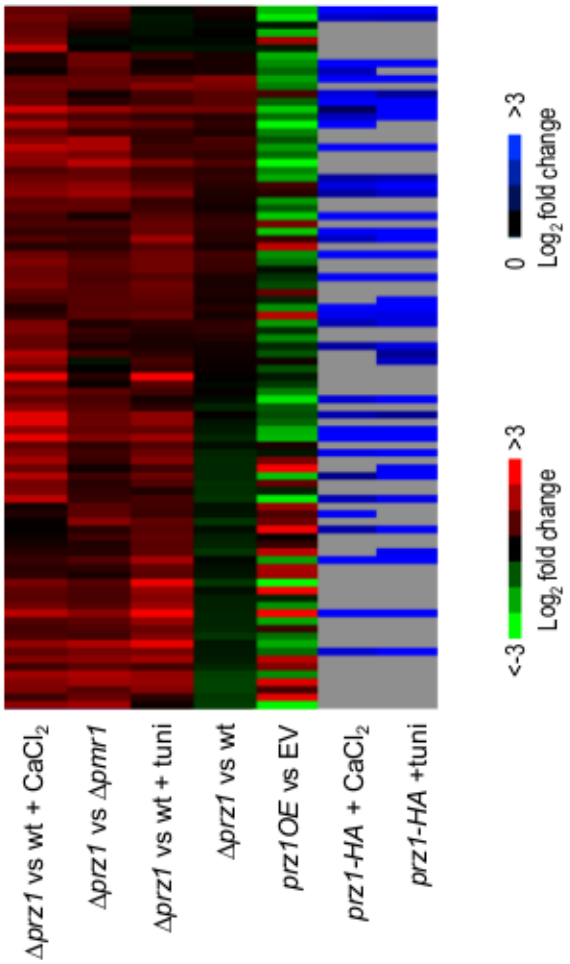

Figure 2.3: The heat map shows the expression profiles of 92 putative target genes that are negatively-regulated by Prz1. The first four columns of the heat map match the expression data from Figure 2.2A while the fifth column shows the expression profiles of the same target genes in a *prz1*$^{+}$ overexpression strain compared to the empty vector (EV) control. The next two columns in the heat map show ChIP-chip analysis of a *prz1-HA* strain treated with 0.15 M CaCl2 or 2.5 µg/mL tunicamycin for 0.5 and 1.5 hours, respectively. The colour bars indicate relative expression and chIP enrichment ratios between experimental and control strains. All microarray expression and chIP-chip experiments were performed in replicate with dye reversal.

Orthologous target genes between S. pombe Prz1 and other fungal Crz1/CrzA

The known target genes of Prz1 are well conserved in *S. cerevisiae*. All of the known Prz1 target genes (*prz1*$^+$, *pmc1*$^+$, *pmr1*$^+$, *ncs1*$^+$ and *cmk1*$^+$) have budding yeast orthologs regulated by Crz1 with the exception of *ncs1*$^+$ (Hamasaki-Katagiri and Ames 2010). However, the proportion of the remaining Prz1 putative target genes that have Crz1 target gene orthologs was considerably lower. There were 24 Crz1 target gene orthologs among the 165 putative target genes upregulated by Prz1 (Tables 2.1 and A4) (Ruiz *et al.* 2008; Yoshimoto *et al.* 2002; Matheos *et al.* 1997; Cai *et al.* 2008; Chua *et al.* 2006; Fardeau *et al.* 2007; Hu et al. 2007). The conservation of target genes is highest for the conserved biological process of cell wall organization or biogenesis in which 40% of the Prz1 putative target genes annotated in this gene ontology category have Crz1 target gene orthologs (Table 2.1). Interestingly, there were eight putative target genes (*atd1*$^+$, *sua1*$^+$, *bfr1*$^+$, SPBC1683.01, *pho84*$^+$, *fhn1*$^+$, *plb1*$^+$ and SPAC513.07) seemingly repressed by Prz1 that had orthologs that were positively regulated by Crz1 (Ruiz *et al.* 2008; Chua *et al.* 2006; Yoshimoto *et al.* 2002). This phenomenon is further supported by the observation that the promoters of seven of these eight genes were bound by Prz1 in one or both of the chIP-chip experiments (Table A5).

The number of orthologous target genes decreases with more distantly-related fungi (Figure 2.4). Comparison with a study in *C. albicans* found that of the 65 Crz1 targets, only five overlap with the 165 positively-regulated targets and two overlap with the negatively-regulated target genes in *S. pombe* (Karababa *et al.* 2006). A similar overlap was also observed between the 34 target genes of *C. glabrata* Crz1 (Chen *et al*. 2012). CrzA target genes in *A. nidulans* and *A. fumigatus* showed even less overlap with

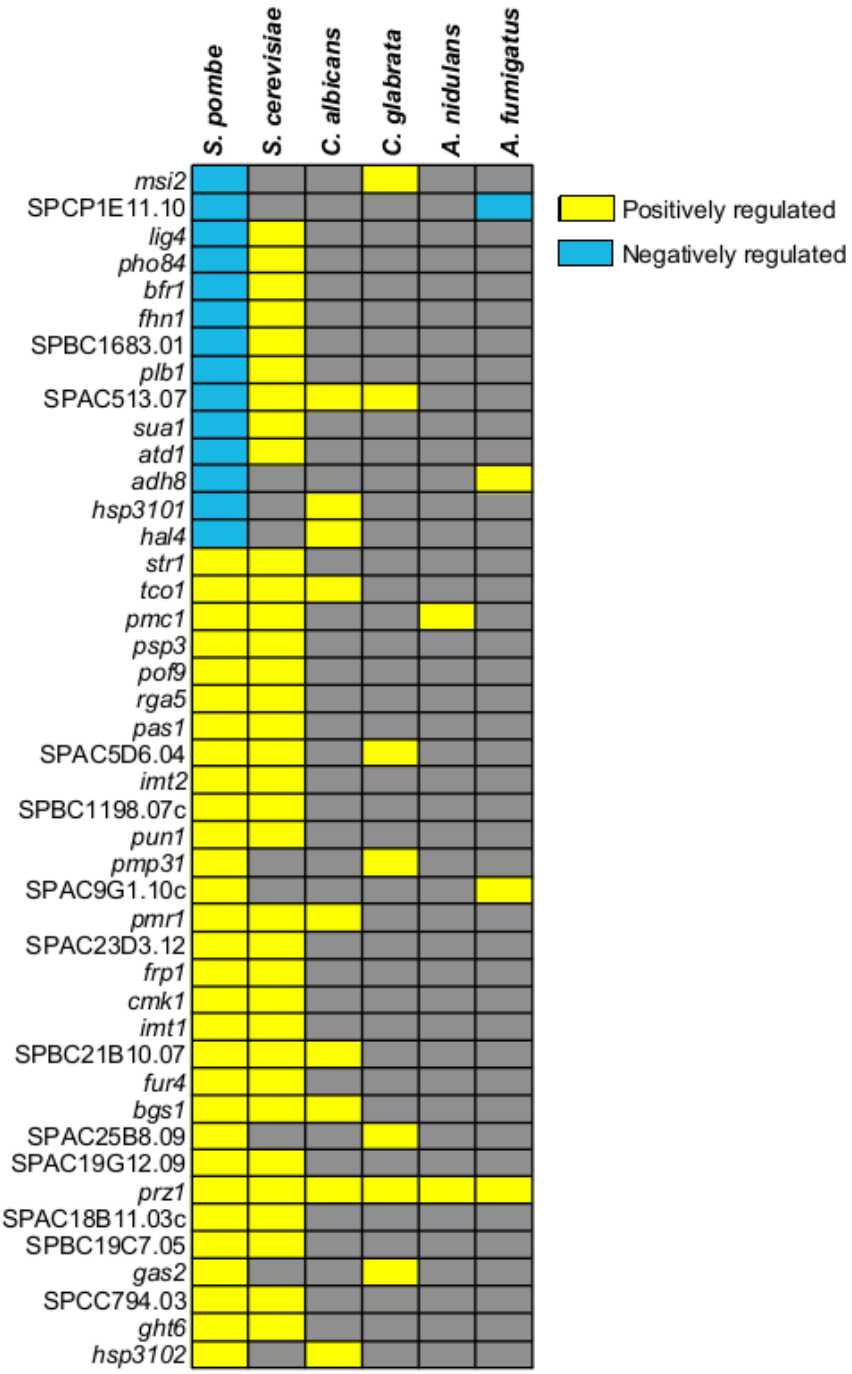

Figure 2.4: The orthologs of the 339 differentially regulated genes in *S. pombe* that are regulated by a Prz1 ortholog in other fungal species. The highest number of orthologs is found between *S. pombe* and *S. cerevisiae*. This is likely due to several factors including the closer evolutionary distance. The other factors include the better characterized ortholog list between *S. pombe* and *S. cerevisiae* as well as the greater number of experiments and conditions used to find Crz1 targets in *S. cerevisiae* compared to the other species included.

the *S. pombe* Prz1 target genes (Hagiwara *et al*. 2008; Soriani *et al.* 2008). Cell wall organization is positively regulated by Prz1, as well as its orthologs in fungi, which would indicate conservation among the target genes implicated in that process. However, this conservation was not as extensive as expected. Only two Prz1 target genes with cell wall functions (SPBC21B10.07 and *bgs1*$^{+}$), share orthologs in *S. cerevisiae* and *C. albicans*. Other cell wall genes like *gas2*$^{+}$ and SPAC9G1.10c were conserved in more distantly-related species *C. glabrata* and *A. fumigatus,* respectively, while not sharing an ortholog in *S. cerevisiae*.

The difference in the number of orthologs suggests an increasingly distant relationship between Prz1 and its Crz1/CrzA orthologs over evolutionary time. However, it may reflect incomplete data because unlike *S. cerevisiae*, the other targets are each determined from a single study (Karababa *et al.* 2006; Chen *et al*. 2012; Hagiwara *et al*. 2008; Soriani *et al.* 2008). The curation of the ortholog lists may also play a role in the overlap observed. The ortholog list between *S. cerevisiae* and *S. pombe* has been extensively refined (Wood *et al.* 2012), whereas with the other species, orthology was determined using Inparanoid datasets (Sonnhammer and Östlund 2015) and the Fungal Orthogroups Repository (Wapinski *et al.* 2007). Although the overlap with these other species offers an interesting look at conserved elements, it is clearly an incomplete picture.

2.4.3 Prz1 activates target genes functioning in cell wall synthesis and structure

The activation of Prz1 upregulates 15 putative target genes implicated in the biosynthesis and structure of the cell wall (Figure 2.5A; Table 2.1). Among these 15

genes, nine contained a CDRE motif in the promoter while Prz1 occupancy was detected in four (Figure 2.5A; Tables 2.1 and A4). To further investigate this, we first determined whether Δ*prz1* and *prz1OE* strains possessed an altered cell wall structure. The Δ*prz1* and *prz1OE* strains were tested for resistance to cell wall degradation by zymolyase (a β glucanase) relative to their controls. The short duration of the zymolyase assay was ideal because of the reduced fitness exhibited by the *prz1OE* strain (Koike *et al*. 2012; Vachon *et al*. 2013). We found that overexpression of *prz1*$^{+}$ with the *nmt1* promoter confers increased resistance to zymolyase ($p=1.0e^{-4}$), suggesting that the upregulation of these target genes could enhance the strength of the cell wall (Figure 2.5B). In contrast, no change in resistance to zymolyase was observed in the Δ*prz1* strain compared to wild type (Figure 2.5B). We next attempted to identify the putative target genes that could be responsible for the increased resistance to zymolyase in the *prz1OE* strain. Loss of these target genes could potentially result in sensitivity to cell wall perturbing agents. Thirteen deletion strains of the Prz1 putative target genes implicated in cell wall processes were assayed for growth sensitivity to the antifungal micafungin, which inhibits β-1,3-glucan production. The remaining two genes *gas2*$^{+}$ and *bgs1*$^{+}$, the latter being an essential gene, were not available in the Bioneer deletion collection. Among the thirteen deletion strains, only Δ*pvg1*, Δ*pvg5*, and Δ*omh1* were sensitive to micafungin (Figure 2.5C). Both *pvg1*$^{+}$ and *pvg5*$^{+}$ function in the synthesis of pyruvated galactose residues in N-linked glycans (Andreishcheva *et al.* 2004; Yoritsune *et al.* 2013), and *omh1*$^{+}$ encodes a putative α1,2-mannosyltransferase for synthesis of O-linked glycans (Ikeda *et al.* 2009). The Δ*prz1* strain, in addition to not being sensitive to zymolyase, was not sensitive to micafungin (Figure 2.5C). The lack of sensitivity is perhaps due to redundancy in the regulation of

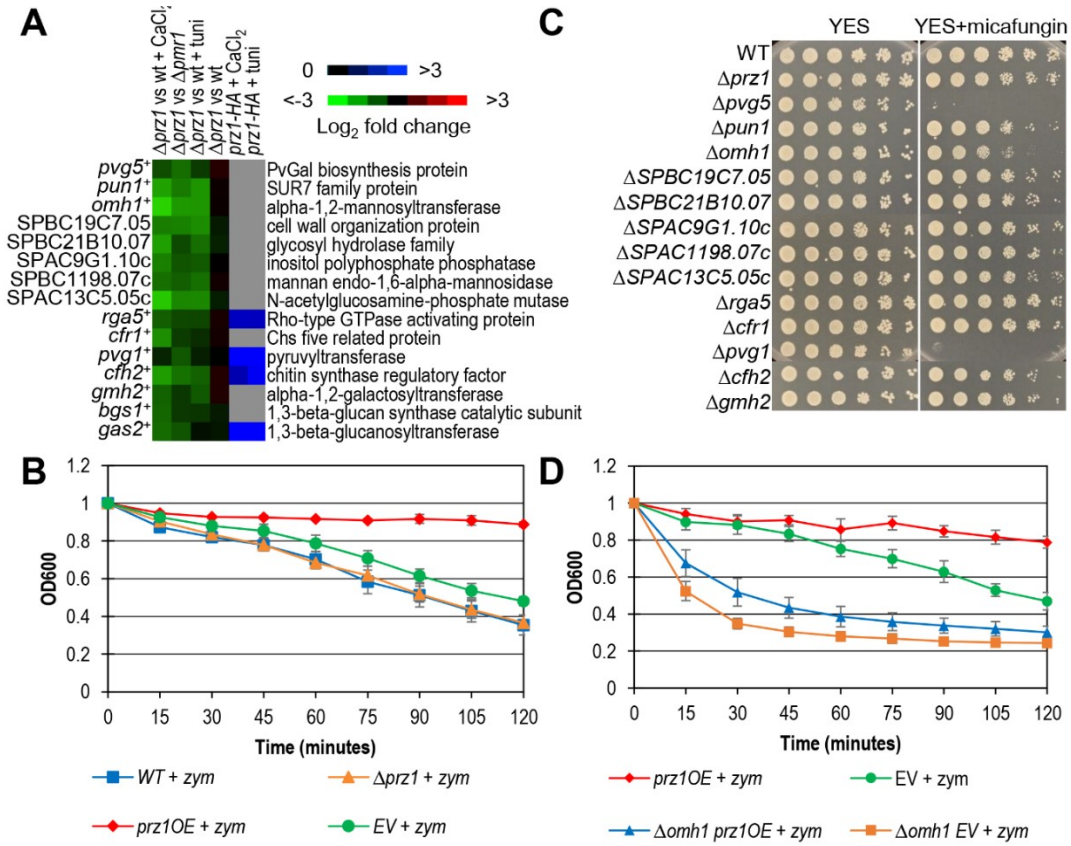

Figure 2.5: Characterization of putative target genes of Prz1 implicated in cell wall-related processes. A) The heat map shows relative expression and Prz1 promoter occupancy for 15 putative target genes annotated to function in cell wall organization or biogenesis. The colour bars indicate relative expression and chIP enrichment ratios between experimental and control strains. All microarray expression and ChIP-chip experiments were performed in replicate with dye reversal. B) Cell wall degradation assays. Wild type and Δ*prz1* strains were grown in liquid YES medium, while *nmt1*-driven *prz1*$^{+}$ or empty vector (EV) were grown in liquid EMM minus thiamine for 18-24 hours. The samples were adjusted to matching cell densities and transferred to test tubes in the presence of 25 U/mL Zymolyase 100T. The samples were shaken at 37°C and OD_{600} readings were taken every 15 minutes to assess the degree of cell wall degradation. Overexpression of *prz1*$^{+}$ caused resistance to the cell wall degrading enzyme zymolyase ($p=1.0e^{-4}$) while *Δprz1* cells did not show significant sensitivity to zymolyase compared to wild type. C) Spot dilution for micafungin sensitivity of deletion strains of the putative Prz1 target genes involved in cell wall-related processes. Exponentially growing wild type and deletion strains were pinned on solid YES medium containing 0.5 µg/mL micafungin and incubated at 30°C for three days. D) Cell wall degradation assays. The *Δomh1* strain was more sensitive to zymolyase treatment than wild-type ($p=1.6e^{-2}$). The zymolyase-resistant phenotype from overexpression of *prz1*$^{+}$ was abrogated by loss of *omh1*$^{+}$ ($p=5.0e^{-4}$). The zymolyase experiments were repeated in triplicate and error bars represent the standard error. The p-values were determined with ANOVA followed by a two-tailed t-test after two hours of zymolyase treatment.

these cell wall target genes by a transcription factor other than Prz1. We then overexpressed *prz1*$^{+}$ with the *nmt1* promoter in the Δ*pvg1*, Δ*pvg5*, and Δ*omh1* strains to determine if the zymolyase resistance exhibited in the *prz1OE* strain was affected by loss of these genes. Consistent with the micafungin assay, the Δ*omh1* strain was more susceptible to degradation by zymolyase than the control after two hours of treatment ($p=1.2e^{-2}$), while the Δ*pvg1* and Δ*pvg5* strains did not show a significant increase in sensitivity (Figures 2.5D and 2.6). Indeed, loss of *omh1*$^{+}$ almost completely abrogated the zymolyase resistance caused by *prz1*$^{+}$ overexpression ($p=5.0e^{-4}$). A similar genetic interaction was also observed in the Δ*pvg1* background except the degree of abrogation was less ($p=6.8e^{-3}$) (Figure 2.6). Together, these results indicate that the cell wall function of Prz1 involves activation of its target genes *omh1*$^{+}$ and *pvg1*$^{+}$.

2.4.4 Prz1 repression of flocculation

The Δ*prz1* strain exhibited a slightly crumbly texture on solid media that is often present in flocculent strains. To determine if Δ*prz1* cells are flocculent, we cultured the strain in liquid YES and EMM with an initial density of ~10^{7} cells/mL for 24 hours. The Δ*prz1* cells, but not wild type, formed large flocs in both EMM and YES media (Figure 2.7A). In contrast, overexpression of *prz1*$^{+}$ did not suppress the flocculation of wild-type cells in flocculation inducing-medium (data not shown). We next examined whether putative target genes in our genome-wide data could be responsible for the constitutive flocculent phenotype of Δ*prz1* cells. Interestingly, several genes implicated in triggering flocculation were upregulated in the Δ*prz1* strain. These upregulated genes (1.6 to 5.3-fold) encoded the flocculins Gsf2 and Pfl3, and the transcription factor Cbf12 which is

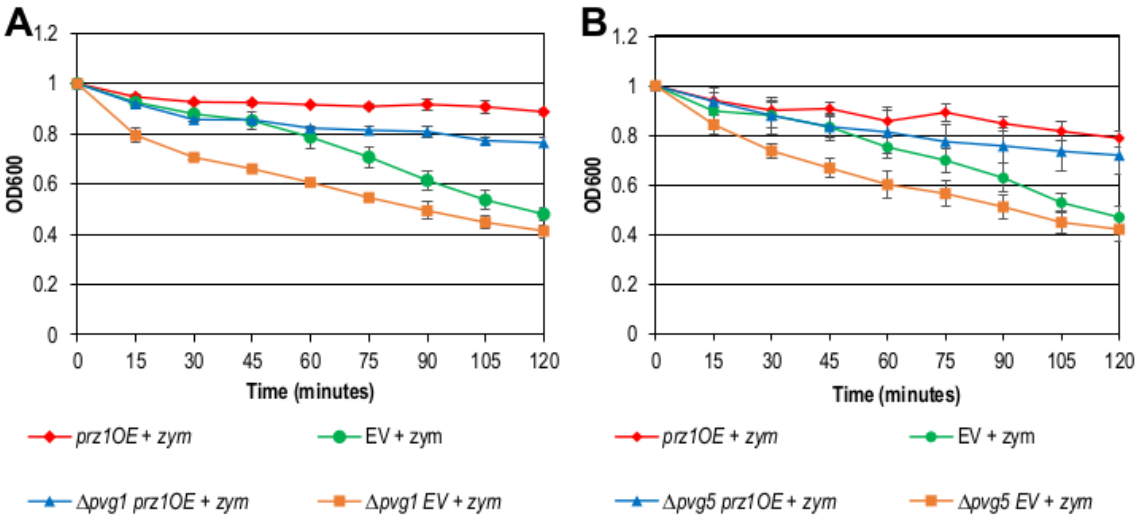

Figure 2.6: Cell wall degradation assays. A) The zymolyase-resistant phenotype from overexpression of *prz1*$^{+}$ was abrogated by loss of *pvg1*$^{+}$ (p=6.8e^{-3}). B) The Δ*pvg5* strain does not suppress the zymolyase-resistant phenotype from overexpression of prz1^{+}. The samples were adjusted to matching cell densities and transferred to test tubes in the presence and absence of 25 U/mL Zymolyase 100T. The samples were shaken at 37°C and OD600 readings were taken every 15 minutes to assess the degree of cell wall degradation. The zymolyase experiments were repeated in triplicate and error bars represent the standard error. The p-values were determined with ANOVA followed by a two-tailed student t-test after two hours of zymolyase treatment.

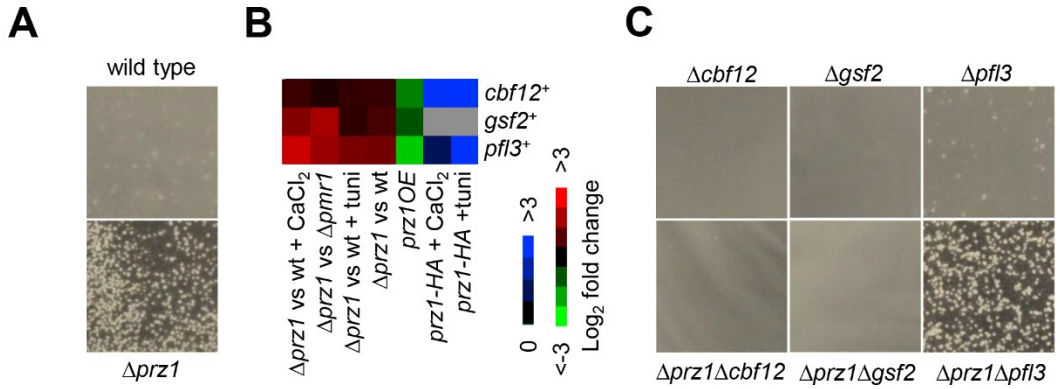

Figure 2.7: Constitutive flocculation of the Δ*prz1* strain. A) Wild type and the Δ*prz1* strain were grown at an initial cell density of ~10^{7} cells/mL in liquid YES medium for 24 hours at 30°C and assayed for flocculation. B) Negative regulation of flocculation genes by Prz1. The heat map shows relative expression and Prz1 promoter occupancy for the flocculation genes *cbf12*$^{+}$, *gsf2*$^{+}$, and *pfl3*$^{+}$. The colour bars indicate relative expression and chIP enrichment ratios between experimental and control strains. All microarray expression and ChIP-chip experiments were performed in replicate with dye reversal. C) The Δ*prz1* flocculation phenotype was abolished by loss of *cbf12*$^{+}$ or *gsf2*$^{+}$. Cells were assayed for flocculation as described for Figure 2.7A.

known to activate *gsf2*$^+$ (Převorovský *et al.* 2015; Kwon *et al.* 2012) (Figure 2.7B). In addition, these three genes were downregulated in the *prz1OE* strain and the promoters of *pfl3*$^+$ and *cbf12*$^+$ were bound by Prz1 in both $CaCl_2$ and tunicamycin treatments (Figure 2.7B). These results suggest that Prz1 inhibits flocculation by repression of *gsf2*$^+$, *pfl3*$^+$, or *cbf12*$^+$. To further confirm this hypothesis, we examined whether the constitutive flocculent phenotype of the Δ*prz1* strain in YES medium could be abrogated in a Δ*gsf2*, Δ*pfl3,* or Δ*cbf12* genetic background. Indeed, we discovered that loss of *gsf2*$^+$ or *cbf12*$^+$, but not *pfl3*$^+$ could abrogate the constitutive flocculation observed in Δ*prz1* cells (Figure 2.7C).

2.5 Discussion

In this study, we substantially expanded the target gene list and implicated new functional roles for the calcineurin-responsive transcription factor Prz1 in *S. pombe*. Moreover, we presented genetic evidence that link putative target genes to these new functions of Prz1. Our results also demonstrate that identification of target genes by genome-wide approaches requires that the transcription factor be active. Transcriptome profiling of the Δ*prz1* strain grown in rich medium did not identify many direct target genes of Prz1. We used several inducing conditions that promote Prz1 activity including chemicals (Ca^{2+} and tunicamycin), overexpression of *prz1*$^+$, and the Δ*pmr1* genetic background. Both Ca^{2+} and tunicamycin and have been shown to activate a CDRE-regulated reporter, and Ca^{2+} has also been shown to cause Prz1 to translocate to the nucleus (Hirayama *et al.* 2003; Deng *et al*. 2006). Systematic overexpression of yeast transcription factors, combined with transcriptome profiling, has been used effectively to

identify direct target genes (Chua *et al.* 2006; Vachon *et al*. 2013, Chua 2013). The *prz1OE* strain displays reduced fitness, which is common for transcription factors overexpressed in fission yeast (Vachon *et al*. 2013). This reduced fitness is likely caused by increased promoter occupancy and aberrant expression of target genes. When overexpressed, Prz1 is still largely localized in the cytoplasm (Hirayama *et al.* 2003). Despite this, Prz1 overproduction allows some of the transcription factors to override the normal cytoplasmic retention signals and enter the nucleus, resulting in differential expression in a large number of putative target genes (893 upregulated and 532 downregulated by more than 2-fold).

2.5.1 Genetic activation of transcription factors

In addition, Prz1 activation was observed in the Δ*pmr1* genetic background. The *pmr1*$^{+}$ gene encodes a Golgi P-type Ca^{2+}/Mn^{2+}-ATPase which functions to reduce abnormally high levels of cytosolic Ca^{2+} (Cortés *et al*. 2004). Therefore, loss of *pmr1*$^{+}$ is expected to cause elevated cytosolic Ca^{2+} relative to wild type and result in the downstream activation of Prz1. Our results show that nuclear localization of Prz1-GFP was increased in Δ*pmr1* cells compared to unperturbed wild-type cells (Figure 2.1). Although the Prz1-GFP nuclear localization in Δ*pmr1* cells was less than wild-type cells treated with Ca^{2+} or tunicamycin, the putative target genes of Prz1 could still be recovered by comparing the transcriptome profiles of Δ*pmr1* and Δ*prz1* strains (Figure 2.2). Interestingly, synthetic lethality is observed in the Δ*pmr1* Δ*prz1* double mutant (Ryan *et al.* 2012) indicating that Prz1 activity is required in the Δ*pmr1* strain. This observation is intriguing as it suggests that synthetic-lethal interactions could be used to

identify genetic backgrounds that contain transcription factors in their active state (genetic activation). Subsequently, the comparison of transcriptomes between the transcription factor deletion strain and a deletion strain with which it shares a synthetic-lethal interaction, could conceivably identify direct target genes. We are currently exploring whether this approach is indeed effective in identifying target genes of transcription factors in *S. pombe*.

2.5.2 Prz1 cellular functions

The annotated functions of the positively-regulated 165 putative target genes of Prz1 align well with certain functions of the fungal Crz1 orthologs: ion homeostasis and transport, lipid metabolism, and cell wall biosynthesis. In *S. pombe*, functional enrichment was only detected for genes implicated in reproduction and cell wall organization or biogenesis. There were 15 putative target genes of Prz1 that have a role in cell wall processes, six of which have orthologs in *S. cerevisiae*. These genes are implicated in β-glucan synthesis (*bgs1+/FKS1* and *rga5+*/*SAC7*), mannosidase activity (SPBC1198.07c/*DFG5*), cell wall integrity (*pun1+/PUN1*), as well as chitin deposition (SPBC19C7.05/*RCR1*) and transglycosylation (SPBC21B10.07/*UTR2*). In contrast, two *S. pombe*-specific target genes ($pvg1^+$ and $pvg5^+$) were involved in the synthesis of pyruvylated galactose residues which are not found in the cell wall of *S. cerevisiae* (Andreishcheva *et al.* 2004; Yoritsune *et al.* 2013). The upregulation of $omh1^+$, which encodes a putative mannosyltransferase, and $pvg1^+$ by $prz1^+$ overexpression contributes to the zymolyase-resistant phenotype of the *prz1OE* strain (Figures 2.5 and 2.6).

In addition, 33 target genes implicated in reproduction were identified as positively-regulated by Prz1. These genes involved in reproduction are consistent with the decreased mating efficiency observed in Δ*prz1* mutants (Sun *et al.* 2013). In *S. cerevisiae*, Crz1 is required for survival in prolonged exposure to mating pheromones (Stathopoulos and Cyert 1997), but pheromone genes have not been identified as targets of Crz1. The function of Prz1 in the mating process is likely different since very few of the target genes have orthologs in *S. cerevisiae* (Table 2.1). Interestingly, we detected Prz1 promoter occupancy of *ste11*$^{+}$, which encodes the primary transcriptional activator of the mating response (Sugimoto *et al.* 1991).

2.5.3 Prz1 binding motif

Our expanded list of 165 putative target genes upregulated by Prz1 identified a CDRE motif in 91 promoters similar to the 5'-AGCCTC-3' motif found by Deng *et al.* (2006). This motif is also similar to the *S. cerevisiae* CDRE motif (5'-TG(C/A)GCCNC-3') (Stathopoulos and Cyert 1997). The apparent conservation in binding specificity of Crz1 and Prz1 indicates the possibility of heterologous complementation. To test this, we overexpressed *CRZ1* with the *nmt1* or *nmt41* promoter in the Δ*prz1* strain. In contrast to *prz1*$^{+}$ overexpression, heterologous overexpression of *CRZ1* did not cause reduced fitness or suppress the calcium sensitivity of the Δ*prz1* strain (data not shown). Transcriptome profiling of *nmt1*-driven *CRZ1* in the Δ*prz1* strain did not result in differential regulation of the Prz1 target genes. The inability of Crz1 to regulate Prz1 target genes may be due to the absence of binding to the CDRE motifs or required trans-acting factors. In contrast,

the *C. albicans* Crz1 was able suppress the Ca^{2+} sensitivity of the *S. cerevisiae* Δ*crz1* strain, as well as drive expression of the CDRE-reporter (Karababa *et al.* 2006).

2.5.4 Gene repression by Prz1

We have also uncovered a novel repressive role of Prz1 in flocculation. Loss of *prz1*$^+$ causes constitutive flocculation in high-density cultures and the induction of both the transcription factor gene *cbf12*$^+$ and the dominant flocculin gene *gsf2*$^+$ (Figures 2.7A and B). The constitutive flocculation is dependent on the presence of *cbf12*$^+$ and *gsf2*$^+$ (Figure 2.7C). Prz1 promoter occupancy was also detected for *cbf12*$^+$ and the *pfl3*$^+$ flocculin gene (Figure 2.7B). Although CDRE motifs were not detected in the promoters of these genes, five copies of the Ca^{2+}-dependent response element (5'-CAACT-3') were present in the *cbf12*$^+$ promoter. Prz1 has been shown to bind to this motif in the *ncs1*$^+$ promoter (Hamasaki-Katagiri and Ames 2010). The repressive flocculation function of Prz1 and the Ca^{2+}-dependent response element have not been discovered in other fungal Crz1 orthologs.

Previous studies on Prz1 orthologs have predominantly focused on positively-regulated functions and target genes. One exception was three genes identified as negatively regulated by *C. glabrata* Crz1 (Chen *et al.* 2012). In *A. fumigatus*, 31 genes were also identified as being downregulated in response to calcium treatment, and some may represent direct targets of CrzA (Soriani *et al.* 2008). The low number of identified negatively-regulated target genes of Prz1 orthologs could be the result of limitations in previous studies, which do not contain genome-wide binding data.

The repression of target genes by Prz1 could be the result of *S. pombe*-specific rewiring of the transcriptional-regulatory network due to an alteration in the amino acid sequence of the transcription factor. In contrast to *S. cerevisiae* Crz1, *S. pombe* Prz1 does not contain a polyglutamine tract domain, which is often associated with transcriptional activation (Hirayama *et al.* 2003). It could be the absence of this domain that provides Prz1 with its transcriptional repressive function. Interestingly, Schaefer *et al.* (2012) observed that considerably fewer *S. pombe* genes (3) compared to *S. cerevisiae* genes (79) contain this domain. In addition, we examined whether the repressed putative targets of Prz1 could be the result of transcriptional interference where a transcribed gene can repress the transcription of the adjacent gene (Martens *et al.* 2004). Among the 92 negatively-regulated putative target genes of Prz1, only 13 (14.1%) are located adjacent to a putative activated target gene. This indicates that the vast majority of putative negatively-regulated target genes of Prz1 are not a result of transcriptional interference. One notable example, SPAC513.07, which encodes a flavonol reductase, is negatively regulated by Prz1 in *S. pombe*, but its orthologs are activated by Crz1 in *S. cerevisiae*, *C. albicans*, and *C. glabrata*. This may indicate a rewiring of the transcriptional regulation of this gene between fungal species. The specific mechanism of Prz1-mediated negative regulation remains unknown, and more experimentation will be needed to determine if there is nucleosome remodeling occurring at these sites or some undiscovered cofactor involved.

2.5.5 Conserved Crz1 targets

Our genome-wide analysis of Prz1 has uncovered gene regulation in conserved and species-specific functions among fungal Crz1 orthologs. Preliminary comparison with other Crz1 target genes among different fungi shows substantial rewiring within the transcriptional-regulatory network controlling calcineurin-mediated processes. This rewiring is evident even in well conserved processes such as cell wall biogenesis, where distinct fungi accomplish a similar function by positive regulation of different target genes. Moreover, this study revealed that the calcineurin-mediated transcriptional-regulatory network of *S. pombe* has undergone substantial rewiring to include negative regulation of target genes implicated in species-specific processes such as flocculation.

Chapter Three: **Genetic interactions of *S. pombe* transcription factors**

Kate Chatfield-Reed and Gordon Chua

This chapter was entirely my own work, although it uses strains constructed in the lab and previously published in Vachon *et al.* (2013). The contents of this chapter are currently being assembled for submission to *G3*.

3.1 Abstract

The interactions of transcription factors and their target genes occur in a complex regulatory network. Transcription factors regulate multiple target genes, and target genes can be regulated by multiple transcription factors. Negative genetic interactions capture relationships between genes by identifying pairs of mutants that are sicker than expected when combined. A synthetic genetic array (SGA) screen was used to map novel interactions between 38 query and 92 array transcription factor deletion strains in *S. pombe*. The screen identified 48 negative interactions, most of which were novel. These negative interactions suggest functional redundancy between the two transcription factors due to overlapping targets, or negative interactions between the downstream targets of transcription factors. Negative genetic interactions between a transcription factor and other genes can reveal their biological function, or potentially be used to identify backgrounds that result in the activation of the transcription factor. A full genome SGA screen of the calcineurin-responsive transcription factor Prz1 detected 62 negative interactions. We tested the activity of Prz1 through fluorescence microscopy and expression microarrays to see if two of the 62 negative interactions could act as genetic

activators of the transcription factor. While the Δ*pmr1* mutant exhibited enhanced Prz1 activity, the Δ*alp31* strain was not able to enhance Prz1 activity over wild-type levels. These experiments show that SGA screens can potentially be used to identify genetic backgrounds that promote activation of the transcription factor.

3.2 Introduction

Full genome deletion analysis revealed that, when assayed in rich media conditions, essential genes comprise only ~20% (Giaever *et al.* 2002) and 26.1% (Kim *et al.* 2010) of the budding and fission yeast genomes, respectively. Genes are often nonessential because they are only needed under specific environmental conditions or because they are functionally redundant with one or more other genes. Chemical and synthetic genetic screens can be used to look for condition-specific function or functional redundancy, respectively, in nonessential genes, which potentially have no visible phenotype (Parsons *et al.* 2006). A synthetic genetic array (SGA) screen tests for functional redundancy between pairs of genes, and buffering between pathways. SGA screens create double mutants in a high-throughput manner by mating single deletion mutants together on high density arrays and selecting for the double deletion progeny (Tong *et al.* 2001). The double deletion mutants are then scored for fitness based on whether they are sicker or healthier than the expected combined fitness of the two single deletions (Tong *et al.* 2001). Sick or lethal combinations are called negative genetic interactions and indicate genes that buffer each other, either directly or through interactions between their pathways. Positive genetic interactions are cases where the combined double deletion is healthier than the expected combined fitness of the two single deletions, such as in some

physical complexes or genetic suppression (Wagih *et al.* 2013). This technique was developed for *S. cerevisiae*, where 75% of the genes have full or partial genetic interaction data (Tong *et al.* 2001; Tong *et al.* 2004; Costanzo *et al.* 2010). This includes mostly nonessential genes as well as some temperature-sensitive essential alleles. These studies can be used to uncover unknown gene function or physical interactions by looking at genes that share similar genetic interaction profiles (Tong *et al.* 2004). The data also shows relationships between different biological processes based on the genetic interactions between genes annotated with different biological functions (Costanzo *et al.* 2010). This technique has been adapted in several other organisms including *S. pombe*, where ~50% of the genome has partial genetic interaction data (Roguev *et al.* 2007; Dixon *et al.* 2008; Ryan *et al.* 2012).

SGA was used to explore the transcription factor interaction network in *S. cerevisiae* (Zheng *et al.* 2010). Zheng *et al.* (2010) used the epistatic miniarray profile approach to look at genetic interactions between general and sequence-specific transcription factors. This approach applies the SGA methodology to a small functionally-related group of genes to look at connections within the network. The sequence-specific transcription factors had fewer genetic interactions than the general transcriptional machinery, and these genetic interactions were enriched for negative interactions over positive interactions. This indicates that sequence-specific transcription factors tend to work in parallel instead of cooperatively or in sequence (Zheng *et al.* 2010). Sequence-specific transcription factors that shared target genes were more likely to share a negative interaction. Of the 49 pairs of sequence-specific transcription factors that shared a significant number of targets, 10 pairs had negative interactions (Zheng *et*

al. 2010). Zheng *et al.* (2010) concluded that negative interactions between sequence-specific transcription factors were not generally the result of genetic interactions between their targets, as transcription factors that shared negative interactions did not have an enrichment of negative interactions between their target genes. The number of genetic interactions increased among the general transcription factors (Zheng *et al.* 2010). Sequence-specific transcription factors were also more likely to interact with a general transcription factor than with a second sequence-specific transcription factor. This is likely because general transcription factors affect many more processes than most sequence-specific transcription factors. This supports the cooperative role between general and sequence-specific transcription factors in regulating gene expression (Zheng *et al.* 2010). Unpublished work from the same group indicated that the same trends held for *S. pombe* transcription factors.

This study looks at the genetic interactions among the sequence-specific transcription factors in *S. pombe.* Thirty-eight query transcription factor deletion strains were mated to 92 array transcription factor deletion strains to uncover genetic interactions among the transcription factors. These screens uncover areas of functional redundancy between the transcription factors. A full genome screen was also performed on *prz1*$^{+}$, which encodes a calcineurin-responsive transcription factor, to identify genes that genetically interact, share functional redundancy, and can act as candidates for genetic activation of the transcription factor. The transcription factor SGA screens uncovered both novel and previously-identified negative interactions between *S. pombe* transcription factors. The *prz1*$^{+}$ whole genome screen also identified genetic interactions with the deletion mutants of the genes encoding the calcium transporter Pmr1 and the β-tubulin

folding cofactor A Alp31. These deletion strains, that were synthetic sick with the Δ*prz1* strain, were tested as candidates for genetic activation of Prz1 (Maeda *et al.* 2004; Radcliffe *et al.* 2000). These experiments show that negative genetic interactions are a potential source for deletions that cause transcription factor activation, but cannot be universally applied.

3.3 Materials and methods

3.3.1 Yeast strains, media, and general methods

Table A6 contains a list of yeast strains used in this study. Strains were grown on YES medium and supplemented, when required, with adenine (225 mg/L), leucine (225 mg/L), and uracil (225 mg/L). Plates used in the SGA screen were also supplemented with histidine (225 mg/L) because of an additional auxotrophic strain used as a control. The drugs genetecin (Kan) and nourseothricin (Nat) were used for selection at 150 mg/L and 100 mg/L, respectively. SPAS media was used for mating and supplemented with adenine (45 mg/L), leucine (45 mg/L), uracil (45 mg/L), and histidine (45 mg/L) in the SGA screens. Standard genetic and molecular methods were performed as described in Moreno *et al.* (1991).

3.3.2 Nat-resistance cassette switch

The Nat-resistant strains were made by PCR amplification of the Nat-resistance cassette, which shares sequence homology in the outer regions with the Kan-resistance cassette. The Nat-resistance cassette was inserted into the Kan-resistant deletion strains via a lithium acetate transformation. Strains were confirmed by checking for the presence

of Nat-resistance and the absence of Kan-resistance, followed by colony PCR. The mating type was switched by mating the Nat-resistance strain to wild type, followed by tetrad dissection to separate and genotype the progeny.

3.3.3 Synthetic genetic array screens

The SGA screen was based on the methodology developed by Dixon *et al.* (2008). In the transcription factor screen, the array strains were knockouts with the transcription factor gene replaced by the Kan-resistance cassette (KanMX6) in a prototrophic background (*972 h*$^{-}$), while in the query strains the transcription factor gene was replaced with the Nat-resistance cassette (NatMX4) in the prototrophic *975 h*$^{+}$. The control for the query strains was the Δ*leu1* mutant which was used to obtain an estimate of the single mutant fitness of the array strains. The procedure was carried out with the Δ*leu1* mutant using the Nat-resistance cassette in the *JK366 h*$^{+}$ background. The Δ*leu1* control was created from the Δ*leu1* in the Bioneer haploid deletion collection v2, and as a result has auxotrophic markers for adenine, leucine, and uracil, that were not present in the other query strains. Since all of the SGA media was supplemented with 225 mg/L of each amino acid and nucleotide, the auxotrophic markers should not affect the fitness unduly. In the Prz1 full genome screen, the array strains were from the Bioneer haploid deletion collection, where the genes are replaced by the Kan-resistance cassette (KanMX4) in a *JK366 h*$^{+}$ background that is auxotrophic for adenine, leucine, and uracil. The Δ*prz1* query strain was made in the *972 h*$^{-}$ background and *prz1*$^{+}$ was replaced with the NatMX4 cassette. The control strain was Δ*leu1* mutant using the Nat-resistance cassette in the *JK366 h*$^{-}$ background.

The screens were performed with an array density of 768 colonies per plate, which was based on a 384 array layout with each array strain present in duplicate. The screens were not performed at a density of 1536 in the early stages of the screen as described in Dixon *et al.* (2008), because the higher density impeded the growth of the colonies. Each array had a border of Δ*his5* to control for spatial bias at the edges of the plate, as well as at least one blank spot. The query and array strains were mated by pinning them one over the other with mixing on SPAS plates with the BM3 BioMatrix Robot (S&P Robotics Inc.). The pins were dipped in sterile water before transferring the array strains to help with the mixing. Once both strains were on the plates the pins were used to gently mix the cells together by repeated contact with the plate. The plates were left at 25°C for 3 days to allow the query and array strains to mate. The plates were then moved to a 42°C incubator for 3 days to select for the mated spores and select against unmated vegetative cells. The spores were pinned onto YES solid medium to recover and left at 30°C for 3 days. The cells were then pinned on YES+Kan+Nat plates to select for recombinants that have both Kan and Nat resistance, which represent the double mutants. In this final step, the two colony replicates were copied to four colonies to give a final array density of 1536 colonies per plate which resulted in four replicates of each double mutant combination. In the transcription factor SGA screen, each array strain was present on the array three times, giving a total of 12 replicates of each double mutant combination at the final step.

The plates were photographed using the spImager-M system (S&P Robotics). The colony sizes were measured and normalized to account for spatial biases that can occur due to competition effects during the protocol. Colonies that are surrounded less densely

because of empty spots or sick mutants on the plate tend to grow larger due to greater availability of nutrients. The screens were also corrected for batch effects, where small variations in factors like media, plate thickness, and humidity can cause the growth of colonies to vary in each screen. The normalized double mutant colony sizes were compared to the colony sizes from the control plates. The double mutants created with the control strain Δ*leu1* were used to obtain a set of mutants that represent the fitness of the single mutant, as the Δ*leu1* should have very little fitness defect in media supplemented with leucine. The fitness scores of the double mutants were determined in relation to these single mutants. In the transcription factor screen, the genes within 200,000 base pairs of the query strain on the chromosome were also removed from consideration. These gene combinations would look like negative genetic interactions, as genetic linkage would make it very unlikely for crossover to occur. None of the transcription factors were within 200,000 base pairs of the $leu1^{+}$ control gene. For the Prz1 full genome screen, the linkage distance was set at 325,000 base pairs from $prz1^{+}$ or $leu1^{+}$, because genetic interactions within this range were strongly enriched for negative interactions. Finally, the four replicates on the plate and across the three replicate experiments were averaged, and scores were also combined for the double mutants which were generated by reciprocal crosses. The cut-offs used to determine a negative or positive genetic interaction were based on interactions that fell more than two standard deviations from the mean value for all of the genetic interaction scores. The final fitness score was based on a multiplicative model, where the single mutant fitness weights were multiplied to generate a predicted double mutant fitness. The array strain single mutant fitness was based on the fitness obtained with that single mutant when crossed to the

Δ*leu1* control, while the query mutant fitness was based on the average fitness for all the array strains crossed with that query mutant. The predicted fitness weight was then subtracted from the double mutant fitness ($W_{ij} - W_i W_j$), where W_{ij} was the observed double mutant fitness, and W_i and W_j were the single mutant fitness values (Wagih *et al.* 2013).

3.3.4 Random spore analysis

Random spore analysis (RSA) was performed to validate some of the negative interactions from the screens. The two strains were mated in 10 µl of sterile water on SPAS plates and incubated for 3 days at 25°C. The patch was checked for the presence of mated spores under light microscopy before being suspended in 1 ml of 0.5% glusalase for 6 hours at 30°C to kill the unmated vegetative cells. The cells were spun down at 3000 RPM for 5 minutes and washed twice in sterile water to remove the glusalase. The resulting cells were diluted by 1/1000 and plated at a ratio of 1:2:2:4 on YES, YES+Kan, YES+Nat, and YES+Kan+Nat solid medium (Dixon *et al.* 2008). The plates were left to grow at 30°C for 3 to 5 days, depending on the growth of the single mutants, before the relative density of colonies on the four plates was compared. Double mutant combinations were considered lethal when fewer than 10 colonies were present on the YES+Kan+Nat plates, while a low colony density relative to the single mutant fitness was considered a moderate negative interaction. Mild genetic interactions were scored when the double mutant colony density was high, but could still be recognized as lower than the single mutants by blind selection.

3.3.5 Tetrad dissection

Tetrad analysis was performed on a Zeiss AxioScope A1 tetrad microscope (Zeiss, Thornwood, NY). Tetrads were selected and the asci were left to break down for 3-5 hours at 37°C. The tetrads were split and left to grow for ~5 days at 30°C.

3.3.6 Microarray expression profiling

The wild-type and deletion mutants were grown concurrently in 100 ml liquid YES at 30°C for 16-20 hours to a matching cell density of ~8×10^6 cells/mL in experimental and control cultures. The mRNA sample preparation, Cy5 and Cy3 labeling, hybridization to 8 × 15,000 Agilent *S. pombe* expression microarrays, and scanning were carried out as described in detail in Kwon *et al.* (2012). All microarray experiments were performed with a single dye-swap and normalized in the R Limma package with Lowess scaling (Smyth and Speed 2003), and the eBayes method was used to combine the replicates by fitting to a linear model (Smyth 2004). Hierarchical clustering was performed using the uncentered Pearson correlation and average linkage with Cluster 3.0 (Eisen *et al.* 1999), while the tree image was generated using Java Treeview (Saldanha 2004).

3.3.7 Fluorescence microscopy

The intracellular localization of natively-regulated Prz1-GFP was determined in wild type and several deletion backgrounds. Cells were grown and treated as described for the expression microarray experiments. Images of live *prz1-GFP* cells were captured

with a Zeiss Imager Z1 microscope and AxioCam MRM digital camera (Zeiss, Thornwood, NY). The nuclear localization was determined by visual inspection.

3.4 Results

3.4.1 SGA screen design

An SGA screen of the sequence-specific transcription factors was performed in triplicate. Ninety-two nonessential transcription factor deletion mutants were used as the array strains and 38 of these 92 deletions were also selected as query strains (Table A7). The query genes were involved in a range of biological processes including the cell cycle, ion homeostasis, reproduction, stress response, and several with no annotated function. Twelve of eighteen DNA-binding domains found among the sequence-specific transcription factors in *S. pombe* were represented in the products of the query genes. The 38 query strains were crossed against the 92 array strains to produce a potential 3496 genetic interactions (38×92) among the *S. pombe* transcription factors. This was reduced to 2714 potential interactions when the double mutants obtained from reciprocal crosses were combined, and double mutants that were linked or self-crossed were omitted (Figure 3.1). This dramatically increased the number of genetic interactions available from previous whole genome SGA studies that looked at 10×10 and 27×37 interactions among the sequence-specific transcription factors (Roguev *et al.* 2007; Ryan *et al*. 2012). These screens resulted in 39 and 824 potential genetic interactions, of which 34 and 554, respectively, overlap with the 2714 potential genetic interactions covered in this study (Roguev *et al.* 2007; Ryan *et al*. 2012). This screen adds a considerable number of transcription factor genetic interactions to those screened in previous works.

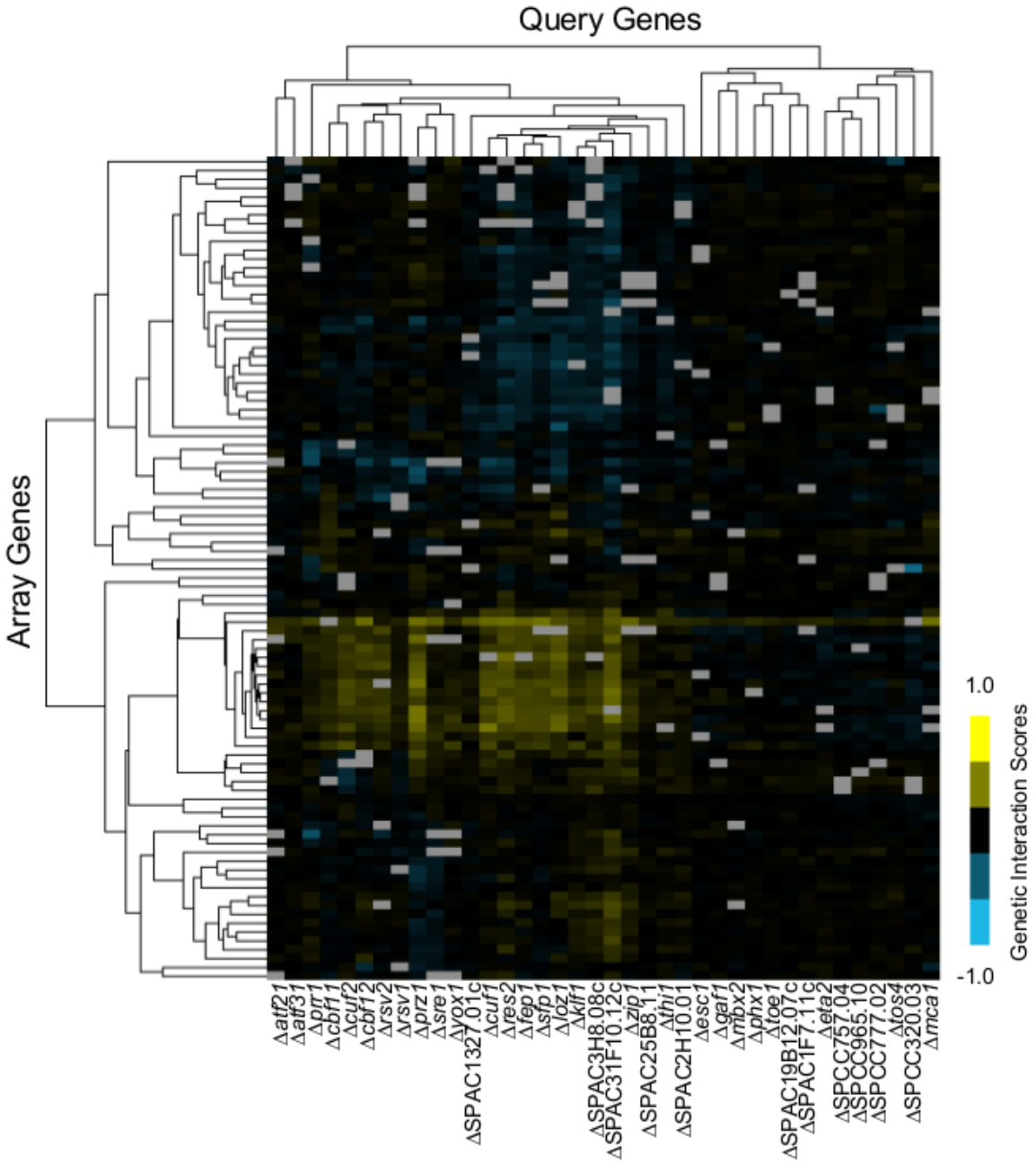

Figure 3.1: A heatmap of the genetic interactions between the 38 query and 92 array transcription factor deletion strains. The interaction scores are mapped to colours as indicated by the colour bar at the bottom right, with negative scores in cyan and positive scores in yellow. The grey squares indicate interactions that were omitted due to the possibility of gene linkage. All of the screens were performed in triplicate, with each array strain at three different locations on the plate.

3.4.2 Negative interactions between S. pombe transcription factors

There were 48 negative genetic interactions using a cut-off of -0.185 (Table A8), which was used because it was two standard deviations below the mean. Of the 48 negative genetic interactions, only eight of these negative interactions were also tested in the genome-wide screen by Ryan *et al*. (2012). The Ryan *et al.* (2012) screen had a total of 29 negative interactions among the transcription factors, but only 12 were also crossed in the present study. Three of the overlapping negative interactions agreed between the two studies (Ryan *et al.* 2012). The conserved negative genetic interactions were between *tos4*$^+$ and *res2*$^+$, *yox1*$^+$ and *sep1*$^+$, and *prz1*$^+$ and *sep1*$^+$ (Ryan *et al.* 2012).

The transcription factor Res2 is part of the MBF transcription factor complex responsible for activating S-phase primarily in the meiotic cell cycle (Zhu *et al.* 1997). The MBF complex detaches from the DNA of its target genes in response to DNA damage, although this seems to be through the essential MBF transcription factor Cdc10 (Ivanonva *et al.* 2013). Tos4 is not well characterized in *S. pombe*, but its *S. cerevisiae* ortholog is involved in the DNA damage response, and it is regulated by the MBF complex in both yeasts (Basto de Oliveira *et al.* 2012; Aligianni *et al.* 2009). The regulation of *tos4*$^+$ by MBF indicates that both transcription factors are normally active during the mitotic/meiotic cell cycle, and this common role could explain the negative interaction between the two genes.

Yox1 is another member of the MBF complex that negatively regulates genes involved in the G1/S transition of the cell cycle (Aligianni *et al.* 2009). The transcription factor Sep1 is involved in activating genes in the M phase of the cell cycle (Rustici *et al.* 2004). The double mutant would be expected to have a higher expression of genes

involved in the G1/S transition of the cell cycle and lower expression of genes involved in the M phase. This extra level of disruption to the cell cycle could result in an increased double mutant fitness defect. Cell cycle transcription factors often work in cascades, and disrupting two points of regulation would increase the likelihood of catastrophic errors.

Prz1 is a calcineurin-responsive transcription factor that plays a role in cell wall biogenesis and reproduction (Sun *et al.* 2013). Prz1 regulates multiple processes, which makes genetic interactions with Prz1 harder to characterize, as they could be the result of its role in the cell wall, ion homeostasis, or reproduction. The *sep1*$^{+}$/*prz1*$^{+}$ negative interaction may be the result of problems with cytokinesis or cell polarity as both Δ*sep1* and Δ*ppb1* (the gene encoding calcineurin which is an upstream regulator of Prz1) have septation defects and hyphal growth (Yoshida *et al.* 1994; Ribár *et al.* 1999).

There were several transcription factors that had a higher number of interactions such as *loz1*$^{+}$ (zinc ion homeostasis), *scr1*$^{+}$ (cellular response to glucose starvation), and SPAC3F10.12c (unknown function), each of which had eight or more negative genetic interactions (Figure 3.1) (Corkins *et al.* 2013; Tanaka *et al.* 1998; Wood *et al.* 2012). This could indicate that some genes interact more readily than others. Eighteen of the 48 negative interactions were tested by RSA. The interactions tested included the eight strongest negative interactions, the reciprocal interactions, the conserved interactions, as well as seven other interactions from the top half of the scores. The relative growth after mating was compared between the wild type, single mutant, and double mutant progeny. Photographs were taken after 3-5 days, depending on the growth of the single mutants. Strikingly, the RSA confirmed 16/18 negative interactions identified by our SGA screen (Table 3.1 and Figure 3.2). The negative interactions often had one single mutant that

Table 3.1: Comparison of the interaction scores among the *S. pombe* transcription factors measured by the SGA screen to the strength of the interaction observed by RSA for the 16 confirmed negative genetic interactions.

Query Strain	Array Strain	Interaction Score	RSA Score
Δ*prr1*	Δ*scr1*	-0.37	Lethal Interaction
Δ*cuf1*	Δ*scr1*	-0.33	
Δ*prr1*	Δ*atf21*	-0.25	
Δ*SPAC3F10.12c*	Δ*scr1*	-0.25	
Δ*SPCC320.03*	Δ*SPAC3C7.04*	-0.58	Moderate Negative Interaction
Δ*loz1*	Δ*sre2*	-0.43	
Δ*prz1*	Δ*sep1*	-0.41	
Δ*prr1*	Δ*SPCC1393.08*	-0.38	
Δ*SPAC3F10.12c*	Δ*mug151*	-0.32	
Δ*res2*	Δ*ace2*	-0.30	
Δ*loz1*	Δ*sep1*	-0.27	
Δ*res2*	Δ*tos4*	-0.25	
Δ*SPAC3F10.12c*	Δ*SPAC3H8.08c*	-0.22	
Δ*prz1*	Δ*SPBC56F2.05c*	-0.34	Mild Negative Interaction
Δ*cbf12*	Δ*scr1*	-0.31	
Δ*cbf12*	Δ*ace2*	-0.24	
Δ*rsv1*	Δ*scr1*	-0.41	No Interaction
Δ*yox1*	Δ*sep1*	-0.20	

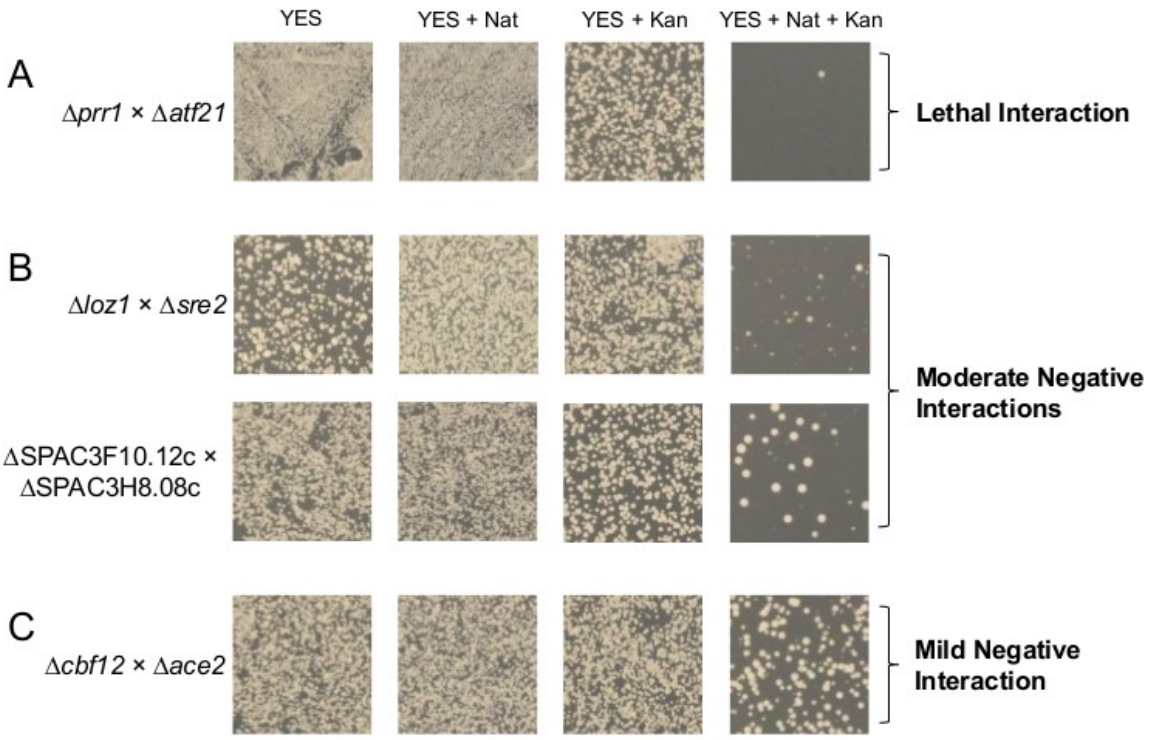

Figure 3.2: Examples of lethal, moderate negative, and mild negative interactions by RSA. A) A lethal interaction between Δ*prr1* and Δ*atf21*. Interactions were considered lethal if there were fewer than 10 colonies on the YES+Kan+Nat plate containing the double mutant. B) Two examples of moderate negative interactions one between Δ*loz1* and Δ*sre2*, and another between Δ*SPAC31F10.12c* and Δ*SPAC3H8.08c*. C) A mild negative interaction between Δ*cbf12* and Δ*ace2*. Negative interactions were considered mild when the colony density on the YES+Kan+Nat plate was high, but still easily chosen as the lowest density plate without prior knowledge of which plates contained which drugs.

was considerably sicker than the other. Interestingly the negative interaction between *yox1*$^{+}$ and *sep1*$^{+}$, which was also observed by Ryan *et al.* (2012), failed to confirm by RSA. The other negative interaction that failed to confirm was between the highly related glucose responsive transcription factors Scr1 and Rsv1 (Saitoh *et al.* 2015).

3.4.3 Positive interactions between S. pombe transcription factors

The transcription factor SGA screen detected 99 positive interactions using a cut-off of 0.204 (Table A9), which was used because it was two standard deviations above the mean. Of the 554 putative transcription factor genetic interactions tested by Ryan *et al.* (2012) 15 were positive. Nine of those were included in our screen, while six of our positive interactions were included in their screen. The overlap of the included, or cross study, interactions only yielded one conserved positive interaction, the interaction between *cuf2*$^{+}$ and *res1*$^{+}$ (Ryan *et al.* 2012). The Cuf2 transcription factor negatively regulates genes during meiosis and has a meiotic defect (Ioannoni *et al.* 2012). The Res1 transcription factor is a member of the MBF complex and is involved in the activation of mitotic G1/S phase genes, whereas its paralog Res2 is associated with meiosis (Caligiuri and Beach 1993). It is possible that the replacement of Res1 with Res2 in the MBF complex in the Δ*res1* strain rescues some of the mating defects associated with the Δ*cuf2* strain by improving the efficiency of meiosis. There was also a genetic interaction that strongly disagreed between the two studies, which was *fep1*$^{+}$ with *php5*$^{+}$, as it displayed a positive interaction in this screen, and a negative interaction in the Ryan *et al.* (2012) screen. The *fep1*$^{+}$ gene encodes a transcription factor involved in iron ion homeostasis which negatively regulates the expression of *php4*$^{+}$. Php4 is a member of the CCAAT-

binding complex that also includes Php5 (Pelletier *et al.* 2002; Mercier *et al.* 2006). The *fep1*$^{+}$ with *php5*$^{+}$ genetic interaction was not negative, nor noticeably positive, when tested by RSA (data not shown). Twelve genes had eight or more positive interactions (Figure 3.1), two of which, *loz1*$^{+}$ and SPAC3F10.12c, also had a high number of negative interactions.

3.4.4 Comparison with S. cerevisiae transcription factors

One aim of mapping the genetic interactions in yeast is to establish a conserved interaction network across species. The transcription factor genetic interaction network has been partially covered in *S. cerevisiae* using SGA (Zheng *et al.* 2010). Thirty-eight of the *S. cerevisiae* sequence-specific transcription factor genes had one or more orthologs present in the *S. pombe* transcription factor array strains (Zheng *et al*. 2010; Wood *et al.* 2012). Some of the transcription factors from one yeast had multiple orthologs in the other, which expanded the 38 transcription factors to a 51×51 matrix containing 1228 potential interactions for comparison. Using the cut-off selected by Zheng *et al*. (2010), there were 18 negative interactions and zero positive interactions among the *S. cerevisiae* transcription factors with *S. pombe* orthologs. This increased to 28 possible overlapping negative interactions when the genetic interactions in transcription factors with multiple orthologs were accounted for. These genetic interactions overlapped poorly between the two screens with only one conserved interaction. The *S. cerevisiae* transcription factor genes *MIG1* and *MIG2* shared a negative interaction, which is orthologous to the negative genetic interaction between *rsv1*$^{+}$ and *scr1*$^{+}$ in *S. pombe*, an interaction that failed to confirm by RSA. This low level of overlap suggests that the transcription factor genetic

interaction network between species has been substantially rewired. Not only were the specific genetic interactions poorly conserved, but the trend of fewer negative than positive interactions was also not observed in the *S. pombe* transcription factor SGA data.

3.4.5 Prz1 full genome screen

Next we performed a full genome screen involving non-transcription factor genes to identify functional redundancy and genetic activation of the transcription factor Prz1. The deletion mutant of the gene encoding the calcineurin-responsive transcription factor Prz1 was crossed against the Bioneer haploid deletion collection v2 (Hirayama *et al*. 2003; Kim *et al.* 2010). This resulted in 2682 interactions, once the genes that were linked with *prz1*$^{+}$ and the *leu1*$^{+}$ control were omitted. Genetic interactions that were more than three standard deviations away from the mean were classified as high stringency interactions, and those that were between two and three standard deviations away from the mean were classified as lower stringency interactions. The negative interaction cut-offs were -0.301 and -0.200 for the high and low stringency, respectively. There were 62 negative interactions, 17 of which were considered high stringency (Table 3.2). These negative interactions were enriched for several membrane components as well as the biological process dolichol-linked oligosaccharide biosynthetic process ($p=5.1e^{-3}$) (Table 3.3). These genetic interactions matched well with the role of Prz1 in cell wall organization or biosynthesis, as creation of cell wall glycoproteins occurs in the endoplasmic reticulum through the transmembrane movement of dolichol-linked oligosaccharides (Helenius and Aebi 2002). The negative interactions were enriched for genes in the endoplasmic reticulum membrane with ten genes localized to that component

Table 3.2: The 17 genes with high stringency negative genetic interactions with *prz1*$^{+}$.

Gene	Interaction Score	Biological Process
SPAC2E1P3.05c	-0.61	Unknown
ctr4^{+}	-0.54	Copper ion import across the plasma membrane
mug134^{+}	-0.46	Regulation of phosphoprotein phosphatase activity
alp31^{+}	-0.44	Post-chaperonin tubulin folding pathway
clr2^{+}	-0.44	Chromatin silencing at centromere/rDNA/silent mating-type cassette
pmr1^{+}	-0.41	Calcium/manganese ion transmembrane transport
ppk11^{+}	-0.39	Signaling
rds1^{+}	-0.38	Unknown
SPAC19A8.11c	-0.37	Unknown
arf6^{+}	-0.35	Endoplasmic reticulum to Golgi vesicle mediated transport
spc2^{+}	-0.34	Protein targeting to endoplasmic reticulum
ckb1^{+}	-0.33	Negative regulation of transcription from RNA polymerase II promoter
zfs1^{+}	-0.33	Pheromone-dependent signal transduction involved in conjugation with cellular fusion
vps26^{+}	-0.32	Retrograde transport, endosome to Golgi
atp16^{+}	-0.32	Mitochondrial ATP synthesis coupled proton transport
swi6^{+}	-0.31	Chromatin silencing at centromere/centromere outer repeat region/silent mating-type cassette/telomere
ypa2^{+}	-0.30	Unknown

Table 3.3: The functional enrichment of GO terms among the 62 genes that share negative interactions with *prz1*$^+$ using the Princeton GO term finder (Boyle *et al.* 2004).

Gene Ontology Term	P-value	Gene List
Dolichol-linked oligosaccharide biosynthetic process (GO:0006488)	5.1e^{-3}	*alg9*$^+$, *alg12*$^+$, *alg10*$^+$
Endoplasmic reticulum membrane (GO:0005789)	5.5e^{-4}	*pmr1*$^+$, *mga2*$^+$, SPAC1071.04c, *sur2*$^+$, *ccr1*$^+$, *pdt1*$^+$, *alg10*$^+$, *alg9*$^+$, SPAC3H5.08c, SPCC1795.10c
Nuclear outer membrane-endoplasmic reticulum membrane network (GO:0042175)	1.1e^{-3}	*pmr1*$^+$, *mga2*$^+$, SPAC1071.04c, *sur2*$^+$, *ccr1*$^+$, *pdt1*$^+$, *alg10*$^+$, *alg9*$^+$, SPAC3H5.08c, SPCC1795.10c
Endoplasmic reticulum part (GO:0044432)	3.3e^{-3}	*pmr1*$^+$, *mga2*$^+$, SPAC1071.04c, *sur2*$^+$, *ccr1*$^+$, *pdt1*$^+$, *alg10*$^+$, *alg9*$^+$, SPAC3H5.08c, SPCC1795.10c
Bounding membrane of organelle (GO:0098588)	6.6e^{-3}	*pmr1*$^+$, *mga2*$^+$, SPAC1071.04c, *sur2*$^+$, *ccr1*$^+$, *pdt1*$^+$, *alg10*$^+$, *alg9*$^+$, SPAC3H5.08c, SPCC1795.10c, *sft2*$^+$, *tom7*$^+$, *arf6*$^+$, *pmc1*$^+$, SPBC25H2.03
Organelle membrane (GO:0031090)	9.5e^{-3}	*pmr1*$^+$, *mga2*$^+$, SPAC1071.04c, *sur2*$^+$, *ccr1*$^+$, *pdt1*$^+$, *alg10*$^+$, *alg9*$^+$, SPAC3H5.08c, SPCC1795.10c, *sft2*$^+$, *arf6*$^+$, *pmc1*$^+$, SPBC25H2.03, *tom7*$^+$, *dsc3*$^+$, *atp16*$^+$, *mpc1*$^+$

(p=5.5e^{-4}). This enrichment was likely due to the disruption of calcium storage in the endoplasmic reticulum, which would be more detrimental to cells without Prz1 (Deng *et al*. 2006). The top ten high stringency negative interactions were tested with RSA and only 4/10 (SPAC19A8.11c, *arf6*$^+$, *rds1*$^+$, *alp31*$^+$) confirmed (data not shown). The ten interactions were also tested by tetrad dissection, where only Δ*pmr1* and Δ*alp31* showed reduced colony sizes for the double mutants. The crosses between Δ*prz1* and Δ*ppk11* generated progeny that only contained kanamycin resistance, indicating that there could be a mating defect. It appears as though the Bioneer strain Δ*ppk11* is homothallic as it

was able to mate to either mating type. The crosses between Δ*prz1* and Δ*rds1* only generated parental ditypes, which usually occurs when genes are linked. However, this was unlikely as the *prz1*$^{+}$ and *rds1*$^{+}$ genes are 878,907 base pairs apart (Wood *et al.* 2012). This could indicate a problem with crossover of genetic material between these two strains.

The positive interaction cut-offs were 0.309 and 0.207 for high and low stringency, respectively. There were 85 positive interactions in the screen, 34 of which were considered high stringency. There was no functional enrichment found among the positively interacting genes using a p-value cut-off of 0.01. Interestingly, positive interactions occurred with three of the four genes in the SGA screen that were part of the CORVET complex, an endosomal tethering complex involved in transport between the Golgi, endoplasmic reticulum, and vacuoles ($p=1.4e^{-2}$) (Peplowska *et al.* 2007). These organelles may affect Prz1 through their role as cellular stores for cytoplasmic Ca^{2+}.

3.4.6 Comparison of Prz1 full genome screens

Many potential *prz1*$^{+}$ interactions were assayed by Ryan *et al.* (2012) as part of a larger screen. Of the 1683 potential interactions between *prz1*$^{+}$ and other genes tested in that screen, 272 were negative interactions and 76 were positive interactions. Our screen identified 62 negative interactions, 39 of which were also measured by Ryan *et al.* (2012). Most of these genes had negative interaction scores in the Ryan *et al.* (2012) screen, though many were not below the cut-off (Figure 3.3A). The two screens shared 14 common negative genetic interactions.

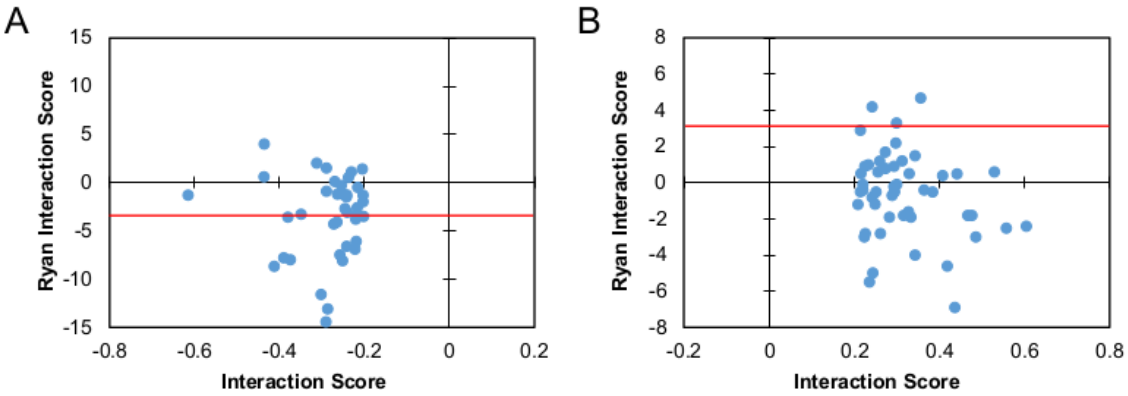

Figure 3.3: Comparison of genetic interactions of *prz1*$^{+}$ from this study and Ryan *et al.* (2012). A) The negative interactions discovered in this study had mostly negative scores in the previous study. Fourteen of the 39 overlapping genetic interactions shown were scored as negative interactions in both. B) The positive interactions do not agree well with the scores obtained in the previous study. Of the 49 overlapping interactions shown only three were considered positive interactions in both. The cut-off scores used by Ryan *et al.* (2012) to determine negative and positive interactions are indicated with red lines.

The positive interactions were far less consistent, with only three shared positive interactions between the two screens. There were also five genes displaying negative interactions with *prz1*$^{+}$ in the Ryan *et al.* (2012) screen that were positive interactions in this screen. Figure 3.3B shows the 49 positive interactions found in this screen that were also measured in Ryan *et al*. (2012), the interaction scores do not match between the screens.

3.4.7 Prz1 SGA and genetic activation

SGA screens can uncover functional redundancy from negative genetic interactions in the double mutants. A negative interaction could also indicate that in each single deletion mutant, the other gene product is likely active in the cell. This is because the activity of the one gene product is required for viability in the other deletion strain. If the

gene product was not active, and compensating for the loss of the first gene, there would be no additional fitness defect in the double mutant. This means that gene deletions that share negative genetic interactions with *prz1*$^+$ could represent backgrounds in which Prz1 is more active. This was the case with Δ*pmr1,* a negative interaction seen in this study as well as by Ryan *et al.* (2012), as was discussed in chapter 2. This particular interaction has a known explanation. Pmr1 is a transporter involved in calcium sequestering in the endoplasmic reticulum, which when removed would result in considerably higher cytoplasmic calcium (Maeda *et al.* 2004). The high cytoplasmic calcium in the Δ*pmr1* mutant would trigger the activation of Prz1. In wild-type cells Prz1 upregulates *pmr1*$^+$, a known downstream target gene, to sequester calcium into the endoplasmic reticulum in response to elevated calcium levels (Maeda *et al.* 2004).

In chapter 2 we performed microarray experiments to look for target genes of Prz1 (Figure 2.2A). The four microarray experiments looked at wild type compared to Δ*prz1*, wild type compared to Δ*prz1* treated with either $CaCl_2$ or tunicamycin, and Δ*pmr1* compared to Δ*prz1*. These experiments identified 339 genes that were differentially regulated by more than two-fold in at least one of the experiments. There are eight genes (SPAC2E1P3.05c, *ctr4*$^+$, *alp31*$^+$, *clr2*$^+$, *pmr1*$^+$, *rds1*$^+$, SPBC1289.14, and *pmc1*$^+$) among the 62 genes that shared negative genetic interactions with *prz1*$^+$ that were up- or down-regulated by more than two-fold in at least one of the four microarray experiments. Six of these genes were among the top eight strongest negative interactions with *prz1*$^+$. Some of these genes, such as *pmr1*$^+$ and *pmc1*$^+$, are known targets of Prz1, and have a clear relationship with the calcium response. These gene targets were downregulated in the Δ*prz1* mutant relative to wild type, along with *clr2*$^+$, a third putative target gene that

encodes a histone deacetylase. The expression change was presumably because they were not activated by the Prz1 response to calcium in the Δ*prz1* mutant. There were also three genes that were upregulated in the Δ*prz1* mutant relative to the wild type or Δ*pmr1* strain. These represent genes whose mRNA levels increase in response to the loss of Prz1, whether by direct DNA binding or indirect mechanisms. The *alp31*$^{+}$ levels increased more than any other gene in the Δ*prz1* mutant relative to wild type (4.9-fold), which further supports a relationship between Prz1 and Alp31 activity. Alp31 is an ortholog to cofactor A, a part of the pathway responsible for folding β-tubulin (Radcliffe *et al.* 2000). We used fluorescence microscopy to look for Prz1 activity in the Δ*alp31* mutant. Prz1-GFP did not localize to the nucleus more frequently in Δ*alp31* than in wild type (data not shown). We also performed a microarray experiment comparing the Δ*alp31* mutant to the Δ*prz1* mutant, looking for increased activity of Prz1 as was observed in the Δ*pmr1* background. The result of the microarray was consistent with the results of the microscope work as Prz1 targets were not activated to a greater degree in the Δ*alp31* mutant than they were in wild type (Figure 3.4). The Δ*prz1* strain compared to Δ*pmr1* microarray experiment shows greater than two-fold differential regulation for 98/165 genes activated by Prz1, and 49/92 genes repressed by Prz1. The Δ*prz1* strain compared to Δ*alp31* microarray experiment shows greater than two-fold differential regulation for only 4/165 genes activated by Prz1, and 8/92 genes repressed by Prz1. This level of differential regulation is similar to the Δ*prz1* strain compared to wild type microarray experiment which had only 5/165 and 5/92 genes differentially regulated by more than two-fold in the activated and repressed target genes, respectively. This indicates that not

all negative genetic interactions involving transcription factors are equally amenable for their activation.

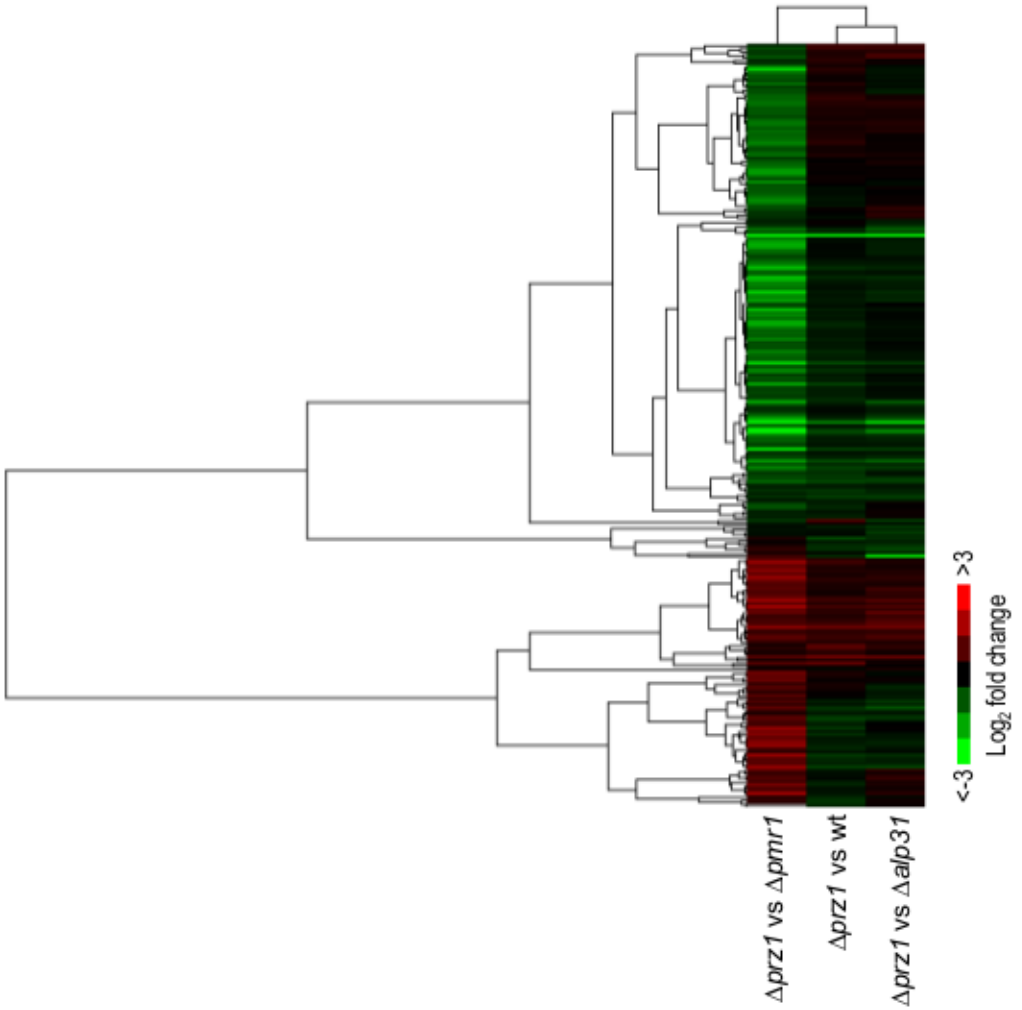

Figure 3.4: The use of negative interactions between *pmr1*$^+$ and *alp31*$^+$, with *prz1*$^+$ to uncover Prz1 target genes using microarray experiments. The heat map shows two-dimensional hierarchical clustering of the 165 positively- and 92 negatively-regulated putative target genes of Prz1. In the heat map, genes upregulated and downregulated in the Δ*prz1* strain relative to the mutant or control are indicated in red and green, respectively. The Δ*pmr1* causes Prz1 activation and results in the differential expression of many of its target genes. This regulation was comparable to activation by a 30 minute treatment with 0.15 M $CaCl_2$ or a 90 minute treatment with 2.5 µg/mL tunicamycin, as discussed in chapter 2. In contrast the Δ*alp31* mutant was not able to activate Prz1 target genes, and the comparison of Δ*prz1* to Δ*alp31* was not considerably different from Δ*prz1* compared to wild type.

3.5 Discussion

The genetic interactions between the sequence-specific *S. pombe* transcription factors were investigated using a SGA screen that identified 48 negative and 99 positive interactions. A quarter of the negative interactions were tested by RSA, and 16/18 interactions were confirmed. A SGA screen of Δ*prz1* crossed to the full haploid deletion collection was also performed. This screen resulted in 62 negative and 85 positive interactions predicted for *prz1*$^{+}$. The negative interactions were enriched for genes involved in the dolichol-linked oligosaccharide biosynthetic process and endoplasmic reticulum localized proteins. The *prz1*$^{+}$ interactions did not confirm as well when tested by RSA and tetrad dissection, with only 5/10 genes confirmed by one or the other method and only one gene confirmed by both.

3.5.1 Noise in SGA data

SGA screens, like many high-throughput methodologies, are inherently noisy. The data from SGA screens are normalized to help account for systematic sources of bias, such as competition effects that change depending on the position on the plate, and the fitness of the neighbouring strains (Baryshnikova *et al.* 2010). Batch effects are another source of systematic error, where small differences in media or the robot used can introduce systematic errors that mask the true interactions (Baryshnikova *et al.* 2010). Although the number of screens performed per query was the same for the transcription factor array and the *prz1*$^{+}$ full genome screen, the transcription factor array had more replicates for each interaction. This was due to each transcription factor array strain being

present at three different locations on the array. This had the added benefit of reducing the effect of spatial bias, and may account for the improved accuracy of the screen as confirmed by the RSA experiments (88.9% compared to 40%).

3.5.2 Redundancy between S. pombe transcription factors

The negative genetic interactions between the transcription factors can describe different regulatory relationships. Two transcription factors could bind the same binding motif and regulate the same target genes either redundantly, or under different conditions. This is more likely to be the case when the transcription factors are paralogs (Zheng *et al.* 2010). The transcription factor pairs could also regulate an overlapping set of target genes through different binding motifs in the promoter region. Finally the transcription factors could regulate different sets of target genes that genetically interact.

There were only two negative interactions of 48 identified that involved transcription factor paralogs in *S. pombe*. The genes encoding the transcription factors Rsv1 and Scr1 are paralogs, although this interaction did not confirm by serial dilution (Villela *et al.* 2009). The genes encoding the transcription factors Prz1 and Ace2 are also paralogs (Villela *et al.* 2009). However, these two transcription factors do not appear to regulate the same target genes or possess the same functions (Alonso-Nuñez *et al*. 2005; Rustici *et al.* 2004). The Sep1 transcription factor is an upstream regulator of the expression of the cell cycle gene $ace2^{+}$ and like $ace2^{+}$ the $sep1^{+}$ gene interacts with $prz1^{+}$ (Garg *et al.* 2015). This is further confirmation that $prz1^{+}$ interacts with the cytokinesis pathway regulated by Sep1 and Ace2, even though the interaction cannot be explained through the transcriptional targets (Garg *et al.* 2015). The negative interaction between

prz1^{+} and *ace2*$^{+}$ could be the result of non-overlapping target genes that negatively interact.

Without prior knowledge of the target genes or functions of the transcription factors involved in a genetic interaction, it is difficult to explain the nature of the relationship. Unlike negative interactions between transcription factors and other genes, negative interactions between two transcription factors in most cases will not reveal overlapping targets with microarray experiments. The possibility of overlapping targets means the target genes may not display differential expression between the two transcription factors. Genetic activation microarray experiments are only able to identify target genes when the transcription factors regulate different genes. However, it is impossible to know with certainty that the two transcription factors do not share target genes, meaning the experimental design may mask any overlap. Zheng *et al.* (2010) observed that genetic interactions between transcription factors were often direct, in that they could not be explained by negative interactions between the target genes of interacting transcription factors.

When the transcription factor double mutant is sick, as opposed to lethal, both of the single mutants and the double mutant can be explored by expression microarrays. Zheng *et al.* (2010) performed expression profiling on four sets of negative interactions between *S. cerevisiae* transcription factors. Two of the negative interaction pairs shared common targets between the transcription factors, with one acting as a major regulator and the other acting as a minor regulator. The expression pattern of the deletion strain of the major regulator was closer to that of the double mutant (Zheng *et al.* 2010). The other two negative interactions involved transcription factors that did not share common

targets. Microarray expression profiling of the single and double transcription factor mutants revealed that often one transcription factor will play a larger role in the fitness defect and that there are multiple reasons for transcription factors to negatively interact (Zheng *et al.* 2010).

The negative interactions between transcription factors could potentially identify backgrounds that result in the activation of one of the transcription factors. A deletion mutant of either transcription factor could enhance the activity of the other and result in differential expression of the target genes. This could be due to either the loss of a regulator to the same set of target genes, or due to stress to a completely different biological process. DNA-binding data from chIP microarray or chIP sequencing experiments for one transcription factor in the deletion mutant of the other transcription factor, should in theory reveal the target gene promoters it binds. This experimental design works whether the target genes of the transcription factors are shared or not, because it does not rely on the expression changes in the two deletion mutants.

3.5.3 SGA and the genetic activation of transcription factors

Negative genetic interactions appear to be a good approach to identify mutations that result in the activation of a transcription factor. If a single deletion mutant is viable on its own, but lethal when combined with the deletion of a transcription factor, then the transcription factor must be active to improve the fitness in the single mutant. This was confirmed by fluorescence microscopy and microarray expression profiling looking at the activity of Prz1 in the Δ*pmr1* mutant. In the Δ*pmr1* strain, Prz1 nuclear localization was enhanced and its target genes were differentially expressed. The Δ*alp31* mutant did not

seem to affect Prz1 activity when assayed by either method, despite the fact that the negative interaction was confirmed by RSA and tetrad dissection. Because the interaction was confirmed, the lack of activation was not due to a false hit caused by noise in the screen. It is possible that even though the basal activity of Prz1 is low, this level of activity is sufficient for viability in the Δ*alp31* strain. Hirayama *et al.* (2003) observed that Prz1 nuclear localization increased in binucleate cells before septum formation. This brief activation of Prz1 during the normal progression of the cell cycle is typical of wild-type cells, and therefore would not result in increased Prz1 activity in Δ*alp31* relative to wild type. In *S. cerevisiae*, Costanzo *et al.* (2010) observed a large number of overlapping genetic interactions between the following biological processes: cell wall biosynthesis and integrity, and genes involved in cell polarity and morphogenesis. The negative interaction between $prz1^+$ and $alp31^+$ could be the result of the interdependence of these two pathways. This demonstrates that not all negative genetic interactions are equally effective at activating a transcription factor.

Costanzo *et al.* (2010) observed that single mutants that were sicker had more genetic interactions than those with a fitness similar to wild type. This was supported by the major and minor players observed by microarray when looking at negative interactions between transcription factors (Zheng *et al.* 2010). The Δ*alp31* mutant was much sicker than the Δ*prz1* mutant, indicating that the former plays a larger role in the defect observed in the double mutant. The fact that $alp31^+$ expression levels are extremely high in the Δ*prz1* mutant relative to wild type, indicates that the Δ*prz1* mutant results in upregulation of $alp31^+$ expression, and that Δ*alp31* does not cause upregulation of $prz1^+$ expression. The health of the interacting partner may be a useful metric to

eliminate poor candidates for genetic activation. Further study will be needed to identify whether negative interactions elucidated with SGA can be generally applied to determine mutants which genetically activate transcription factors.

Chapter Four: **Identification of novel putative regulators of fission yeast transcription factors by synthetic dosage lethality**

Kate Chatfield-Reed and Gordon Chua

This chapter was entirely my own work, although it uses strains constructed in the lab and previously published in Vachon *et al.* (2013). The contents of this chapter are currently being assembled for submission to *G3*.

4.1 Abstract

The regulation of transcription factors is necessary to ensure the appropriate abundance of mRNAs in the cell in response to various environmental and physiological conditions. Here, we developed a synthetic genetic array (SGA)-based method for systematic screening of synthetic dosage lethal (SDL) interactions to identify novel regulators of several transcription factors in the fission yeast *Schizosaccharomyces pombe*. Fourteen transcription factor overexpression strains were mated by SGA to a miniarray of 279 strains, containing gene deletions encoding primarily posttranslational modifying enzymes, and subsequently assayed for SDL interactions. The frequency of SDL interactions isolated in our screens was ~5% and consisted of known and putative regulators often implicated in similar cellular processes as the transcription factor. We discovered that the ubiquitin ligase Ubr1 and putative E2/E3-interacting protein Mua1 both function to degrade the glucose repressor Scr1 in response to low glucose. In addition, certain components of the SAGA complex appeared to be required for activation of the pyrimidine-salvage target genes by Toe1. Our study reveals that SDL

screening is an effective approach to uncover novel regulators of transcription factors and their target genes.

4.2 Introduction

Cells need to regulate gene expression in response to external stimuli during growth and development. Transcription factors are an integral component of this regulation as they activate and repress mRNA synthesis of the appropriate target genes. Transcription factors themselves are also regulated to control their abundance, localization, and activity in the cell. They undergo posttranslational modifications (e.g. phosphorylation, acetylation, ubiquitination, methylation, and sumoylation) that modulate their activity via alterations in intracellular localization, stability, or protein-protein interactions (Hirayama *et al.* 2003; Barlev *et al.* 2001; Huang *et al.* 2007). The interactions between different upstream regulators create a complex network that controls the activity of each transcription factor accordingly (Chuikov *et al.* 2004; Gostissa *et al.* 1999). The elucidation of the upstream regulators of each transcription factor is necessary to understand the establishment of gene expression programs.

A synthetic dosage lethality (SDL) interaction is when overexpression of a gene is normally viable, but is lethal in certain deletion backgrounds. SDL interactions usually involve two genes with opposing regulatory roles and result in the hyperactivation of a pathway that is detrimental to cell viability (Measday *et al.* 2005; Sopko et al. 2006). For example, SDL could potentially occur if the deletion of a repressor further increases the activity of an overexpressed protein. This is in contrast to synthetic lethal/synthetic sick interactions in double deletion strains, which usually involve two genes in redundant

pathways (Tong *et al.* 2001; Costanzo *et al.* 2010; Dixon *et al*. 2008; Ryan *et al*. 2012). SDL interactions can also involve genes whose products are components of the same complex. In this case, the SDL interactions are attributed to a disruption in the stoichiometry of the protein complex (Duffy *et al.* 2012).

Several large-scale systematic screens have used the synthetic genetic array (SGA) approach to identify SDL interactions in *S. cerevisiae*. (Measday *et al.* 2005; Sopko *et al.* 2006; Liu *et al.* 2009; Sharifpoor *et al.* 2012; Duffy *et al.* 2012). Similar to deletion mutants, overexpression of the vast majority of genes does not result in a large fitness defect under standard laboratory conditions (Sopko *et al.* 2006). The availability of a full-genome overexpression array in budding yeast allows for comprehensive screening of SDL interactions by systematic mating between a deletion query strain and the overexpression array strains. SDL has been used to explore chromosome segregation, the kinome, the ubiquitinome, and the acetylome in *S. cerevisiae* (Measday *et al.* 2005; Liu *et al.* 2009; Sharifpoor *et al.* 2012; Duffy *et al.* 2012).

SGA protocols have been developed for *S. pombe*, but not adapted for SDL screening. The nature of SDL interactions and the availability of SGA-based screening make it an attractive screen to elucidate upstream regulators of transcription factors, which has not been attempted to date. Moreover, a collection of 99 overexpression strains covering almost all *S. pombe* transcription factor ORFs, under control of the *nmt1* promoter, has been previously constructed and used to identify direct target genes by expression microarrays and ChIP-chip (Kwon *et al.* 2012; Vachon *et al.* 2013). When overexpressed, approximately two thirds of transcription factors exhibited mild to severe fitness defects that were presumably due to aberrant expression of their target genes

(Vachon *et al.* 2013). Therefore, SDL interactions could be used as genetic backgrounds that exacerbate the aberrant regulation of target genes in the transcription factor overexpression strain. These genetic backgrounds could represent putative negative regulators of transcription factor activity.

Here, we developed a modified SGA method to screen for SDL interactions in *S. pombe* and applied the protocol to search for upstream regulators of several transcription factors. Fourteen transcription factor overexpression strains were systematically crossed to a regulator miniarray, consisting of 279 strains deleted for genes primarily encoding posttranslational modifying enzymes, to select for SDL interactions (Table A11). SDL interactions revealed a known upstream regulator for each of the transcription factors Scr1 and Yox1 (Gómez-Escoda *et al.* 2011; Saitoh *et al.* 2015). It also revealed several novel regulatory interactions with Scr1, including the E3 ubiquitin ligase Ubr1 and the zf-MYND type zinc finger protein Mua1/SPBC31F10.10c, both of which cause accumulation of the Scr1 protein when deleted. These regulators appeared to be repressors of their respective transcription factors, indicating that the SDL interactions may be due to an increase in aberrant regulation of target genes in the deletion backgrounds compared to the transcription factor overexpression strain alone. In addition, the screens uncovered a role for components of the SAGA complex and the Set1 histone lysine methyltransferase in the transcriptional regulation of Toe1 target genes. These results demonstrate that SDL screening is a useful tool in identifying upstream regulators of transcription factors.

4.3 Materials and methods

4.3.1 Yeast strains, media and general methods

Table A10 contains a list of yeast strains used in this study. Strains were grown on YES or EMM supplemented with 225 mg/L each for adenine (A), leucine (L) or uracil (U) and 15 μM thiamine when required. The glucose concentration of YES low glucose medium was 0.08% instead of 3%. Cells were mated on SPAS medium supplemented with 45 mg/L each for adenine, leucine, and uracil. Selection of deletion mutants containing the *pREP1* vector, overexpressing the transcription factor ORF by the *nmt1* promoter, was performed on PMG medium containing 225 mg/L each for adenine and uracil as well as 300 mg/L geneticin (Kan). All media used in the SDL protocol was supplemented with 2% galactose to limit cell-cell adhesion and promote better pinning. The Kan concentration was increased to 300 mg/L because PMG medium was observed to reduce the Kan sensitivity of strains that did not contain the *KanMX4* cassette (Figure 4.1A). The miniarray consisted of 279 Bioneer haploid deletions, with the *KanMX4* cassette in place of their ORFs, whose genes encode potential regulators of transcription factors including kinases, phosphatases, ubiquitin ligases, SUMO transferases, chromatin remodelling enzymes, and RNA-binding proteins (Table A11). The vectors for the query strains were constructed in Vachon *et al.* (2013) and contained transcription factor ORFs cloned in the *pREP1* vector (*LEU2*-marked) and overexpressed by the *nmt1* promoter. The vectors were transformed into the *JK366 h*$^{-}$ strain, so that the query strains would have the same auxotrophic background as the array strains. The endogenously-tagged *scr1GFP* strain was created by PCR-amplification of the *EGFP* ORF and *KanMX4* cassette from the pYM27 plasmid (Janke *et al.* 2004), which were PCR-stitched to

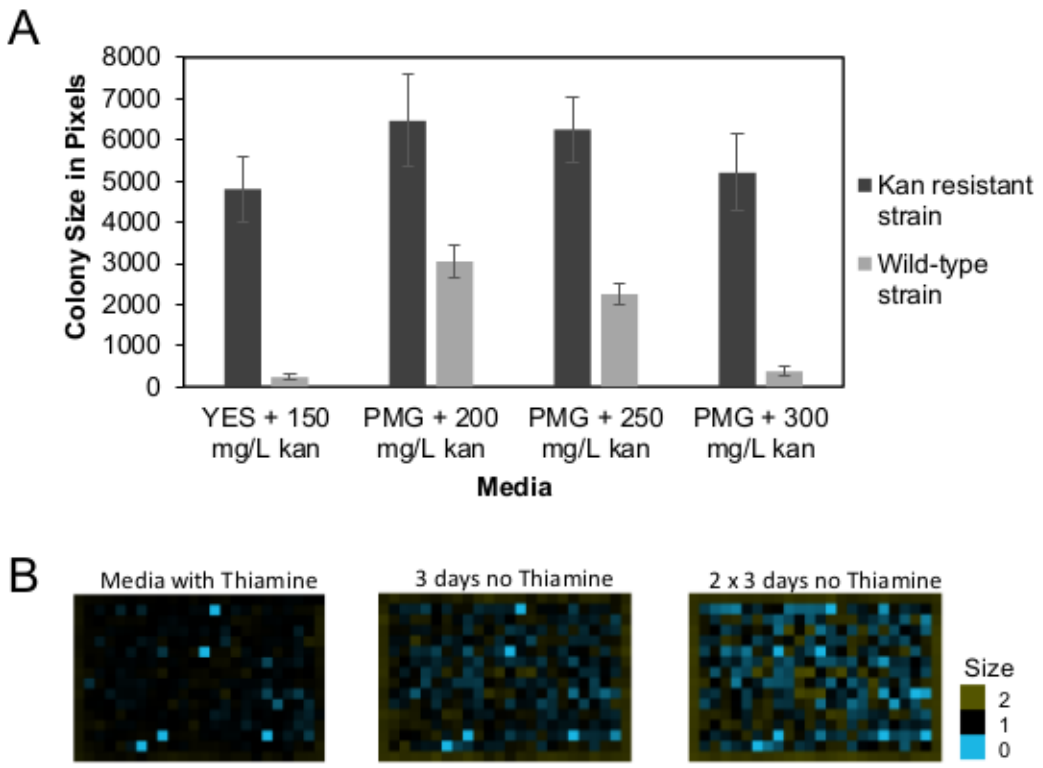

Figure 4.1: Experiments that determined the variables used for selection of the deletion mutants and induction of the overexpression plasmid. Minimal medium is required to maintain leucine selection of the transcription factor overexpression plasmid during the *S. pombe* SDL procedure. Standard minimal medium is not conducive to Kan selection, so Pombe Minimal Glutamate (PMG) medium was used instead. A) Several trials were performed to test the impact of the minimal media on Kan selection. PMG medium reduces the Kan sensitivity of the strains without the Kan-resistance cassette, relative to the fitness observed in rich medium. Increasing the concentration of Kan counteracts the increased growth and improves the selection. B) The *nmt1* promoter is induced by the absence of thiamine in the media. The colony size is reduced after three days on plates without thiamine as seen in the difference between the first two figures. Three additional days on fresh minus thiamine plates increases the growth defect even further.

homologous flanking regions, and inserted in-frame at the C-terminal end of the *scr1*$^{+}$ ORF. Standard genetic and molecular methods were performed as described in Moreno *et al.* (1991).

4.3.2 SDL screens

A systematic SDL screening method was developed in *S. pombe* by modifying the SGA procedure from Dixon *et al.* (2008). SDL screening to identify deletion backgrounds of regulator genes that cause lethality in a transcription factor overexpression strain was conducted with a BM3 SGA Robot (S&P Robotics). The regulator gene deletions (miniarray strains) and the transcription factor overexpressor (query strain) were assembled in a 384 colony format on YES+Kan and EMM+AU with thiamine plates, respectively, and incubated at 30°C for three days. The query and miniarray strains were mated to introduce the transcription factor overexpression vector into the regulator gene deletion strains by pinning onto a common SPAS plate. To improve mating efficiency, the robotic pins were dipped in sterile water before the first transfer and cells were gently mixed. The SPAS plates were incubated for three days at 25°C to allow mating, and then incubated at 42°C for three days to select for spores and kill unmated vegetative cells. The spores were subsequently transferred through pinning onto EMM+AU with thiamine plates and incubated for three days at 30°C to allow for germination. The colonies were then pinned onto PMG+AU+Kan without thiamine plates and incubated for six days at 30°C to select for regulator gene deletion strains and allow induction of the *nmt1* promoter and overexpression of the transcription factor ORF. There was an intervening pinning step after three days to reduce the amount of carryover of

cells from the previous pinning and allowed for better detection of SDL interactions (Figure 4.1B). The final set of plates was then photographed and colony sizes determined using the spImager-M system (S&P Robotics).

Normalization to correct for spatial biases, resulting from variation in the media or local environment on the plate, was performed with SGAtools (Wagih *et al.* 2013). The screen was also performed with an empty vector control strain as the query to obtain an estimate for the single mutant fitness of the deletion strains. The normalized colony size of the regulator gene deletion strain with the overexpressed transcription factor ORF was then compared to the expected fitness of the combination, which was generated using a multiplicative model of the individual fitness of the query and miniarray strains. The predicted fitness was subtracted from the double mutant fitness ($W_{ij} - W_i W_j$), where W_{ij} was the observed double mutant fitness, and W_i and W_j were the single mutant fitness values (Wagih *et al.* 2013). A conservative cut-off for SDL interactions of -0.5 was selected to reduce false positives, where a cut-off of -0.3 is normally considered a strong effect (Wagih *et al.* 2013).

Serial spot dilutions were used to confirm putative SDL interactions. The transcription factor overexpression vector was retransformed into candidate regulator deletion strains and their fitness were compared to the empty vector control, transcription factor overexpression strain, and the regulator gene deletion containing the empty vector. The comparisons were performed on EMM+AU media in the presence and absence of thiamine after three to five days growth at 30°C.

4.3.3 Microscopy

The intracellular localization and intensity of natively-regulated Scr1-GFP was compared in wild type and gene deletion backgrounds that exhibited SDL interactions when *scr1*$^{+}$ was overexpressed. Strains were logarithmically grown for 6 hours in YES and YES low glucose media and live cell images were captured with a Zeiss Imager Z1 microscope and AxioCam MRM digital camera (Zeiss, Thornwood, NY). The quantification of GFP signal intensity was assessed for the entire cell area using ImageJ (v1.48, NIH). The corrected total cellular fluorescence was calculated as described by McCloy *et al*. (2014) and represented 30 cells over three biological replicates. Three different locations per image were selected for background corrections. The significant difference of corrected total cellular Scr1-GFP fluorescence, between the wild type and gene deletion backgrounds, was determined with a two-tailed t-test.

Colony morphology was examined and compared between wild type and various deletion backgrounds that displayed SDL interactions with *yox1*$^{+}$ overexpression. Strains were grown for 24 hours at 30°C on EMM+AU plates, then streaked onto a new plate and incubated for another 24 hours to allow full *yox1*$^{+}$ overexpression. Colony morphology was examined at this point with a Zeiss AxioScope A1 tetrad microscope (Zeiss, Thornwood, NY).

4.3.4 Quantitative PCR

Deletion strains of SAGA components and wild type were cultured to mid-exponential phase in liquid YES medium for 18-20 hours at 30°C. The mRNA expression levels of *toe1*$^{+}$ and its target genes were compared between the SAGA deletion strains

and wild type by quantitative PCR as previously described in Vachon *et al.* (2013). Three technical replicates were performed for each gene-strain combination, with *act1*$^{+}$ used as the reference gene, and fold changes were determined by the ΔΔCt method.

4.4 Results

4.4.1 SDL screens and known interactions

A systematic SDL screening method using SGA was developed and applied in *S. pombe* to identify potential regulators of transcription factors (Figure 4.2). The SDL screens involved mating query strains containing the *pREP1* vector with transcription factor ORFs overexpressed by the *nmt1* promoter to a miniarray of 279 Bioneer haploid deletion strains of mainly posttranslational-modifying enzymes including kinases, phosphatases, ubiquitin ligases, SUMO transferases, and chromatin remodeling factors (Table A11). Fourteen transcription factor overexpression strains were selected as queries for the SDL screens. These fourteen included the transcription factors Cbf11, Eta2, Sre2, Sfp1, Scr1, Toe1, Mbx1, Tos4, and Yox1, which have been implicated in a variety of biological processes including cell cycle regulation, glucose metabolism, pyrimidine salvage, and flocculation. The remainder were the uncharacterized transcription factors SPAC1F7.11c, SPAC19B12.07c, SPBC19G7.04, SPBC29A10.12, and SPBC530.08. Seven of the fourteen transcription factors have predicted human orthologs. The transcription factor overexpression strains exhibited fitness defects ranging from similar to wild type, to severe. Robotic pinning of the transcription factor overexpression strains in the absence of thiamine exhibited fitness defects that agreed with those previously observed in Vachon *et al.* (2013) with the exception of Toe1 (Figure 4.3). Five additional

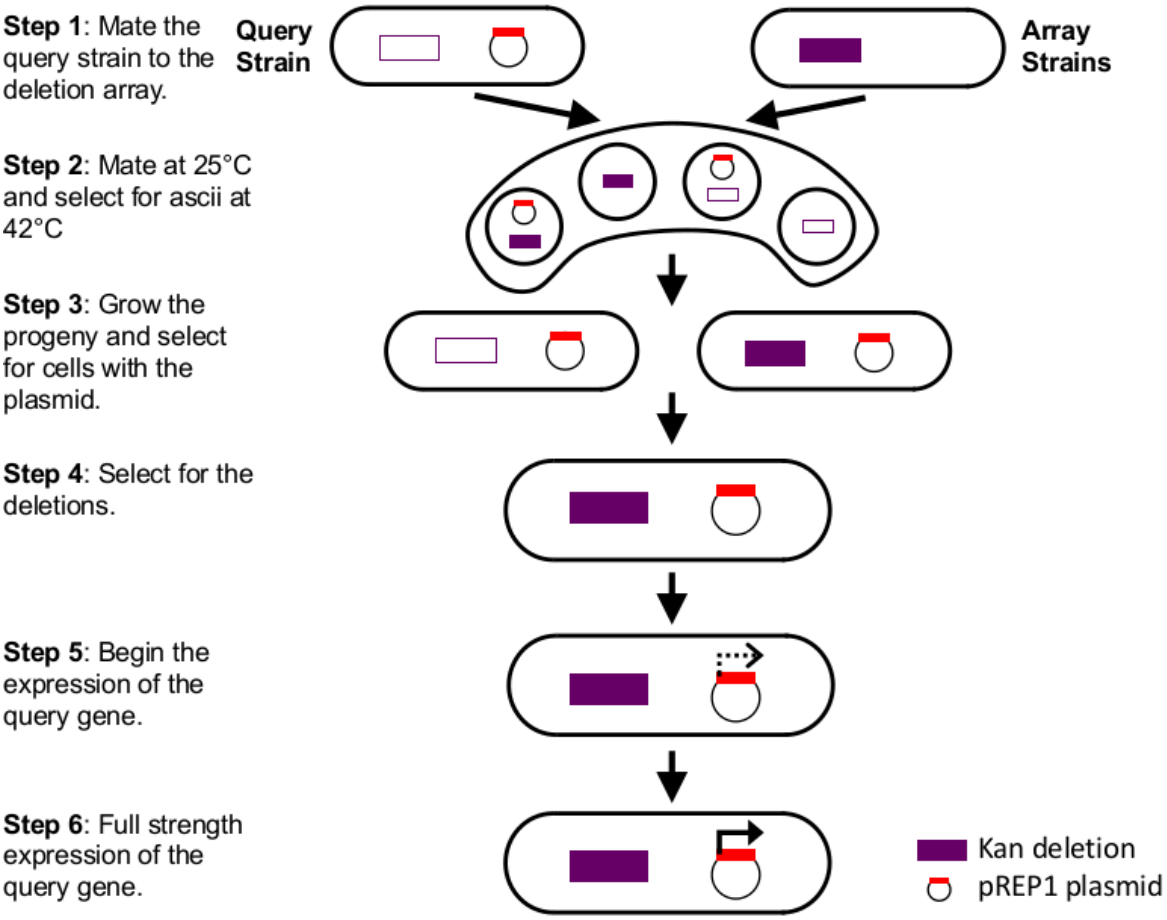

Figure 4.2: The SGA-based screening protocol for identifying SDL interactions in *S. pombe*. The 279 deletion array strains were arrayed on a single plate at a colony density of 384. The *nmt1*-driven overexpression query strain was crossed to the deletion miniarray in Step 1. The selection of mated spores in Step 2 was similar to the SGA protocol outlined by Dixon *et al.* (2008) with a 3-day incubation on SPAS plates at 25°C followed by another 3-day incubation at 42°C for mating and selection of spores, respectively. This was followed by a 3-day incubation on EMM+AU medium supplemented with thiamine to allow for spore germination and growth of vegetative cells. The selection of the double deletion mutants and induction of the *nmt1* promoter was performed in Steps 5 and 6 to detect putative SDL interactions. PMG+AU+Kan was used to select for both the gene deletion and the plasmid, while overexpressing the transcription factor target gene. The final colony size was imaged with the spImager-M system (S&P Robotics) and scored using SGAtools (Wagih *et al.* 2013).

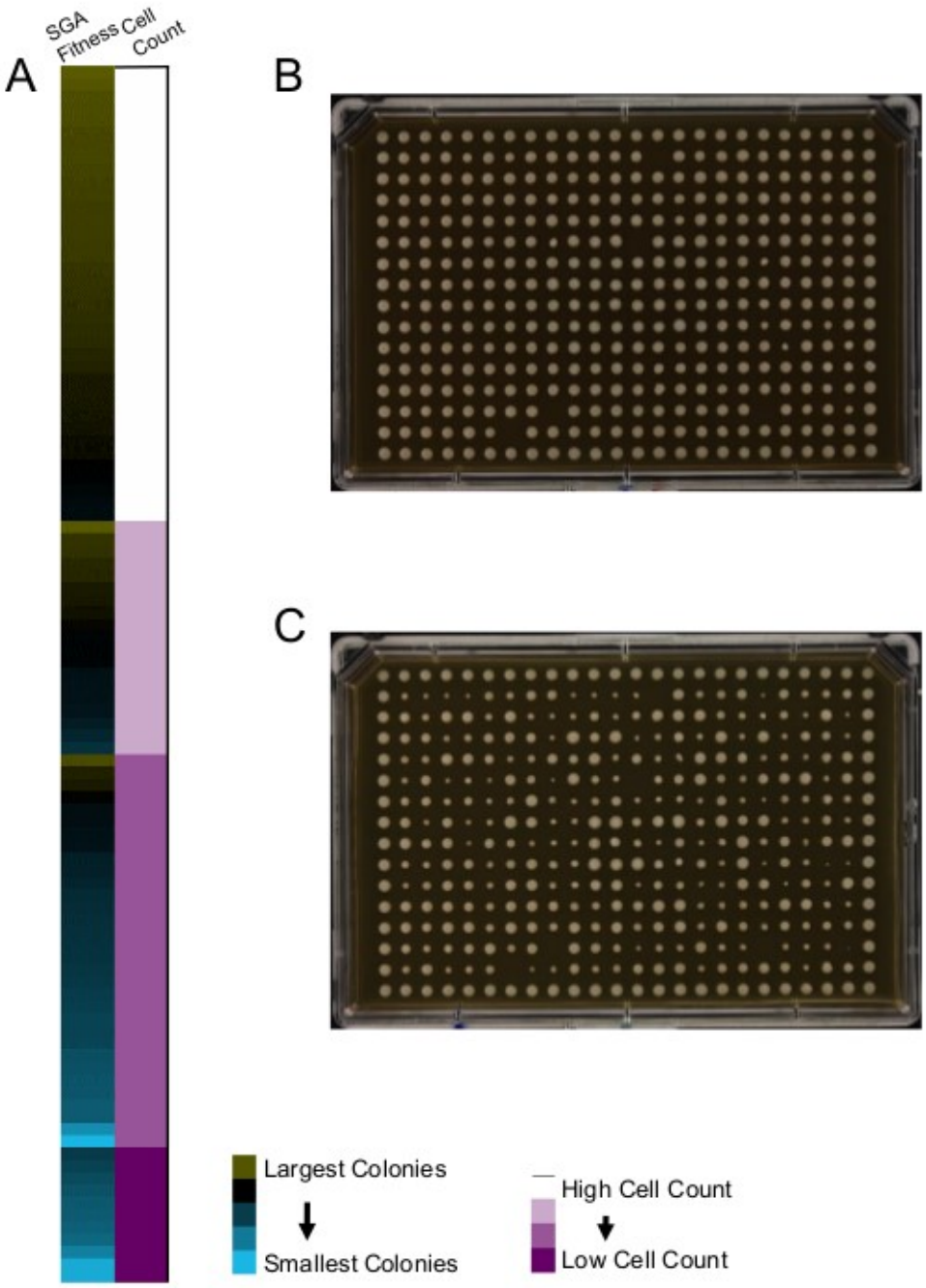

Figure 4.3: **Correspondence of reduced fitness of transcription factor overexpression strains detected by robotic pinning and microscope visualization of cells/colony from Vachon *et al.* (2013).** A) The fitness scores of the transcription factor overexpression strains from SGA screening are located on the left and the manual scores of cells/colony are on the right side of the heat map. The difference in colony size between plates with thiamine and without thiamine (ectopic expression of the transcription factor gene) in the medium after robotic pinning are shown in B) and C), respectively.

transcription factors (*prz1*$^+$, *map1*$^+$, SPCC1393.08, *grt1*$^+$, and *gaf1*$^+$) were also selected as queries for the SDL screen were omitted due to irregular growth on multiple replicates.

The total frequency of putative SDL interactions in our screens was 195 of a potential 3906 genetic interactions (~5%) based on an interaction score cut-off of -0.5 (Figure 4.4 and Table A12). Forty-three of the 195 SDL interactions were tested by serial dilution. Approximately 51% of the SDL interactions identified from SGA screening confirmed by serial dilutions, while ~23% did not. The remaining ~26% of interactions could not be confirmed because some of the SDL strains also exhibited a severe fitness defect when grown on thiamine-containing medium, which should repress the *nmt1*-driven transcription factor gene. An explanation for the fitness defect in repressive thiamine-containing medium is that the *nmt1* promoter is leaky, and the deletion background in these SDL strains may be highly sensitive to elevated expression of the transcription factor gene. In addition, some of the single deletion mutants were extremely sick, which also prevented confirmation by serial dilution. Altogether, these results were comparable to the false discovery rates obtained from other SGA-based SDL screens (Liu *et al.* 2009; Sharifpoor *et al.* 2012).

Five of the transcription factor genes in the SDL screens have 20 putative upstream regulators previously reported (Saitoh *et al.* 2015; Matsuzawa *et al*. 2012; Gómez-Escoda *et al.* 2011; Papadopoulou *et al.* 2008; Takada *et al.* 2010; Papadopoulou *et al.* 2010; Stewart *et al.* 2011; Stewart *et al.* 2012), eight of which were represented on the miniarray. Two of the eight regulatory interactions appeared as SDL interactions in the screen: *yox1*$^+$ and *scr1*$^+$ overexpression with deletions of *cds1*$^+$ and *sds23*$^+$,

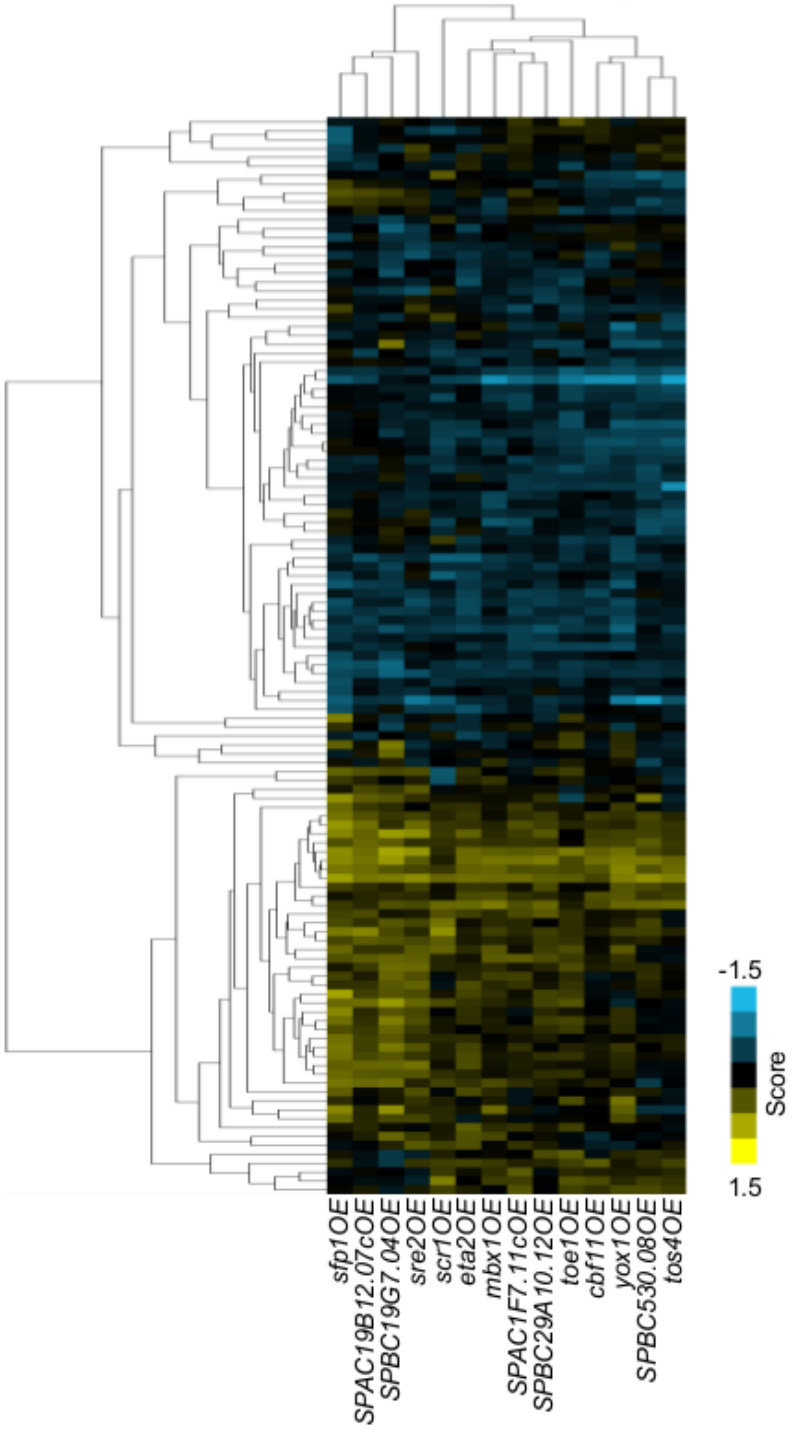

Figure 4.4: The *S. pombe* genetic interactions from the SDL screens. The 121 of 279 genes that showed a genetic interaction score of either >0.5 or <-0.5 with one of the 14 transcription factor query strains are shown in the heat map. Each column represents an overexpression query strain and each row represents a deletion array strain. Positive interactions are indicated in yellow and negative interactions (SDL) are indicated in cyan.

respectively (Gómez-Escoda *et al.* 2011; Saitoh *et al.* 2015). Both of these SDL interactions involved known negative regulators of their respective transcription factors. The Cds1 kinase phosphorylates and inhibits Yox1 in response to DNA damage (Gómez-Escoda *et al.* 2011), while the Sds23 kinase phosphorylates Scr1 to prevent its nuclear translocation under low glucose conditions (Saitoh *et al.* 2015). An SDL interaction was not detected between *scr1*$^+$ overexpression and loss of *ssp2*$^+$ despite the latter having the same effect on Scr1 nuclear localization as observed in the Δ*sds23* strain (Matsuzawa *et al.* 2012). The known interaction of *dsc1*$^+$ and *sre2*$^+$, which encode a putative ubiquitin ligase and SREBP transcription factor, respectively, was not recovered in our SDL screens. In this case Dsc1 positively regulates Sre2 by cleaving it from the membrane, which allows translocation into the nucleus (Stewart *et al.* 2011). Although the sample size is small, these results indicate that SDL interactions may be enriched for negative regulators of transcription factors.

4.4.2 Novel SDL interactions of scr1$^+$

The Scr1 transcription factor represses its target genes (*inv1*$^+$, *fbp1*$^+$, *gld1*$^+$, and *ght5*$^+$) in response to glucose (Tanaka *et al.* 1998; Janoo *et al.* 2001; Matsuzawa *et al.* 2010; Saitoh *et al.* 2015). Scr1 displays nuclear localization when wild-type cells are grown in rich media but remains localized in the cytoplasm under low glucose conditions (Saitoh *et al.* 2015). In addition to *sds23*$^+$, we discovered five other genes that exhibited SDL interactions with *scr1*$^+$ overexpression when deleted (Figure 4.5A). Two of these genes, *amk2*$^+$ and *gad8*$^+$, encode kinases that are known to be responsive to glucose levels (Valbuena and Moreno 2012; Hatano *et al.* 2015). Gad8 has been shown to have a

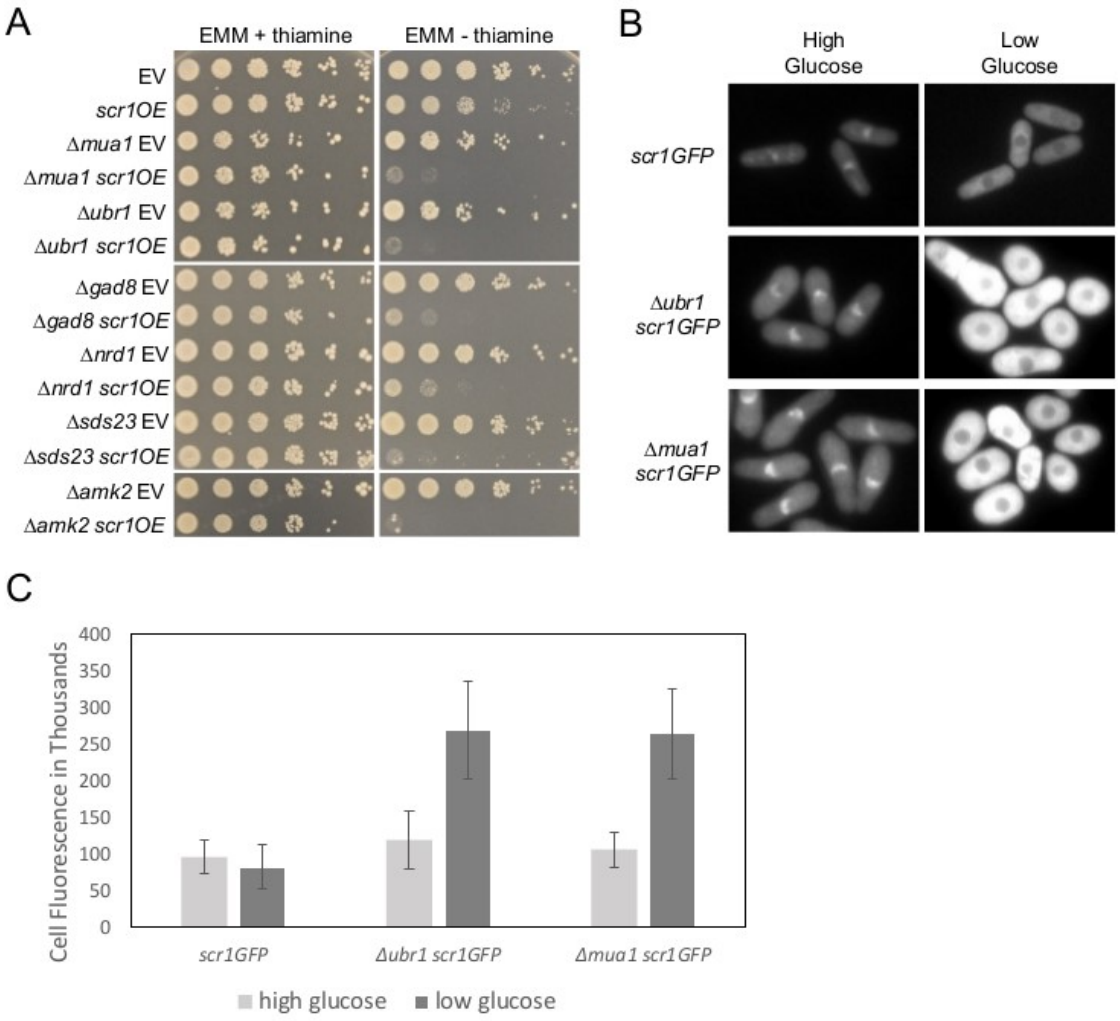

Figure 4.5: SDL interactions of *scr1*$^{+}$. A) Confirmation of SDL interactions with *scr1*$^{+}$ by serial dilutions. B) Fluorescence microscopy images of Scr1-GFP under either high or low glucose conditions in wild-type, Δ*ubr1*, and Δ*mua1* strains. C) The quantification of the Scr1-GFP total corrected cellular fluorescence in the three corresponding strains at the two different concentrations of glucose. The Scr1-GFP level in low glucose was significantly higher in the Δ*ubr1* and Δ*mua1* strains than in wild type ($p<0.0001$). The Scr1-GFP level in high glucose was significantly higher in the Δ*ubr1* strain than in wild type ($p=0.0072$). The total corrected cellular fluorescence values were calculated as described by McCloy *et al*. (2014) and represent 30 cells over three biological replicates.

role in the proper localization of the Scr1 putative target gene *ght5*$^{+}$, which encodes a hexose transporter in the plasma membrane (Saitoh *et al.* 2015; Matsuzawa *et al.* 2012). Two other gene deletions that shared a SDL interaction with overexpression of *scr1*$^{+}$ were Δ*ubr1* and ΔSPBC31F10.10c. Ubr1, a putative E3 ubiquitin ligase, appears orthologous to *S. cerevisiae* Ubr2, which interacts in a protein complex containing Rad6 and Mub1 to degrade its protein targets Rpn4, Sml1, and Dsn1 (Ju *et al.* 2008; Andreson *et al*. 2010; Akiyoshi *et al.* 2013). SPBC31F10.10c appears to be the *S. pombe* ortholog of Mub1 and may interact with Ubr1. As a result, we designate SPBC31F10.10c as Mua1 (MYND-type domain Ubr1 associated) hereafter. We next determined whether these SDL genes could regulate the intracellular localization and abundance of Scr1 by examining natively-expressed Scr1-GFP in the corresponding deletion strains in both high (3%) and low (0.08%) glucose medium. None of these deletion strains changed the intracellular localization of Scr1 that was observed with the Δ*sds23* strain. Interestingly, both Δ*ubr1* and ΔSPBC31F10.10c backgrounds displayed a significantly higher amount of Scr1-GFP relative to wild type under low glucose conditions ($p<0.0001$) (Figure 4.5B and C). The differences in high glucose conditions were not as pronounced, but Scr1-GFP levels in the Δ*ubr1* cells was still significantly higher than wild type ($p=0.0072$) (Figures 4.5B and C). Altogether, these data suggest that Scr1 may be degraded in response to its inactivation in low glucose by Ubr1 and Mua1.

4.4.3 SDL interactions of toe1^{+} *with set1*$^{+}$ *and SAGA genes*

Toe1 is a transcription factor that functions to positively regulate the pyrimidine-salvage genes *urg1*$^{+}$, *urg2*$^{+}$, *urg3*$^{+}$, and SPAC1399.04c (Vachon *et al.* 2013). SDL

interactions were observed between *toe1*$^+$ overexpression and loss of *sgf29*$^+$ and *ubp8*$^+$, both of which encode components of the SAGA complex (Figure 4.6A). SAGA (Spt-Ada-Gcn5-acetyltransferase) is a transcriptional coactivator complex that regulates numerous genes by coordinating posttranslational modifications of histones (Hemlinger *et al.* 2008). In *S. pombe*, the SAGA components Gcn5 and Spt8 have opposing roles in sexual differentiation (Helmlinger *et al.* 2008). Neither the loss of *gcn5*$^+$ nor *spt8*$^+$ exhibited a SDL interaction with *toe1*$^+$ overexpression (Figure 4.6A). In *S. cerevisiae* and humans, Sgf29 recruits the SAGA complex to H3K4me2/3, which promotes an increase in histone H3 acetylation by Gcn5 (Bian *et al.* 2011). This was interesting because loss of *set1*$^+$, which encodes the sole H3K4 methyltransferase, also exhibited a strong SDL interaction with *toe1*$^+$ overexpression (Figure 4.6A) (Noma and Grewal 2002).

The results above suggest that certain components of the SAGA complex may transcriptionally regulate the expression of *toe1*$^+$ or its targets. To address this possibility, we used quantitative PCR to compare the expression of *toe1*$^+$ and its target genes (*urg1*$^+$, *urg2*$^+$, *urg3*$^+$, and SPAC1399.04c) in deletion strains of *set1*$^+$, *sgf29*$^+$, and *gcn5*$^+$ relative to wild type. Expression of *toe1*$^+$ decreased in the Δ*set1* strain, but remained unchanged in the Δ*sgf29* and Δ*gcn5* strains compared to wild type (Figure 4.6B). However, the Toe1 target genes displayed lower expression levels in Δ*set1*, Δ*sgf29,* and Δ*gcn5* strains relative to wild type (Figure 4.6B). These results suggest that the SAGA complex is required for the expression of *urg1*$^+$, *urg2*$^+$, *urg3*$^+$, and SPAC1399.04c independent of Toe1. In contrast, Set1 appears to regulate these target genes by controlling the expression of *toe1*$^+$ as well.

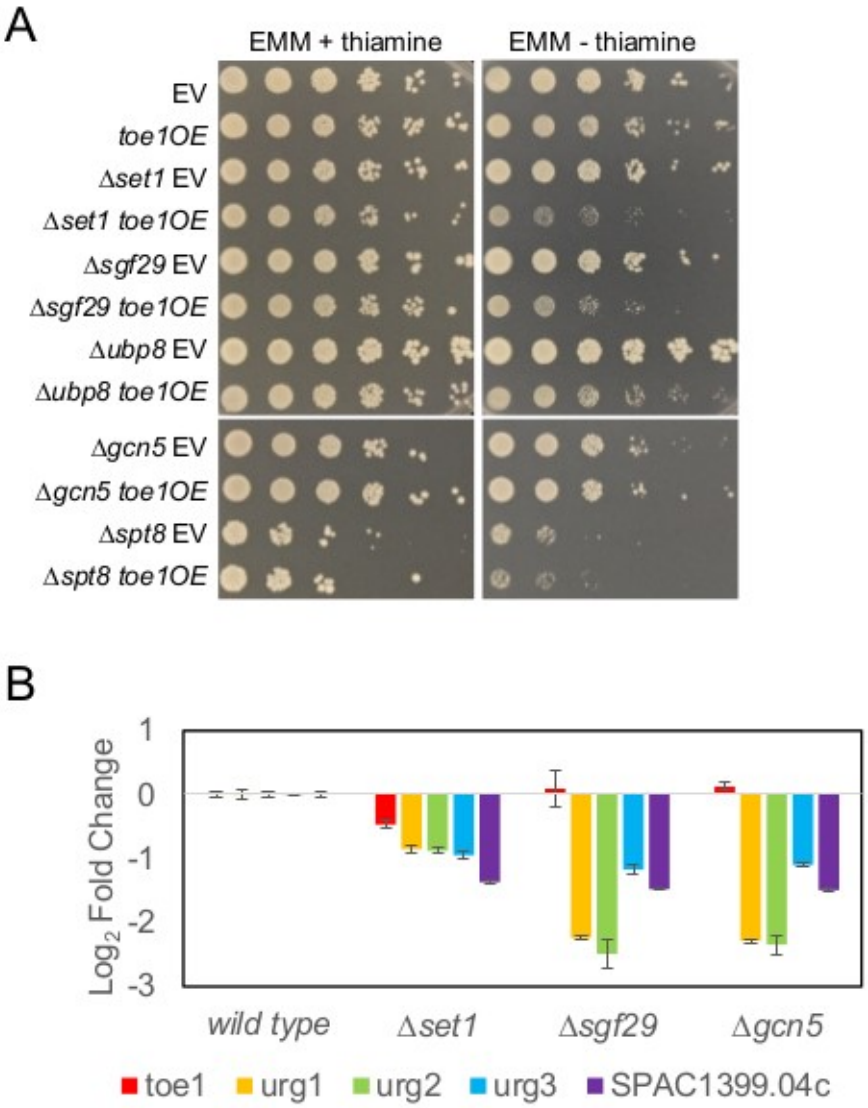

Figure 4.6: SDL interactions of *toe1*$^{+}$ overexpression with gene deletions of the SAGA complex and the Set1 histone lysine methyltransferase. A) Confirmation of SDL interactions of *toe1*$^{+}$ by serial dilutions. B) Quantitative PCR of *toe1*$^{+}$ and its pyrimidine-salvage target genes in wild type, Δ*set1*, and SAGA mutant backgrounds. Three replicates of the quantitative PCR were performed for each gene and mutant pairing. The Δ*set1* and SAGA mutants reduced the expression of Toe1 target genes relative to wild type.

4.4.4 Novel SDL interactions of cell cycle transcription factor genes

Yox1 functions as a repressor of the MBF transcription factor complex, which regulates target genes important in the G1/S transition of the cell cycle (Aligianni *et al.* 2009). Besides *cds1*$^{+}$, we identified an additional eight genes (Table A12) that exhibited SDL interactions with *yox1*$^{+}$ overexpression when deleted that confirmed by serial dilution (data not shown). These previously-undiscovered SDL interactions primarily involved genes related to cell cycle regulation or chromatin remodeling. These included the genes encoding the kinases Oca1, Pef1, and Cdr1, with the latter two involved in the regulation of the G1/S and G2/M transition, respectively (Tanaka and Okayama 2000; Coleman *et al.* 1993). Despite confirmation of the SDL interactions by serial dilutions, we did not detect additive effects in cell morphology when *pef1*$^{+}$ or *cdr1*$^{+}$ were deleted in combination with *yox1*$^{+}$ overexpression (data not shown). Interestingly, the Δ*pef1* and Δ*cdr1* strains also share a synthetic negative interaction with the Δ*yox1* strain (Ryan *et al.* 2012). Altogether, these results suggest that the presence of either gene is crucial when *yox1*$^{+}$ is aberrantly expressed.

Our SDL screens revealed that that the uncharacterized transcription factor SPBC530.08 may be implicated in cell cycle regulation. SPBC530.08 clustered most closely with Tos4 when comparing the interaction profiles obtained from our SDL screens (Figure 4.4). This observation suggests that SPBC530.08 may play a role in the DNA damage checkpoint based on the known function of Tos4 in *S. cerevisiae* (Basto de Oliveira *et al.* 2012). Tos4 is regulated by the MBF complex in both budding and fission yeast, making it possible that SPBC530.08 has some role in the G1/S transition (Basto de Oliveira *et al.* 2012; Aligianni *et al.* 2009).

4.5 Discussion

In this study, we developed a modified SGA method for high-throughput screening of SDL interactions in *S. pombe*, and demonstrate its utility in identifying upstream regulators of transcription factors. The SDL screens were able to identify known regulators of transcription factors including the Sds23 and Cds1 kinases upstream of Scr1 and Yox1 transcription factors, respectively, as well as Ubr1 and Mua1 as novel putative regulators of Scr1. These regulators appeared to be repressors of their associated transcription factors, indicating that these SDL interactions may be due to an increase in aberrant regulation of target genes compared to the transcription factor overexpression strain alone. In addition, the screens uncovered a role for components of the SAGA complex, as well as the Set1 histone lysine methyltransferase, in the transcriptional regulation of Toe1 target genes.

4.5.1 Gene overexpression strains not amenable to SGA based SDL screens

Not all of the transcription factor overexpression strains were equally amenable to the SDL screening process. The SDL screens involving overexpression of the transcription factor genes *prz1*$^{+}$, *map1*$^{+}$, and SPCC1393.08 did not provide consistent results, as indicated by irregular growth and colony morphology. In these cases it is likely that the leakiness of the *nmt1* promoter caused increased expression of the transcription factor despite repressing conditions due to the presence of thiamine. Even mild overexpression of these transcription factors may result in fitness defects that make them less amenable to the SGA screening process. Defects in growth, cell adhesion, or mating

efficiency could alter the effectiveness of the robotic pinning or mating steps of the SGA procedure. SPCC1393.08 exhibited the most severe growth defect among the transcription factor genes in our SDL screens. Overexpression of *grt1*$^{+}$ and *gaf1*$^{+}$ transcription factor genes by the *nmt1* promoter were less problematic as SDL query strains, but did not result in three acceptable replicates and were therefore omitted. In the future, the complications associated with the *nmt1* promoter could be alleviated by using a weaker promoter such as *nmt41* or *nmt81* to overexpress the transcription factor gene.

4.5.2 Putative proteolysis of Scr1 protein by Ubr1 and Mua1

The increased levels of Scr1-GFP in the Δ*ubr1* strain suggested that Ubr1 is an E3 ubiquitin ligase that may target Scr1 for degradation. The regulation of Scr1 activity through degradation via the proteasome has not been shown. This result does not confirm that Ubr1 directly ubiquitinates Scr1, as Ubr1 could interact with another regulator or pathway that impinges on Scr1. Interestingly, the Δ*mua1* strain also exhibited higher levels of Scr1-GFP, providing additional support that Scr1 may be a substrate of Ubr1. The *S. cerevisiae* Mua1 ortholog, Mub1, interacts with Ubr2 in an E3 ubiquitin ligase complex (Ju *et al.* 2008; Andreson et al. 2010; Akiyoshi *et al.* 2013). The degradation of Sml1, an inhibitor of ribonucletide reductase, by the Rad6-Ubr2-Mub1 ubiquitin ligase is dependent on its phosphorylation upon exposure to DNA damage (Andreson *et al.* 2010). A similar mechanism may occur in the degradation of Scr1 as it is phosphorylated in response to low glucose levels in the cell (Matsuzawa *et al.* 2012).

4.5.3 Regulation of Toe1 target genes by the SAGA complex

We also discovered SDL interactions between *toe1*$^+$ overexpression and deletions of the SAGA genes *sgf29*$^+$ and *ubp8*$^+$, as well as the histone lysine methyltransferase encoded by *set1*$^+$. There is a strong connection between the H3K4 methylation by Set1 and the deubiquitination activity of Ubp8 in *S. cerevisiae,* which subsequently influence the HAT activity of Gcn5 (Henry *et al.* 2003; Dover *et al.* 2002). The connection between Ubp8 and Gcn5 mediated histone acetylation may not be as strong in *S. pombe* based on the divergence of transcriptome profiles in their respective deletion mutants (Helmlinger *et al.* 2011). Ubp8 deubiquitinates H2BK123 in *S. cerevisiae* which results in an increase in gene transcription in affected promoters (Henry *et al.* 2003). The loss of Ubp8 and subsequent increase in H2BK123 ubiquitination causes a specific increase of H3K4me3 by Set1 (Henry *et al.* 2003). Our observations of SDL interactions between the loss of *ubp8*$^+$ or *set1*$^+$ and the overexpression of *toe1*$^+$ would suggest a matching regulatory role for those two genes, which is not consistent with the results from Henry *et al.* (2003) which predict an increase in H3K4me3 in the Δ*ubp8* and a decrease in H3K4me3 in the Δ*set1*. It is possible that this pattern of histone modification may occur in genes other than *toe1*$^+$.

The reduced fitness from *toe1*$^+$overexpression is presumably caused by the inappropriate upregulation of its target genes. Therefore, the additive fitness reduction in SDL interactions involving *toe1*$^+$overexpression could be due to further aberrant regulation of its target genes. If this was the case, then we would anticipate that deletion of *sgf29*$^+$, *ubp8*$^+$, or *set1*$^+$ would result in an upregulation of Toe1 targets compared to wild type. This prediction was not supported, as expression of the Toe1 target genes

urg1$^+$, *urg2*$^+$, *urg3*$^+$, and SPAC1399.04c were downregulated in the Δ*set1* and Δ*sgf29* strains relative to wild type. One possible explanation for this discrepancy could be that Sgf29 or Set1 is required for activation of Toe1 target genes and that *toe1*$^+$overexpression in the Δ*sgf29* or Δ*set1* strain may result in the regulation of off-target genes with lower binding affinity motifs in their promoters, thereby causing cellular toxicity. Alternatively, *toe1*$^+$overexpression could regulate other genes that are synthetic-lethal with loss of *urg1*$^+$, *urg2*$^+$, *urg3*$^+$, or SPAC1399.04c function caused in the Δ*sgf29* or Δ*set1* backgrounds. Similarly, the Toe1 target genes were also downregulated in the Δ*gcn5* strain relative to wild type. However, *gcn5*$^+$ may have differing effects on gene expression compared to the rest of the SAGA genes in this study (Helmlinger *et al.* 2008). Consistent with this is that the loss of *gcn5*$^+$ did not exhibit a SDL interaction with *toe1*$^+$overexpression.

4.5.4 SDL interactions with S. pombe transcription factors

Transcription factors are highly regulated by multiple signaling elements (Chuikov *et al.* 2004; Gostissa *et al.* 1999; Salghetti *et al.* 2001; Andreson *et al.* 2010) that can be identified using SDL screening. The SDL interactions recovered from our screens appeared to be biased for repressors of the transcription factor. This SDL approach can allow for comprehensive identification of posttranslational regulators of transcription factors, as well as provide a better view of the genetic crosstalk of transcription factors with other systems.

Chapter Five: **Discussion**

5.1 Summary of key findings

This work looked at transcriptional regulation at multiple levels in *S. pombe*. This included looking for the downstream target genes of Prz1, functional redundancy between transcription factors, and the upstream regulators of fourteen transcription factors. Finding the target genes of the transcription factor Prz1 illuminated its role within the cell and expanded the transcriptional network in *S. pombe*. The conservation of target genes across species revealed conserved and diverged downstream processes. Only five downstream target genes had previously been identified for Prz1. This work expanded the number of putative target genes activated by Prz1 to 165, as assessed under three different inducing conditions. Surprisingly, 92 putative negatively regulated target genes were also discovered, and showed good enrichment for Prz1 binding. These negative target genes included several involved in flocculation. The identification of genes inhibited by Prz1 was surprising as none of its Crz1 orthologues in yeast had been identified as negative regulators of transcription. Prz1 did have a conserved role in cell wall biogenesis or organization, and a novel role in reproduction.

The genetic interactions between transcription factors have only been sparsely mapped in *S. pombe.* Genetic screens reveal the genetic interaction network topology of the cell, and can be used in comparative studies. *S. cerevisiae* and *S. pombe* are separated by ~380 million years of evolution, and because of this large divergence any genetic interactions that are conserved are also more likely to be conserved in higher eukaryotes (Tosti *et al*. 2014; Vizeaccoumar *et al.* 2013). This conservation is critical as negative genetic interactions make good candidates for targets in cancer therapies (Tosti *et al.*

2014; Vizeaccoumar *et al.* 2013). A drug target that is lethal in combination with cancerous mutations but not lethal in a normal cell line, should have fewer negative side effects (Tosti *et al.* 2014; Vizeaccoumar *et al.* 2013). The genetic interactions identified in this SGA screen dramatically increased the number of negative and positive interactions mapped in *S. pombe* transcription factors. This screen shows transcription factors that may share common targets or cause disruption to related systems. We performed a Prz1 full genome screen which had been previously done by Ryan *et al.* (2012). These two screens only show moderate agreement due to the noise inherent in high-throughput SGA screens, and differences in methodology (Dixon *et al.* 2008; Roguev *et al.* 2008). Two of the genes that negatively interacted with *prz1*$^{+}$ were used to look at genetic activation. The first gene, *pmr1*$^{+}$, worked well as a genetic activator of Prz1 when deleted, while the second gene, *alp31*$^{+}$, did not increase Prz1 activity when deleted.

Finally, we used a new SDL screen design for *S. pombe* to look for regulators of fourteen transcription factors. The screen uncovered several novel SDL interactions between the transcription factors and the regulators on the miniarray. The methodology was confirmed with the discovery of two known interactions between Δ*cds1* and *yox1OE*, and between Δ*sds23* and *scr1OE*. The screen predicted two novel putative upstream regulators of Scr1: Ubr1 and Mua1, an E3 ligase and a MYND domain protein, respectively. A deletion in either gene increased Scr1-GFP levels in the cell, suggesting that these proteins regulate Scr1 protein levels. The *S. cerevisiae* orthologs of these two genes encode for Ubr2 and Mub1 which physically associate in a ubiquitin ligase complex to degrade their target proteins (Ju *et al.* 2008; Andreson *et al*. 2010; Akiyoshi

et al. 2013). The screen also uncovered a relationship between the *toe1OE* and several components of the SAGA complex.

5.2 Future directions

The negative regulation of Prz1 target genes prompts several interesting questions. One of which is whether this mechanism is conserved in other species. Because most of the experiments in other species do not use chIP data, it is possible that negatively-regulated target genes were missed in the analysis (Yoshimoto *et al.* 2002; Karababa *et al.* 2006; Chen *et al*. 2012; Hagiwara *et al*. 2008; Soriani *et al.* 2008). Two studies in *C. glabrata* and *A. fumigatus* identified negatively-regulated target genes, but the regulation was not confirmed with direct DNA-binding data (Chen *et al*. 2012; Soriani *et al.* 2008). This leaves open the possibility that negative regulation is a conserved function for Prz1 orthologs. One study in the rice blast fungus, *Magnaporthe oryzae*, identified 19 genes negatively regulated by MoCRZ1 that overlapped with their chIP-binding data (Kim *et al.* 2010b). This indicates that negative regulation may be conserved in at least some of the orthologs, and is not unique to *S. pombe*. Interestingly, the MoCRZ1 paper found two binding motifs among their positive and negative targets, a sequence similar to the CDRE motif, 5'-CAC[AT]GCC-3', and a second sequence 5'-TTGNTTG-3'. The evolution of a second binding motif may be a component of the negative regulation, as a second motif, 5'-CAACT-3', has also been suggested in *S. pombe* (Hamasaki-Katagiri and Ames 2010). An in vitro binding study of Prz1 could be used to confirm the predicted binding sequences for the transcription factor and potentially clarify the role of the DNA sequence specificity in the divergent regulation of the target genes. Regulatory cofactors

can also alter the nature of transcriptional regulation. Studies looking at protein association, as well as the location of the Prz1 binding site relative to the promoter, could illuminate the nature of the negative regulation.

While the SGA *S. pombe* transcription factor screen dramatically increased the number of putative pairwise interactions explored, it is still an incomplete network. The next step would be to complete the full 92×92 genetic map to create the full genetic interaction network among *S. pombe* transcription factors. Once the network is complete, a more comprehensive analysis of the conserved interactions with *S. cerevisiae* can be explored. This includes an exploration of the network trends between the two networks (Zheng *et al.* 2010). Surprisingly, the *S. pombe* network shows more negative interactions than the *S. cerevisiae* screen, despite the fact that *S. pombe* has fewer transcription factors, which might suggest lower functional overlap (Zheng *et al.* 2010; Beskow and Wright 2006). There were also differences between the *S. pombe* genetic interactions identified by this screen and the ones identified by Ryan *et al.* (2012). These differences could be the result of noise, differences in experimental procedure, or in the case of the *S. cerevisiae* screen, evolutionary divergence.

One example of a difference in procedure was that the Zheng *et al.* (2010) and Ryan *et al.* (2012) screens resulted in a homogenous population of mating types, while the protocol used in this study from Dixon *et al.* (2008) resulted in a heterogeneous population of the two mating types. Another difference is the selection of mated cells. In *S. cerevisiae,* haploids are selected by transferring the cells to media with low levels of carbon and nitrogen (Zheng *et al.* 2010), while cycloheximide drug resistance selection markers were employed by Ryan *et al.* (2012) in *S. pombe*. The protocol in some *S.*

pombe studies, including this study, use a heat selection step at 42°C to kill unmated cells (Dixon *et al.* 2008). There were also differences in the normalization and scoring used (Zheng *et al.* 2010; Dixon *et al.* 2008). Each difference in methodology potentially changes the genetic interactions observed. The decision of what cut-off to use to define genetic interactions would also affect the overlap by altering the number of hits. In fact, slightly relaxing the cut-off used by Zheng *et al.* (2010) adds a biologically conserved interaction between SPBC3F10.12c and *php3*$^{+}$ with their *S. cerevisiae* orthologs *CBF1* and *HAP3*. However, to obtain this single new point of overlap, 1089 new interactions are predicted, in addition to 3333 discovered in the screen with the original cut-off value. This illustrates the critical challenge of picking a cut-off to maximize the signal to noise ratio.

The hypothesis that negative genetic interactions could be used to identify genetic backgrounds that result in activation of a transcription factor was demonstrated. The deletion of the calcium ion transporter gene, *pmr1*$^{+}$, was able to increase the activity of Prz1. However, the deletion of *alp31*$^{+}$, involved in the β-tubulin pathway, did not increase Prz1 activity. The main difference observed between these two genetic interactions was the severity of the single mutant growth defect. The Δ*alp31* strain was much sicker than Δ*pmr1* strain. This could suggest that very sick mutants do not make good genetic backgrounds for the activation of transcription factors. In addition the expression of *alp31*$^{+}$ was increased in the Δ*prz1* mutant relative to wild type. This may indicate that *alp31*$^{+}$ is the dominant gene in the negative interaction, and in this case, loss of *prz1*$^{+}$ may induce Alp31 activity. This suggests that genes that exhibit increased expression in the transcription factor mutant may fail to genetically activate a

transcription factor. This would not always be the case as some highly expressed genes could be direct targets repressed by the transcription factor. Moreover, it would not predict cases where the activity of the protein changed without a matching increase in gene expression in the transcription factor deletion strain. This analysis is only possible in cases where microarray data is available for the transcription factor of interest, which is a limiting factor in *S. pombe*. This analysis might be more useful for finding genetic activators in *S. cerevisiae* where both large scale SGA data and microarray screens are available (Costanzo *et al.* 2010; Hu *et al.* 2007).

Other high-throughput genetic screens have been designed in *S. cerevisiae* that could be applied to better identify instances of genetic activation of transcription factors. Two-colour cell array screens use high-throughput robotic pinning to mate a variety of deletion mutants to a GFP reporter that has been fused to a promoter of interest (Fillingham *et al.* 2009). The fluorescent intensity of the GFP reporter is measured with a scanning fluorimager and normalized relative to the expression of an RFP control driven by a ribosomal promoter (Fillingham *et al.* 2009). This technique was used to find transcriptional regulators of the *S. cerevisiae* histone genes (Fillingham *et al.* 2009). It could be applied to look for genetic activation in cases where at least one direct target gene of the transcription factor has been identified. This could be auto-regulation in the case of Prz1, or a downstream target gene promoter.

A second technique, high-content screening (HCS), mates a strain containing an endogenous GFP-tagged gene of interest with a library of deletion mutants (Vizeacoumar *et al.* 2010). This is combined with high-throughput microscopy and image analysis to see the effect of each mutation on the activity of the protein (Vizeacoumar *et al.* 2010).

This approach was used to look for genes that caused defects in spindle morphogenesis with a GFP-tagged tubulin gene (Vizeacoumar *et al.* 2010). In some cases, these screens would work to identify genetic perturbations that induce transcription factor activity. This technique would be applicable to transcription factors like Prz1, where activation involves a localization shift from the cytoplasm to the nucleus (Hirayama *et al.* 2003). While this screen is more complicated because of the added step of high-throughput fluorescence microscopy, it has the added benefit of potentially detecting upstream regulators as well.

The *S. pombe* SDL screen was able to detect multiple novel interactions. This screen was able to uncover interactions that likely result in the direct posttranslational modification of the transcription factor. In addition, it uncovered the regulation of transcription factor target genes at the chromatin level. The diversity of genetic interactions generated by the SDL screen allows it to uncover a wide variety of regulatory interactions. The downside is that it can be difficult to pin down the nature of each SDL interaction. SDL interactions can also miss physical interactions that have a neutral or positive effect on colony growth. The screen was not able to detect the known relationship between Scr1 and Ssp2 because the combination of mutants did not cause a fitness defect. Other known interactions such as the physical one between Sre2 and Dsc1 or the genetic one between *mbx1*$^{+}$ and *pmk1*$^{+}$ were also missed by the screen. Some of these interactions may have been caught with a dosage suppression screen (Magtanong *et al.* 2011), but many interactions cannot be detected based on a simple fitness readout. These screens become more powerful when combined with other types of data. Multiple experiments would work to clarify the data such as affinity purification, protein

microarrays, yeast two-hybrid, computational modeling, or high-throughput genetic technique like HCS. The presence of O-phospho-L-serine and O-phospho-L-threonine modification sites in the Sfp1 transcription factor suggests that the strong genetic interaction with the gene encoding the serine/threonine protein kinase Ppk25 may be the result of a physical interaction (Koch *et al.* 2011; Wood *et al.* 2012).

Like SGA, the power of SDL performed in yeast is amplified by studies in distantly-related species. To our knowledge, high-throughput SDL screens have not been performed in multicellular organisms. The availability of a technique in a second model organism will increase the predictive power of the SDL interactions discovered in yeast. SDL interactions that are conserved across the evolutionary distance between *S. cerevisiae* and *S. pombe* are more likely to be predictive of interactions conserved in humans. These conserved interactions could be applicable to medicine as some cancers are characterized by gain-of-function mutations (Cermelli *et al.* 2014).

5.3 Thoughts and considerations

This study has substantially expanded our knowledge of transcription factors in the fission yeast *S. pombe*. We conducted expression and chIP microarrays to uncover target genes of Prz1, we performed a genetic interactions screen among the sequence-specific transcription factors, and developed a SDL screen to further explore SDL interactions with *S. pombe* transcription factors. This work substantially increased the number of target genes for Prz1 and uncovered an undocumented role as a repressor of some of its target genes. The functional redundancy between transcription factors was mapped by SGA, and very low conservation was discovered with *S. cerevisiae*. This provides

evidence that the transcription genetic interaction network may not be well conserved between species. We also explored negative interactions discovered by SGA screens as a source for genetic backgrounds that increase transcriptional activity. With further refinement this could be a new systematic approach for finding activating conditions for transcription factors. We developed a protocol for measuring SDL interactions in *S. pombe*. This protocol has proven useful for finding regulators of transcription factors and could be applied to other cellular processes in *S. pombe*. High-throughput genetics offers a platform to look at transcriptional regulation. The work in *S. pombe* could in isolation, or in combination with studies in *S. cerevisiae,* predict specific interactions or general mechanisms of transcriptional-regulatory networks. These prediction may have implications in our broader understanding of transcription programs and the treatment of complex genetic diseases.

References

Aberle, H., A. Bauer, J. Stappert, A. Kispert, and R. Kemler, 1997 Beta-catenin is a target for the ubiquitin-proteasome pathway. EMBO J 16: 3797–3804.

Akiyoshi, B., C. R. Nelson, N. Duggan, S. Ceto, J. A. Ranish, *et al.*, 2013 The Mub1/Ubr2 ubiquitin ligase complex regulates the conserved Dsn1 kinetochore protein. PLoS Genet 9: e1003216.

Aligianni, S., D. H. Lackner, S. Klier, G. Rustici, B. T. Wilhelm, *et al.*, 2009 The fission yeast homeodomain protein Yox1p binds to MBF and confines MBF-dependent cell-cycle transcription to G1-S via negative feedback. PLoS Genet 5: e1000626.

Alonso-Nuñez, M. L., H. An, A. B. Martín-Cuadrado, S. Mehta, C. Petit, *et al.*, 2005 Ace2p controls the expression of genes required for cell seperation in *Schizosaccharomyces pombe*. Mol Biol Cell 16: 2003–2017.

Andreishcheva, E. N., J. P. Kunkel, T. R. Gemmill, and R. B. Trimble, 2004 Five genes involved in biosynthesis of the pyruvylated Galβ1,3-Epitope in *Schizosaccharomyces Pombe* N-linked glycans. J Biol Chem 279: 35644-35655.

Andreson, B. L., A. Gupta, B. P. Georgieva, and R. Rothstein, 2010 The ribonucleotide reductase inhibitor, Sml1, is sequentially phosphorylated, ubiquitylated and degraded in response to DNA damage. Nucleic Acids Res 38: 6490–6501.

Araki, Y., H. Wu, H. Kitagaki, T. Akao, H. Takagi, *et al*., 2009 Ethanol stress stimulates the Ca^{2+}-mediated calcineurin/Crz1 pathway in *Saccharomyces cerevisiae*. J Biosci Bioeng 107: 1-6.

Atanesyan, L., V. Günther, B. Dichtl, O. Georgiev, and W. Schaffner, 2012 Polyglutamine tracts as modulators of transcriptional activation from yeast to mammals. Biol Chem 393: 63–70.

Bailey, T. L., and C. Elkan, 1994 Fitting a mixture model by expectation maximization to discover motifs in biopolymers. Proc Sec Int Conf Intell Syst Mol Biol: 28-36.

Babu, M., J. J. Díaz-Mejía, J. Vlasblom, A. Gagarinova, S. Phanse, *et al.,* 2011 Genetic interaction maps in *Escherichia coli* reveal functional crosstalk among cell envelope biogenesis pathways. PLoS Genet 7: e1002377.

Badis, G., E. T. Chan, H. van Bakel, L. Pena-Castillo, D. Tillo, *et al.,* 2008 A library of yeast transcription factor motifs reveals a widespread function for Rsc3 in targeting nucleosome exclusion at promoters. Mol Cell 32: 878-887.

Bai, C., P. Sen, K. Hofmann, L. Ma, M. Goebi, *et al.*, 1996 SKP1 connects cell cycle regulators to the ubiquitin proteolysis machinery through a novel motif, the F-box. Cell 86: 263-274.

Barlev, N. A., L. Liu, N. H. Chehab, K. Mansfield, K. G. Harris, *et al.*, 2001 Acetylation of p53 activates transcription through recruitment of coactivators/histone acetyltransferases. Mol Cell 8: 1243–1254.

Baryshnikova, A., M. Costanzo, Y. Kim, H. Ding, J. Koh, *et al*., 2010 Quantitative analysis of fitness and genetic interactions in yeast on a genome scale. Nat Methods 7: 1017-1024.

Bastos de Oliveira, F. M., M. R. Harris, P. Brazauskas, R. A. M. de Bruin, and M. B. Smolka, 2012 Linking DNA Replication Checkpoint to MBF Cell-Cycle Transcription Reveals a Distinct Class of G1/S Genes. EMBO J 31: 1798–1810.

Beskow, A., and A. P. H. Wright, 2006 Comparative analysis of regulatory transcription factors in *Schizosaccharomyces pombe* and budding yeasts. Yeast 23: 929-935.

Bian, C., C. Xu, J. Ruan, K. K. Lee, T. L. Burke, *et al.*, 2011 Sgf29 binds histone H3K4me2/3 and is required for SAGA complex recruitment and histone H3 acetylation. EMBO J 30: 2829–2842.

Bodvard, K., A. Jörhov, A. Blomberg, M. Molin, and M. Käll, 2013 The yeast transcription factor Crz1 Is activated by light in a Ca^{2+}/calcineurin-dependent and PKA-independent manner. PloS One 8: e53404.

Boyer, L. A., T. I. Lee, M. F. Cole, S. E. Johnstone, S. S. Levine, *et al.*, 2005 Core transcriptional regulatory circuitry in human embryonic stem cells. Cell 122: 947-956.

Boyle, E. I., S. Weng, J. Gollub, H. Jin, D. Botstein, *et al.*, 2004 GO::TermFinder-open source software for accessing Gene Ontology information and finding significantly enriched Gene Ontology terms associated with a list of genes. Bioinformatics 20: 3710-3715.

Brownell, J. E., J. Zhou, T. Ranalli, R. Kobayashi, D. G. Edmondson, *et al*., 1996 Tetrahymena histone acetyltransferase A: a homologue to yeast Gcn5p linking histone acetylation to gene activation. Cell 84: 843-851.

Buck, M. J., A. B. Nobel, and J. D. Lieb. 2005 ChIPOTle: A user-friendly tool for the analysis of chIP-chip data. Genome Biol 6: R97.

Byrne, A. B., M. T. Weirauch, V. Wong, M. Koeva, S. J. Dixon, *et al*., 2007 A global analysis of genetic interactions in *Caenorhabditis elegans*. J Biol 6: 8.

Cai, L., C. K. Dalal, and M. B. Elowitz, 2008 Frequency-modulated nuclear localization bursts coordinate gene regulation. Nature 455: 485-490.

Caligiuri, M., and D. Beach, 1993 Sct1 functions in partnership with Cdc10 in a transcription complex that activates cell cycle START and inhibits differentiation. Cell 72: 607–619.

Cam, H. P., T. Sugiyama, E. S. Chen, X. Chen, P. C. FitzGerald, *et al.*, 2005 Comprehensive analysis of heterochromatin- and RNAi-mediated epigenetic control of the fission yeast genome. Nat Genet 37: 809-819.

Cermelli, S., I. S. Jang, B. Bernard, and C. Grandori, 2014 Understand and treat MYC-driven cancers. Cold Spring Harb Perspect Med 4: a014209.

Chan, E. T., G. T. Quon, G. Chua, T. Babak, M. Trochesset, *et al*., 2009 Conservation of core gene expression in vertebrate tissues. J Biol 8: 33.

Chatfield-Reed, K., L. Vachon, E.-J. G. Kwon, and G. Chua, 2016 Conserved and diverged functions of the calcineurin-activated Prz1 transcription factor in fission yeast. Genetics 202: 1365–1375.

Chen, J. L., L. D. Attardi, C. P. Verrijzer, K. Yokomori, and R. Tjian, 1994 Assembly of recombinant TFIID reveals differential coactivator requirements for distinct transcriptional activators. Cell 79: 93–105.

Chen, Y.-L., J. H. Konieczka, D. J. Springer, S. E. Bowen, J. Zhang, *et al*., 2012 Convergent evolution of calcineurin pathway roles in thermotolerance and virulence in *Candida glabrata*. G3 2: 675-691.

Chen, D., C. R. M. Wilkinson, S. Watt, C. J. Penkett, W. M. Toone, *et al.*, 2008 Multiple pathways differentially regulate global oxidative stress responses in fission yeast. Mol Biol Cell 19: 308-317.

Chi, Y., M. J. Huddleston, X. Zhang, R. A. Young, R. S. Annan, *et al.*, 2001 Negative regulation of Gcn4 and Msn2 transcription factors by Srb10 cyclin-dependent kinase. Genes Dev 15: 1078-1092.

Chua, G., 2013 Systematic genetic analysis of transcription factors to map the fission yeast transcription-regulatory network. Bioc Soc T 41: 1696-1700.

Chua, G., Q. D. Morris, R. Sopko, M. D. Robinson, O. Ryan, *et al.*, 2006 Identifying transcription factor functions and targets by phenotypic activation. P Natl Acad Sci USA 103: 12045-12050.

Chuikov, S., J. K. Kurash, J. R. Wilson, B. Xiao, N. Justin, *et al*., 2004 Regulation of p53 activity through lysine methylation. Nature 432: 353–360.

Chwang, W. B., K. J. O'Riordan, J. M. Levenson, and J. D. Sweatt, 2006 ERK/MAPK regulates hippocampal histone phosphorylation following contextual fear conditioning. Learn Memory 13: 322–328.

Cisneros-Barroso, E., T. Yance-Chávez, A. Kito, R. Sugiura, A. Gómez-Hierro, *et al.*, 2014 Negative feedback regulation of calcineurin-dependent Prz1 transcription factor by the CaMKK-CaMK1 axis in fission yeast. Nucleic Acids Res 42: 9573-9587.

Clipstone, N. A., and G. R. Crabtree, 1992 Identification of calcineurin as a key signalling enzyme in T-lymphocyte activation. Nature 357: 695-697.

Coleman, T. R., Z. Tang, and W. G. Dunphy, 1993 Negative regulation of the Wee1 protein kinase by direct action of the Nim1/Cdr1 mitotic inducer. Cell 72: 919–929.

Corey, L. L., C. S. Weirich, I. J. Benjamin, and R. E. Kingston, 2003 Localized recruitment of a chromatin-remodeling activity by an activator in vivo drives transcriptional elongation. Genes Dev 17: 1392–1401.

Corkins, M. E., M. May, K. M. Ehrensberger, Y.-M. Hu, Y.-H. Liu, *et al.*, 2013 Zinc finger protein Loz1 is required for zinc-responsive regulation of gene expression in fission yeast. Proc. Natl. Acad. Sci. U.S.A. 110: 15371–15376.

Cortés, J. C. G., R. Katoh-Fukui, K. Moto, J. C. Ribas, and J. Ishiguro, 2004 *Schizosaccharomyces pombe* Pmr1p is essential for cell wall integrity and is required for polarized cell growth and cytokinesis. Eukaryot Cell 3: 1124-1135.

Costanzo, M., A. Baryshnikova, J. Bellay, Y. Kim, E. D. Spear, *et al*., 2010 The genetic landscape of a cell. Science 327: 425–431.

Deng, L., R. Sugiura, M. Takeuchi, M. Suzuki, H. Ebina, *et al*., 2006 Real-time monitoring of calcineurin activity in living cells: evidence for two distinct Ca^{2+}-dependent pathways in fission yeast. Mol Biol Cell 17: 4790-4800.

Deplancke, B., A. Mukhopadhyay, W. Ao, A. M. Elewa, C. A. Grove, *et al*., 2006 A gene-centered *C. elegans* protein-DNA interaction network. Cell 125: 1193–1205.

Deshpande, R., M. K. Asiedu, M. Klebig, S. Sutor, E. Kuzmin, *et al*., 2013 A comparative genomic approach for identifying synthetic lethal interactions in human cancer. Cancer Res 73: 6128–6136.

Dixon, S. J., Y. Fedyshyn, J. L. Y. Koh, T. S. K. Prasad, C. Chahwan, *et al.*, 2008 Significant conservation of synthetic lethal genetic interaction networks between distantly related eukaryotes. Proc. Natl. Acad. Sci. U.S.A. 105: 16653–16658.

Dover, J., J. Schneider, M. A. Tawiah-Boateng, A. Wood, K. Dean, *et al*., 2002. Methylation of histone H3 by COMPASS requires ubiquitination of histone H2B by Rad6. J Biol Chem 277: 28368–71.

Duffy, S. K., H. Friesen, A. Baryshnikova, J.P. Lambert, Y. T. Chong, *et al*., 2012 Exploring the yeast acetylome using functional genomics. Cell: 149: 936-948.

Dürr, G., J. Strayle, R. Plemper, S. Elbs, S. K. Klee, *et al.*, 1998 The medial-Golgi ion pump Pmr1 supplies the yeast secretory pathway with Ca^{2+} and Mn^{2+} required for glycosylation, sorting, and endoplasmic reticulum-associated protein degradation. Mol Biol Cell 9: 1149-1162.

Ea, C.-K., and D. Baltimore, 2009 Regulation of NF-kappaB activity through lysine monomethylation of p65. Proc. Natl. Acad. Sci. U.S.A. 106: 18972–18977.

Edlind, T., L. Smith, K. Henry, S. Katiyar, and J. Nickels, 2002 Antifungal activity in *Saccharomyces cerevisiae* is modulated by calcium signalling. Mol Microbiol 46: 257-268.

Eisen, M. B., P. T. Spellman, P. O. Brown, and D. Botstein, 1999 Cluster analysis and display of genome-wide exopresion patterns. P Natl Acad Sci USA 95: 12930-12933.

Fardeau, V., G. Lelandais, A. Oldfield, H. Salin, S. Lemoine, *et al.*, 2007 The central role of PDR1 in the foundation of yeast drug resistance. J Biol Chem 282: 5063-5074.

Ferreira, R. T., A. R. Courelas Silva, C. Pimentel, L. Batista-Nascimento, C. Rodrigues-Pousada, *et al.*, 2012 Arsenic stress elicits cytosolic Ca^{2+} bursts and Crz1 activation in *Saccharomyces cerevisiae*. Microbiol 158: 2293-2302. acetylome using functional genomics. Cell 149: 936–948.

Fiedler, D., H. Braberg, M. Mehta, G. Chechik, G. Cagney, *et al.*, 2009 Functional organization of the *S. cerevisiae* phosphorylation network. Cell 136: 952–963.

Fillingham, J., P. Kainth, J. P. Lambert, H. van Bakel, K. Tsui, L. *et al.*, 2009 Two-color cell array screen reveals interdependent roles for histone chaperones and a chromatin boundary regulator in histone gene repression. Mol Cell 35: 340–351.

Garg, A., B. Futcher, and J. Leatherwood, 2015 A new transcription factor for mitosis: in *Schizosaccharomyces pombe*, the RFX transcription factor Sak1 works with forkhead factors to regulate mitotic expression. Nucleic Acids Res 43: 6874–6888.

Gerber, A. P., D. Herschlag, and P. O. Brown, 2004 Extensive association of functionally and cytotopically related mRNAs with Puf family RNA-binding proteins in yeast. PLoS Biol 2: 342–354.

Gerber, A. P., S. Luschnig, M. A. Krasnow, P. O. Brown, and D. Herschlag, 2006 Genome-wide identification of mRNAs associated with the translational regulator PUMILIO in *Drosophila melanogaster*. Proc. Natl. Acad. Sci. U.S.A. 103: 4487–4492.

Giaever, G., A. M. Chu, L. Ni, C. Connelly, L. Riles, *et al.*, 2002 Functional profiling of the *Saccharomyces cerevisiae* genome. Nature 418: 387–391.

Gómez-del Arco, P., J. Koipally, and K. Georgopoulos, 2005 Ikaros SUMOylation: switching out of repression. Mol Cell Biol 25: 2688–2697.

Gómez-Escoda, B., T. Ivanova, I. A. Calvo, I. Alves-Rodrigues, E. Hidalgo, *et al.*, 2011 Yox1 links MBF-dependent transcription to completion of DNA synthesis. EMBO Rep 12: 84–89.

Gostissa, M., A. Hengstermann, V. Fogal, P. Sandy, S. E. Schwarz, *et al.*, 1999 Activation of p53 by conjugation to the ubiquitin-like protein SUMO-1. EMBO J 18: 6462–6471.

Graef, I. A., F. Chen, L. Chen, A. Kuo, and G. R. Crabtree, 2001 Signals transduced by Ca^{2+}/calcineurin and NFATc3/c4 pattern the developing vasculature. Cell 105: 863-875.

Hagen, G., S. Müller, M. Beato, and G. Suske, 1994 Sp1-mediated transcriptional activation is repressed by Sp3. EMBO J 13: 3843–3851.

Hagiwara, D., A. Kondo, T. Fujioka, and K. Abe, 2008 Functional analysis of C_2H_2 zinc finger transcription factor CrzA involved in calcium signaling in *Aspergillus nidulans*. Curr Genet 54: 325-338.

Hamasaki-Katagiri, N., and J. B. Ames, 2010 Neuronal calcium sensor-1 (Ncs1p) is up-regulated by calcineurin to promote Ca^{2+} tolerance in fission yeast. J Biol Chem 285: 4405-4414.

Harbison, C. T., D. B. Gordon, T. I. Lee, N. J. Rinaldi, K. D. Macisaac, *et al*., 2004 Transcriptional regulatory code of eukaryotic genome. Nature 431: 99–104.

Harrison, C., S. Katayama, S. Dhut, D. Chen, N. Jones, *et al.*, 2005 SCF(Pof1)-ubiquitin and its target Zip1 transcription factor mediate cadmium response in fission yeast. EMBO J 24: 599–610.

Hatano, T., S. Morigasaki, H. Tatebe, K. Ikeda, and K. Shiozaki, 2015 Fission yeast Ryh1 GTPase activates Tor Complex 2 in response to glucose. Cell Cycle 14: 848–856.

Helenius, J., and M. Aebi, 2002 Transmembrane movement of dolichol linked carbohydrates during N-glycoprotein biosynthesis in the endoplasmic reticulum. Semin Cell Dev Biol 13: 171–178.

Helmlinger, D., S. Marguerat, J. Villén, S. P. Gygi, J. Bähler, *et al.*, 2008 The *S. pombe* SAGA complex controls the switch from proliferation to sexual differentiation through the opposing roles of its subunits Gcn5 and Spt8. Genes Dev 22: 3184–3195.

Helmlinger, D., S. Marguerat, J. Villén, D. L. Swaney, S. P. Gygi, *et al*., 2011. Tra1 has specific regulatory roles, rather than global functions, within the SAGA co-activator complex. EMBO J 30: 2843–2852.

Hendey, B., C. B. Klee, and F. R. Maxfield, 1992 Inhibition of neutrophil chemokinesis on vitronectin by inhibitors of calcineurin. Science 258: 296-299.

Henry, K. W., A. Wyce, W.-S. Lo, L. J. Duggan, N. C. T. Emre, *et al*., 2003 Transcriptional activation via sequential histone H2B ubiquitylation and deubiquitylation, mediated by SAGA-associated Ubp8. Genes Dev 17: 2648–2663.

Hirayama, S., R. Sugiura, Y. Lu, T. Maeda, K. Kawagishi, *et al*., 2003 Zinc finger protein Prz1 regulates Ca^{2+} but not Cl^{-} homeostasis in fission yeast. Identification of distinct branches of calcineurin signaling pathway in fission yeast. J Biol Chem 278: 18078–18084.

Hoppe, T., K. Matuschewski, M. Rape, S. Schlenker, H. D. Ulrich, *et al.*, 2000 Activation of a membrane-bound transcription factor by regulated ubiquitin/proteasome-dependent processing. Cell 102: 577–586.

Hu, Z., P. J. Killion, and V. R. Iyer. 2007 Genetic reconstruction of a functional transcriptional regulatory network. Nat Genet 39: 683-687.

Huang, J., R. Sengupta, A. B. Espejo, M. G. Lee, J. A. Dorsey, *et al*., 2007 p53 is regulated by the lysine demethylase LSD1. Nature 449: 105–109.

Huang, S., M. Litt, and G. Felsenfeld, 2005 Methylation of histone H4 by arginine methyltransferase PRMT1 is essential in vivo for many subsequent histone modifications. Genes and Development 19: 1885–1893.

Ikeda, Y., T. Ohashi, N. Tanaka, and K. Takegawa. 2009 Identification and characterization of a gene required for α1,2-mannose extension in the O-linked glycan synthesis pathway in *Schizosaccharomyces pombe*. FEMS Yeast Res 9: 115-125.

Ioannoni, R., J. Beaudoin, L. Lopez-Maury, S. Codlin, J. Bähler, 2012 Cuf2 is a novel meiosis-specific regulatory factor of meiosis maturation. PLoS ONE 7: e36338.

Ivanova, T., I. Alves-Rodrigues, B. Gómez-Escoda, C. Dutta, J. A. DeCaprio, *et al.*, 2013 The DNA damage and the DNA replication checkpoints converge at the MBF transcription factor. Mol Biol Cell 24: 3350–3357.

Janke, C., M. M. Magiera, N. Rathfelder, C. Taxis, S. Reber, *et al*., 2004 A versatile toolbox for PCR-based tagging of yeast genes: New fluorescent proteins, more markers and promoter substitution cassettes. Yeast 21: 947–962.

Janoo, R. T. K., L. A. Neely, B. R. Braun, S. K. Whitehall, and C. S. Hoffman, 2001 Transcriptional regulators of the *Schizosaccharomyces pombe fbp1* gene include two redundant Tup1p-like corepressors and the CCAAT binding factor activation complex. Genetics 157: 1205–1215.

Jarvela, A. M. C., and V. F. Hinman, 2015 Evolution of transcription factor function as a mechanism for changing metazoan developmental gene regulatory networks. EvoDevo 6: 3.

Joo, H.-Y., L. Zhai, C. Yang, S. Nie, H. Erdjument-Bromage, *et al.*, 2007 Regulation of cell cycle progression and gene expression by H2A deubiquitination. Nature 449: 1068–1072.

Ju, D., X. Wang, H. Xu, and Y. Xie, 2008 Genome-wide analysis identifies MYND-domain protein Mub1 as an essential factor for Rpn4 ubiquitylation. Mol Cell Biol 28: 1404–1412.

Kadam, S., and B. M. Emerson, 2003 Transcriptional specificity of human SWI/SNF BRG1 and BRM chromatin remodeling complexes. Mol Cell 11: 377–389.

Kakkis, E., K. J. Riggs, W. Gillespie, and K. Calame, 1989 A transcriptional repressor of c-Myc. Nature 339: 718–721.

Karababa, M., E. Valentino, G. Pardini, A. T. Coste, J. Bille, *et al.*, 2006 CRZ1, a target of the calcineurin pathway in *Candida albicans*. Mol Microbiol 59: 1429-1451.

Käufer, N F, and J Potashkin, 2000 Analysis of the splicing machinery in fission yeast: A comparison with budding yeast and mammals. Nucleic Acids Res 28: 3003–3010.

Käufer, N. F., V. Simanis, and P. Nurse, 1985 Fission yeast *Schizosaccharomyces pombe* correctly excises a mammalian RNA transcript intervening sequence. Nature 318: 78–80.

Kennedy, P. J., A. A. Vashisht, K. L. Hoe, D. U. Kim, H. O. Park, *et al.*, 2008 A genome-wide screen of genes involved in cadmium tolerance in *Schizosaccharomyces pombe*. Toxicol Sci 106: 124–139.

Kim, D.-U., J. Hayles, D. Kim, V. Wood, H.-O. Park, *et al.*, 2010 Analysis of a genome-wide set of gene deletions in the fission yeast *Schizosaccharomyces pombe*. Nat Biotechnol 28: 617–623.

Kim, S., J. Hu, Y. Oh, J. Park, J. Choi, *et al*., 2010b Combining chIP-Chip and expression profiling to model the MoCRZ1 mediated circuit for Ca2+/calcineurin signaling in the rice blast fungus. PLoS Pathog 6: e1000909.

Kim, Y. K., C. F. Bourgeois, C. Isel, M. J. Churcher, and J. Karn, 2002 Phosphorylation of the RNA polymerase II carboxyl-terminal domain by CDK9 is directly responsible for human immunodeficiency virus type 1 Tat-activated transcriptional elongation. Mol Cell Biol 22: 4622–4637.

Kim, Y.-J., S. Björklund, Y. Li, M. H. Sayre, and R. D. Kornberg, 1994 A multiprotein mediator of transcriptional activation and its interaction with the C-terminal repeat domain of RNA polymerase II. Cell 77: 599–608.

Koch, A., K. Krug, S. Pengelley, B. Macek, and S. Hauf, 2011 Mitotic substrates of the kinase Aurora with roles in chromatin regulation identified through quantitative phosphoproteomics of fission yeast. Sci Signal 4: rs6.

Koike, A., T. Kato, R. Sugiura, Y. Ma, Y. Tabata, *et al.*, 2012 Genetic screening for regulators of Prz1, a transcriptional factor ccting downstream of calcineurin in fission yeast. J Biol Chem 287: 19294-19303.

Kontaki, H., and I. Talianidis, 2010 Lysine methylation regulates E2F1-induced cell death. Mol Cell 39: 152–160.

Kroll, E. S., K. M. Hyland, P. Hieter, and J. J. Li, 1996 Establishing genetic interactions by a synthetic dosage lethality phenotype. Genet 143: 95–102.

Kummerfeld, S. K., and S. A. Teichmann, 2006 DBD: A transcription factor prediction database. Nucleic Acids Res 34: D74–D81.

Kuras, L., A. Rouillon, T. Lee, R. Barbey, M. Tyers, *et al.*, 2002 Dual regulation of the Met4 transcription factor by ubiquitin-dependent degradation and inhibition of promoter recruitment. Mol Cell 10: 69–80.

Kwon, E. J. G., A. Laderoute, K. Chatfield-Reed, L. Vachon, J. Karagiannis, *et al.*, 2012 Deciphering the transcriptional-regulatory network of flocculation in *Schizosaccharomyces pombe*. PLoS Genet 8: e1003104.

Lee, D. Y., J. J. Hayes, D. Pruss, and A. P. Wolffe, 1993 A positive role for histone acetylation in transcription factor access to nucleosomal DNA. Cell 72: 73–84.

Lee, T. I., N. J. Rinaldi, F. Robert, D. T. Odom, Z. Bar-Joseph, *et al*., 2002 Transcriptional regulatory networks in *Saccharomyces cerevisiae*. Science 298: 799–804.

Lehner, B., C. Crombie, J. Tischler, A. Fortunato, and A. G. Fraser, 2006 Systematic mapping of genetic interactions in *Caenorhabditis elegans* identifies common modifiers of diverse signaling pathways. Nat Genet 38: 896–903.

Lemercier, C., R. Q. To, R. A. Carrasco, and S. F. Konieczny, 1998 The basic helix-loop-helix transcription factor Mist1 functions as a transcriptional repressor of MyoD. EMBO J 17: 1412–1422.

Lillycrop, K. A., S. J. Dawson, J. K. Estridge, T. Gerster, P. Matihias, *et al.*, 1994 Repression of a herpes simplex virus immediate-early promoter by the Oct-2 transcription factor is dependent on an inhibitory region at the N terminus of the protein. Mol Cell Biol 14: 7633–7642.

Liu, C., D. van Dyk, Y. Li, B. Andrews, and H. Rao, 2009 A genome-wide synthetic dosage lethality screen reveals multiple pathways that require the functioning of ubiquitin-binding proteins Rad23 and Dsk2. BMC Biol 7: 75.

Lo, W.-S., L. Duggan, N. C. T. Emre, R. Belotserkovskya, W. S. Lane, *et al.*, 2001 Snf1: A histone kinase that works in concert with the histone acetyltransferase Gcn5 to regulate transcription. Science 293: 1142–1146.

Lorković, Z. J., and A. Barta, 2002 Genome analysis: RNA recognition motif (RRM) and K homology (KH) domain RNA-binding proteins from the flowering plant *Arabidopsis thaliana*. Nucleic Acids Res 30: 623–635.

Lu, J., T. A. McKinsey, C.-L. Zhang, and E. N. Olson, 2000 Regulation of skeletal myogenesis by association of the MEF2 transcription factor with class II histone deacetylases. Mol Cell 6: 233–244.

Lukashchuk, N., and K. H. Vousden, 2007 Ubiquitination and degradation of mutant p53. Mol Cell Biol 27: 8284–8295.

Luscombe, N. M., M. M. Babu, H. Yu, M. Snyder, S. A. Teichmann, and M. Gerstein, 2004 Genomic analysis of regulatory network dynamics reveals large topological changes. Nature 431: 308–312.

Macian, F., 2005 NFAT proteins: key regulators of T-cell development and function. Nat Rev Immunol 5: 472-484.

Maeda, T., R. Sugiura, A. Kita, M. Saito, L. Deng, *et al.*, 2004 Pmr1, a P-type ATPase, and Pdt1, and Nramp homologue, cooperatively regulate cell morphogenesis in fission yeast: the importance of Mn^{2+} homeostasis. Genes Cells 9: 71–82.

Magtanong, L., C. H. Ho, S. L. Barker, W. Jiao, A. Baryshnikova, *et al.*, 2011. Dosage suppression genetic interaction networks enhance functional wiring diagrams of the cell. Nat Biotechnol 29: 505–511.

Mansuy, I. M., D. G. Winder, T. M. Moallem, M. Osman, M. Mayford, *et al.*, 1998 Inducible and reversible gene expression with the rtTA system for the study of memory. Neuron 21: 257-265.

Marbach, D., S. Roy, F. Ay, P. E. Meyer, R. Candeias, *et al.*, 2012 Predictive regulatory models in *Drosophila melanogaster* by integrative inference of transcriptional networks. *Genome Res* 22: 1334–1349.

Marion, R. M., A. Regev, E. Segal, Y. Barash, D. Koller, *et al.*, 2004 Sfp1 Is a stress- and nutrient-sensitive regulator of ribosomal protein gene expression. Proc. Natl. Acad. Sci. U.S.A. 101: 14315–14322.

Martens, J.A., L. Laprade, and F. Winston, 2004 Intergenic transcription is required to repress the *Saccharomyces cerevisiae* SER3 gene. Nature 429: 571-574.

Matheos, D. P., T. J. Kingsbury, U. S. Ahsan, and K. W. Cunningham, 1997 Tcn1p/Crz1p, a calcineurin-dependent transcription factor that differentially regulates gene expression in *Saccharomyces cerevisiae*. Gene Dev 11: 3445-3458.

Matsuzaki, H., H. Daitoku, M. Hatta, H. Aoyama, K. Yoshimochi, *et al.*, 2005 Acetylation of Foxo1 alters its DNA-binding ability and sensitivity to phosphorylation. Proc. Natl. Acad. Sci. U.S.A. 102: 11278–11283.

Matsuzawa, T., Y. Fujita, H. Tohda, and K. Takegawa, 2012 Snf1-like protein kinase Ssp2 regulates glucose derepression in *Schizosaccharomyces pombe.* Eukaryot Cell 11: 159–167.

Matsuzawa, T., T. Ohashi, A. Hosomi, N. Tanaka, H. Tohda, *et al.*, 2010 The *gld1*$^{+}$ gene encoding glycerol dehydrogenase is required for glycerol metabolism in *Schizosaccharomyces pombe*. Appl Microbiol Biol 87: 715–727.

Maundrell, K., 1993 Thiamine-repressible expression vectors pREP and pRIP for fission yeast. Gene 123: 127–130.

McCloy, R. A., S. Rogers, C. E. Caldon, T. Lorca, A. Castro, *et al*., 2014 Partial inhibition of Cdk1 in G_2 phase overrides the SAC and decouples mitotic events. Cell Cycle 13: 1400–1412.

Measday, V., K. Baetz, J. Guzzo, K. Yuen, T. Kwok, *et al.*, 2005 Systematic yeast synthetic lethal and synthetic dosage lethal screens identify genes required for chromosome segregation. Proc. Natl. Acad. Sci. U.S.A. 102 (39): 13956–13961.

Measday, V., P. Hieter, 2002 Synthetic dosage lethality. Guide to Yeast Genetics and Molecular and Cell Biology, Parts B and C. Method Enzymol 350: 316-326.

Mercier, A., B. Pelletier, and S. Labbé, 2006 A transcription factor cascade involving Fep1 and the CCAAT-binding factor Php4 regulates gene expression in response to iron deficiency in the fission yeast *Schizosaccharomyces pombe*. Eukaryot Cell 5: 1866–1881.

Molkentin, J. D., J-R Lu, C. L. Antos, B. Markham, J. Richardson, *et al.*, 1998 A calcineurin-dependent transcriptional pathway for cardiac hypertrophy. Cell 93: 215-228.

Moreno, S, A Klar, and P Nurse, 1991 Molecular genetic analysis of fission yeast *Schizosaccharomyces pombe*. Method Enzymol 194: 795–823.

Noma, K., and S. I S Grewal, 2002 Histone H3 lysine 4 methylation is mediated by Set1 and promotes maintenance of active chromatin states in fission yeast. Proc. Natl. Acad. Sci. U.S.A. 99: 16438–16445.

Noma, K., C. D. Allis, and S. I. S. Grewal, 2001 Transitions in distinct histone H3 methylation patterns at the heterochromatin domain boundaries. Science 293: 1150–1155.

Nurse, P 1975 Genetic control of cell size at cell division in yeast. Nature 256: 547–551.

Nurse, P., P. Thuriaux, and K. Nasmyth, 1976 Genetic control of the cell division cycle in the fission yeast *Schizosaccharomyces pombe.* Mol Gen Genet 146: 167–178.

Ogryzko, V. V., R. L. Schiltz, V. Russanova, B. H. Howard, and Y. Nakatani, 1996 The transcriptional coactivators p300 and CBP are histone acetyltransferases. Cell 87: 953–959.

Papadopoulou, K., J.-S. Chen, E. Mead, A. Feoktistova, C. Petit, *et al.*, 2010 Regulation of cell cycle-specific gene expression in fission yeast by the Cdc14p-like phosphatase Clp1p. J Cell Sci 123: 4374–4381.

Papadopoulou, K., S. S. Ng, H. Ohkura, M. Geymonat, S. G. Sedgwick, *et al.*, 2008 Regulation of gene expression during M-G1-phase in fission yeast through Plo1p and forkhead transcription factors. J Cell Sci 121: 38–47.

Parsons, A. B., A. Lopez, I. E. Givoni, D. E. Williams, C. A. Gray, *et al*., 2006 Exploring the mode-of-action of bioactive compounds by chemical-genetic profiling in yeast. Cell 126: 611–625.

Pelletier, B., J. Beaudoin, Y. Mukai, and S. Labbé, 2002 Fep1, an iron sensor regulating iron transporter gene expression in *Schizosaccharomyces pombe*. J Biol Chem 277: 22950–22958.

Peng, S. S.-Y., C.-Y. A. Chen, N. Xu, and A.-B. Shyu, 1998 RNA stabilization by the AU-rich element binding protein, HuR, an ELAV protein. EMBO J 17: 3461–3470.

Peplowska, K., D. F. Markgraf, C. W. Ostrowicz, G. Bange, and C. Ungermann, 2007 The CORVET tethering complex interacts with the yeast Rab5 homolog Vps21 and is involved in endo-lysosomal biogenesis. Dev Cell 12: 739–750.

Převorovský, M., M. Oravcová, J. Tvarůžková, R. Zach, P. Folk, *et al.*, 2015 Fission yeast CSL transcription factors: mapping their target genes and biological roles. PloS One 10: e0137820.

Radcliffe, P. A., M. A. Garcia, and T. Toda. 2000. The cofactor-dependent pathways for α- and β-tubulins in microtubule biogenesis are functionally different in fission yeast. Genet 156: 93–103.

Ribár, B., A. Grallert, E. Oláh, and Z. Szállási, 1999 Deletion of the sep1(+) forkhead transcription factor homologue is not lethal but causes hyphal growth in Schizosaccharomyces pombe. Biochem Bioph Res Commun 263: 465–474.

Robzyk, K., J. Recht, and M. A. Osley, 2000 Rad6-dependent ubiquitination of histone H2B in yeast. Science 287: 501–504.

Roguev, A., D. Talbot, G. L. Negri, M. Shales, G. Cagney, *et al.*, 2013 Quantitative genetic-interaction mapping in mammalian cells. Nat Methods 10: 432–437.

Roguev, A., M. Wiren, J. S. Weissman, and N. J. Krogan, 2007 High-throughput genetic interaction mapping in the fission yeast *Schizosaccharomyces pombe*. Nature Methods 4: 861–866.

Ruiz, A., R. Serrano, and J. Ariño, 2008 Direct regulation of genes involved in glucose utilization by the calcium/calcineurin pathway. J Biol Chem 283: 13923-13933.

Russell, P., and P. Nurse, 1987 Negative regulation of mitosis by *wee1*$^{+}$, a gene encoding a protein kinase homolog. Cell 49: 559–567.

Rustici, G., J. Mata, K. Kivinen, P. Lió, C. J. Penkett, *et al.*, 2004 Periodic gene expression program of the fission yeast cell cycle. Nat Genet 36: 809–817.

Rustici, G., H. van Bakel, D. H. Lackner, F. C. Holstege, C. Wijmenga, *et al.*, 2007 Global transcriptional responses of fission and budding yeast to changes in copper and iron levels: A comparative study. Genome Biol 8: R73.

Ryan, C. J., A. Roguev, K. Patrick, J. Xu, H. Jahari, *et al*., 2012 Hierarchical modularity and the evolution of genetic interactomes across species. Mol Cell 46: 691–704.

Sachdev, S., L. Bruhn, H. Sieber, A. Pichler, F. Melchior, *et al.*, 2001 PIASy, a nuclear matrix-associated SUMO E3 ligase, represses LEF1 activity by sequestration into nuclear bodies. Genes Dev 15: 3088–3103.

Saitoh, S., A. Mori, L. Uehara, F. Masuda, S. Soejima, *et al.*, 2015. Mechanisms of expression and translocation of major fission yeast glucose transporters regulated by CaMKK/phosphatases, nuclear shuttling, and TOR. Mol Biol Cell 26: 373–386.

Sakaguchi, K., J. E. Herrera, S. Saito, T. Miki, M. Bustin, *et al*, 1998 DNA damage activates p53 through a phosphorylation – acetylation cascade. Genes Dev 12: 2831–2841.

Saldanha, A. J., 2004 Java Treeview-extensible visualization of microarray data. Bioinformatics 20: 3246-3248.

Salghetti, S. E., A. A. Caudy, J. G. Chenoweth, and W. P. Tansey, 2001 Regulation of transcriptional activation domain function by ubiquitin. Science 293: 1651–1653.

Santiago, A, D. Li, L. Y. Zhao, A. Godsey, and D. Liao, 2013 p53 SUMOylation promotes its nuclear export by facilitating its release from the nuclear export receptor CRM1. Mol Biol Cell 24: 2739–2752.

Satoh, R., A. Tanaka, A. Kita, T. Morita, Y. Matsumura, *et al.*, 2012 Role of the RNA-binding protein Nrd1 in stress granule formation and its implication in the stress response in fission yeast. PLoS ONE 7: e29683.

Schaefer, M. H., E. E. Wanker, M. A. Andrade-Navarro, 2012 Evolution of CAG/polyglutamine repeats in protein-protein interaction networks. Nucleic Acids Res 40: 4273-4287.

Serrano, R. A. Ruiz, D. Bernal, J. R. Chambers, and J. Ariño, 2002 The transcriptional response to alkaline pH in *Saccharomyces cerevisiae*: evidence for calcium-mediated signalling. Mol Microbiol 46: 1319-1333.

Sharifpoor, S., D. van Dyk, M. Costanzo, A. Baryshnikova, H. Friesen, *et al*., 2012 Functional wiring of the yeast kinome revealed by global analysis of genetic network motifs. Genome Res 22: 791–801.

Smyth, G. K., and T. Speed, 2003 Normalization of cDNA microarray data. Methods 31: 265-273.

Smyth, G. K., 2004 Linear models and empirical Bayes methods for assessing differential expression in microarray experiments. Stat Appl Genet Mol 3: 1-25.

Sonnhammer, E. L. and G. Östlund, 2015 InParanoid 8: orthology analysis between 273 proteomes, mostly eukaryotic. Nucleic Acids Res 43: D234-239.

Sopko, R., D. Huang, N. Preston, G. Chua, B. Papp, *et al.*, 2006 Mapping pathways and phenotypes by systematic gene overexpression. Mol Cell 21: 319–330.

Soriani, F. M., I. Malavazi, M. E. Da Silva Ferreira, M. Savoldi, M. R. Von Zeska Kress, *et al.*, 2008 Functional characterization of the *Aspergillus fumigatus* CRZ1 homologue, CrzA. Mol Microbiol 67: 1274-1291.

Soutoglou, E., N. Katrakili, and I. Talianidis, 2000 Acetylation regulates transcription factor activity at multiple levels. Mol Cell 5: 745–751.

Stathopoulos, A. M., and M. S. Cyert, 1997 Calcineurin acts through the CRZ1/TCN1-encoded transcription factor to regulate gene expression in yeast. Gene Dev 11: 3432-3444.

Stathopoulos-Gerontides, A., J. J. Guo, and M. S. Cyert, 1999 Yeast calcineurin regulates nuclear localization of the Crz1p transcription factor through dephosphorylation. Gene Dev 13: 798-803.

Stewart, E. V., S. J. A. Lloyd, J. S. Burg, C. C. Nwosu, R. E. Lintner, *et al.*, 2012. Yeast sterol regulatory element-binding protein (SREBP) cleavage requires Cdc48 and Dsc5, a ubiquitin regulatory X domain-containing subunit of the Golgi Dsc E3 ligase. J Biol Chem 287: 672–681.

Stewart, E. V., C. C. Nwosu, Z. Tong, A. Roguev, T. D. Cummins, *et al.*, 2011 Yeast SREBP cleavage activation requires the Golgi Dsc E3 ligase complex. Mol Cell 42: 160–171.

Stringer, K. F., C. J. Ingles, and J. Greenblatt, 1990 Direct and selective binding of an acidic transcriptional activation domain to the TATA-box factor TFIID. Nature 345: 783–786.

Suka, N., K. Luo, and M. Grunstein, 2002 Sir2p and Sas2p opposingly regulate acetylation of yeast histone H4 lysine16 and spreading of heterochromatin. Nat Genet 32: 378–383.

Sugimoto, A., Y. Iino, T. Maeda, Y. Watanabe, and M.asayuki Yamamoto, 1991 *Schizosaccharomyces pombe* ste11^{+} encodes a transcription factor with an HMG motif that is a critical regulator of sexual development. *Gene Dev* 5: 1990-1999.

Sun, L.-L., M. Li, F. Suo, X.-M. Liu, E.-Z. Shen, *et al.*, 2013 Global analysis of fission yeast mating genes reveals new autophagy factors. PLoS Genet 9: e1003715.

Sun, Z.-W., and C. D. Allis, 2002 Ubiquitination of histone H2B regulates H3 gethylation and gene silencing in yeast. Nature 418: 104–108.

Takada, H., A. Nishida, M. Domae, A. Kita, Y. Yamano, *et al.*, 2010 The cell surface protein gene *ecm33*$^{+}$ is a target of the two transcription factors Atf1 and Mbx1 and negatively regulates Pmk1 MAPK cell integrity signaling in fission yeast. Mol Biol Cell 21: 674–685.

Tanaka, K., and H. Okayama, 2000 A Pcl-like cyclin activates the Res2p-Cdc10p cell cycle 'start' transcriptional factor complex in fission yeast. Mol Biol Cell 11: 2845–2862.

Tanaka, N., N. Ohuchi, Y. Mukai, Y. Osaka, Y. Ohtani, *et al.*, 1998 Isolation and characterization of an invertase and its repressor genes from *Schizosaccharomyces pombe*. Biochem Bioph Res Commun 245: 246–253.

Thewes, S., 2014 Calcineurin-Crz1 signaling in lower eukaryotes. Eukaryot Cell 13: 694-705.

Todd, B. L., E. V. Stewart, J. S. Burg, A. L. Hughes, and P. J. Espenshade, 2006 Sterol regulatory element binding protein is a principal regulator of anaerobic gene expression in fission yeast. Mol Cell Biol 26: 2817–2831.

Tong, A. H. T., M. Evangelista, A. B. Parsons, H. Xu, G. D. Bader, *et al.,* 2001 Systematic genetic analysis with ordered arrays of yeast deletion mutants. Science 294: 2364–2368.

Tong, A. H. Y., G. Lesage, G. D. Bader, H. Ding, H. Xu, *et al.*, 2004 Global mapping of the yeast genetic interaction network. Science 303: 808–813.

Tosti, E., J. A. Katakowski, S. Schaetzlein, H.-S. Kim, C. J. Ryan, *et al*., 2014 Evolutionarily conserved genetic interactions with budding and fission yeast MutS identify orthologous relationships in mismatch repair-deficient cancer cells. Genome Med 6: 68.

Vachon, L., J. Wood, E.-J. G. Kwon, A. Laderoute, K. Chatfield-Reed, *et al.*, 2013. Functional characterization of fission yeast transcription factors by overexpression analysis. Genetics 194: 873–884.

Valbuena, N., and S. Moreno, 2012 AMPK phosphorylation by Ssp1 is required for proper sexual differentiation in fission yeast. J Cell Sci 125: 2655–2664. doi:10.1242/jcs.098533.

Viladevall, L., R. Serrano, A. Ruiz, G. Domenech, J. Giraldo, *et al.*, 2004 Characterization of the calcium-mediated response to alkaline stress in *Saccharomyces cerevisiae*. J Biol Chem 279: 43614-43624.

Vilella, A. J., J. Severin, A. Ureta-Vidal, L. Heng, R. Durbin, *et al.*, 2009 EnsemblCompara GeneTrees: complete, duplication-aware phylogenetic trees in vertebrates. Genome Res 19: 327–335.

Vizeacoumar, F. J., R. Arnold, F. S. Vizeacoumar, M. Chandrashekhar, A. Buzina, *et al*., 2013 A negative genetic interaction map in isogenic cancer cell lines reveals cancer cell vulnerabilities. Mol Syst Biol 9: 791-801.

Vizeacoumar, F. J., N. Van Dyk, F. S. Vizeacoumar, V. Cheung, J. Li, *et al.*, 2010. Integrating high-throughput genetic interaction mapping and high-content screening to explore yeast spindle morphogenesis. J Cell Biol 188: 69–81.

Wagih, O., M. Usaj, A. Baryshnikova, B. VanderSluis, E. Kuzmin, *et al.*, 2013 SGAtools: One-stop analysis and visualization of array-based genetic interaction screens. Nucleic Acids Res 41: W591–W596.

Wang, H., N. Pathan, I. M. Ethell, S. Krajewski, Y. Yamaguchi, *et al*., 1999 Ca^{2+}-induced apoptosis through calcineurin dephosphorylation of BAD. Science 284: 339-343.

Wapinski, H., A. Pfeffer, N. Friedman, and A. Regev, 2007 Automatic genome-wide reconstruction of phylogenetic gene trees. Bioinformatics 23: i549-i558.

Wood, V., M. A. Harris, M. D. McDowall, K. Rutherford, B. W. Vaughan, *et al.*, 2012 PomBase: a comprehensive online resource for fission yeast. Nucleic Acids Res 40: D695-D699.

Wood, V., R. Gwilliam, M. A. Rajandream, M. Lyne, R. Lyne, *et al*., 2002 The genome sequence of *Schizosaccharomyces pombe*. Nature 415: 871–880.

Yamagata, K., H. Daitoku, Y. Takahashi, K. Namiki, K. Hisatake, *et al.*, 2008 Arginine methylation of FOXO transcription factors inhibits their phosphorylation by Akt. Mol Cell 32: 221–231.

Yang, S.-H., and A. D. Sharrocks, 2004 SUMO promotes HDAC-mediated transcriptional repression. Mol Cell 13: 611–617.

Yao, Y.-L., W.-M. Yang, and E. Seto, 2001 Regulation of transcription factor YY1 by acetylation and deacetylation. Mol Cell Biol 21: 5979–5991.

Yet, S.-F., M. M. McA'Nulty, S. C. Folta, H.-W. Yen, M. Yoshizumi, *et al.*, 1998 Human EZF, a Krüppel-like zinc finger protein, is expressed in vascular endothelial cells and contains transcriptional activation and repression domains. J Biol Chem 273: 1026–1031.

Yoritsune, K., T. Matsuzawa, T. Ohashi, and K. Takegawa, 2013 The fission yeast Pvg1p has galactose-specific pyruvyltransferase activity. FEBS Lett 587: 917-921.

Yoshida, T., T. Toda, and M. Yanagida, 1994 A calcineurin-like gene *ppb1*$^{+}$ in fission yeast: mutant defects in cytokinesis, cell polarity, mating and spindle pole body positioning. *J. Cell Sci* 107: 1725-1735.

Yoshimoto, H., K. Saltsman, A. P. Gasch, H. X. Li, N. Ogawa, *et al*., 2002 Genome-wide analysis of gene expression regulated by the calcineurin/Crz1p signaling pathway in *Saccharomyces cerevisiae*. J Biol Chem 277: 31079-31088.

Yudkovsky, N., J. A. Ranish, and S. Hahn, 2000 A transcription reinitiation intermediate that is stabilized by activator. Nature 408: 225–229.

Zakrzewska, A., A. Boorsma, S. Brul, J. K. Hellingwerf, and F. M. Klis, 2005 Transcriptional response of Saccharomyces cerevisiae to the plasma membrane-perturbing compound chitosan. Eukaryot Cell 4: 703-715.

Zhang, Y.-Q., and R. Rao, 2007 Global disruption of cell cycle progression and nutrient response by the antifungal agent amiodarone. J Biol Chem 282: 37844-37853.

Zheng, J., J. J. Benschop, M. Shales, P. Kemmeren, J. Greenblatt, G. Cagney, *et al.*, 2010 Epistatic relationships reveal the functional organization of yeast transcription factors. Mol Syst Biol: 420.

Zhu, C., K. Byers, R. McCord, Z. Shi, M. Berger, *et al.*, 2009 High-resolution DNA binding specificity analysis of yeast transcription factors. Genome Res 19: 556–566.

Zhu, Y., T. Takeda, S. Whitehall, N. Peat, and N. Jones, 1997 Functional characterization of the fission yeast start-specific transcription factor res2. EMBO J 16: 1023–1034.

Appendix A: Additional tables

Table A1: *Schizosaccharomyces pombe* strains used in chapter 2.

Strain	Genotype	Reference
972h-	*972 h⁻*	JK
JK366	*ade6-M216 leu1-32 ura4D18 h⁺*	JK
GCY978	Δ*prz1::KanMX6 h⁻*	This work
V3-P12-91	Δ*prz1::KanMX4 ade6-M216 leu1-32 ura4D18 h⁺*	Bioneer
V3-P11-56	Δ*pmr1::KanMX4 ade6-M216 leu1-32 ura4D18 h⁺*	Bioneer
GCY3020	*pREP1-prz1⁺ ade6-M216 leu1-32 ura4D18 h⁻*	This work
GCY2829	*pREP1 ade6-M216 leu1-32 ura4D18 h⁻*	This work
GCY3232	*pREP2-prz1⁺ ura4D18 h⁻*	This work
GCY1893	*pREP2 ura4D18 h⁻*	This work
V3-P19-71	Δ*pvg1::KanMX4 ade6-M216 leu1-32 ura4D18 h⁺*	Bioneer
V3-P18-22	Δ*pvg5::KanMX4 ade6-M216 leu1-32 ura4D18 h⁺*	Bioneer
V3-P17-24	Δ*omh1::KanMX4 ade6-M216 leu1-32 ura4D18 h⁺*	Bioneer
V3-P16-38	Δ*pun1::KanMX4 ade6-M216 leu1-32 ura4D18 h⁺*	Bioneer
V3-P25-37	Δ*SPBC19C7.05::KanMX4 ade6-M216 leu1-32 ura4D18 h⁺*	Bioneer
V3-P18-64	Δ*SPBC21B10.07::KanMX4 ade6-M216 leu1-32 ura4D18 h⁺*	Bioneer
V3-P29-15	Δ*SPAC9G1.10c::KanMX4 ade6-M216 leu1-32 ura4D18 h⁺*	Bioneer
V3-P03-55	Δ*SPAC13C5.05c::KanMX4 ade6-M216 leu1-32 ura4D18 h⁺*	Bioneer
V3-P07-61	Δ*rga5::KanMX4 ade6-M216 leu1-32 ura4D18 h⁺*	Bioneer
V3-P36-40	Δ*cfr1::KanMX4 ade6-M216 leu1-32 ura4D18 h⁺*	Bioneer
V3-P17-70	Δ*cfh2::KanMX4 ade6-M216 leu1-32 ura4D18 h⁺*	Bioneer
V3-P16-79	Δ*gmh2::KanMX4 ade6-M216 leu1-32 ura4D18 h⁺*	Bioneer
GCY3204	*pREP1-prz1⁺ ade6-M216 leu1-32 ura4D18 h⁺*	This work
GCY3205	*pREP1 ade6-M216 leu1-32 ura4D18 h⁺*	This work
GCY3250	Δ*pvg1::KanMX4 pREP1-prz1+ ade6-M216 leu1-32 ura4D18 h⁺*	This work
GCY3216	Δ*pvg5::KanMX4 pREP1-prz1+ ade6-M216 leu1-32 ura4D18 h⁺*	This work
GCY3212	Δ*omh1::KanMX4 pREP1-prz1+ ade6-M216 leu1-32 ura4D18 h⁺*	This work
GCY3251	Δ*pvg1::KanMX4 pREP1 ade6-M216 leu1-32 ura4D18 h⁺*	This work
GCY3217	Δ*pvg5::KanMX4 pREP1 ade6-M216 leu1-32 ura4D18 h⁺*	This work
GCY3213	Δ*omh1::KanMX4 pREP1 ade6-M216 leu1-32 ura4D18 h⁺*	This work
GCY1038	Δ*cbf12::KanMX6 h⁻*	This work
GCY3235	Δ*gsf2::KanMX6 h⁻*	This work
GCY3237	Δ*pfl3::KanMX6 h⁻*	This work
GCY3238	Δ*prz1::NatMX4* Δ*cbf12::KanMX6 h⁻*	This work
GCY3236	Δ*prz1::KanMX6* Δ*gsf2::KanMX6 h⁻*	This work
GCY3238	Δ*prz1::KanMX6* Δ*pfl3::KanMX6 h⁻*	This work
GCY3051	*prz1-GFP::KanMX6 ade6-M216 leu1-32 ura4D18 h⁻*	This work
GCY3128	Δ*pmr1::KanMX4 prz1-GFP::NatMX4 ade6-M216 leu1-32 ura4D18 h⁻*	This work
GCY3264	*pREP1-CRZ1⁺ leu1-32 h⁻*	This work
GCY3252	Δ*prz1::KanMX4 pREP1-CRZ1+ ade6-M216 leu1-32 ura4D18 h⁺*	This work
GCY3253	Δ*prz1::KanMX4 pREP1 ade6-M216 leu1-32 ura4D18 h⁺*	This work
GCY3254	Δ*prz1::KanMX4 pREP41-CRZ1+ ade6-M216 leu1-32 ura4D18 h⁺*	This work
GCY3255	Δ*prz1::KanMX4 pREP41 ade6-M216 leu1-32 ura4D18 h⁺*	This work
GCY3161	*prz1-HA::KanMX6 ade6-M216 leu1-32 ura4D18 h⁻*	This work

Table A2: ChIP-chip analysis of *Prz1-HA* with $CaCl_2$ treatment.

Chromosome Location	Genes	High Ratio	P-value
chr1:0066080-0066130	SPAC977.17 (PR 1013), dak2 (ORF 549)	1.361	2.94E-05
chr1:0104111-0104169	pdc101 (PR 567), SPAC1F8.08 (ORF 170)	2.958	1.12E-13
chr1:0158612-0158671	SPAC5H10.07 (PR 532), adh4 (PR 796)	2.409	4.81E-11
chr1:0192884-0192939	asl1 (ORF 949)	1.668	1.94E-06
chr1:0239554-0239613	SPAC806.11 (PR 2124)	4.185	1.54E-20
chr1:0341162-0341220	mcp60 (ORF 635)	1.602	3.26E-06
chr1:0381582-0381635	gti1 (PR 1228)	2.835	1.33E-13
chr1:0528104-0528163	lys3 (PR 2359), psf3 (ORF 608)	1.949	4.26E-08
chr1:0577540-0577599	erg11 (PR 918), mcp7 (PR 922)	2.920	2.06E-12
chr1:0790669-0790728	prz1 (PR 1505)	3.422	1.47E-16
chr1:0869924-0869983	sib1 (PR 397), sib2 (PR 1042)	1.615	3.10E-06
chr1:0934099-0934154	erg31 (PR 145)	2.552	3.96E-11
chr1:0947541-0947600	puf3 (PR 1614), tim10UTR 364)	2.311	3.06E-09
chr1:0960805-0960853	sno1 (PR 2455), seb1 (ORF 744)	2.655	1.14E-12
chr1:0969468-0969522	atp2 (ORF 838)	1.285	7.50E-05
chr1:1003930-1003988	sod1 (PR 467), pro1 (PR 2406)	2.394	4.84E-11
chr1:1066622-1066673	SPAC1A6.02 (PR 2058)	1.126	4.47E-04
chr1:1073304-1073362	SPAC1A6.11 (PR 172), SPAC1A6.03c (PR 1291)	2.558	1.10E-11
chr1:1078278-1078336	plb1 (PR 1660)	3.535	5.15E-17
chr1:1150276-1150335	SPAC56F8.15 (PR 1733), SPAC56F8.13UTR 60)	5.169	1.65E-25
chr1:1155169-1155219	esc1 (ORF 436)	1.507	9.77E-06
chr1:1184309-1184368	SPAC22A12.14c (PR 1938), acl2 (PR 1946), bip1 (ORF 935)	2.074	5.18E-09
chr1:1206531-1206589	sir1 (PR 1033)	3.208	1.33E-14
chr1:1238387-1238446	mug134 (PR 450)	2.664	2.48E-12
chr1:1263416-1263475	SPAC1420.01c (PR 656)	2.126	5.82E-09
chr1:1360735-1360791	pas1 (PR 1780)	1.371	2.63E-05
chr1:1479975-1480034	SPAC9.08c (PR 1913)	2.579	4.07E-12
chr1:1494482-1494541	mug116 (PR 129), mtf2 (PR 658)	1.827	4.71E-07
chr1:1544002-1544053	hul5 (PR 2451)	1.637	9.77E-07
chr1:1572391-1572449	ecm33 (PR 1131), rbx1 (PR 2961)	2.492	3.27E-11
chr1:1598263-1598322	gln1 (PR 692), SPAC23H4.05c (PR 1009)	1.899	1.88E-07
chr1:1667662-1667720	rds1 (PR 351)	2.264	2.59E-10
chr1:1700814-1700871	SPAC824.09c (ORF 730)	1.540	3.38E-06
chr1:1711708-1711759	rps1602 (PR 641), rlp7 (PR 1058), rpl13 (ORF 494)	1.986	1.13E-08
chr1:1727955-1728013	SPAC664.13 (PR 1492)	1.341	3.92E-05
chr1:1756339-1756383	dbr1 (PR 701), rpl301 (ORF 230)	1.437	2.24E-05
chr1:1823613-1823669	SPAC1002.20 (PR 303), psu1 (PR 424), itt1 (PR 1116)	3.255	1.32E-14
chr1:1850841-1850899	SPAC1399.01c (PR 1728)	3.050	1.26E-14
chr1:1890283-1890341	pof15 (PR 579), arv1 (PR 2213)	1.501	9.93E-06
chr1:1898489-1898545	arb1 (PR 1507), gar2 (ORF 966)	1.892	7.67E-08
chr1:1906256-1906313	ppk1 (PR 1955)	2.681	8.49E-13
chr1:1944243-1944302	SPAC3H1.06c (PR 1457), aru1 (ORF 12)	1.606	1.97E-06
chr1:1957074-1957133	hsr1 (PR 2178)	1.928	2.38E-08
chr1:2095433-2095492	obr1 (PR 542), SPAC3C7.13c (PR 2491)	4.184	1.89E-19
chr1:2106416-2106475	bdf2 (PR 995), acp2 (PR 1167)	4.096	2.87E-19
chr1:2177184-2177243	gld1 (PR 824)	1.656	1.67E-06
chr1:2203009-2203068	pap1 (PR 762), atg12 (PR 3045)	1.728	6.28E-07
chr1:2296578-2296629	erg7 (PR 1462), upf3 (PR 2350)	1.617	2.22E-06

chr1:2329670-2329728	meu43 (PR 1427), cit1 (ORF 995)	1.395	1.98E-05
chr1:2440894-2440953	meu26 (PR 1736)	1.440	1.31E-05
chr1:2581616-2581675	SPAC823.02 (PR 2129)	1.454	2.55E-05
chr1:2664127-2664183	hxk2 (PR 1633)	3.979	2.00E-19
chr1:2718514-2718571	pmc1 (PR 1583)	3.574	1.15E-17
chr1:2792534-2792593	fmt1 (PR 1313), rpl14 (PR 2345)	1.302	6.05E-05
chr1:2872144-2872201	pvg1 (PR 819)	3.487	4.28E-17
chr1:2875908-2875967	SPACUNK4.16c (PR 1552), SPACUNK4.17 (PR 1659), mug153 (ORF 20)	2.015	4.84E-08
chr1:2892973-2893032	SPACUNK4.10 (PR 446)	1.524	1.22E-05
chr1:2925439-2925498	amt3 (ORF 948)	1.939	4.82E-08
chr1:2936646-2936704	SPAC2E1P3.05c (PR 543)	1.648	6.53E-06
chr1:2960494-2960553	SPAPB24D3.07c (PR 1568)	3.792	1.29E-18
chr1:3004178-3004232	pac2 (PR 1906)	3.919	1.58E-19
chr1:3033855-3033912	SPAC1786.02 (PR 970), SPAC1786.04 (ORF 4)	2.528	8.29E-12
chr1:3070036-3070095	shm1 (ORF 922)	1.801	1.27E-07
chr1:3342665-3342724	bud23 (PR 2060)	1.228	1.76E-04
chr1:3368799-3368856	dph1 (PR 887), SPAC26A3.14c (PR 1743), nsp1 (ORF 663)	1.220	1.52E-04
chr1:3384227-3384286	rad24 (PR 0), SPAC8E11.01c (PR 1761)	2.966	1.28E-13
chr1:3456712-3456771	nde2 (PR 502)	2.511	2.86E-11
chr1:3502803-3502850	SPAC16E8.02 (PR 1411)	1.361	4.37E-05
chr1:3530907-3530963	sua7 (ORF 570)	1.940	4.05E-08
chr1:3571119-3571176	ntr2 (PR 2040)	2.181	1.57E-09
chr1:3575935-3575994	SPAC17A2.10c (PR 248), SPAC17A2.11 (PR 1115)	4.365	4.72E-20
chr1:3647913-3647958	dtd1 (PR 1601)	2.401	3.75E-11
chr1:3655237-3655295	ppr4 (PR 1802), rps5 (ORF 93)	1.159	3.96E-04
chr1:3664409-3664461	prr1 (PR 1546), SPAC8C9.12c (PR 2010)	2.432	8.96E-11
chr1:3747828-3747886	per1 (PR 1809)	2.082	6.84E-09
chr1:3841052-3841108	SPAC4H3.08 (PR 473), rdl2 (PR 1672), SPAC4H3.09 (PR 2308)	3.338	4.86E-16
chr1:3868369-3868424	rpp203 (PR 721)	2.791	6.07E-13
chr1:3870401-3870460	rps1502 (PR 1441)	3.236	8.84E-15
chr1:3874055-3874114	pma1 (ORF 565)	1.429	1.62E-05
chr1:3885334-3885393	stp1 (PR 1243), rlc1 (PR 2177), SPAC926.02 (ORF 790)	2.011	2.66E-08
chr1:3985627-3985685	SPAPB18E9.04c (PR 523)	5.049	6.76E-25
chr1:4004142-4004199	yih1 (PR 308)	4.472	6.53E-22
chr1:4007114-4007170	SPAC27E2.03c (PR 86)	2.140	3.02E-09
chr1:4051921-4051979	mce1 (ORF 793)	1.283	7.53E-05
chr1:4058919-4058978	SPAC19G12.09 (PR 1274)	3.478	9.47E-17
chr1:4090577-4090636	SPAC23A1.07 (PR 1693)	1.045	1.19E-03
chr1:4104186-4104230	SPAC23A1.14c (PR 1231), sec20 (ORF 392)	1.301	6.73E-05
chr1:4128992-4129051	pot1 (PR 478)	1.852	7.75E-08
chr1:4134936-4134995	SPAC26H5.07c (PR 1473), bgl2 (ORF 592)	2.344	3.23E-09
chr1:4172201-4172257	SPAC25B8.11 (PR 1802), SPAC25B8.10 (ORF 25)	2.774	3.04E-13
chr1:4177239-4177298	SPAC25B8.12c (ORF 634)	1.344	1.67E-04
chr1:4189290-4189349	ypf1 (PR 1004), tyw3 (PR 2065), SPAC25B8.18 (PR 2264)	1.575	4.68E-06
chr1:4218729-4218783	pkd2 (PR 1218), spt6 (PR 1926), has1 (ORF 371)	1.547	3.32E-06
chr1:4228753-4228812	hsp3105 (PR 2038)	1.582	1.79E-05
chr1:4244412-4244471	dal2 (PR 1368), SPAC1F7.10 (ORF 443)	1.403	2.00E-05
chr1:4307452-4307511	his1 (PR 1672)	1.615	2.06E-06
chr1:4410087-4410146	uso1 (PR 749), nnf1 (ORF 314)	1.326	4.44E-05

chr1:4429007-4429066	ura2 (PR 202), dus3 (PR 618), srp2 (PR 2042)	2.420	1.16E-10
chr1:4450156-4450213	ypt2 (PR 639), rad26 (PR 902)	2.637	3.31E-12
chr1:4487438-4487483	pnu1 (PR 1444), alg8 (ORF 584)	1.421	1.66E-05
chr1:4517462-4517514	omt2 (PR 28), etf1 (PR 1532)	1.401	2.66E-05
chr1:4525694-4525753	SPAC27D7.09c (PR 1155)	4.347	5.54E-22
chr1:4716367-4716425	mug51 (PR 145)	3.940	7.16E-19
chr1:4782268-4782325	fta6 (PR 0), arp2 (PR 730), SPAC11H11.03c (PR 2019)	3.533	1.07E-17
chr1:4855818-4855862	fta1 (ORF 275)	1.962	1.59E-08
chr1:4875051-4875107	SPAC19B12.01 (PR 468), hit1 (PR 2298)	3.392	3.24E-16
chr1:4905347-4905406	SPAC19B12.11c (PR 1171), cox1102 (PR 1572)	3.361	1.13E-16
chr1:4953413-4953469	vma3 (PR 1165), rpb10 (PR 2179)	1.352	4.13E-05
chr1:5080375-5080432	och1 (PR 0), rgf2 (PR 673), mcp3 (PR 2381)	1.448	1.05E-05
chr1:5138906-5138965	cam2 (PR 920), cbf5 (PR 1442)	2.246	8.51E-10
chr1:5151635-5151693	hgh1 (PR 2239)	2.879	1.01E-13
chr1:5168762-5168821	gyp51 (PR 1926)	3.124	6.70E-14
chr1:5195432-5195490	Tf2-7 (PR 287)	1.561	6.91E-06
chr1:5264024-5264080	dpp1 (PR 2271), abp1 (ORF 950)	2.903	4.06E-14
chr1:5301481-5301540	SPAC11E3.10 (ORF 699)	1.231	2.28E-04
chr1:5314746-5314804	rpl22 (PR 58)	3.021	6.61E-14
chr1:5473718-5473777	gto1 (ORF 771)	2.298	1.56E-10
chr1:5511640-5511699	SPAC869.03c (PR 1058), SPAC869.04 (ORF 670)	4.223	2.01E-19
chr2:0072724-0072782	SPBPB21E7.08 (ORF 379)	2.046	3.33E-08
chr2:0107709-0107768	alr2 (PR 0)	2.622	1.63E-11
chr2:0133003-0133062	SPBC1683.01 (PR 1241)	1.969	2.31E-08
chr2:0156603-0156662	ght4 (PR 893)	2.256	3.13E-09
chr2:0230344-0230403	SPBC660.16 (PR 0)	1.863	1.00E-07
chr2:0352799-0352852	tgp1 (PR 430)	2.669	5.35E-12
chr2:0465205-0465264	met17 (PR 369)	1.676	1.07E-06
chr2:0525286-0525342	fhn1 (PR 749)	3.990	1.00E-18
chr2:0576710-0576769	gpd3 (PR 1962)	2.779	2.41E-13
chr2:0606755-0606814	cta3 (PR 1357), rps1701 (PR 2378)	3.616	5.63E-18
chr2:0627693-0627752	tef103 (PR 205), thf1 (PR 278)	2.341	3.06E-10
chr2:0675081-0675140	naa38 (PR 1489), pfl3 (PR 2420)	2.665	1.17E-12
chr2:0721502-0721559	sco1 (PR 2200), lsb1 (ORF 784)	1.147	3.49E-04
chr2:0812081-0812135	mrl1 (PR 1582), anc1 (ORF 246)	2.115	4.66E-09
chr2:0844163-0844222	mfs3 (ORF 902)	1.547	4.48E-06
chr2:0889846-0889904	pmp3 (PR 1695)	3.190	1.04E-15
chr2:0966634-0966693	txc1 (PR 18)	2.289	1.80E-10
chr2:0993393-0993452	swc2 (PR 2026), puf2 (ORF 506)	1.754	2.16E-07
chr2:1045871-1045930	ubi4 (PR 305), erg28 (PR 1605), ecm14 (PR 1912)	1.950	1.41E-07
chr2:1082607-1082658	mas5 (ORF 888)	1.746	3.50E-07
chr2:1107501-1107554	dus2 (PR 1174)	2.546	9.76E-12
chr2:1152419-1152478	SPBC409.08 (ORF 340)	2.184	3.28E-09
chr2:1268491-1268550	but2 (PR 1198)	4.573	1.08E-22
chr1:1308365-1308424	adn1 (PR 2475)	2.787	3.20E-13
chr2:1392387-1392446	mde3 (PR 1008), SPBC8D2.18c (ORF 522)	1.348	4.16E-05
chr2:1448366-1448410	rps1002 (ORF 358)	2.028	5.71E-09
chr2:1455045-1455104	nep2 (PR 1611)	3.120	2.95E-15
chr2:1476350-1476407	act1 (ORF 869)	1.933	4.04E-08
chr2:1533526-1533577	SPBC83.13 (ORF 223)	1.383	3.37E-05
chr2:1546043-1546100	fic1 (PR 1277)	2.431	2.52E-11
chr2:1555219-1555278	isp4 (PR 2428)	2.099	4.60E-09
chr2:1572085-1572139	mgr2 (PR 1233), mep33 (PR 2388), sua1 (ORF 818)	2.147	2.89E-09

chr2:1688312-1688371	fba1 (PR 0), mug124 (PR 1107), prp38 (PR 1777)	3.442	4.43E-16
chr2:1742677-1742736	byr2 (PR 381)	2.174	1.12E-09
chr2:1751303-1751362	scr1 (PR 2227)	1.923	6.07E-08
chr2:1776029-1776073	sce3 (ORF 824)	1.722	3.86E-07
chr2:1792797-1792855	rpl701 (PR 582), rps1601 (PR 1092), ppr2 (PR 2115), rpsl402 (ORF 413)	2.308	2.97E-10
chr2:1873591-1873650	SPBC3H7.05c (PR 809)	2.520	2.06E-11
chr2:1887684-1887743	SPBC3H7.02 (PR 686)	1.953	1.59E-08
chr2:1948797-1948848	zrg17 (PR 2475)	1.846	6.73E-08
chr2:1970240-1970299	SPBC1E8.05 (PR 615)	3.098	3.93E-15
chr2:2020008-2020058	SPBP23A10.11c (ORF 631)	1.614	1.36E-06
chr2:2113282-2113341	rga7 (PR 388), mat1-Mc (PR 1141)	1.494	1.17E-05
chr2:2201223-2201279	eno101 (PR 0)	3.470	1.89E-16
chr2:2215204-2215260	meu17 (PR 1832), arc1 (ORF 766)	1.484	1.23E-05
chr2:2300656-2300712	pfk1 (PR 362)	4.100	2.42E-18
chr2:2471250-2471309	SPBC12C2.04 (PR 1035), SPBC12C2.03c (PR 2321)	1.937	6.94E-08
chr2:2486559-2486618	rga5 (PR 189), nak1 (PR 2239)	2.275	6.40E-10
chr2:2553803-2553862	gas2 (PR 185)	3.200	2.88E-15
chr2:2586307-2586362	SPBC2G5.05 (PR 159), erv41 (PR 2072)	1.690	7.64E-07
chr2:2591032-2591090	hmt2 (PR 553)	2.883	3.98E-13
chr2:2807283-2807332	tdh1 (PR 305)	4.133	7.20E-21
chr2:2826999-2827058	SPBC19C7.04c (PR 933)	3.176	4.96E-14
chr2:2901986-2902043	aco2 (PR 1060)	2.465	3.16E-11
chr2:3009114-3009170	klp9 (PR 1361)	4.582	8.63E-22
chr2:3155724-3155783	SPBC609.01 (PR 1814)	1.879	9.84E-08
chr2:3408769-3408828	ptr2 (PR 1077)	3.140	1.92E-13
chr2:3425718-3425777	usp102 (PR 1487), ght2 (PR 1795)	1.402	2.33E-05
chr2:3484218-3484275	zfs1 (ORF 393)	1.553	4.62E-06
chr2:3493957-3494016	SPBPB7E8.01 (PR 501)	2.204	1.92E-09
chr2:3498257-3498312	SPBPB7E8.02 (PR 820)	2.163	4.86E-09
chr2:3514431-3514490	exg1 (PR 648), cbp1 (PR 2092)	2.467	1.50E-11
chr2:3532148-3532207	SPBC1105.13c (PR 0), rsv2 (PR 724)	2.091	2.00E-08
chr2:3606372-3606431	zrt1 (PR 1459)	1.961	1.44E-08
chr2:3612719-3612775	sir2 (PR 1163)	1.344	6.37E-05
chr2:3664844-3664903	dbp2 (ORF 398)	1.551	5.43E-06
chr2:3811022-3811081	car2 (PR 295), trm140 (PR 2227)	3.412	2.55E-16
chr2:3862275-3862334	ssn6 (PR 1171)	2.262	2.49E-10
chr2:3922777-3922833	pgi1 (ORF 621)	1.274	8.43E-05
chr2:3975013-3975072	SPBC26H8.11c (PR 120), cyc3 (PR 1769)	1.414	2.83E-05
chr2:3983169-3983226	ste11 (PR 2360)	2.811	3.39E-13
chr2:4035607-4035666	gpd1 (PR 148)	2.614	9.67E-12
chr2:4056405-4056464	SPBC215.13 (ORF 237)	1.345	4.14E-05
chr2:4081666-4081720	sro1 (PR 487), arp1 (PR 2217)	2.282	8.21E-10
chr2:4087240-4087291	mrm1 (PR 802), ilv5 (ORF 802)	1.666	1.08E-06
chr2:4130584-4130643	abp2 (PR 1059), cnp3 (PR 2016)	3.348	5.15E-15
chr2:4159869-4159927	pgk1 (PR 453)	4.348	7.82E-21
chr2:4163020-4163075	rli1 (PR 1584), sam1 (ORF 601)	1.580	4.20E-06
chr2:4216804-4216863	SPBC16G5.03 (PR 1811), rtt109 (PR 2055), rbk1 (ORF 240)	1.233	1.30E-04
chr2:4253556-4253612	SPBC1652.01 (ORF 276)	1.902	3.15E-08
chr2:4284839-4284890	nrm1 (PR 1152), oga1 (ORF 901)	1.223	1.69E-04
chr2:4443198-4443256	pho84 (PR 996), SPBC8E4.02c (ORF 43)	4.042	5.49E-20
chr2:4447242-4447301	pho1 (PR 256)	3.513	1.98E-17

chr3:0072846-0072905	SPCC757.12 (PR 578), SPCC757.11c (PR 1790)	3.755	5.42E-17
chr3:0170988-0171046	SPCC320.03 (PR 2463)	2.858	7.69E-14
chr3:0229405-0229461	ght8 (PR 1005), dbl5 (PR 3762)	3.646	2.69E-18
chr3:0236215-0236274	SPCC1529.01 (PR 1280), ght1 (PR 1708)	2.663	9.01E-12
chr3:0242461-0242518	zwf2 (PR 1253), wtf5 (PR 1337)	3.079	7.87E-15
chr3:0252523-0252572	SPCC794.04c (PR 2329)	4.082	2.43E-19
chr3:0277647-0277706	mae2 (PR 436), SPCC794.15 (PR 1200), SPCC553.12c (PR 1728)	3.762	1.63E-17
chr3:0285518-0285577	SPCC553.10 (PR 1047), spb70 (PR 2063)	2.975	6.03E-13
chr3:0348496-0348555	pil1 (PR 617)	3.194	8.00E-14
chr3:0352550-0352609	SPCC594.01 (PR 1847)	3.659	7.30E-18
chr3:0361424-0361479	SPCC594.02c (PR 1691), SPCC594.03 (ORF 68)	3.995	3.42E-19
chr3:0425096-0425154	wtf8 (PR 2291)	1.549	3.31E-06
chr3:0470946-0471004	aph1 (PR 1258)	1.380	3.20E-05
chr3:0539962-0540020	SPCC962.01 (PR 1255)	1.928	8.29E-08
chr3:0564189-0564248	sap1 (PR 1072)	4.346	3.52E-21
chr3:0612436-0612489	rpl101 (ORF 61)	1.540	1.42E-05
chr3:0673838-0673895	scw1 (ORF 362)	1.373	2.65E-05
chr3:0716417-0716475	bfr1 (PR 2410)	2.349	6.50E-10
chr3:0750444-0750503	ump1 (PR 1914), SPCC1020.13c (PR 1971)	1.928	2.26E-08
chr3:0762789-0762840	oca2 (PR 1936)	1.977	1.12E-08
chr3:0798993-0799050	fta4 (PR 793), spt2 (PR 1024)	1.576	2.67E-06
chr3:0811388-0811447	SPCC1393.08 (PR 1208)	3.121	2.25E-15
chr3:0862469-0862528	eis1 (PR 184), pup3 (PR 2076)	1.736	5.37E-07
chr3:0939338-0939397	tpi1 (PR 548), pog1 (PR 2019)	2.437	7.18E-11
chr3:0949877-0949936	ade10 (PR 288)	2.063	1.95E-08
chr3:0975674-0975732	SPCC1795.10c (PR 1709), sum3 (ORF 939)	1.663	1.19E-06
chr3:1029458-1029517	psy1 (PR 312)	3.806	4.64E-16
chr3:1157402-1157459	ipk1 (PR 689), set9 (PR 1796)	2.790	5.07E-13
chr3:1303802-1303861	SPCC1322.09 (PR 2333), srk1 (ORF 902)	1.118	6.17E-04
chr3:1310383-1310436	rpl2302 (PR 1216), SPCC1322.10 (ORF 603)	1.940	1.94E-08
chr3:1393591-1393641	ole1 (ORF 488)	2.303	1.61E-10
chr3:1413240-1413299	hta1 (PR 1318)	1.580	2.84E-06
chr3:1420299-1420349	gdh1 (ORF 463)	1.757	3.33E-07
chr3:1452582-1452641	SPCC11E10.01 (PR 601)	3.298	3.41E-14
chr3:1526122-1526181	SPCC584.16c (PR 910)	1.901	4.73E-08
chr3:1547787-1547846	tol1 (PR 2158)	2.177	6.43E-09
chr3:1591272-1591331	adh1 (PR 28)	3.423	4.43E-17
chr3:1634971-1635030	pmd1 (PR 944)	2.800	1.73E-13
chr3:1661814-1661872	trp663 (PR 2031), SPCC663.15c (ORF 383)	1.469	8.23E-06
chr3:1669943-1669998	gaf1 (PR 1066), SPCC417.03 (PR 2005)	2.327	2.25E-10
chr3:1676653-1676709	cfh2 (ORF 247)	2.087	9.32E-09
chr3:1703929-1703987	SPCC417.15 (PR 1087), SPCC191.01 (PR 2474)	2.199	1.32E-09
chr3:1859508-1859567	SPCC1223.09 (PR 1275)	2.555	1.03E-10
chr3:1871070-1871129	cbf12 (PR 621), meu10 (PR 1340)	2.955	3.10E-14
chr3:2010362-2010421	SPCC4F11.05 (PR 81), imt2 (PR 1166), mpg1 (PR 2421)	4.633	8.12E-22
chr3:2056880-2056937	ssa2 (PR 306)	3.620	1.20E-15
chr3:2085849-2085908	tpx1 (PR 235), bxi1 (PR 969)	2.416	6.50E-10
chr3:2095809-2095864	rps20 (PR 694), SPCC576.06c (PR 2172), rps2 (ORF 124)	1.827	8.23E-08
chr3:2113865-2113921	SPCC576.17c (PR 475)	2.958	3.95E-13
chr3:2257908-2257967	sal3 (PR 2315)	1.343	8.58E-05
chr3:2310074-2310131	SPCC965.13 (PR 2349)	2.212	1.90E-09

chr3:2378874-2378932	pcy1 (PR 747)	1.496	9.74E-06
chr3:2423607-2423662	SPCC569.05c (PR 674), SPCC569.06 (PR 1507)	2.721	5.29E-13

Table A3: ChIP-chip analysis of *Prz1-HA* with tunicamycin treatment.

Chromosome Location	Genes	High Average Ratio	P-value
chr1:0066080-0066130	SPAC977.17 (PR 1013), dak2 (ORF 549)	2.781	4.48E-08
chr1:0104111-0104169	pdc101 (PR 567), SPAC1F8.08 (ORF 170)	3.224	2.25E-10
chr1:0158612-0158671	SPAC5H10.07 (PR 532), adh4 (PR 796)	2.463	1.26E-06
chr1:0239554-0239613	SPAC806.11 (PR 2124)	4.918	3.92E-22
chr1:0361565-0361624	erg25 (PR 603), mug177 (ORF 8)	1.952	1.23E-04
chr1:0383251-0383310	loc1 (PR 1317)	3.356	4.02E-11
chr1:0460258-0460315	SPAC24H6.13 (PR 582), uba3 (PR 1624)	2.151	2.31E-05
chr1:0577540-0577599	erg11 (PR 918), mcp7 (PR 922)	3.105	1.00E-09
chr1:0660380-0660431	lkh1 (PR 1548)	2.165	2.05E-05
chr1:0790669-0790728	prz1 (PR 1505)	3.679	4.56E-13
chr1:0869924-0869983	sib1 (PR 397), sib2 (PR 1042)	2.507	8.12E-07
chr1:0934099-0934154	erg31 (PR 145)	2.659	1.68E-07
chr1:0947541-0947600	puf3 (PR 1614)	2.615	2.67E-07
chr1:0960805-0960853	sno1 (PR 2455), seb1 (ORF 744)	2.398	2.38E-06
chr1:1003742-1003801	sod1 (PR 279)	2.861	1.81E-08
chr1:1078278-1078336	plb1 (PR 1660)	3.879	2.32E-14
chr1:1150276-1150335	SPAC56F8.15 (PR 1733)	5.416	1.74E-26
chr1:1184125-1184180	SPAC22A12.14c (PR 1754), acl2 (PR 2134)	2.017	7.22E-05
chr1:1206531-1206589	sir1 (PR 1033)	4.127	4.76E-16
chr1:1238387-1238446	mug134 (PR 450)	3.110	9.44E-10
chr1:1241843-1241901	SPAC10F6.17c (PR 188), SPAC56E4.03 (PR 2150)	1.816	3.51E-04
chr1:1263416-1263475	SPAC1420.01c (PR 656)	2.542	5.66E-07
chr1:1286457-1286516	SPAPB17E12.12c (PR 973)	2.413	2.05E-06
chr1:1290863-1290922	rcf2 (PR 356)	2.656	1.74E-07
chr1:1361063-1361122	pas1 (PR 1449)	2.422	1.88E-06
chr1:1398392-1398451	SPAC20G8.04c (PR 469)	2.360	3.43E-06
chr1:1479975-1480034	SPAC9.08c (PR 1913)	2.522	6.99E-07
chr1:1494103-1494161	mtf2 (PR 279), mug116 (PR 509), vps74 (PR 2349)	3.242	1.80E-10
chr1:1540726-1540785	pabp (PR 2080), SPAC57A7.05 (PR 2125)	3.500	5.75E-12
chr1:1544002-1544053	hul5 (PR 2451)	1.688	8.97E-04
chr1:1572029-1572088	ecm33 (PR 769)	2.609	2.84E-07
chr1:1598263-1598322	gln1 (PR 692), SPAC23H4.05c (PR 1009)	2.500	8.70E-07
chr1:1667662-1667720	rds1 (PR 351)	4.020	2.62E-15
chr1:1823613-1823669	SPAC1002.20 (PR 303), psu1 (PR 424), itt1 (PR 1116)	4.285	3.50E-17
chr1:1830056-1830115	SPAC1002.16c (PR 686), urg3 (PR 2342)	2.301	5.99E-06
chr1:1835020-1835079	urg1 (PR 390)	2.858	1.88E-08
chr1:1849519-1849578	SPAC1399.02 (PR 1629)	2.688	1.23E-07
chr1:1875458-1875517	SPAPB1A10.08 (PR 754), SPAPB1A10.07c (PR 1661)	1.699	8.26E-04
chr1:1889000-1889053	pof15 (PR 1867)	4.125	4.86E-16
chr1:1906256-1906313	ppk1 (PR 1955)	3.209	2.72E-10
chr1:1919252-1919310	pss1 (ORF 850)	1.805	3.83E-04
chr1:1944243-1944302	SPAC3H1.06c (PR 1457), aru1 (ORF 12)	2.567	4.38E-07
chr1:1957074-1957133	hsr1 (PR 2178)	2.393	2.49E-06
chr1:2095433-2095492	obr1 (PR 542), SPAC3C7.13c (PR 2491)	5.347	7.39E-26
chr1:2106416-2106475	bdf2 (PR 995), acp2 (PR 1167)	4.094	8.11E-16
chr1:2203189-2203248	pap1 (PR 942)	2.450	1.43E-06
chr1:2276774-2276831	idn1 (PR 368), cmb1 (PR 525)	1.892	1.98E-04
chr1:2322652-2322711	msa1 (PR 2413)	1.694	8.57E-04

chr1:2424038-2424093	SPAC6B12.07c (PR 877), mug185 (PR 2098)	2.682	1.32E-07
chr1:2508728-2508787	bub3 (PR 1422), ssr2 (PR 2464), gly1 (ORF 256)	2.011	7.62E-05
chr1:2520015-2520074	avl9 (PR 1624), gpa2 (PR 1700)	2.978	4.63E-09
chr1:2625294-2625351	SPAC7D4.08 (PR 0), trx1 (PR 106), alg3 (PR 1232), ost4 (PR 1256)	1.894	1.94E-04
chr1:2651002-2651061	spp42 (ORF 264)	1.902	1.83E-04
chr1:2664127-2664183	hxk2 (PR 1633)	4.727	1.44E-20
chr1:2718514-2718571	pmc1 (PR 1583), vma5 (PR 2383)	4.290	3.20E-17
chr1:2792534-2792593	fmt1 (PR 1313), rpl14 (PR 2345)	1.983	9.54E-05
chr1:2872144-2872201	pvg1 (PR 819)	3.623	1.02E-12
chr1:2875908-2875967	SPACUNK4.16c (PR 1552), SPACUNK4.17 (PR 1659), mug153 (ORF 20)	3.500	5.79E-12
chr1:2892973-2893032	SPACUNK4.10 (PR 446)	1.691	8.77E-04
chr1:2925439-2925498	amt3 (ORF 948)	2.780	4.51E-08
chr1:2936646-2936704	SPAC2E1P3.05c (PR 543)	3.303	8.16E-11
chr1:2960494-2960553	SPAPB24D3.07c (PR 1568)	4.516	6.47E-19
chr1:3004178-3004232	pac2 (PR 1906)	4.506	7.74E-19
chr1:3006589-3006648	pac2 (ORF 451)	1.699	8.31E-04
chr1:3033547-3033603	SPAC1786.02 (PR 1279), SPAC1786.04 (ORF 313)	3.137	6.71E-10
chr1:3076919-3076974	SPAC16A10.01 (PR 702), spn5 (PR 931)	2.491	9.53E-07
chr1:3374830-3374889	SPAC8E11.08c (PR 627), SPAC8E11.10 (PR 846), alp31 (PR 2259), rmt2 (PR 2348)	1.809	3.70E-04
chr1:3384227-3384286	rad24 (PR 0), SPAC8E11.01c (PR 1761)	3.371	3.30E-11
chr1:3456712-3456771	nde2 (PR 502)	2.650	1.86E-07
chr1:3478402-3478459	tps1 (PR 855)	2.951	6.41E-09
chr1:3499935-3499993	shd1 (ORF 886)	1.886	2.06E-04
chr1:3537243-3537302	deb1 (ORF 616)	1.753	5.63E-04
chr1:3577151-3577200	SPAC17A2.10c (PR 1464), SPAC17A2.11 (ORF 42)	4.607	1.28E-19
chr1:3647913-3647958	dtd1 (PR 1601)	2.670	1.49E-07
chr1:3664409-3664461	prr1 (PR 1546), SPAC8C9.12c (PR 2010)	2.978	4.65E-09
chr1:3723531-3723590	hal3 (PR 243), SPAC15E1.02c (PR 1775)	1.747	5.86E-04
chr1:3747828-3747886	per1 (PR 1809)	2.963	5.54E-09
chr1:3841052-3841108	SPAC4H3.08 (PR 473), rdl2 (PR 1672), SPAC4H3.09 (PR 2308)	3.722	2.43E-13
chr1:3870124-3870179	rps1502 (PR 1164)	4.442	2.38E-18
chr1:3874055-3874114	pma1 (ORF 565)	2.862	1.79E-08
chr1:3885334-3885393	stp1 (PR 1243), rlc1 (PR 2177), SPAC926.02 (ORF 790)	2.976	4.77E-09
chr1:3929084-3929139	rim1 (PR 767), rpa49 (PR 1824), SPAC2F3.05c (ORF 497)	1.841	2.91E-04
chr1:3933166-3933224	kap104 (ORF 844)	2.836	2.42E-08
chr1:3981714-3981773	ppk18 (PR 1025)	3.137	6.79E-10
chr1:3985627-3985685	SPAPB18E9.04c (PR 523)	5.375	4.11E-26
chr1:4004142-4004199	yih1 (PR 308)	4.722	1.57E-20
chr1:4007114-4007170	SPAC27E2.03c (PR 86)	2.742	6.83E-08
chr1:4046899-4046947	cda1 (PR 1194), cut20 (PR 2480), pms1 (ORF 551)	1.812	3.63E-04
chr1:4058919-4058978	SPAC19G12.09 (PR 1274)	3.568	2.24E-12
chr1:4127959-4128018	pot1 (PR 1511)	1.908	1.74E-04
chr1:4133592-4133650	SPAC26H5.07c (PR 129)	4.335	1.50E-17
chr1:4172201-4172257	SPAC25B8.11 (PR 1802), SPAC25B8.10 (ORF 25)	2.528	6.56E-07
chr1:4177239-4177298	SPAC25B8.12c (ORF 634)	2.391	2.53E-06
chr1:4189290-4189349	ypf1 (PR 1004), tyw3 (PR 2065), SPAC25B8.18 (PR 2264)	2.286	6.86E-06
chr1:4228753-4228812	hsp3105 (PR 2038)	1.890	1.99E-04

chr1:4409918-4409977	uso1 (PR 580), nnf1 (ORF 145)	1.734	6.43E-04
chr1:4429007-4429066	ura2 (PR 202), dus3 (PR 618), srp2 (PR 2042)	2.976	4.74E-09
chr1:4433575-4433634	sfp1 (PR 0), SPAC9E9.01 (PR 1227)	2.608	2.87E-07
chr1:4449858-4449916	ypt2 (PR 341), rad26 (PR 1199), SPAC9E9.06c (PR 2390)	3.368	3.43E-11
chr1:4457512-4457571	atd1 (PR 2441)	1.823	3.35E-04
chr1:4517462-4517514	omt2 (PR 28), etf1 (PR 1532)	1.706	7.86E-04
chr1:4525694-4525753	SPAC27D7.09c (PR 1155)	4.574	2.32E-19
chr1:4716367-4716425	mug51 (PR 145)	4.185	1.85E-16
chr1:4762285-4762344	cox24 (PR 735), SPAC1782.02c (PR 1399), ypa2 (PR 2105), saf3 (ORF 478)	1.688	8.94E-04
chr1:4782268-4782325	fta6 (PR 0), arp2 (PR 730), SPAC11H11.03c (PR 2019)	3.892	1.91E-14
chr1:4855818-4855862	fta1 (ORF 275)	2.693	1.17E-07
chr1:4875051-4875107	SPAC19B12.01 (PR 468), hit1 (PR 2298)	3.632	8.99E-13
chr1:4905347-4905406	SPAC19B12.11c (PR 1171), cox1102 (PR 1572)	3.944	8.62E-15
chr1:5080375-5080432	och1 (PR 0), rgf2 (PR 673), mcp3 (PR 2381)	1.694	8.56E-04
chr1:5118019-5118076	pex3 (PR 1597), hal4 (PR 1605), srs1 (ORF 802)	2.262	8.53E-06
chr1:5151635-5151693	hgh1 (PR 2239)	3.866	2.83E-14
chr1:5168762-5168821	gyp51 (PR 1926)	3.801	7.60E-14
chr1:5195712-5195771	Tf2-7 (PR 567)	2.545	5.53E-07
chr1:5264024-5264080	dpp1 (PR 2271), abp1 (ORF 950)	4.158	2.84E-16
chr1:5309290-5309349	gas5 (PR 693)	1.711	7.61E-04
chr1:5314746-5314804	rpl22 (PR 58)	4.081	9.98E-16
chr1:5354943-5354999	pop2 (PR 132), pgc1 (PR 1271)	1.726	6.83E-04
chr1:5443137-5443196	SPAC29B12.14c (PR 1543), SPAC1039.01 (PR 2154)	1.934	1.41E-04
chr1:5473718-5473777	gto1 (ORF 771)	2.970	5.14E-09
chr1:5511404-5511461	SPAC869.03c (PR 1296), SPAC869.04 (ORF 908)	4.191	1.65E-16
chr2:0072724-0072782	SPBPB21E7.08 (ORF 379)	3.667	5.46E-13
chr2:0107709-0107768	alr2 (PR 0)	3.962	6.54E-15
chr2:0133736-0133795	SPBC1683.01 (PR 508)	2.134	2.69E-05
chr2:0156603-0156662	ght4 (PR 893)	2.290	6.61E-06
chr2:0230344-0230403	SPBC660.16 (PR 0)	2.546	5.45E-07
chr2:0352799-0352852	tgp1 (PR 430)	3.450	1.14E-11
chr2:0358643-0358702	SPBC1271.07c (PR 153), mug96 (PR 1201)	1.683	9.28E-04
chr2:0465205-0465264	met17 (PR 369)	3.335	5.31E-11
chr2:0525286-0525342	fhn1 (PR 749)	3.964	6.30E-15
chr2:0576710-0576769	gpd3 (PR 1962)	2.689	1.21E-07
chr2:0606755-0606814	cta3 (PR 1357), rps1701 (PR 2378)	3.789	9.03E-14
chr2:0627693-0627752	tef103 (PR 205), thf1 (PR 278), see1 (PR 2496)	2.299	6.09E-06
chr2:0675081-0675140	naa38 (PR 1489), pfl3 (PR 2420)	3.225	2.22E-10
chr2:0715215-0715272	ubc4 (PR 61)	2.373	3.03E-06
chr2:0813394-0813449	anc1 (PR 1013)	2.316	5.19E-06
chr2:0889846-0889904	pmp3 (PR 1695)	3.703	3.21E-13
chr2:0966634-0966693	txc1 (PR 18)	2.665	1.58E-07
chr2:1045871-1045930	ubi4 (PR 305), erg28 (PR 1605), ecm14 (PR 1912)	2.336	4.31E-06
chr2:1108553-1108612	dus2 (PR 116), erg27 (PR 2278)	2.390	2.56E-06
chr2:1152419-1152478	SPBC409.08 (ORF 340)	1.736	6.36E-04
chr2:1188946-1189005	SPBC4.02c (PR 1622)	2.024	6.83E-05
chr2:1268491-1268550	but2 (PR 1198)	4.520	6.11E-19
chr2:1308471-1308530	adn1 (PR 2475)	3.134	6.98E-10
chr2:1352723-1352780	SPBC27B12.12c (ORF 962)	1.913	1.67E-04
chr2:1448366-1448410	rps1002 (ORF 358)	1.790	4.29E-04

chr2:1455045-1455104	nep2 (PR 1611)	4.303	2.58E-17
chr2:1476350-1476407	act1 (ORF 869)	2.741	6.93E-08
chr2:1513530-1513589	rpl4302 (ORF 150)	1.754	5.59E-04
chr2:1546043-1546100	fic1 (PR 1277), atf1 (PR 1561)	3.251	1.59E-10
chr2:1555219-1555278	isp4 (PR 2428)	2.295	6.32E-06
chr2:1573465-1573524	sua1 (PR 508), mep33 (PR 1003)	2.676	1.39E-07
chr2:1688312-1688371	fba1 (PR 0), mug124 (PR 1107), prp38 (PR 1777)	3.790	8.87E-14
chr2:1742677-1742736	byr2 (PR 381)	2.303	5.85E-06
chr2:1751303-1751362	scr1 (PR 2227)	2.793	3.90E-08
chr2:1872821-1872879	SPBC3H7.05c (PR 1580), pof9 (ORF 974)	3.212	2.63E-10
chr2:1888046-1888105	SPBC3H7.02 (PR 1048)	2.632	2.23E-07
chr2:1948559-1948603	zrg17 (PR 2237)	2.090	3.92E-05
chr2:1970240-1970299	SPBC1E8.05 (PR 615)	3.352	4.26E-11
chr2:2021877-2021935	SPBP23A10.11c (PR 1188), frg1 (PR 2014)	3.289	9.79E-11
chr2:2113539-2113598	rga7 (PR 645), mat1-Mc (PR 884)	1.979	9.89E-05
chr2:2143288-2143335	rpl401 (ORF 151)	2.008	7.80E-05
chr2:2201035-2201088	eno101 (PR 149)	3.636	8.52E-13
chr2:2300656-2300712	pfk1 (PR 362)	4.456	1.85E-18
chr2:2471250-2471309	SPBC12C2.04 (PR 1035), SPBC12C2.03c (PR 2321)	3.263	1.36E-10
chr2:2486240-2486299	rga5 (PR 508), nak1 (PR 1920)	2.237	1.08E-05
chr2:2553803-2553862	gas2 (PR 185)	3.400	2.25E-11
chr2:2586307-2586362	SPBC2G5.05 (PR 159), erv41 (PR 2072)	2.981	4.49E-09
chr2:2591032-2591090	hmt2 (PR 553)	3.320	6.50E-11
chr2:2780304-2780349	SPBC685.08 (PR 967), orc2 (PR 1609), rpl2701 (ORF 304)	1.843	2.87E-04
chr2:2807283-2807332	tdh1 (PR 305)	5.338	8.90E-26
chr2:2826999-2827058	SPBC19C7.04c (PR 933)	3.745	1.74E-13
chr2:2887138-2887189	rsv1 (PR 1261)	2.677	1.38E-07
chr2:2901986-2902043	aco2 (PR 1060)	3.622	1.04E-12
chr2:2969861-2969920	SPBC2D10.03c (PR 1066), SPBC2D10.04 (PR 2276)	2.518	7.28E-07
chr2:3009114-3009170	klp9 (PR 1361)	4.668	4.24E-20
chr2:3155487-3155545	SPBC609.01 (PR 2052)	2.828	2.63E-08
chr2:3242944-3243003	mcs6 (PR 426), meu22 (PR 1997), rps401 (PR 2140)	1.921	1.56E-04
chr2:3380905-3380964	dsd1 (PR 898), SPBC3B8.08 (PR 2466)	1.923	1.55E-04
chr2:3408769-3408828	ptr2 (PR 1077)	3.216	2.51E-10
chr2:3425489-3425548	usp102 (PR 1258), ght2 (PR 2024)	2.741	6.89E-08
chr2:3486604-3486663	zfs1 (PR 1936)	1.858	2.56E-04
chr2:3493957-3494016	SPBPB7E8.01 (PR 501)	2.803	3.49E-08
chr2:3498257-3498312	SPBPB7E8.02 (PR 820)	2.966	5.34E-09
chr2:3514431-3514490	exg1 (PR 648), cbp1 (PR 2092)	3.102	1.04E-09
chr2:3532376-3532435	SPBC1105.13c (PR 188), rsv2 (PR 496)	2.439	1.60E-06
chr2:3573311-3573370	sur2 (PR 1050), SPBC887.16 (PR 1551)	1.761	5.31E-04
chr2:3606372-3606431	zrt1 (PR 1459)	1.862	2.48E-04
chr2:3663145-3663204	mpe1 (PR 1524)	2.160	2.13E-05
chr2:3811022-3811081	car2 (PR 295), trm140 (PR 2227)	3.526	4.01E-12
chr2:3975013-3975072	SPBC26H8.11c (PR 120), cyc3 (PR 1769)	2.055	5.26E-05
chr2:3983169-3983226	ste11 (PR 2360)	2.771	5.01E-08
chr2:4008480-4008539	ctf1 (PR 453), dad4 (PR 2146), trs23 (ORF 296)	1.943	1.32E-04
chr2:4035268-4035322	gpd1 (PR 492)	3.019	2.84E-09
chr2:4081666-4081720	sro1 (PR 487), arp1 (PR 2217)	3.312	7.27E-11
chr2:4130584-4130643	abp2 (PR 1059), cnp3 (PR 2016)	3.728	2.23E-13
chr2:4159869-4159927	pgk1 (PR 453)	4.406	4.43E-18

chr2:4163020-4163075	rli1 (PR 1584), sam1 (ORF 601)	1.735	6.38E-04
chr2:4238790-4238843	rps3 (ORF 483)	1.705	7.95E-04
chr2:4253099-4253158	SPBC1652.01 (PR 122)	1.906	1.76E-04
chr2:4443198-4443256	pho84 (PR 996), SPBC8E4.02c (ORF 43)	4.468	1.50E-18
chr2:4447039-4447098	pho1 (PR 459)	3.518	4.51E-12
chr3:0067289-0067347	rnc1 (PR 604), vph2 (PR 1265)	1.742	6.06E-04
chr3:0071775-0071830	SPCC757.11c (PR 719), SPCC757.12 (PR 1653)	3.648	7.20E-13
chr3:0173772-0173829	SPCC1235.01 (PR 354)	4.458	1.80E-18
chr3:0229405-0229461	ght8 (PR 1005)	4.717	1.72E-20
chr3:0236215-0236274	SPCC1529.01 (PR 1280), ght1 (PR 1708)	2.374	2.99E-06
chr3:0242461-0242518	zwf2 (PR 1253), wtf5 (PR 1337)	3.287	9.96E-11
chr3:0252523-0252572	SPCC794.04c (PR 2329)	4.377	7.35E-18
chr3:0277647-0277706	mae2 (PR 436), SPCC794.15 (PR 1200), SPCC553.12c (PR 1728)	4.061	1.37E-15
chr3:0285518-0285577	SPCC553.10 (PR 1047), spb70 (PR 2063)	3.608	1.26E-12
chr3:0346785-0346843	pil1 (PR 2329)	3.877	2.41E-14
chr3:0352550-0352609	SPCC594.01 (PR 1847)	4.173	2.25E-16
chr3:0361424-0361479	SPCC594.02c (PR 1691), SPCC594.03 (ORF 68)	3.942	8.84E-15
chr3:0471433-0471485	aph1 (PR 1745), ser3 (ORF 583)	1.925	1.52E-04
chr3:0536887-0536946	eft202 (PR 380)	2.215	1.31E-05
chr3:0564189-0564248	sap1 (PR 1072)	4.870	9.80E-22
chr3:0713267-0713321	bfr1 (ORF 686)	2.235	1.10E-05
chr3:0716417-0716475	bfr1 (PR 2410)	4.345	1.26E-17
chr3:0749928-0749985	ump1 (PR 1398), SPCC1020.13c (PR 2489)	1.761	5.32E-04
chr3:0762789-0762840	oca2 (PR 1936)	3.476	8.05E-12
chr3:0798993-0799050	fta4 (PR 793), spt2 (PR 1024), ers1 (PR 2147)	1.745	5.94E-04
chr2:0812081-0812135	SPCC1393.08 (PR 1208)	3.933	1.02E-14
chr3:0820048-0820105	mrpl20 (PR 1539), ten1 (ORF 52)	1.852	2.69E-04
chr3:0863006-0863063	eis1 (ORF 294)	1.840	2.94E-04
chr3:0867096-0867155	sfk1 (PR 841)	2.699	1.10E-07
chr3:0939338-0939397	tpi1 (PR 548), pog1 (PR 2019)	2.802	3.53E-08
chr3:0949877-0949936	ade10 (PR 288)	2.716	9.08E-08
chr1:0960805-0960853	SPCPB16A4.06c (PR 1974)	1.918	1.60E-04
chr3:1029458-1029517	psy1 (PR 312)	3.228	2.15E-10
chr3:1157402-1157459	ipk1 (PR 689), set9 (PR 1796)	2.942	7.15E-09
chr3:1309596-1309655	SPCC1322.10 (PR 125), rpl2302 (PR 1997)	2.379	2.84E-06
chr1:1398392-1398451	wtf11 (PR 974), gst4 (ORF 161)	1.766	5.10E-04
chr3:1412814-1412865	hta1 (PR 892), htb1 (ORF 330)	1.788	4.34E-04
chr3:1431832-1431891	SPCC622.15c (PR 1053)	2.551	5.19E-07
chr3:1438151-1438210	jmj4 (PR 165)	2.250	9.57E-06
chr3:1452232-1452291	SPCC11E10.01 (PR 951)	3.867	2.80E-14
chr3:1525817-1525876	SPCC584.16c (PR 605)	1.829	3.19E-04
chr3:1545337-1545396	git3 (PR 756)	1.688	8.95E-04
chr3:1591272-1591331	adh1 (PR 28)	3.855	3.36E-14
chr3:1634971-1635030	pmd1 (PR 944)	3.531	3.74E-12
chr3:1669943-1669998	gaf1 (PR 1066), SPCC417.03 (PR 2005)	3.359	3.86E-11
chr3:1677442-1677501	cfh2 (PR 486)	2.870	1.63E-08
chr3:1694441-1694500	SPCC417.09c (PR 9), dal51 (PR 1226)	1.710	7.68E-04
chr3:1703929-1703987	SPCC417.15 (PR 1087), SPCC191.01 (PR 2474)	3.284	1.05E-10
chr3:1827219-1827278	rps2802 (ORF 82)	1.861	2.50E-04
chr3:1859282-1859341	SPCC1223.09 (PR 1049)	3.277	1.14E-10
chr3:1871070-1871129	cbf12 (PR 621), meu10 (PR 1340)	3.461	9.89E-12
chr3:2010362-2010421	SPCC4F11.05 (PR 81), imt2 (PR 1166), mpg1 (PR 2421)	4.583	1.99E-19

chr3:2056880-2056937	ssa2 (PR 306)	3.904	1.60E-14
chr3:2068596-2068648	amt1 (PR 1158)	1.840	2.95E-04
chr3:2085849-2085908	tpx1 (PR 235), bxi1 (PR 969)	3.235	1.97E-10
chr3:2095392-2095439	rps20 (PR 1119), SPCC576.06c (PR 1755), rps2 (ORF 549)	2.002	8.14E-05
chr3:2113865-2113921	SPCC576.17c (PR 475)	3.060	1.74E-09
chr3:2310074-2310131	SPCC965.13 (PR 2349)	2.489	9.68E-07
chr3:2352794-2352853	SPCC70.03c (PR 588)	2.121	3.00E-05
chr3:2380567-2380626	SPCC1827.03c (PR 544), vms1 (PR 2106), pcy1 (PR 2440)	2.340	4.12E-06
chr3:2423607-2423662	SPCC569.05c (PR 674), SPCC569.06 (PR 1507)	2.882	1.43E-08

Table A4: The 165 putative target genes positively regulated by Prz1.

Systematic ID	Name	$CaCl_2$ chIP	tuni chIP	Motif	*CRZ1* regulated *S. cerevisiae* orthologs
SPBC4F6.09	str1	NA	NA	No	ENB1
SPAC17C9.16c	mfs1	NA	NA	No	No
SPBC1709.12	rid1	NA	NA	No	No
SPAC17G6.02c	tco1	NA	NA	No	PUG1, RTA1, YLR046C
SPAC22E12.11c	set3	NA	NA	No	No
SPBC1E8.05	SPBC1E8.05	3.098	3.352	Yes	No
SPAPB2B4.04c	pmc1	3.574	4.290	Yes	PMC1
SPAC630.04c	SPAC630.04c	NA	NA	Yes	No
SPAC22F8.02c	pvg5	NA	NA	Yes	No
SPAC23G3.03	sib2	1.615	2.507	Yes	No
SPAC824.08	gda1	NA	NA	Yes	No
SPAC1039.07c	SPAC1039.07c	NA	NA	Yes	No
SPCC737.03c	ima1	NA	NA	No	No
SPAC8C9.16c	mug63	NA	NA	No	No
SPAC1687.07	SPAC1687.07	NA	NA	Yes	No
SPBC713.12	erg1	NA	2.543	Yes	No
SPBC19F8.03c	yap18	NA	NA	Yes	No
SPAC23G3.07c	snf30	NA	NA	No	No
SPAC22E12.09c	krp1	NA	NA	No	No
SPAC26F1.12c	hgh1	2.879	3.866	No	No
SPAC1B3.17	clr2	NA	NA	Yes	No
SPAC8F11.10c	pvg1	3.487	3.623	Yes	No
SPAC1006.01	psp3	NA	NA	No	PRB1
SPMTR.01	matPc	NA	NA	Yes	No
SPCC4B3.10c	ipk1	2.790	2.942	Yes	No
SPCC1682.09c	ggc1	NA	NA	No	No
SPBC83.11	pet2	NA	NA	No	No
SPCC794.15	SPCC794.15	1.327	1.848	No	No
SPCC1753.02c	git3	2.177	1.688	Yes	No
SPAC5H10.13c	gmh2	NA	NA	Yes	No
SPAC29A4.11	rga3	NA	NA	No	No
SPBC3H7.06c	pof9	NA	3.212	Yes	SAF1
SPCC417.05c	cfh2	2.087	2.870	Yes	No
SPAC1F3.05	gga21	NA	NA	Yes	No
SPCC4B3.02c	SPCC4B3.02c	NA	NA	Yes	No
SPAC821.10c	sod1	2.394	2.861	Yes	No
SPBC17F3.01c	rga5	2.275	2.237	Yes	BAG7
SPAC19E9.03	pas1	1.371	2.422	No	PCL5
SPAC5D6.04	SPAC5D6.04	NA	NA	Yes	YBR287W
SPCC1020.13c	SPCC1020.13c	1.928	1.761	No	No
SPAPB1A10.08	SPAPB1A10.08	NA	1.699	Yes	No
SPCC4F11.04c	imt2	4.633	4.583	No	SUR1
SPCC553.12c	SPCC553.12c	3.762	4.061	No	No
SPBC365.14c	uge1	NA	NA	No	No
SPAC22A12.06c	SPAC22A12.06c	NA	NA	Yes	No
SPBC1198.07c	SPBC1198.07c	NA	NA	No	DFG5
SPAC15A10.09c	pun1	NA	NA	No	PUN1
SPBP35G2.05c	cki2	NA	NA	No	No
SPBC216.02	mcp5	NA	NA	Yes	No

SPCC1183.09c	pmp31	NA	NA	No	No
SPBC19C7.12c	omh1	NA	NA	Yes	No
SPAC9G1.10c	SPAC9G1.10c	NA	NA	Yes	No
SPBC83.19c	SPBC83.19c	NA	NA	Yes	No
SPAC6G9.12	cfr1	NA	NA	No	No
SPBPB2B2.18	SPBPB2B2.18	NA	NA	Yes	No
SPCC417.06c	ppk35	NA	NA	Yes	No
SPAC6F6.05	ost2	NA	NA	Yes	No
SPCC4B3.12	set9	2.790	2.942	No	No
SPAC750.04c	SPAC750.04c	NA	NA	Yes	No
SPCC1259.14c	meu27	NA	NA	Yes	No
SPBC31E1.02c	pmr1	NA	NA	Yes	PMR1
SPCC613.09	sen54	NA	NA	No	No
SPBC14C8.05c	meu17	1.484	NA	No	No
SPBC354.08c	rsn1	NA	NA	No	No
SPAC1A6.11	SPAC1A6.11	2.558	NA	Yes	No
SPCC584.16c	SPCC584.16c	1.901	1.829	Yes	No
SPAC13G7.04c	mac1	NA	NA	Yes	No
SPAC23D3.12	SPAC23D3.12	NA	NA	No	PHO84
SPAC212.02	SPAC212.02	NA	NA	Yes	No
SPAC22F8.04	pet1	NA	NA	No	No
SPBC1683.09c	frp1	NA	NA	Yes	FRE1
SPCC1529.01	SPCC1529.01	2.663	2.374	No	No
SPAC11E3.06	map1	NA	NA	No	No
SPBC4C3.08	mug136	NA	NA	No	No
SPBP4G3.03	SPBP4G3.03	NA	NA	Yes	No
SPAC32A11.02c	SPAC32A11.02c	NA	NA	Yes	No
SPBC119.05c	lsb1	1.147	NA	Yes	No
SPAPB24D3.07c	SPAPB24D3.07c	3.792	4.516	Yes	No
SPCC330.03c	SPCC330.03c	NA	NA	No	No
SPBC660.06	SPBC660.06	NA	NA	Yes	No
SPAC18B11.04	ncs1	NA	NA	Yes	No
SPBC24C6.06	gpa1	NA	NA	Yes	No
SPAC11H11.04	mam2	NA	NA	No	No
SPAC4C5.03	SPAC4C5.03	NA	NA	Yes	No
SPCPB1C11.02	SPCPB1C11.02	NA	NA	Yes	No
SPAPB1A10.14	pof15	3.884	4.125	No	No
SPACUNK12.02c	cmk1	NA	NA	No	CMK2
SPAC824.02	bst1	NA	NA	Yes	No
SPAC29A4.12c	mug108	NA	NA	Yes	No
SPAC227.06	yip5	NA	NA	Yes	No
SPAC821.13c	dnf1	NA	NA	Yes	No
SPBC1271.07c	SPBC1271.07c	NA	1.683	Yes	No
SPAC13C5.05c	SPAC13C5.05c	NA	NA	Yes	No
SPAC27E2.05	cdc1	NA	NA	No	No
SPBC1198.14c	fbp1	NA	NA	No	No
SPBC1271.03c	SPBC1271.03c	NA	NA	No	No
SPAC4G9.07	mug133	NA	NA	Yes	No
SPAC17G8.13c	mst2	NA	NA	No	No
SPAC22H10.07	scd2	NA	NA	Yes	No
SPBC36B7.02	SPBC36B7.02	NA	NA	Yes	No
SPAC20G8.03	itr2	NA	NA	Yes	No
SPBC16C6.05	SPBC16C6.05	NA	NA	Yes	No
SPAC144.10c	gwt1	NA	NA	No	No

SPAC14C4.07	SPAC14C4.07	NA	NA	Yes	No
SPAC2F3.01	imt1	NA	NA	Yes	SUR1
SPBPB2B2.12c	gal10	NA	NA	Yes	No
SPBC21B10.07	SPBC21B10.07	NA	NA	No	CRH1
SPAC4A8.07c	lcb4	NA	NA	No	No
SPAC4H3.13	pcc1	NA	NA	Yes	No
SPAC1399.03	fur4	NA	NA	No	FUI1
SPAC6F12.04	tvp15	NA	NA	Yes	No
SPAC3A11.10c	SPAC3A11.10c	NA	NA	Yes	No
SPAC27F1.03c	uch1	NA	NA	Yes	No
SPCC4F11.05	SPCC4F11.05	4.633	4.583	Yes	No
SPBCPT2R1.02	SPBCPT2R1.02	NA	NA	Yes	No
SPBC19G7.05c	bgs1	NA	NA	No	FKS2
SPAC23C11.06c	SPAC23C11.06c	NA	NA	Yes	No
SPCC4F11.03c	SPCC4F11.03c	NA	NA	No	No
SPAC25B8.09	SPAC25B8.09	NA	NA	Yes	No
SPAC19G12.10c	cpy1	NA	NA	Yes	No
SPBC119.03	SPBC119.03	NA	NA	Yes	No
SPAC19G12.09	SPAC19G12.09	3.478	3.568	Yes	YDL124W
SPAC4A8.10	rog1	NA	NA	No	No
SPAC1687.08	SPAC1687.08	NA	NA	No	No
SPAC15A10.10	mde6	NA	NA	No	No
SPAC212.01c	SPAC212.01c	NA	NA	Yes	No
SPBC19G7.07c	ppr3	NA	NA	Yes	No
SPAC4G8.13c	prz1	3.422	3.679	No	CRZ1
SPAC25G10.04c	rec10	NA	NA	No	No
SPBP35G2.13c	swc2	1.754	NA	Yes	No
SPBC32C12.02	ste11	2.811	2.771	No	No
SPAC25B8.03	psd2	NA	NA	No	No
SPAC18B11.03c	SPAC18B11.03c	NA	NA	Yes	SLI1
SPCC737.04	SPCC737.04	NA	NA	Yes	No
SPBPB21E7.04c	SPBPB21E7.04c	NA	NA	Yes	No
SPBC15C4.06c	SPBC15C4.06c	NA	NA	No	No
SPBC19G7.06	mbx1	NA	NA	Yes	No
SPBC19C7.04c	SPBC19C7.04c	3.176	3.745	Yes	No
SPBC19C7.05	SPBC19C7.05	NA	NA	Yes	RCR1
SPAC20G4.03c	hri1	NA	NA	No	No
SPAC1039.09	isp5	NA	NA	Yes	No
SPAC869.02c	SPAC869.02c	NA	NA	Yes	No
SPAC869.05c	SPAC869.05c	NA	NA	Yes	No
SPAC977.02	SPAC977.02	NA	NA	No	No
SPBC29A10.08	gas2	3.200	3.400	No	No
SPBC1348.03	SPBC1348.03	NA	NA	Yes	No
SPBC11B10.08	SPBC11B10.08	NA	NA	No	No
SPAPJ691.02	SPAPJ691.02	NA	NA	No	No
SPBC19F8.06c	meu22	NA	1.921	Yes	No
SPAC750.01	SPAC750.01	NA	NA	No	No
SPAC186.08c	SPAC186.08c	NA	NA	No	No
SPAC32A11.01	mug8	NA	NA	No	No
SPCC794.03	SPCC794.03	NA	NA	No	TPO5
SPBC646.17c	dic1	NA	NA	No	No
SPCC1682.08c	mcp2	NA	NA	No	No
SPCC1322.10	pwp1	1.940	2.379	Yes	No
SPAC977.14c	SPAC977.14c	NA	NA	No	No

SPAC222.15	meu13	NA	NA	Yes	No
SPBC1198.01	fmd2	NA	NA	No	No
SPAC212.05c	SPAC212.05c	NA	NA	No	No
SPAC1F8.05	isp3	NA	NA	No	No
SPAC869.03c	SPAC869.03c	4.223	4.191	No	No
SPAC27D7.03c	mei2	NA	NA	No	No
SPAC1565.04c	ste4	NA	NA	Yes	No
SPAC513.03	mfm2	NA	NA	No	No

Table A5: The 92 putative target genes negatively regulated by Prz1.

Systematic ID	Name	$CaCl_2$ chIP	tuni chIP	*CRZ1* regulated *S. cerevisiae* orthologs
SPBC8E4.01c	pho84	4.042	4.468	PHO84
SPCC18B5.01c	bfr1	2.349	2.235	PDR10
SPAC186.01	pfl9	NA	NA	No
SPBPB2B2.08	SPBPB2B2.08	NA	NA	No
SPAC869.01	SPAC869.01	NA	NA	No
SPAC186.02c	SPAC186.02c	NA	NA	No
SPCPB1C11.03	SPCPB1C11.03	NA	NA	No
SPBC8E4.02c	SPBC8E4.02c	4.042	4.468	No
SPAC4G8.12c	SPAC4G8.12c	2.212	NA	No
SPBC1685.13	fhn1	3.990	3.964	FHN1
SPBP26C9.02c	car1	NA	NA	No
SPBC215.05	gpd1	2.614	1.861	No
SPBC3D6.02	but2	4.573	4.520	No
SPBC947.04	pfl3	1.068	3.225	No
SPBC1347.11	sro1	2.282	3.312	No
SPBC36.03c	mfs3	4.261	NA	No
SPAPB8E5.03	mae1	NA	NA	No
SPCC1742.01	gsf2	NA	NA	No
SPBP4G3.02	pho1	3.513	3.518	No
SPBC36.02c	SPBC36.02c	NA	NA	No
SPBPB10D8.01	SPBPB10D8.01	NA	NA	No
SPBP16F5.08c	SPBP16F5.08c	NA	NA	No
SPBC1683.01	SPBC1683.01	1.969	2.134	PHO84
SPBC1271.09	tgp1	2.669	3.450	No
SPAC3H1.11	hsr1	1.928	2.393	No
SPAC29B12.10c	pgt1	NA	NA	No
SPBP8B7.05c	nce103	NA	NA	No
SPAC1A6.04c	plb1	3.535	3.879	PLB1, PLB3
SPAC2H10.01	SPAC2H10.01	NA	NA	No
SPCC553.10	SPCC553.10	2.975	3.608	No
SPAC343.12	rds1	2.264	4.020	No
SPCC1223.03c	gut2	NA	NA	No
SPAC17A2.10c	SPAC17A2.10c	3.799	4.744	No
SPCC965.07c	gst2	NA	NA	No
SPAC513.07	SPAC513.07	NA	NA	ARI1
SPBC32H8.02c	nep2	3.120	4.303	No
SPAC17D4.01	pex7	NA	NA	No
SPCC1393.12	SPCC1393.12	NA	NA	No
SPAC23H3.13c	gpa2	NA	2.978	No
SPBC1861.02	abp2	3.348	3.728	No
SPBC354.12	gpd3	2.779	2.689	No
SPBC27.08c	sua1	2.147	2.676	MET3
SPAC5D6.09c	mug86	NA	NA	No
SPAC19G12.16c	adg2	NA	NA	No
SPBC3H7.02	SPBC3H7.02	1.953	2.632	No
SPAC9E9.09c	atd1	NA	1.728	ALD4, ALD6
SPAC1002.17c	urg2	NA	2.282	No
SPBPB2B2.15	SPBPB2B2.15	NA	NA	No
SPAPB1A11.02	SPAPB1A11.02	NA	NA	No
SPBC1348.06c	SPBC1348.06c	NA	NA	No

SPAPB1A11.03	SPAPB1A11.03	NA	NA	No
SPBC3H7.05c	SPBC3H7.05c	2.520	3.212	No
SPCC191.11	inv1	NA	NA	No
SPBC29B5.02c	isp4	2.099	1.737	No
SPAC1039.02	SPAC1039.02	NA	NA	No
SPCC794.04c	SPCC794.04c	4.082	4.377	No
SPAC806.11	SPAC806.11	4.185	4.918	No
SPAC13C5.06c	mug121	NA	NA	No
SPAC1751.01c	gti1	2.835	4.409	No
SPBC1773.06c	adh8	NA	NA	No
SPAC1002.19	urg1	NA	2.858	No
SPAC2E1P3.05c	SPAC2E1P3.05c	1.648	3.303	No
SPBC1683.06c	SPBC1683.06c	NA	NA	No
SPAC1039.10	mmf2	NA	NA	No
SPBPB7E8.01	SPBPB7E8.01	2.204	2.803	No
SPBPB21E7.01c	eno102	NA	NA	No
SPAC1399.01c	SPAC1399.01c	3.050	NA	No
SPBC1289.16c	cao2	NA	NA	No
SPACUNK4.17	SPACUNK4.17	2.015	3.500	No
SPCC757.07c	ctt1	NA	NA	No
SPAC22H12.01c	mug35	NA	NA	No
SPAC2F3.05c	SPAC2F3.05c	NA	2.836	No
SPAC27D7.09c	SPAC27D7.09c	4.347	4.574	No
SPAC2E1P3.01	SPAC2E1P3.01	NA	NA	No
SPBC725.03	SPBC725.03	NA	NA	No
SPBPB2B2.05	SPBPB2B2.05	NA	NA	No
SPAC139.05	SPAC139.05	NA	NA	No
SPAC13C5.04	SPAC13C5.04	NA	NA	No
SPAC27D7.11c	SPAC27D7.11c	NA	NA	No
SPAC4H3.08	SPAC4H3.08	3.338	3.722	No
SPAC27D7.10c	SPAC27D7.10c	NA	NA	No
SPCC757.03c	hsp3101	NA	NA	No
SPBC23G7.10c	SPBC23G7.10c	NA	NA	No
SPBC1289.14	SPBC1289.14	NA	NA	No
SPCC1223.09	SPCC1223.09	2.555	3.277	No
SPBC24C6.09c	SPBC24C6.09c	NA	NA	No
SPBC1773.05c	tms1	NA	NA	No
SPAC22A12.17c	SPAC22A12.17c	NA	NA	No
SPBPB2B2.01	SPBPB2B2.01	NA	NA	No
SPAC513.02	SPAC513.02	NA	NA	No
SPAC13F5.07c	hpz2	NA	NA	No
SPBPB2B2.06c	SPBPB2B2.06c	NA	NA	No

Table A6: *Schizosaccharomyces pombe* strains used in chapter 3.

Strain	Genotype	Reference
972h-	*972 h$^-$*	JK
JK366	*ade6-M216 leu1-32 ura4D18 h$^+$*	JK
GCY1876	Δ*leu1::NatMX4 ade6-M216 leu1-32 ura4D18 h$^-$*	This work
GCY1232	Δ*leu1::NatMX4 ade6-M216 leu1-32 ura4D18 h$^+$*	This work
GCY978	Δ*prz1::KanMX6 h$^-$*	This work
GCY2806	Δ*prz1::NatMX4 ade6-M216 leu1-32 ura4D18 h$^-$*	This work
V3-P12-91	Δ*prz1::KanMX4 ade6-M216 leu1-32 ura4D18 h$^+$*	Bioneer
V3-P11-56	Δ*pmr1::KanMX4 ade6-M216 leu1-32 ura4D18 h$^+$*	Bioneer
V3-P01-91	Δ*alp31::KanMX4 ade6-M216 leu1-32 ura4D18 h$^+$*	Bioneer
V3-P26-42	Δ*SPAC2E1P3.05c::KanMX4 ade6-M216 leu1-32 ura4D18 h$^+$*	Bioneer
V3-P34-46	Δ*ctr4::KanMX4 ade6-M216 leu1-32 ura4D18 h$^+$*	Bioneer
V3-P03-31	Δ*mug134::KanMX4 ade6-M216 leu1-32 ura4D18 h$^+$*	Bioneer
V3-P12-46	Δ*clr2::KanMX4 ade6-M216 leu1-32 ura4D18 h$^+$*	Bioneer
V3-P05-16	Δ*ppk11::KanMX4 ade6-M216 leu1-32 ura4D18 h$^+$*	Bioneer
V3-P32-09	Δ*rds1::KanMX4 ade6-M216 leu1-32 ura4D18 h$^+$*	Bioneer
V3-P01-33	Δ*SPAC19A8.11c::KanMX4 ade6-M216 leu1-32 ura4D18 h$^+$*	Bioneer
V3-P02-26	Δ*arf6::KanMX4 ade6-M216 leu1-32 ura4D18 h$^+$*	Bioneer
GCY3051	*prz1-GFP::KanMX6 ade6-M216 leu1-32 ura4D18 h$^-$*	This work
GCY3128	Δ*pmr1::KanMX4 prz1-GFP::NatMX4 ade6-M216 leu1-32 ura4D18 h$^-$*	This work
GCY3130	Δ*alp31::KanMX4 prz1-GFP::NatMX4 ade6-M216 leu1-32 ura4D18 h$^-$*	This work

Table A7: The transcription factor query strain from chapter 3.

Systematic ID	Name	DNA-Binding Motif	Biological Process
SPBC2F12.09c	atf21	Leucine zipper/bZIP	Meiotic cell cycle
SPAC22F3.02	atf31	Leucine zipper/bZIP	Meiotic cell cycle
SPCC736.08	cbf11	CBF/LAG-1	Lipid metabolic process
SPCC1223.13	cbf12	CBF/LAG-1	Cell adhesion
SPAC31A2.11c	cuf1	Copperfist	Iron ion homeostasis
SPCC584.02	cuf2	Copperfist	Meiosis
SPAC56F8.16	esc1	Helix-loop-helix	Induction of conjugation upon carbon/nitrogen starvations
SPAC31G5.10	eta2	Myb-like	Termination of RNA polymerase I transcription
SPAC23E2.01	fep1	GATA Zn finger	Iron ion homeostasis
SPCC1902.01	gaf1	GATA Zn finger	Negative regulation of induction to conjugation
SPAC1039.05c	klf1	C2H2 Zn Finger	Fungal-type cell wall organization
SPAC25B8.19c	loz1	C2H2 Zn Finger	Zinc ion homeostasis
SPBC317.01	mbx2	SRF-type	Cell adhesion
SPAPB1A11.04c	mca1	Fungal Zn(2)-Cys(6)	Response to copper starvation
SPAC32A11.03c	phx1	Homeobox	Glycolytic fermentation to ethanol
SPAC8C9.14	prr1	HSF-type	Response to oxidative stress
SPAC4G8.13c	prz1	C2H2 Zn Finger	Calcium ion homeostasis
SPAC22F3.09c	res2	APSES	G1/S transition of mitotic cell cycle
SPBP4H10.09	rsv1	C2H2 Zn Finger	Response to glucose starvation
SPBC1105.14	rsv2	C2H2 Zn Finger	Meiotic cell cycle
SPAC16.05c	sfp1	C2H2 Zn Finger	Unknown
SPAC1327.01c	SPAC1327.01c	Fungal Zn(2)-Cys(6)	Unknown
SPAC19B12.07c	SPAC19B12.07c	C2H2 Zn Finger	Unknown
SPAC1F7.11c	SPAC1F7.11c	Fungal Zn(2)-Cys(6)	Unknown
SPAC25B8.11	SPAC25B8.11	Fungal Zn(2)-Cys(6)	Unknown
SPAC2H10.01	SPAC2H10.01	Fungal Zn(2)-Cys(6)	Unknown
SPAC3F10.12c	SPAC3F10.12c	Helix-loop-helix	Unknown
SPAC3H8.08c	SPAC3H8.08c	Fungal Zn(2)-Cys(6)	Unknown
SPCC320.03	SPCC320.03	Fungal Zn(2)-Cys(6)	Unknown
SPCC757.04	SPCC757.04	Fungal Zn(2)-Cys(6)	Unknown
SPCC777.02	SPCC777.02	Fungal Zn(2)-Cys(6)	Unknown
SPCC965.10	SPCC965.10	Fungal Zn(2)-Cys(6)	Unknown
SPBC354.05c	sre2	Helix-loop-helix	Unknown
SPAC1486.10	thi1	Fungal Zn(2)-Cys(6)	Thiamine biosynthetic process
SPAC1399.05c	toe1	Fungal Zn(2)-Cys(6)	Pyrimidine-containing compound salvage
SPAP14E8.02	tos4	Forkhead	Response to DNA damage stimulus
SPBC21B10.13c	yox1	Homeobox	G1/S transition of mitotic cell cycle
SPAC25G10.03	zip1	Leucine zipper/bZIP	Response to cadmium

Table A8: The 48 negative interactions between *Schizosaccharomyces pombe* transcription factors.

Query Strain	Array Strain	Interaction Scores
SPCC320.03	SPAC3C7.04	-0.580
loz1	sre2	-0.428
prz1	sep1	-0.410
rsv1	scr1	-0.410
prr1	SPCC1393.08	-0.376
prr1	scr1	-0.366
prz1	SPBC56F2.05c	-0.342
cuf1	scr1	-0.336
rsv2	SPBC15D4.02	-0.332
SPAC3F10.12c	mug151	-0.319
SPAC3F10.12c	SPBC17D1.01	-0.317
cbf12	scr1	-0.314
prz1	ace2	-0.301
res2	ace2	-0.301
loz1	sep1	-0.277
SPAC3F10.12c	SPBC56F2.05c	-0.274
prz1	scr1	-0.264
res2	scr1	-0.263
tos4	res2	-0.252
prr1	atf21	-0.251
SPAC3F10.12c	matmc_2	-0.249
res2	SPBC17D1.01	-0.247
SPAC3F10.12c	scr1	-0.246
SPAC3F10.12c	ace2	-0.244
cbf12	ace2	-0.243
loz1	mug151	-0.235
klf1	ace2	-0.234
prz1	rep1	-0.232
prz1	SPBC1773.12	-0.232
res2	mug151	-0.227
SPAC3H8.08c	SPAC3F10.12c	-0.224
loz1	ace2	-0.217
SPAC3F10.12c	map1	-0.214
fep1	mug151	-0.211
cuf2	SPCC1393.08	-0.208
loz1	pap1	-0.207
klf1	mug151	-0.204
loz1	SPCC1393.08	-0.201
yox1	sep1	-0.200
loz1	toe2	-0.198
SPAC3F10.12c	esc1	-0.197
res2	sre2	-0.195
zip1	SPAC3F10.12c	-0.194
loz1	scr1	-0.194
SPAC3F10.12c	php3	-0.191
fep1	toe2	-0.190
cuf1	sep1	-0.189
cuf1	sre2	-0.188

Table A9: The 99 positive interactions between *Schizosaccharomyces pombe* transcription factors.

Query Strain	Array Strain	Interaction Scores
cuf1	sak1	0.468
prz1	zas1	0.458
prz1	php5	0.455
prz1	atf1	0.411
SPAC3F10.12c	zas1	0.400
prz1	sak1	0.397
loz1	sak1	0.394
SPAC3F10.12c	sfc2	0.391
prz1	moc3	0.369
SPAC3F10.12c	atf1	0.368
loz1	zas1	0.367
SPAC3F10.12c	php5	0.347
res2	zas1	0.347
prz1	SPBC30D10.02	0.342
loz1	atf1	0.326
res2	php5	0.320
res2	sfc2	0.318
SPAC3F10.12c	moc3	0.314
res2	SPBC30D10.02	0.313
SPAC3F10.12c	SPBC30D10.02	0.312
loz1	SPBC30D10.02	0.305
cuf1	php5	0.301
SPAC3F10.12c	php2	0.300
loz1	bdp1	0.300
cbf11	SPAPB1A11.04c	0.299
prz1	SPAPB1A11.04c	0.299
cuf2	res1	0.295
res2	atf1	0.294
prz1	rst2	0.291
cbf12	bdp1	0.287
sfp1	php5	0.285
res2	moc3	0.284
cuf2	php5	0.284
cuf1	moc3	0.284
rsv2	SPBC30D10.02	0.283
fep1	zas1	0.281
loz1	php5	0.278
sfp1	zas1	0.278
fep1	sak1	0.278
cbf11	cuf1	0.278
SPAC3F10.12c	thi5	0.275
cuf2	sfc2	0.275
sfp1	sak1	0.273
cuf1	res1	0.273
cbf11	prz1	0.271
cbf11	res2	0.271
res2	pcr1	0.269
cbf11	sfp1	0.269
SPAC3F10.12c	pcr1	0.268
cuf2	sak1	0.268

SPAC3F10.12c	SPBC29A10.12	0.264
rsv2	pcr1	0.264
fep1	sfc2	0.263
fep1	php5	0.263
SPAC3F10.12c	SPBC530.05	0.262
SPAC3F10.12c	res1	0.261
loz1	moc3	0.258
cuf2	atf1	0.254
sfp1	atf1	0.254
fep1	pcr1	0.254
sfp1	sfc2	0.253
res2	sak1	0.252
fep1	atf1	0.250
cuf1	zas1	0.249
fep1	bdp1	0.249
cbf12	SPBC30D10.02	0.248
res2	bdp1	0.236
res2	php2	0.235
loz1	sfc2	0.234
loz1	php2	0.234
klf1	zas1	0.233
cbf11	cbf12	0.233
klf1	res1	0.233
cuf1	php2	0.229
prz1	sfc2	0.227
cuf1	bdp1	0.225
sfp1	res1	0.225
rsv2	bdp1	0.225
SPAC3H8.08c	php5	0.223
prz1	pcr1	0.223
loz1	nht1	0.222
cuf1	SPBC30D10.02	0.222
yox1	res1	0.221
SPAC3F10.12c	sak1	0.219
cbf12	php5	0.218
SPAC3F10.12c	cha4	0.216
fep1	SPBC30D10.02	0.216
cuf1	res2	0.215
cuf1	sfc2	0.215
klf1	pcr1	0.214
sfp1	SPBC30D10.02	0.212
SPAC3H8.08c	sfc2	0.210
yox1	zas1	0.209
cbf11	fep1	0.209
cuf1	rst2	0.207
SPAC3F10.12c	bdp1	0.206
prz1	bdp1	0.206
atf21	pcr1	0.206
rsv2	zas1	0.205

Table A10: *Schizosaccharomyces pombe* strains used in chapter 4.

Strain	Genotype	Reference
JK366	*ade6-M216 leu1-32 ura4D18 h*$^{+}$	JK
GCY2517	*pREP1 ade6-M216 leu1-32 ura4D18 h*$^{+}$	This work
GCY2833	*pREP1-scr1*$^{+}$ *ade6-M216 leu1-32 ura4D18 h*$^{-}$	This work
GCY3350	Δ*mua1::KanMX4 pREP1 ade6-M216 leu1-32 ura4D18 h*$^{+}$	This work
GCY3450	Δ*mua1::KanMX4 pREP1-scr1*$^{+}$ *ade6-M216 leu1-32 ura4D18 h*$^{+}$	This work
GCY3351	Δ*ubr1::KanMX4 pREP1 ade6-M216 leu1-32 ura4D18 h*$^{+}$	This work
GCY3482	Δ*ubr1::KanMX4 pREP1-scr1*$^{+}$ *ade6-M216 leu1-32 ura4D18 h*$^{+}$	This work
GCY3189	Δ*gad8::KanMX4 pREP1 ade6-M216 leu1-32 ura4D18 h*$^{+}$	This work
GCY3188	Δ*gad8::KanMX4 pREP1-scr1*$^{+}$ *ade6-M216 leu1-32 ura4D18 h*$^{+}$	This work
GCY3185	Δ*nrd1::KanMX4 pREP1 ade6-M216 leu1-32 ura4D18 h*$^{+}$	This work
GCY3184	Δ*nrd1::KanMX4 pREP1-scr1*$^{+}$ *ade6-M216 leu1-32 ura4D18 h*$^{+}$	This work
GCY3187	Δ*sds23::KanMX4 pREP1 ade6-M216 leu1-32 ura4D18 h*$^{+}$	This work
GCY3186	Δ*sds23::KanMX4 pREP1-scr1*$^{+}$ *ade6-M216 leu1-32 ura4D18 h*$^{+}$	This work
GCY3183	Δ*amk2::KanMX4 pREP1 ade6-M216 leu1-32 ura4D18 h*$^{+}$	This work
GCY3182	Δ*amk2::KanMX4 pREP1-scr1*$^{+}$ *ade6-M216 leu1-32 ura4D18 h*$^{+}$	This work
GCY3090	*scr1-GFP::KanMX6 ade6-M216 leu1-32 ura4D18 h*$^{-}$	This work
GCY3484	Δ*mua1::KanMX4 scr1-GFP::KanMX6 ade6-M216 leu1-32 ura4D18 h*$^{-}$	This work
GCY3451	Δ*ubr1::KanMX4 scr1-GFP::KanMX6 ade6-M216 leu1-32 ura4D18 h*$^{-}$	This work
GCY2831	*pREP1-toe1*$^{+}$ *ade6-M216 leu1-32 ura4D18 h*$^{-}$	This work
GCY2933	Δ*set1::KanMX4 pREP1 ade6-M216 leu1-32 ura4D18 h*$^{+}$	This work
GCY2925	Δ*set1::KanMX4 pREP1-toe1*$^{+}$ *ade6-M216 leu1-32 ura4D18 h*$^{+}$	This work
GCY2931	Δ*sgf29::KanMX4 pREP1 ade6-M216 leu1-32 ura4D18 h*$^{+}$	This work
GCY2924	Δ*sgf29::KanMX4 pREP1-toe1*$^{+}$ *ade6-M216 leu1-32 ura4D18 h*$^{+}$	This work
GCY3553	Δ*ubp8::KanMX4 pREP1 ade6-M216 leu1-32 ura4D18 h*$^{+}$	This work
GCY3552	Δ*ubp8::KanMX4 pREP1-toe1*$^{+}$ *ade6-M216 leu1-32 ura4D18 h*$^{+}$	This work
GCY2935	Δ*gcn5::KanMX4 pREP1 ade6-M216 leu1-32 ura4D18 h*$^{+}$	This work
GCY2927	Δ*gcn5::KanMX4 pREP1-toe1*$^{+}$ *ade6-M216 leu1-32 ura4D18 h*$^{+}$	This work
GCY3551	Δ*spt8::KanMX4 pREP1 ade6-M216 leu1-32 ura4D18 h*$^{+}$	This work
GCY3550	Δ*spt8::KanMX4 pREP1-toe1*$^{+}$ *ade6-M216 leu1-32 ura4D18 h*$^{+}$	This work
V3-P31-90	Δ*set1::KanMX4 ade6-M216 leu1-32 ura4D18 h*$^{+}$	Bioneer
V3-P34-42	Δ*sgf29::KanMX4 ade6-M216 leu1-32 ura4D18 h*$^{+}$	Bioneer
V3-P20-56	Δ*gcn5::KanMX4 ade6-M216 leu1-32 ura4D18 h*$^{+}$	Bioneer

Table A11: The genes present on the SDL miniarray.

Systematic ID	Name	Description
SPCC24B10.08c	ada2	SAGA complex subunit
SPAC23H4.12	alp13	MRG family Clr6 histone deacetylase complex subunit
SPCC1919.03c	amk2	AMP-activated protein kinase beta subunit
SPAC27D7.05c	apc14	Anaphase-promoting complex subunit
SPBC83.04	apc15	Anaphase-promoting complex, platform subcomplex scaffold subunit
SPCC63.08c	atg1	Autophagy and CVT pathway serine/threonine protein kinase
SPAC1556.03	azr1	Serine/threonine protein phosphatase
SPBC21D10.10	bdc1	Bromodomain containing protein 1
SPAP32A8.03c	bop1	Ubiquitin-protein ligase E3 (predicted)
SPCC1919.15	brl1	Ubiquitin-protein ligase E3
SPCC970.10c	brl2	Ubiquitin-protein ligase E3
SPCC1322.12c	bub1	Mitotic spindle checkpoint kinase
SPAC1D4.13	byr1	MAP kinase kinase
SPBC1D7.05	byr2	MAP kinase kinase kinase
SPCC18.06c	caf1	CCR4-Not complex CAF1 family ribonuclease subunit
SPCC31H12.08c	ccr4	CCR4-Not complex subunit (predicted)
SPBC18H10.15	cdk11	Serine/threonine protein kinase
SPAC644.06c	cdr1	NIM1 family serine/threonine protein kinase
SPAC57A10.02	cdr2	Serine/threonine protein kinase
SPCC18B5.11c	cds1	Replication checkpoint kinase
SPAC17H9.19c	cdt2	WD repeat protein
SPCC1450.11c	cek1	Serine/threonine protein kinase
SPAC1851.03	ckb1	CK2 family regulatory subunit
SPBC2G5.02c	ckb2	CK2 family regulatory subunit (predicted)
SPBP35G2.05c	cki2	Serine/threonine protein kinase
SPAC1805.05	cki3	Serine/threonine protein kinase
SPCC1919.01	ckk2	Calmodulin-dependent kinase kinase 2
SPAC1782.09c	clp1	Cdc14-related protein phosphatase
SPBC800.03	clr3	Histone deacetylase (class II)
SPBC428.08c	clr4	Histone H3 lysine methyltransferase
SPACUNK12.02c	cmk1	Calcium/calmodulin-dependent protein kinase
SPAC23A1.06c	cmk2	MAPK-activated protein kinase
SPAC1610.03c	crp79	Poly(A) binding protein
SPAC1D4.06c	csk1	Cyclin-dependent kinase/ cyclin-dependent kinase activating kinase
SPCC1840.11	csl4	Exosome subunit
SPAC17A2.09c	csx1	RNA-binding protein
SPCC1739.07	cti1	Cut3 interacting protein, predicted exosome subunit
SPAC24H6.03	cul3	Cullin 3
SPBC23E6.01c	cxr1	mRNA processing factor
SPAC21E11.05c	cyp8	Cyclophilin family peptidyl-prolyl cis-trans isomerase
SPAC328.02	dbl4	Ubiquitin-protein ligase E3 involved in sporulation
SPCC548.05c	dbl5	Ubiquitin-protein ligase E3
SPAC17H9.10c	ddb1	Damaged DNA binding protein
SPBC776.02c	dis2	Serine/threonine protein phosphatase PP1
SPAC17G8.10c	dma1	Mitotic spindle checkpoint ubiquitin ligase
SPBC14F5.07	doa10	ER-localized ubiquitin-protein ligase E3 (predicted)
SPBC947.10	dsc1	Golgi Dsc E3 ligase complex subunit
SPBC530.14c	dsk1	SR protein-specific kinase
SPAC6F6.09	eaf6	Mst2/NuA4 histone acetyltransferase complex subunit

SPBC16A3.19	eaf7	Histone acetyltransferase complex subunit
SPBC2F12.03c	ebs1	EST1 family nonsense-mediated mRNA decay (NMD) pathway protein (predicted)
SPAC29A4.20	elp3	Elongator complex subunit (predicted)
SPAC19E9.02	fin1	Serine/threonine protein kinase, NIMA related
SPCC24B10.07	gad8	AGC family protein kinase
SPAC1952.05	gcn5	SAGA complex histone acetyltransferase catalytic subunit
SPBC29A3.03c	gid2	GID complex ubiquitin-protein ligase E3 subunit (predicted)
SPAC17A5.09c	glc8	Protein phosphatase regulatory subunit (predicted)
SPAC1687.15	gsk3	Serine/threonine protein kinase
SPBC8D2.01	gsk31	Serine/threonine protein kinase (predicted)
SPAC29A4.16	hal4	Serine/threonine protein kinase
SPAC139.06	hat1	Histone acetyltransferase
SPBC887.18c	hfi1	SAGA complex subunit
SPAC23C4.12	hhp2	Serine/threonine protein kinase
SPAC3G9.07c	hos2	Histone deacetylase (class I)
SPBC17D11.02c	hrd1	Synviolin family ubiquitin-protein ligase E3
SPBC28F2.08c	hrd3	HRD ubiquitin ligase complex subunit (predicted)
SPAC20G4.03c	hri1	eIF2 alpha kinase
SPAC222.07c	hri2	eIF2 alpha kinase
SPAC23C4.03	hrk1	Haspin related kinase
SPCC132.02	hst2	Sirtuin family histone deacetylase
SPCC622.08c	hta1	Histone H2A alpha
SPAC19G12.06c	hta2	Histone H2A beta
SPAC167.07c	hul5	HECT-type ubiquitin-protein ligase E3 (predicted)
SPAC30D11.13	hus5	SUMO conjugating enzyme E2
SPBC839.07	ibp1	Cdc25 family phosphatase
SPAC167.01	ire1	Serine/threonine protein kinase, sensor for unfolded proteins in the ER
SPBC4F6.06	kin1	Microtubule affinity-regulating kinase
SPAC1565.07c	knd1	Cullin-associated NEDD8-dissociated protein (predicted)
SPBC16E9.13	ksp1	Serine/threonine protein kinase (predicted)
SPAC1D4.11c	lkh1	Dual specificity protein kinase
SPBC530.13	lsc1	Lsk1 associated cyclin
SPCC4B3.08	lsg1	Lsk1 complex gamma subunit
SPAC2F3.15	lsk1	P-TEFb-associated cyclin-dependent protein kinase
SPBC887.04c	lub1	WD repeat protein
SPAC1834.08	mak1	Histidine kinase
SPAC27E2.09	mak2	Histidine kinase
SPCC74.06	mak3	Histidine kinase
SPCC1682.08c	mcp2	Pumilio family RNA-binding protein
SPBC8D2.19	mde3	Serine/threonine protein kinase, meiotic
SPBC119.04	mei3	Meiosis inducing protein
SPAC14C4.03	mek1	Cds1/Rad53/Chk2 family protein kinase
SPAC3A12.03c	meu34	Ubiquitin-protein ligase E3 (predicted)
SPBC660.14	mik1	Mitotic inhibitor kinase
SPCC338.05c	mms2	Ubiquitin conjugating enzyme
SPAC16C9.04c	mot2	CCR4-Not complex ubiquitin-protein ligase E3 subunit (predicted)
SPAC4G9.05	mpf1	Meiotic pumilio family RNA-binding protein (predicted)
SPBC106.01	mph1	Dual specificity protein kinase
SPAC343.11c	msc1	Swr1 complex subunit
SPAC17G8.13c	mst2	Histone acetyltransferase
SPCC417.06c	mug27	Meiosis specific protein kinase

SPCC825.04c	naa40	Histone N-acetyltransferase (predicted)
SPAC14C4.06c	nab2	Poly(A) binding protein (predicted)
SPAC3H8.09c	nab3	Poly(A) binding protein (predicted)
SPBC3B8.10c	nem1	Nem1-Spo7 phosphatase complex catalytic subunit (predicted)
SPBC28F2.10c	ngg1	SAGA complex subunit
SPCC4G3.15c	not2	CCR4-Not complex subunit (predicted)
SPAC1B3.05	not3	CCR4-Not complex subunit (predicted)
SPAC2F7.11	nrd1	RNA-binding protein
SPBC17D11.04c	nto1	Histone acetyltransferase complex subunit (predicted)
SPCC1020.10	oca2	Serine/threonine protein kinase
SPBC6B1.08c	ofd1	2-oxoglutarate and Fe(II) dioxygenase domain containing protein 1
SPBC16E9.12c	pab2	Poly(A) binding protein
SPAC57A7.04c	pabp	mRNA export shuttling protein
SPAC1783.07c	pap1	Transcription factor
SPBC17A3.10	pas4	Peroxisomal ubiquitin-protein ligase E3 (predicted)
SPCC126.07c	pbr1	Ubiquitin-protein ligase E3 (predicted)
SPBC32F12.06	pch1	P-TEFB associated cyclin, cyclin T
SPAC17G8.14c	pck1	Protein kinase C (PKC)-like
SPBC19G7.10c	pdc2	Topoisomerase II-associated deadenylation-dependent mRNA-decapping factor (predicted)
SPCC16C4.11	pef1	Pho85/PhoA-like cyclin-dependent kinase
SPBC543.07	pek1	MAP kinase kinase
SPCC790.02	pep3	HOPS/CORVET complex subunit, ubiquitin-protein ligase E3 (predicted)
SPAPB17E12.03	pex12	Ubiquitin-protein ligase E3 (predicted)
SPBC15D4.15	pho2	4-nitrophenylphosphatase
SPBC14F5.13c	pho8	Vacuolar membrane alkaline phosphatase (predicted)
SPAC3C7.06c	pit1	Serine/threonine protein kinase, meiotic
SPBC106.10	pka1	cAMP-dependent protein kinase catalytic subunit
SPAC644.11c	pkp1	Mitochondrial pyruvate dehydrogenase (lipoamide) kinase (predicted)
SPAC1687.05	pli1	SUMO E3 ligase
SPBC119.08	pmk1	MAP kinase
SPBC1685.01	pmp1	Dual-specificity MAP kinase phosphatase
SPBC1709.11c	png2	ING family homolog
SPAC29E6.01	pof11	F-box protein
SPBC56F2.01	pof12	F-box protein
SPBC1271.01c	pof13	F-box protein
SPAC13D6.01	pof14	F-box protein
SPAC2F7.03c	pom1	DYRK family protein kinase
SPAC16C9.07	pom2	DYRK family protein kinase
SPAC823.15	ppa1	Minor serine/threonine protein phosphatase
SPBC16H5.07c	ppa2	Serine/threonine protein phosphatase
SPAC22H10.04	ppa3	Protein phosphatase type 2A
SPBP4H10.04	ppb1	Calcium-dependent serine/threonine protein phosphatase calcineurin A, catalytic subunit
SPCC1739.12	ppe1	Serine/threonine protein phosphatase
SPBC26H8.05c	pph3	Serine/threonine protein phosphatase, PP4 complex subunit (predicted)
SPAC110.01	ppk1	Serine/threonine protein kinase (predicted)
SPAC2C4.14c	ppk11	PAK-related kinase
SPAC3H1.13	ppk13	Serine/threonine protein kinase (predicted)

SPAC4G8.05	ppk14	Serine/threonine protein kinase (predicted)
SPAC823.03	ppk15	Serine/threonine protein kinase (predicted)
SPAC890.03	ppk16	Serine/threonine protein kinase (predicted)
SPBC1778.10c	ppk21	Serine/threonine protein kinase
SPBC1861.09	ppk22	Serine/threonine protein kinase (predicted)
SPBC21.07c	ppk24	Serine/threonine protein kinase
SPBC32C12.03c	ppk25	Serine/threonine protein kinase (predicted)
SPBC336.14c	ppk26	Protein kinase like PAN complex subunit
SPBC337.04	ppk27	Serine/threonine protein kinase (predicted)
SPBC557.04	ppk29	Ark1/Prk1 family protein kinase
SPAC15A10.13	ppk3	Protein kinase domain and HEAT repeat protein
SPBC6B1.02	ppk30	Ark1/Prk1 family protein kinase
SPBC725.06c	ppk31	Serine/threonine protein kinase (predicted)
SPBP23A10.10	ppk32	Serine/threonine protein kinase (predicted)
SPCC162.10	ppk33	Serine/threonine protein kinase (predicted)
SPCP1E11.02	ppk38	Ark1/Prk1 family protein kinase
SPAC1805.01c	ppk6	Serine/threonine protein kinase (predicted)
SPAC22G7.08	ppk8	Serine/threonine protein kinase (predicted)
SPAC23H4.02	ppk9	Serine/threonine protein kinase (predicted)
SPCC4G3.08	psk1	Serine/threonine protein kinase
SPAC2F7.02c	psr1	NLI interacting factor family phosphatase (predicted)
SPCC1223.11	ptc2	Protein phosphatase 2C
SPAC2G11.07c	ptc3	Protein phosphatase 2c homolog 3
SPAC4A8.03c	ptc4	Protein phosphatase 2C
SPBC609.02	ptn1	Phosphatidylinositol-3,4,5-trisphosphate3-phosphatase
SPAC11G7.02	pub1	HECT-type ubiquitin-protein ligase E3
SPAC1805.15c	pub2	HECT-type ubiquitin-protein ligase E3
SPBC16E9.11c	pub3	HECT-type ubiquitin-protein ligase E3 (predicted)
SPBC56F2.08c	puf1	Pumilio family RNA-binding protein (predicted)
SPBP35G2.14	puf2	Pumilio family RNA-binding protein
SPAC1687.22c	puf3	Pumilio family RNA-binding protein (predicted)
SPAC6G9.14	puf4	Pumilio family RNA-binding protein (predicted)
SPAC4G8.03c	puf5	Pumilio family RNA-binding protein (predicted)
SPCP1E11.11	puf6	Pumilio family RNA-binding protein (predicted)
SPAC26F1.10c	pyp1	Tyrosine phosphatase
SPAC19D5.01	pyp2	Tyrosine phosphatase
SPAC11E3.09	pyp3	Protein-tyrosine phosphatase
SPAC57A7.08	pzh1	Serine/threonine protein phosphatase
SPAC8E11.02c	rad24	14-3-3 protein
SPAC17A2.13c	rad25	14-3-3 protein
SPAC13G6.01c	rad8	Ubiquitin-protein ligase E3
SPBC17G9.05	rct1	RRM-containing cyclophilin regulating transcription
SPAC19A8.10	rfp1	SUMO-targeted ubiquitin-protein ligase subunit
SPAC343.18	rfp2	SUMO-targeted ubiquitin-protein ligase subunit
SPCC330.01c	rhp16	Rad16 homolog ATP-dependent DNA helicase/ ubiquitin protein ligase E3
SPBC1734.06	rhp18	Rad18 homolog ubiquitin protein ligase E3
SPBC2D10.12	rhp23	Rad23 homolog
SPAC18B11.07c	rhp6	Rad6 homolog, ubiquitin conjugating enzyme E2
SPBC21D10.09c	rkr1	RQC complex ubiquitin-protein ligase E3 (predicted)
SPCC757.09c	rnc1	RNA-binding protein that suppresses calcineurin deletion
SPBP8B7.23	rnf10	Ubiquitin-protein ligase E3 implicated in transcription (predicted)
SPAC17A2.12	rrp1	ATP-dependent DNA helicase/ ubiquitin-protein ligase E3

		(predicted)
SPBC23E6.02	rrp2	ATP-dependent DNA helicase, ubiquitin-protein ligase E3 (predicted)
SPAC23A1.16c	rtr1	RNA polymerase II CTD phosphatase (predicted)
SPBC342.06c	rtt109	RTT109 family histone lysine acetyltransferase
SPBC2A9.04c	san1	Sir antagonist, ubiquitin-protein ligase E3
SPAC1B9.02c	sck1	Serine/threonine protein kinase
SPAC22E12.14c	sck2	Serine/threonine protein kinase
SPBC646.13	sds23	PP2A-type phosphatase inhibitor
SPAC11E3.05	sea3	Ubiquitin-protein ligase E3, coatamer related complex subunit (predicted)
SPAC12G12.01c	sea4	SEA complex subunit, ubiquitin-protein ligase E3, (predicted)
SPCC306.04c	set1	Histone lysine methyltransferase
SPAC29B12.02c	set2	Histone lysine methyltransferase
SPAC22E12.11c	set3	Histone lysine methyltransferase
SPCC1739.05	set5	Histone lysine methyltransferase (predicted)
SPBP8B7.07c	set6	Histone lysine methyltransferase (predicted)
SPCC297.04c	set7	Histone lysine methyltransferase (predicted)
SPCC4B3.12	set9	Histone lysine H3-K20 methyltransferase
SPAC57A10.14	sgf11	SAGA complex subunit
SPBC1921.07c	sgf29	SAGA complex subunit
SPCC126.04c	sgf73	SAGA complex subunit
SPAC22F8.12c	shf1	Small histone ubiquitination factor
SPAC1F5.09c	shk2	PAK-related kinase
SPBC16D10.07c	sir2	Sirtuin family histone deacetylase
SPAC12B10.01c	SPAC12B10.01c	HECT-type ubiquitin-protein ligase E3 (predicted)
SPAC144.05	SPAC144.05	ATP-dependent DNA helicase/ ubiquitin-protein ligase E3 (predicted)
SPAC16A10.03c	SPAC16A10.03c	Ubiquitin-protein ligase E3 Pep5/Vps11-like (predicted)
SPAC16E8.13	SPAC16E8.13	Ubiquitin-protein ligase E3 (predicted)
SPAC23A1.07	SPAC23A1.07	Ubiquitin-protein ligase E3 (predicted)
SPAC2F3.16	SPAC2F3.16	Ubiquitin-protein ligase E3 (predicted)
SPAC57A7.09	SPAC57A7.09	E3 ubiquitin-protein ligase, human RNF family homolog
SPAC6B12.07c	SPAC6B12.07c	Ubiquitin-protein ligase E3 (predicted)
SPBC1271.03c	SPBC1271.03c	NLI interacting factor family phosphatase (predicted)
SPBC13E7.03c	SPBC13E7.03c	RNA hairpin binding protein (predicted)
SPBC14F5.10c	SPBC14F5.10c	Ubiquitin-protein ligase E3 (predicted)
SPBC15C4.06c	SPBC15C4.06c	Ubiquitin-protein ligase E3 (predicted)
SPBC16G5.03	SPBC16G5.03	Ubiquitin-protein ligase E3 (predicted)
SPBC17A3.03c	SPBC17A3.03c	Phosphoprotein phosphatase (predicted)
SPBC17A3.06	SPBC17A3.06	Phosphoprotein phosphatase (predicted)
SPBC17D11.08	SPBC17D11.08	WD repeat protein, DDB1 and CUL4-associated factor 7 (predicted)
SPBC1861.07	SPBC1861.07	elongin C (predicted)
SPBC31F10.10c	SPBC31F10.10c	zf-MYND type zinc finger protein
SPBC32F12.07c	SPBC32F12.07c	Ubiquitin-protein ligase E3, MARCH family (predicted)
SPBC36B7.05c	SPBC36B7.05c	Ubiquitin-protein ligase E3/phosphatidylinositol(3)-phosphate binding protein (predicted)
SPBC3F6.01c	SPBC3F6.01c	Serine/threonine protein phosphatase (predicted)
SPCC1020.05	SPCC1020.05	Phosphoprotein phosphatase involved in unfolded protein response (predicted)
SPCC1223.01	SPCC1223.01	Ubiquitin-protein ligase E3 (predicted)
SPCC18.03	SPCC18.03	Shuttle craft like ubiquitin-protein ligase E3 (predicted)
SPAC31G5.09c	spk1	MAP kinase

SPBC21C3.18	spo4	Serine/threonine protein kinase
SPBC1778.04	spo6	Spo4-Spo6 kinase complex regulatory subunit
SPAC4D7.10c	spt20	SAGA complex subunit
SPCC61.02	spt3	SAGA complex subunit
SPBC14C8.17c	spt8	SAGA complex subunit
SPAC23H4.17c	srb10	Cyclin-dependent protein Srb mediator subunit kinase
SPCC1322.08	srk1	MAPK-activated protein kinase
SPCC74.03c	ssp2	AMP-activated protein serine/threonine kinase alpha subunit
SPBC776.09	ste13	ATP-dependent RNA helicase
SPAC1071.12c	stp1	Protein tyrosine phosphatase
SPAC24B11.06c	sty1	MAP kinase
SPAC12B10.14c	tea5	Pseudokinase
SPCC23B6.03c	tel1	ATM checkpoint kinase
SPBP16F5.03c	tra1	SAGA complex phosphatidylinositol pseudokinase
SPBC2D10.20	ubc1	Ubiquitin conjugating enzyme (predicted)
SPAC11E3.04c	ubc13	Ubiquitin conjugating enzyme E2
SPAC1250.03	ubc14	Ubiquitin conjugating enzyme E2 (predicted)
SPBC1105.09	ubc15	Ubiquitin conjugating enzyme E2
SPBC1198.09	ubc16	Ubiquitin conjugating enzyme E2 (predicted)
SPAC10F6.05c	ubc6	Ubiquitin conjugating enzyme E2 (predicted)
SPAC11G7.04	ubi1	Ribosomal-ubiquitin fusion protein (predicted)
SPAC589.10c	ubi5	Ribosomal-ubiquitin fusion protein (predicted)
SPAC13A11.04c	ubp8	SAGA complex ubiquitin C-terminal hydrolase
SPBC19C7.02	ubr1	N-end-recognizing protein, UBR ubiquitin-protein ligase E3
SPAC15A10.11	ubr11	UBR ubiquitin-protein ligase E3
SPAC20H4.10	ufd2	Ubiquitin-protein ligase E4 (predicted)
SPAC17A2.06c	vps8	WD repeat protein (predicted)
SPCC18B5.03	wee1	M phase inhibitor protein kinase
SPBC409.07c	wis1	MAP kinase kinase
SPAC9G1.02	wis4	MAP kinase kinase kinase
SPAC17G8.07	yaf9	YEATS family histone acetyltransferase subunit
SPBC1718.07c	zfs1	CCCH tandem zinc finger protein, human Tristetraprolin homolog, involved in mRNA catabolism
SPCC1442.16c	zta1	NADPH quinone oxidoreductase/ARE-binding protein (predicted)

Table A12: The 195 SDL interactions between the miniarray and 14 transcription factor query strains.

Query Strain	Array Strain	Interaction Score
cbf11	mst2	-1.189
cbf11	gad8	-0.657
cbf11	pom1	-0.595
cbf11	brl1	-0.568
cbf11	pho8	-0.559
cbf11	spk1	-0.553
cbf11	sea3	-0.529
cbf11	alp13	-0.518
cbf11	rnc1	-0.504
eta2	cdr1	-0.795
eta2	spo4	-0.689
eta2	sgf29	-0.643
eta2	oca2	-0.608
eta2	pka1	-0.603
eta2	ubi1	-0.599
eta2	mst2	-0.589
eta2	apc14	-0.562
eta2	rfp1	-0.559
eta2	pom1	-0.550
eta2	SPAC2F3.16	-0.528
eta2	pdc2	-0.525
eta2	ppk21	-0.518
eta2	pkp1	-0.506
mbx1	mst2	-0.898
mbx1	spt3	-0.730
mbx1	ppk13	-0.707
mbx1	SPBC31F10.10c	-0.618
mbx1	SPBC3F6.01c	-0.592
mbx1	pof11	-0.590
mbx1	ubc15	-0.519
mbx1	cdr1	-0.513
scr1	cdr1	-0.809
scr1	SPAC2F3.16	-0.793
scr1	ste13	-0.756
scr1	amk2	-0.729
scr1	sds23	-0.699
scr1	nrd1	-0.611
scr1	ubr1	-0.599
scr1	gad8	-0.573
scr1	SPBC31F10.10c	-0.544
scr1	mst2	-0.533
scr1	cki3	-0.522
scr1	spo4	-0.501
sfp1	ste13	-0.778
sfp1	ppk25	-0.775
sfp1	nrd1	-0.765
sfp1	cds1	-0.738
sfp1	mst2	-0.735
sfp1	ppk21	-0.712
sfp1	oca2	-0.655

sfp1	ubc13	-0.652
sfp1	spo4	-0.640
sfp1	pyp2	-0.604
sfp1	SPBC3F6.01c	-0.598
sfp1	SPBC17A3.06	-0.559
sfp1	dbl4	-0.556
sfp1	puf3	-0.544
sfp1	SPAC2F3.16	-0.542
sfp1	pka1	-0.531
sfp1	not3	-0.511
SPAC19B12.07c	ppk21	-0.928
SPAC19B12.07c	ptc2	-0.707
SPAC19B12.07c	pho8	-0.669
SPAC19B12.07c	ubi1	-0.609
SPAC19B12.07c	cdr1	-0.607
SPAC19B12.07c	gsk3	-0.605
SPAC19B12.07c	apc14	-0.593
SPAC19B12.07c	oca2	-0.590
SPAC19B12.07c	not3	-0.562
SPAC19B12.07c	mst2	-0.548
SPAC19B12.07c	pom1	-0.525
SPAC19B12.07c	cds1	-0.503
SPAC1F7.11	mst2	-0.884
SPAC1F7.11	pyp3	-0.633
SPAC1F7.11	SPBC31F10.10c	-0.617
SPAC1F7.11	ubi1	-0.548
SPAC1F7.11	ubr1	-0.546
SPAC1F7.11	pom1	-0.539
SPAC1F7.11	pka1	-0.530
SPAC1F7.11	brl1	-0.529
SPAC1F7.11	rad24	-0.528
SPAC1F7.11	ppk21	-0.522
SPAC1F7.11	pho8	-0.515
SPAC1F7.11	pli1	-0.513
SPBC19G7.04	SPBC3F6.01c	-1.063
SPBC19G7.04	rfp1	-1.012
SPBC19G7.04	ppk21	-0.883
SPBC19G7.04	puf6	-0.841
SPBC19G7.04	rrp1	-0.814
SPBC19G7.04	ppk13	-0.738
SPBC19G7.04	pit1	-0.653
SPBC19G7.04	pka1	-0.618
SPBC19G7.04	mde3	-0.616
SPBC19G7.04	SPBC1861.07	-0.586
SPBC19G7.04	ppk26	-0.580
SPBC19G7.04	yaf9	-0.528
SPBC19G7.04	pkp1	-0.525
SPBC19G7.04	caf1	-0.511
SPBC19G7.04	bop1	-0.506
SPBC19G7.04	dbl4	-0.502
SPBC29A10.12	mst2	-0.727
SPBC29A10.12	ibp1	-0.618
SPBC29A10.12	gsk3	-0.560
SPBC29A10.12	ubi1	-0.550

SPBC29A10.12	SPBC3F6.01c	-0.544
SPBC29A10.12	pef1	-0.512
SPBC29A10.12	ubc16	-0.510
SPBC29A10.12	oca2	-0.510
SPBC530.08	ste13	-1.320
SPBC530.08	mst2	-0.823
SPBC530.08	alp13	-0.807
SPBC530.08	pef1	-0.703
SPBC530.08	rhp6	-0.682
SPBC530.08	ufd2	-0.655
SPBC530.08	SPBC31F10.10c	-0.640
SPBC530.08	sty1	-0.623
SPBC530.08	ubp8	-0.612
SPBC530.08	gad8	-0.589
SPBC530.08	brl1	-0.570
SPBC530.08	spt8	-0.563
SPBC530.08	zta1	-0.547
SPBC530.08	pdc2	-0.533
SPBC530.08	pof11	-0.530
SPBC530.08	clr4	-0.519
SPBC530.08	spk1	-0.514
SPBC530.08	brl2	-0.509
SPBC530.08	wis1	-0.504
sre2	SPBC3F6.01c	-0.975
sre2	srk1	-0.913
sre2	rnc1	-0.741
sre2	ste13	-0.712
sre2	oca2	-0.673
sre2	rhp16	-0.663
sre2	bop1	-0.661
sre2	ubc15	-0.646
sre2	dbl4	-0.608
sre2	spo4	-0.601
sre2	pka1	-0.583
sre2	ppk13	-0.575
sre2	ppk14	-0.572
sre2	meu34	-0.560
sre2	rrp2	-0.526
sre2	SPBC13E7.03c	-0.518
toe1	mst2	-0.996
toe1	brl1	-0.778
toe1	set1	-0.631
toe1	rhp6	-0.625
toe1	ubp8	-0.613
toe1	pof12	-0.598
toe1	hrd3	-0.578
toe1	sgf29	-0.573
toe1	pho8	-0.548
toe1	ubr1	-0.548
toe1	pef1	-0.544
toe1	brl2	-0.544
toe1	pyp1	-0.530
toe1	hat1	-0.514
toe1	ptc2	-0.513

toe1	pyp3	-0.504
tos4	mst2	-1.344
tos4	wee1	-1.184
tos4	gad8	-0.735
tos4	brl1	-0.732
tos4	rhp6	-0.709
tos4	ste13	-0.701
tos4	clr4	-0.661
tos4	brl2	-0.636
tos4	hfi1	-0.628
tos4	alp13	-0.621
tos4	SPBC31F10.10c	-0.617
tos4	cdt2	-0.603
tos4	spk1	-0.549
tos4	shf1	-0.532
tos4	pdc2	-0.510
tos4	ubr1	-0.510
tos4	ufd2	-0.503
yox1	mst2	-1.203
yox1	ste13	-1.028
yox1	cdt2	-0.913
yox1	ubi1	-0.823
yox1	rhp6	-0.736
yox1	cds1	-0.731
yox1	pef1	-0.679
yox1	gad8	-0.669
yox1	brl1	-0.655
yox1	pho8	-0.624
yox1	ptc2	-0.620
yox1	cdr1	-0.602
yox1	oca2	-0.600
yox1	ppe1	-0.555
yox1	alp13	-0.543
yox1	hat1	-0.543
yox1	pdc2	-0.536
yox1	pub1	-0.532
yox1	eaf6	-0.515

Appendix B: Copyright permissions

Genetics Society of America LICENSE TERMS AND CONDITIONS

Jun 28, 2016

This is a License Agreement between Kate Chatfield ("You") and Genetics Society of America ("Genetics Society of America") provided by Copyright Clearance Center ("CCC"). The license consists of your order details, the terms and conditions provided by Genetics Society of America, and the payment terms and conditions.

All payments must be made in full to CCC. For payment instructions, please see information listed at the bottom of this form.

License Number	3897760557302
License date	Jun 26, 2016
Licensed content publisher	Genetics Society of America
Licensed content title	Genetics
Licensed content date	Dec 31, 1969
Type of Use	Thesis/Dissertation
Requestor type	Academic institution
Format	Print, Electronic
Portion	chapter/article
Title or numeric reference of the portion(s)	Full work
Title of the article or chapter the portion is from	Conserved and Diverged Functions of the Calcineurin-Activated Prz1 Transcription Factor in Fission Yeast
Editor of portion(s)	N/A
Author of portion(s)	Kate Chatfield-Reed
Volume of serial or monograph.	N/A
Page range of the portion	
Publication date of portion	2016
Rights for	Main product
Duration of use	Life of current edition
Creation of copies for the disabled	no
With minor editing privileges	yes
For distribution to	Canada
In the following language(s)	Original language of publication
With incidental promotional use	no
The lifetime unit quantity of new product	Up to 499
Made available in the following markets	Academic
Specified additional	I would like to put my article with minor editing privileges as a

information	chapter of my thesis.
The requesting person/organization is:	Kate Chatfield-Reed
Order reference number	
Author/Editor	Kate Chatfield-Reed
The standard identifier of New Work	Thesis
Title of New Work	Identifying genetic interactions and target genes of Schizosaccharomyces pombe transcription factors by functional genomics
Publisher of New Work	University of Calgary
Expected publication date	Jun 2016
Estimated size (pages)	200
Total (may include CCC user fee)	0.00 USD
Terms and Conditions	

TERMS AND CONDITIONS
The following terms are individual to this publisher:

None

Other Terms and Conditions:
STANDARD TERMS AND CONDITIONS

1. Description of Service; Defined Terms. This Republication License enables the User to obtain licenses for republication of one or more copyrighted works as described in detail on the relevant Order Confirmation (the "Work(s)"). Copyright Clearance Center, Inc. ("CCC") grants licenses through the Service on behalf of the rightsholder identified on the Order Confirmation (the "Rightsholder"). "Republication", as used herein, generally means the inclusion of a Work, in whole or in part, in a new work or works, also as described on the Order Confirmation. "User", as used herein, means the person or entity making such republication.

2. The terms set forth in the relevant Order Confirmation, and any terms set by the Rightsholder with respect to a particular Work, govern the terms of use of Works in connection with the Service. By using the Service, the person transacting for a republication license on behalf of the User represents and warrants that he/she/it (a) has been duly authorized by the User to accept, and hereby does accept, all such terms and conditions on behalf of User, and (b) shall inform User of all such terms and conditions. In the event such person is a "freelancer" or other third party independent of User and CCC, such party shall be deemed jointly a "User" for purposes of these terms and conditions. In any event, User shall be deemed to have accepted and agreed to all such terms and conditions if User republishes the Work in any fashion.

3. Scope of License; Limitations and Obligations.

3.1 All Works and all rights therein, including copyright rights, remain the sole and exclusive property of the Rightsholder. The license created by the exchange of an Order Confirmation (and/or any invoice) and payment by User of the full amount set forth on that document includes only those rights expressly set forth in the Order Confirmation and in these terms and conditions, and conveys no other rights in the Work(s) to User. All rights not expressly granted are hereby reserved.

3.2 General Payment Terms: You may pay by credit card or through an account with us payable at the end of the month. If you and we agree that you may establish a standing account with CCC, then the following terms apply: Remit Payment to: Copyright Clearance Center, Dept 001, P.O. Box 843006, Boston, MA 02284-3006. Payments Due: Invoices are payable upon their delivery to you (or upon our notice to you that they are available to you

for downloading). After 30 days, outstanding amounts will be subject to a service charge of 1-1/2% per month or, if less, the maximum rate allowed by applicable law. Unless otherwise specifically set forth in the Order Confirmation or in a separate written agreement signed by CCC, invoices are due and payable on "net 30" terms. While User may exercise the rights licensed immediately upon issuance of the Order Confirmation, the license is automatically revoked and is null and void, as if it had never been issued, if complete payment for the license is not received on a timely basis either from User directly or through a payment agent, such as a credit card company.

3.3 Unless otherwise provided in the Order Confirmation, any grant of rights to User (i) is "one-time" (including the editions and product family specified in the license), (ii) is non-exclusive and non-transferable and (iii) is subject to any and all limitations and restrictions (such as, but not limited to, limitations on duration of use or circulation) included in the Order Confirmation or invoice and/or in these terms and conditions. Upon completion of the licensed use, User shall either secure a new permission for further use of the Work(s) or immediately cease any new use of the Work(s) and shall render inaccessible (such as by deleting or by removing or severing links or other locators) any further copies of the Work (except for copies printed on paper in accordance with this license and still in User's stock at the end of such period).

3.4 In the event that the material for which a republication license is sought includes third party materials (such as photographs, illustrations, graphs, inserts and similar materials) which are identified in such material as having been used by permission, User is responsible for identifying, and seeking separate licenses (under this Service or otherwise) for, any of such third party materials; without a separate license, such third party materials may not be used.

3.5 Use of proper copyright notice for a Work is required as a condition of any license granted under the Service. Unless otherwise provided in the Order Confirmation, a proper copyright notice will read substantially as follows: "Republished with permission of [Rightsholder's name], from [Work's title, author, volume, edition number and year of copyright]; permission conveyed through Copyright Clearance Center, Inc. " Such notice must be provided in a reasonably legible font size and must be placed either immediately adjacent to the Work as used (for example, as part of a by-line or footnote but not as a separate electronic link) or in the place where substantially all other credits or notices for the new work containing the republished Work are located. Failure to include the required notice results in loss to the Rightsholder and CCC, and the User shall be liable to pay liquidated damages for each such failure equal to twice the use fee specified in the Order Confirmation, in addition to the use fee itself and any other fees and charges specified.

3.6 User may only make alterations to the Work if and as expressly set forth in the Order Confirmation. No Work may be used in any way that is defamatory, violates the rights of third parties (including such third parties' rights of copyright, privacy, publicity, or other tangible or intangible property), or is otherwise illegal, sexually explicit or obscene. In addition, User may not conjoin a Work with any other material that may result in damage to the reputation of the Rightsholder. User agrees to inform CCC if it becomes aware of any infringement of any rights in a Work and to cooperate with any reasonable request of CCC or the Rightsholder in connection therewith.

4. Indemnity. User hereby indemnifies and agrees to defend the Rightsholder and CCC, and their respective employees and directors, against all claims, liability, damages, costs and expenses, including legal fees and expenses, arising out of any use of a Work beyond the scope of the rights granted herein, or any use of a Work which has been altered in any unauthorized way by User, including claims of defamation or infringement of rights of copyright, publicity, privacy or other tangible or intangible property.

5. Limitation of Liability. UNDER NO CIRCUMSTANCES WILL CCC OR THE RIGHTSHOLDER BE LIABLE FOR ANY DIRECT, INDIRECT, CONSEQUENTIAL OR INCIDENTAL DAMAGES (INCLUDING WITHOUT LIMITATION DAMAGES FOR LOSS OF BUSINESS PROFITS OR INFORMATION, OR FOR BUSINESS

INTERRUPTION) ARISING OUT OF THE USE OR INABILITY TO USE A WORK, EVEN IF ONE OF THEM HAS BEEN ADVISED OF THE POSSIBILITY OF SUCH DAMAGES. In any event, the total liability of the Rightsholder and CCC (including their respective employees and directors) shall not exceed the total amount actually paid by User for this license. User assumes full liability for the actions and omissions of its principals, employees, agents, affiliates, successors and assigns.

6. Limited Warranties. THE WORK(S) AND RIGHT(S) ARE PROVIDED "AS IS". CCC HAS THE RIGHT TO GRANT TO USER THE RIGHTS GRANTED IN THE ORDER CONFIRMATION DOCUMENT. CCC AND THE RIGHTSHOLDER DISCLAIM ALL OTHER WARRANTIES RELATING TO THE WORK(S) AND RIGHT(S), EITHER EXPRESS OR IMPLIED, INCLUDING WITHOUT LIMITATION IMPLIED WARRANTIES OF MERCHANTABILITY OR FITNESS FOR A PARTICULAR PURPOSE. ADDITIONAL RIGHTS MAY BE REQUIRED TO USE ILLUSTRATIONS, GRAPHS, PHOTOGRAPHS, ABSTRACTS, INSERTS OR OTHER PORTIONS OF THE WORK (AS OPPOSED TO THE ENTIRE WORK) IN A MANNER CONTEMPLATED BY USER; USER UNDERSTANDS AND AGREES THAT NEITHER CCC NOR THE RIGHTSHOLDER MAY HAVE SUCH ADDITIONAL RIGHTS TO GRANT.

7. Effect of Breach. Any failure by User to pay any amount when due, or any use by User of a Work beyond the scope of the license set forth in the Order Confirmation and/or these terms and conditions, shall be a material breach of the license created by the Order Confirmation and these terms and conditions. Any breach not cured within 30 days of written notice thereof shall result in immediate termination of such license without further notice. Any unauthorized (but licensable) use of a Work that is terminated immediately upon notice thereof may be liquidated by payment of the Rightsholder's ordinary license price therefor; any unauthorized (and unlicensable) use that is not terminated immediately for any reason (including, for example, because materials containing the Work cannot reasonably be recalled) will be subject to all remedies available at law or in equity, but in no event to a payment of less than three times the Rightsholder's ordinary license price for the most closely analogous licensable use plus Rightsholder's and/or CCC's costs and expenses incurred in collecting such payment.

8. **Miscellaneous.**

8.1 User acknowledges that CCC may, from time to time, make changes or additions to the Service or to these terms and conditions, and CCC reserves the right to send notice to the User by electronic mail or otherwise for the purposes of notifying User of such changes or additions; provided that any such changes or additions shall not apply to permissions already secured and paid for.

8.2 Use of User-related information collected through the Service is governed by CCC's privacy policy, available online here:
http://www.copyright.com/content/cc3/en/tools/footer/privacypolicy.html.

8.3 The licensing transaction described in the Order Confirmation is personal to User. Therefore, User may not assign or transfer to any other person (whether a natural person or an organization of any kind) the license created by the Order Confirmation and these terms and conditions or any rights granted hereunder; provided, however, that User may assign such license in its entirety on written notice to CCC in the event of a transfer of all or substantially all of User's rights in the new material which includes the Work(s) licensed under this Service.

8.4 No amendment or waiver of any terms is binding unless set forth in writing and signed by the parties. The Rightsholder and CCC hereby object to any terms contained in any writing prepared by the User or its principals, employees, agents or affiliates and purporting to govern or otherwise relate to the licensing transaction described in the Order Confirmation, which terms are in any way inconsistent with any terms set forth in the Order Confirmation and/or in these terms and conditions or CCC's standard operating procedures, whether such writing is prepared prior to, simultaneously with or subsequent to the Order Confirmation, and whether such writing appears on a copy of the Order Confirmation or in a

separate instrument.

8.5 The licensing transaction described in the Order Confirmation document shall be governed by and construed under the law of the State of New York, USA, without regard to the principles thereof of conflicts of law. Any case, controversy, suit, action, or proceeding arising out of, in connection with, or related to such licensing transaction shall be brought, at CCC's sole discretion, in any federal or state court located in the County of New York, State of New York, USA, or in any federal or state court whose geographical jurisdiction covers the location of the Rightsholder set forth in the Order Confirmation. The parties expressly submit to the personal jurisdiction and venue of each such federal or state court.If you have any comments or questions about the Service or Copyright Clearance Center, please contact us at 978-750-8400 or send an e-mail to info@copyright.com.

v 1.1

Questions? customercare@copyright.com or +1-855-239-3415 (toll free in the US) or +1-978-646-2777.

Gmail Kate Chatfield-Reed [redacted]

Permission to use Genetics Paper

Lianne Vachon [redacted] Thu, Jun 30, 2016 at 2:20 AM
To: Kate Chatfield-Reed [redacted]

Do I need to email someone else or just you?

If just you, of course that's perfectly alright.

Lianne

From: Kate Chatfield-Reed [redacted]
Sent: June 29, 2016 1:23 PM
To: Gordon Chua; Gina Kwon; Lianne Vachon
Subject: Permission to use Genetics Paper

Hi coauthors,

I am writing to get your permission to use the paper "Conserved and Diverged Functions of the Calcineurin-Activated Prz1 Transcription Factor in Fission Yeast" as a chapter in my PhD thesis. The paper, as part of the thesis, will be added to the repository at the University of Calgary as well as the Library and Archives Canada. Below are some links about these resources:

University of Calgary Theses Repository – The Vault: http://theses.ucalgary.ca/

The Vault at the University of Calgary:Home

theses.ucalgary.ca

This repository is a digital archive of University of Calgary theses submitted after June 28, 2012. How to submit: You may submit your thesis to this repository, if ...

Library and Archives Canada: http://collectionscanada.gc.ca/obj/s4/f2/frm-nl59-2-e.pdf

A quick email indicating that you agree to this use of the material is sufficient.

Thank you,

Gmail Kate Chatfield-Reed [redacted]

Permission to use Genetics Paper

Gina Kwon [redacted] Wed, Jun 29, 2016 at 9:53 PM
To: Kate Chatfield-Reed [redacted]

Of course, Kate.
Gina

On Jun 29, 2016, at 2:23 PM, Kate Chatfield-Reed [redacted] wrote:

> Hi coauthors,
>
> I am writing to get your permission to use the paper "Conserved and Diverged Functions of the Calcineurin-Activated Prz1 Transcription Factor in Fission Yeast" as a chapter in my PhD thesis. The paper, as part of the thesis, will be added to the repository at the University of Calgary as well as the Library and Archives Canada. Below are some links about these resources:
>
> University of Calgary Theses Repository – The Vault: http://theses.ucalgary.ca/
>
> Library and Archives Canada: http://collectionscanada.gc.ca/obj/s4/f2/frm-nl59-2-e.pdf
>
> A quick email indicating that you agree to this use of the material is sufficient.
>
> Thank you,
>
> Kate Chatfield-Reed

Gmail Kate Chatfield-Reed [redacted]

Permission to use Genetics Paper

Gordon Chua [redacted] Wed, Jun 29, 2016 at 3:24 PM
Reply-To: [redacted]
To: Kate Chatfield-Reed [redacted]

Hi Kate,

I agree to the use of your Genetics paper for your thesis.

Kind regards,

Gordon

Gordon Chua, Ph.D.
Associate professor,
Department of Biological Sciences
Biological Sciences Building, Room 560
University of Calgary
2500 University Drive, N.W.
Calgary, Alberta
Canada T2N 1N4
[redacted]

> Hi coauthors,
>
> I am writing to get your permission to use the paper "Conserved and
> Diverged Functions of the Calcineurin-Activated Prz1 Transcription Factor
> in Fission Yeast" as a chapter in my PhD thesis. The paper, as part of
> the
> thesis, will be added to the repository at the University of Calgary as
> well as the Library and Archives Canada. Below are some links about these
> resources:
>
> University of Calgary Theses Repository – The Vault:
> http://theses.ucalgary.ca/
>
> Library and Archives Canada:
> http://collectionscanada.gc.ca/obj/s4/f2/frm-nl59-2-e.pdf
>
> A quick email indicating that you agree to this use of the material is
> sufficient.
>
> Thank you,
>
> Kate Chatfield-Reed
>